UNIVERSITY OF SOUTHAMPTON

Faculty of Natural and Environmental Sciences

Centre for Biological Sciences

The impact of systemic inflammation on neuroinflammation and tau phosphorylation in healthy ageing and pathology

by

Alexander William Collcutt BSc. (Hons)

Thesis for the degree of Doctor of Philosophy

August 2017

UNIVERSITY OF SOUTHAMPTON

ABSTRACT

FACULTY OF NATURAL AND ENVIRONMENTAL SCIENCES

Biological Sciences

Thesis for the degree of Doctor of Philosophy

THE IMPACT OF SYSTEMIC INFLAMMATION ON NEUROINFLAMMATION AND TAU PHOSPHORYLATION IN HEALTHY AGEING AND PATHOLOGY

Alexander William Collcutt BSc. (hons)

Systemic infections accelerate the progression of neurodegenerative conditions, such as Alzheimer's disease (AD), but reasons for this remain unclear. Previous studies utilising the bacterial mimetic lipopolysaccharide (LPS), suggest that systemic inflammation exacerbates and/or induces proinflammatory processes in the brain. In turn, this results in an imbalance in kinase and phosphatase activity with subsequent pathological hyperphosphorylation of tau - a key neuropathological hallmark of AD. However, these findings have not been corroborated with examples of common bacterial infections.

To address this issue, adult (3-4 month old) wild-type mice were infected with an attenuated strain of the bacterium S. Typhimurium. The bacteria induced a diverse systemic and neuroinflammatory response up to 4 weeks post infection, with the elevation of proinflammatory cytokines such as IFN-γ, IL-1β and IL-6, and microglia phenotype changes including increased FcγRI expression. Cells associated with the cerebral vasculature expressed MHCII while there was evidence of IgG infiltration into the brain parenchyma. While microglial expression of FcγRI and CD11b expression increased following multiple systemic LPS challenges, this model displayed no alterations at the cerebral vasculature and an attenuated central immune response, with only modest elevations in IL-1β and mKC, suggesting the development of endotoxin tolerance. Nevertheless, neither systemic LPS challenge nor S. Typhimurium infection induced tau phosphorylation in adult wild-type mice.

As age is the biggest risk factor for neurodegenerative disease, the effects of these two models of systemic inflammation were investigated in middle-age (11-12 month old) wild-type mice. While a similar peripheral and neuroinflammatory immune profile was observed in the middle-aged and adult mice, a trend suggested S. Typhimurium caused increased tau phosphorylation in middle-aged wild-type mice, 4 weeks post infection. As the opposite trend was observed following multiple LPS challenges, differences between the models, including S. Typhimurium-induced IgG infiltration, may be responsible.

An additional pathological hallmark of AD is the deposition of Aβ protein. Using an aged (16-17 month old) transgenic mouse model that develops extensive Aβ plaque pathology (Tg2576), it was shown that the presence of these deposits induced tau phosphorylation. However, when infected with S. Typhimurium, only the aged non-transgenic mice displayed significantly increased tau phosphorylation with no additional effect observed in the Tg2576 mice. In conclusion, these studies suggest the ageing brain is vulnerable to the deleterious effects of systemic inflammation.

Table of Contents

List of Tables

List of Figures

Declaration of Authorship

I Alexander William Collcutt,

declare that this thesis and the work presented in it are my own and has been generated by me as the result of my own original research.

The impact of systemic inflammation on neuroinflammation and tau phosphorylation in healthy ageing and pathology

I confirm that:

1. This work was done wholly or mainly while in candidature for a research degree at this University;
2. Where any part of this thesis has previously been submitted for a degree or any other qualification at this University or any other institution, this has been clearly stated;
3. Where I have consulted the published work of others, this is always clearly attributed;
4. Where I have quoted from the work of others, the source is always given. With the exception of such quotations, this thesis is entirely my own work;
5. I have acknowledged all main sources of help;
6. Where the thesis is based on work done by myself jointly with others, I have made clear exactly what was done by others and what I have contributed myself;
7. None of this work has been published before submission

Signed: .....

Date:.....

Acknowledgements

First and foremost I would like to thank my supervisors, Prof. Jessica Teeling and Dr. Ayodeji Asuni, for their help and support over the past 4 years. I really appreciate the time and care you have given, not just for my studies, but also my wellbeing during this time. Thank you to Deji for continuing to offer invaluable advice from overseas, especially with the late-evening skype calls. Thank you Jessica for the encouragement and positivity that the PhD required, and putting up with my early morning grumpiness at lab meetings. I have been to some wonderful places and met some great people over the last 4 years, and I was always be grateful for these opportunities. I would like to express my gratitude to The Gerald Kerkut Charitable Trust for funding this project and continued support throughout.

I wish to give massive thanks to everyone who taught me all the methods and techniques I have used in the project, and the friendships along the way. Especially to James Fuller and Ursula Püetener for helping me get started in the lab and Jo Bailey and Matt Davies for their help with Western Blotting. I would like to express my gratitude to the Biomedical Research Facility for their help and advice with animal husbandry and the Biomedical Imaging Unit for the training and support provided for confocal microscopy.

Thanks are also due to Elena Pipi, Joanna Gould, Katie Askew, Gemma Fryatt, Julian Obst, Daniel Cohn, Georgie Dawes, Emilie Simon and Chrysia Pegasiou for always being willingly distracted by inappropriate jokes and any chance to mess with someone's chair, computer or desk. To Matt, thank you for being an adequate soundboard, above average housemate and excellent friend. Thanks also to Renzo for keeping up with English football for 9am recaps, and teaching me everything he knew from 'when he was in Barcelona'.

A special thanks to Paul, without whom I don't think I would have completed the PhD. Thanks for always putting other people's problems above your own and never thinking twice about helping out. Even though your reckless file naming and questionable music taste leave a lot to be desired, thanks for having an equally turbulent journey alongside me.

Lastly, I would like to thank my friends and family. To mum and dad, thank you for always supporting my education and going along with any decisions I made, although you may been under the impression that I would cure Alzheimer's. To Becky, I'm sorry that our holidays were dependant on the life cycles of mice. Thank you for your love, support and understanding over the past 4 years.

Definitions and Abbreviations

AA - Amino acid

ACH - Amyloid-Cascade Hypothesis

ACTH - Adrenocorticotrophic hormone

AD - Alzheimer's Disease

ADCC - Antibody dependent cellular cytotoxicity

ANOVA- Analysis of variance

APC - Antigen presenting cell

APO - Apolipoprotein

APP - Amyloid Precursor Protein

Aβ - Amyloid beta

BBB - Blood brain barrier

BCSFB - Blood-cerebrospinal fluid barrier

BSA - Bovine serum albumin

CAA - Cerebral amyloid angiopathy

CBD - Corticobasal degeneration

CRH - Corticotrophin-releasing hormone

CFU - Colony forming units

CNS - Central nervous system

CP - Choroid plexus

CRP - C-reactive protein

CSF - Cerebrospinal Fluid

CVO - Circumventricular organ

DAB - 3,3 Diaminobenzidine

DAMP - Damage-associated molecular pattern

ELISA - Enzyme linked immunosorbent assay

EOAD - Early-onset Alzheimer's Disease

ERK - Extracellular-signal-regulated kinase

ET - Endotoxin tolerance

FAD - Familial Alzheimer's Disease

FcRn - Neonatal Fc receptor

FcγR - Fc gamma receptor

FISH - Fluorescent in situ hybridization

FTDP-17 - Fronto-temporal dementia and parkinsonism linked to chromosome 17

GFAP - Glial fibrillary acidic protein

GSK3β - Glycogen synthase kinase 3 beta

GWAS - Genome-wide association study

HC - Hippocampus

HPA axis - Hypothalamic–pituitary–adrenal axis

HRP - Horseradish peroxidase

I.C.- Intracranial

IFN - Interferon

IgG - Immuno gamma globulin

IL-Interleukin

iNOS - Inducible Nitric Oxide Synthase

I.P. - Intraperitoneal

ISF - Interstitial fluid

ITAM - Immuno tyrosine activating motif

ITIM - Immuno tyrosine inhibitory motif

I.V. - Intravenous

JNK - JUN N-terminal kinase

kDa - Kilo Dalton

K/O - Knockout

LM - Lipid mediator

LOAD - Late-onset Alzheimer's Disease

LPS - Lipopolysaccharide

LRP1 - Low density lipo-protein receptor 1

LTP - Long term potentiation

MAC - Membrane attack complex

MAP - Microtubule-associated Protein

MAPK - Mitogen-activated protein kinase

MBD - Microtubule binding domain

MCI - Mild cognitive impairment

MHC - Major-histocompatability complex

MMP - Matrix metallo-proteinase

MRI - Magnetic resonance imaging

MTs - Microtubules

MYD88 - Myeloid differentiation primary response gene 88

NFT - Neurofibrillary tangle

NO - Nitric oxide

NSAID - Non-steroidal anti-inflammatory drug

NT - Neuropil thread

nTg - Non-transgenic

OCT - Optimum cutting temperature

PAMP - Pathogen associated molecular pattern

PART - Primary age-related tauopathy

PD – Pick's disease

PRR - Pattern recognition receptor

PBS - Phosphate buffered saline

PET - Positron emission topography

PG - Prostaglandin

PHF - Paired helical filament

PI3K - Phospho-inositol 3 kinase

PLC - Phospholipase C

PSP - Supranuclear palsy

ROS - Reactive oxygen species

RSV - Respiratory syncytial virus

S. Typhimurium - Salmonella enterica subsp. enterica serovar Typhimurium

SCV - Salmonella-containing vacuole

SD - Standard deviation

SF - straight filament

SPM - Specialised pro-resolving mediators

SYK - Splenic tyrosine kinase

TCR - T-cell receptor

TGF - Transforming Growth Factor

Tg - Transgenic

TH1/2 - T helper cell ½

TIR - Toll-interleukin-1 receptor

TNF - Tumour necrosis factor

TLR - Toll-like receptor

T_{reg} - Regulatory T-cell

VRS - Virchow–Robin space

WT - Wild type

Chapter 1: Introduction

1.1 Dementia

Dementia refers to a class of diseases presenting clinically with cognitive deficits such as memory loss, problems with communication and changes in personality. These symptoms are often caused by an underlying neurodegenerative disease whereby neuronal dysfunction and eventual loss affects the mental capacity of the individual involved, often in a progressive nature. According to the 'World Alzheimer Report 2015' (Prince et al. 2015), it is estimated that 46.8 million people are living with dementia worldwide, a figure set to rise to 131.5 million by 2050. In the UK, dementia is thought to be directly responsible for 150,000 deaths a year, although other diseases such as bronchial pneumonia can trigger regression (Prince et al. 2014).

In addition to the frustration, confusion and anxiety felt by an individual living with dementia, the real cost spans further than the patient affected. Individuals require a considerable amount of care as their condition worsens, with help primarily provided by family members or trained carers. In reality, the cost to the UK economy is estimated at £26.3 billion, and with more people diagnosed each year, this figure is likely to rise (Prince et al. 2014).

Age is the greatest risk factor, evident as one third of people over 95 harbour some form of dementia (Prince et al. 2014). Therefore countries that have an ageing population, such as UK, should expect dementia to become an ever increasing healthcare concern (Office for National Statistics 2015).

1.2 Alzheimer's Disease

The most common form of dementia is Alzheimer's Disease (AD), contributing to approximately 60% of all cases in the UK (Prince et al. 2014). It was first described clinically by German neurologist Alois Alzheimer in 1907, who observed deposits of Aβ plaques and tau neurofibrillary tangles (NFTs), in addition to neuroinflammation (Alzheimer 1907). These proteinaceous features spread throughout the brain as neuron loss increases, accompanied by a progressive decline in cognitive function.

AD is further categorised, based on genetics and time of onset. AD occurring before 65 years of age is classed as Early-onset Alzheimer's Disease (EOAD), while disease arising later is referred to as Late-onset Alzheimer's Disease (LOAD) (Bertram et al. 2010). The majority of LOAD subjects are termed 'sporadic' as there is no clear genetic component to the development of the disease. Although not exclusively, cases of EOAD are predominantly of a genetic Mendelian pattern of inheritance, known as FAD (Familial Alzheimer's Disease) and account for 5-10% of AD cases (Lunnon and Mill 2013).

FAD is largely associated with mutations involving critical genes implicated in the processing of the amyloid precursor protein (APP). Mutations have been reported in the presenilin genes (PSEN-1,-2) that cleave APP, as well as the protein itself, leading to the generation of multiple Aβ species, of which Aβ42 is considered to be the most pathogenic and the driver of FAD development (Crouch et al. 2008) (Fig 1.1). Conversely, the A673T (Icelandic) mutation on the APP gene provides significant protection from AD by both decreasing the production of Aβ, along with its propensity to aggregate (Maloney et al. 2014).

As further evidence of APP's involvement in AD, individuals with Down's Syndrome develop similar neuropathology which is a contributing factor to their low mean life-span of 49 years (Yang et al. 2002). This disease is caused by triplication of chromosome 21 (trisomy 21), and associated with this, the replication of gene products which include APP. This increased expression may explain the amyloid-driven development of AD-like pathology (Glenner et al. 1984). These pieces of evidence form the basis of the AD causation theory known as the Amyloid-Cascade hypothesis (ACH).

The original ACH outlined a process in which the deposition of Aβ plaques was thought to be one of the leading events in the pathogenesis of AD (Hardy and Higgins 1992). These neurotoxic plaques were suggested to trigger elevations in neuronal calcium levels, the deposition of tau NFTs and eventual cell death. The theory has since been modified as plaque deposition poorly correlates with cognitive alterations, both in mice and humans (Games et al. 1995; Price et al. 2009). There is now evidence to suggest soluble oligomers of Aβ hold greater toxicity (Glabe 2006), although their mechanism of action remains elusive and controversial (for review see (Kayed and Lasagna-Reeves 2012)).

Based on the evidence from FAD and Down's Syndrome, therapeutics have been developed to target components of the ACH, however, the results have not proved significantly beneficial, and in some cases have been detrimental (for review see (Karran and De Strooper 2016)). One approach has focussed on disrupting secretase activity. Of these, Semagacestat, targeting γ-secretase, reached Phase III, but the trials were terminated following an increased incidence of skin cancer and worsening of cognition in trial participants (Imbimbo et al. 2011).

Other strategies, besides inhibiting key enzymes, have been centred on utilising antibodies and the immune system to remove Aβ. For example, a Phase III trial of the monoclonal antibody Solanezumab was conducted in patients with mild dementia (Doody et al. 2014; Liu-Seifert et al. 2015; Siemers et al. 2016). However, this failed to meet primary endpoints which has led many to further question amyloidocentric therapies and the ACH as a whole. Despite these concerns, numerous trials targeting components of the ACH are still ongoing in patients with mild AD, and the field waits with anticipation for the results (for review see (Karran and De Strooper 2016)). Although the majority agree that targeting AD in the earlier stages of the disease is the correct approach going forward, many believe that shifting focus to other two main pathologies; tau and neuroinflammation, may yield more positive results. It is evident that AD is a multifactorial disease, and a combined therapy targeting all three pathologies may be required to achieve clinically relevant changes.

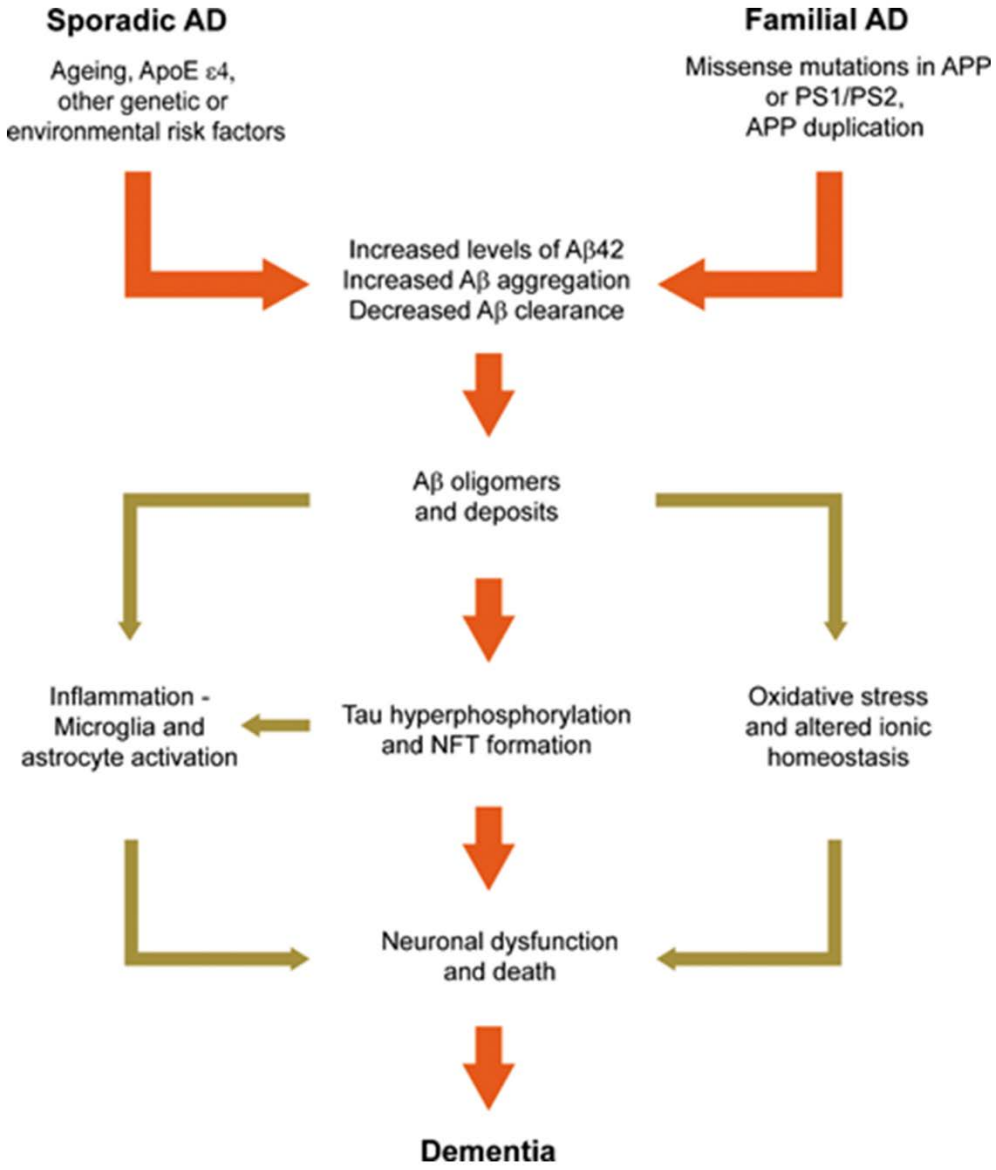

Fig 1.1:- The original Amyloid-Cascade Hypothesis. Familial AD arises from mutations in key genes involved in APP processing, resulting in elevated levels of Aβ42 with an increased propensity to aggregate. Together with decreased clearance, Aβ42 forms into oligomers and amyloid plaques develop. The presence of these deposits induces neuronal stress, causes the hyperphosphorylation of tau and NFT formation and an inflammatory reaction involving microglial activation and gliosis. These preceding pathological events induce neuronal dysfunction and death, before symptoms of dementia arise. Ageing and associated environmental and genetic risk factors e.g. Apoε4, are involved in the development of sporadic AD/LOAD which feeds into a similar pathological sequence as the familial form. Figure adapted from (Philipson et al. 2010).

1.3 Tau

1.3.1 Structure

Under physiological conditions, tau exists as a natively unfolded and highly soluble protein whose role is primarily determined by its association with microtubules (MTs) (Ackmann et al. 2000; Noble et al. 2013). In the neurons where it is primarily found, tau is present at a concentration of approximately 2μM along the axons, although evidence suggests it may also have a role to play within dendrites (Ittner et al. 2010) and at synapses (Pooler et al. 2014).

The alternative splicing of the MAPT pre-mRNA, located at chromosome 17q21.3, gives rise to 6 molecular isoforms of the protein in the human brain. These vary in length and number of amino acids, resulting in different sizes ranging from 45-65 KDa (Buée et al. 2000). Tau protein can be subdivided into 4 regions consisting of the N-terminal projection region, the proline-rich domain, the microtubule-binding domain (MBD) and a C-terminal region. The positive net charge generated from the MBD and adjacent regions in tau is thought to orchestrate its binding to the negatively charged residues in tubulin, which constitute the MTs (Jho et al. 2010). The N-terminal region is thought to bring tau into contact with lipid rafts and other signalling platforms at the cell membrane (Pooler et al. 2012). Tau protein contains multiple phosphorylation sites which are located in the proline-rich domain, a region important in binding the SH3 domains of other proteins such as the tyrosine kinase Fyn (Lee et al. 1998).

Isoforms of tau are distinguished by the numbers of N-terminal (N) and MBD (R) repeats which they contain, with the former determined by inclusion of exon 2 and 3, and the latter by inclusion or exclusion of exon 10 (Morris et al. 2011). While the adult central nervous system (CNS) contains all 6 isoforms, the developing foetal brain only expresses the 0N3R isoform. This is thought to occur as the 3R isoforms bind less efficiently to MTs, important at a time of embryogenesis when dynamic neurodevelopment is required (Hanger et al. 2009). The ratio of 3R:4R isoforms is approximately 1 in the adult CNS, however, this is altered in many diseases where tau exists as the primary pathology (Noble et al. 2013).

Human and mouse tau are highly homologous with 92% sequence similarity shared between the N1 and C terminus. However, differences arise at the N-terminal header, where only 57% sequence similarity is shared (Goedert et al. 1988; Adams et al. 2009). Additionally, mice exclusively express the 4R isoforms of tau in adulthood with only transient expression of 3R tau observed in newborns (Kosik et al. 1989; Takuma et al. 2003; Llorens-Martin et al. 2012).

1.3.2 Function

Evidence suggests tau is a protein with numerous functions (Table 1.1), as it has the capacity to bind a number of entities such as cytoskeletal elements, signalling molecules and lipids. The most extensively studied of these functions is tau's ability to bind the cytoskeleton, with dynamic phosphorylation of the protein regulating its attachment with axons. Binding of tau promotes MT assembly and stabilisation, while aiding reorganisation of the cytoskeleton (Weingarten et al. 1975; Feinstein and Wilson 2005). Interestingly, tau has been shown to interfere with axonal transport *in vitro*, for example, through competition with the motor proteins kinesin and dynein for MT binding (Dixit et al. 2008). However, tau deletion or overexpression in mouse models appears to have limited impact, suggesting mechanisms counteracting this disruption are present *in vivo* (Yuan et al. 2008).

A significant portion of what is known about tau's function has come from studies in tau K/O mice. These mice show no overt pathology, owing to compensatory actions by other microtubule-associated proteins (MAPs) such as MAP1A (Harada et al. 1994). Recent studies do suggest abnormalities in neuronal activity, neurogenesis, iron export and synaptic plasticity (Roberson et al. 2007; Hong et al. 2010; Lei et al. 2012; Frandemiche et al. 2014), however, these studies are controversial as investigations exploring hyperexcitability have only been carried out under pathological conditions such as seizure models (DeVos et al. 2013). Additionally, neurogenesis impairment is dependent on the line of tau K/O mouse utilised (Fuster-Matanzo et al. 2009; Hong et al. 2010). Therefore, although tau's main function of MT assembly and stabilisation is established, further investigation is required into the other roles this protein may possess.

Table 1.1:- Known functions of tau protein (for reviews see (Morris et al. 2011; Wang and Mandelkow 2015)

Function	Reference
Assembly, stability and reorganisation of MTs in axons.	(Weingarten et al. 1975; Feinstein and Wilson 2005)
Interference with axonal transport through competition with motor proteins *in vitro* (not *in vivo*).	(Dixit et al. 2008; Yuan et al. 2008)
Facilitation of axonal elongation and maturation	(Caceres and Kosik 1990; Knops et al. 1991)
Regulation of synaptic plasticity	(Ahmed et al. 2014; Frandemiche et al. 2014; Kimura et al. 2014)
Maintenance of the integrity of genomic DNA, cytoplasmic RNA and nuclear RNA.	(Sultan et al. 2011; Violet et al. 2014)
Regulation of neuronal activity.	(Roberson et al. 2007; DeVos et al. 2013)
Involvement in neurogenesis.	(Fuster-Matanzo et al. 2009; Hong et al. 2010)
Role in iron export.	(Lei et al. 2012)
Facilitation of cytoskeletal stability through interactions with actin.	(Biernat et al. 2002; Whiteman et al. 2009)

1.3.3 Hyperphosphorylation and Toxicity

Phosphorylation has long been considered a critical post-translational modification that tau undergoes, with over 85 potential phosphorylation sites comprising of serine, threonine and tyrosine residues (Noble et al. 2013). By neutralising the positive charge of tau and altering the conformation of the MBD in the protein, kinases phosphorylate tau to induce detachment from the MTs. However, this is a reversible process with phosphatases dephosphorylating tau and allowing reattachment (Jho et al. 2010; Morris et al. 2011).

In addition to altered tau isoform ratios between a developing embryo and adult, the level of phosphorylation at these stages also differs. Together with exclusive expression of the 0N3R isoform, which binds MTs less readily, greater phosphorylation is required at a time when neurons are developing and MTs are dynamically assembling (Hanger et al. 2009). When neurons are fully differentiated in adults, all 6 tau isoforms are expressed and a reduced phosphorylation profile is observed (Noble et al. 2013). There is evidence that phosphorylation varies depending on the location of tau with a gradient of phosphorylation along the axon, and least phosphorylation occurring in the white matter and distal axons (Lovestone and Reynolds 1997).

Although phosphorylation of tau regulates its physiological function: hyperphosphorylation is a key characteristic observed in neurodegenerative diseases such as AD (Grundke-Iqbal et al. 1986). Approximately 1.9 moles of phosphate, per mole of tau, are found in a healthy human brain in comparison to the 6-8 moles of phosphate, per mole of tau, found in abnormal filaments of AD patients (Ksiezak-Reding et al. 1992). It is worth noting that an increase in phosphorylation is not detrimental per se, as it is seen reversibly in hypothermia, hibernation and early foetal brain development as mentioned previously (Spillantini and Goedert 2013). However, a key question that still remains regarding tau hyperphosphorylation is whether site-specific or overall phosphorylation is important in pathological conditions (Crespo-Biel et al. 2012). The majority of phosphorylation sites found in pathological paired-helical filament (PHF) tau are additionally observed in biopsy-derived human tau and normal mouse brain, providing evidence for the latter (Morris et al. 2015). However, there are sites exclusively phosphorylated in AD brain such as Ser214, Ser262 and Ser356, and therefore specific epitope phosphorylation may still be a factor in pathology (Martin et al. 2013).

The first proposed mechanism by which hyperphosphorylation of tau exerts toxicity, is through loss of function (Fig 1.2). Tau is a multifunctional protein and therefore disruption to normal function could conceivably have catastrophic consequences to the neuron, chief of which being the disassembly of MTs. For example, phosphorylation at Ser262, Thr231, Ser235 and Ser396 are all implicated in reducing tau's ability to bind MTs. Phosphorylation of Thr231 causes a *trans*-to-*cis* isomerisation and conformational shift, reducing the affinity of tau for MTs (Hoover et al. 2010). The importance of this post-

translational change is evident as hyperphosphorylated tau has an increased propensity to aggregate *in vitro* (Chohan et al. 2005), while dephosphorylation of soluble tau inhibits polymerisation and restores MT stability (Iqbal et al. 1998).

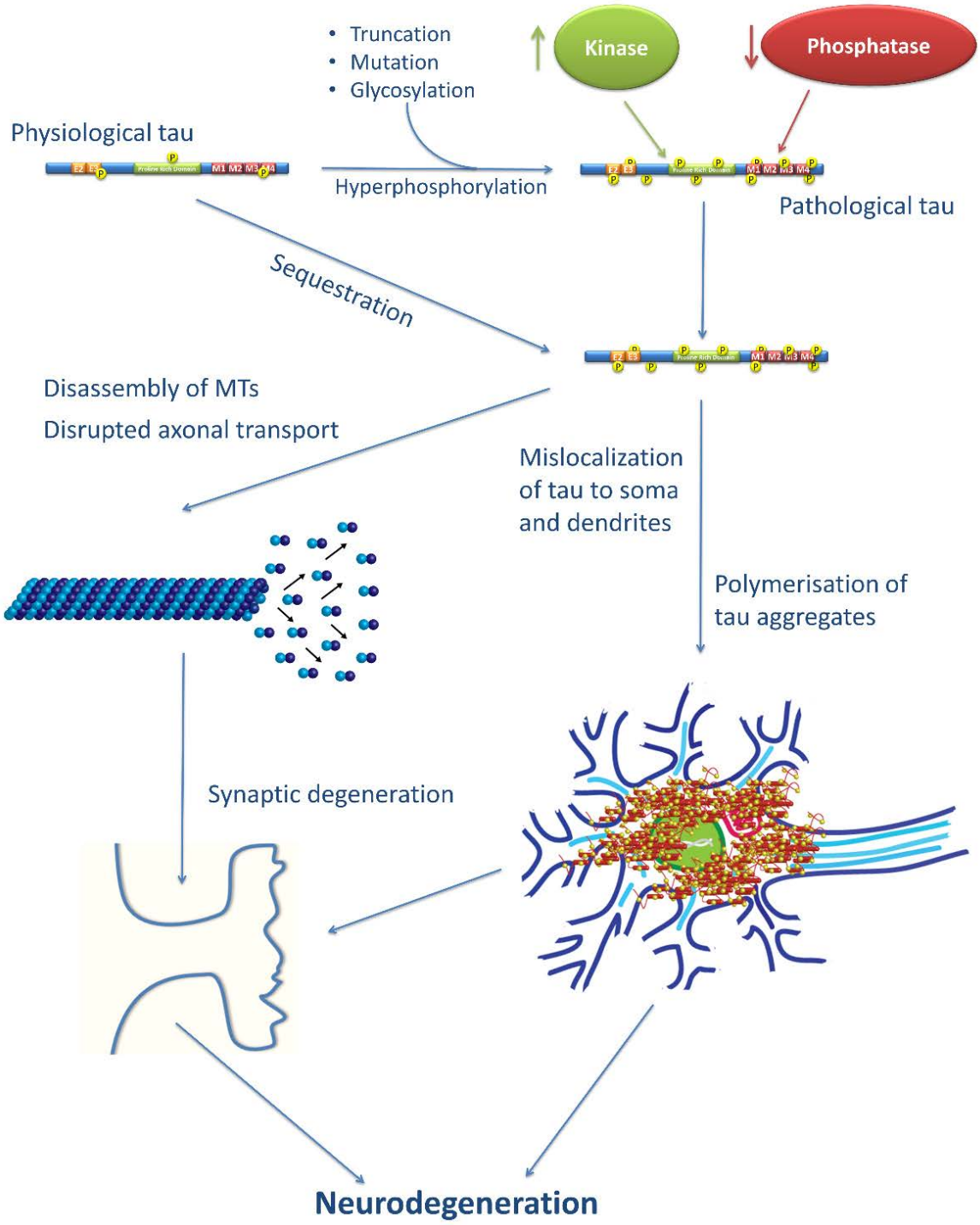

Fig 1.2:- Proposed mechanism of tau toxicity. Tau's toxicity is thought to arise from an imbalance in kinase and phosphatase activity, driving hyperphosphorylation of the protein. Mutations in tau and post translational modifications such as truncation and glycosylation have the capacity to facilitate this process. Loss of tau function results in disassembly of microtubules and disrupted axonal transport, while a toxic gain of function causes mislocalization and aggregation of the tau protein. Additionally, physiological tau and other MAPs are sequestered with the hyperphosphorylated tau. These sequence of events drive synaptic breakdown, before neurodegeneration occurs.

Tau K/O mice have proved useful in gaining insights into tau function and dysfunction. Recent studies suggest these mice show abnormalities in neuronal activity, neurogenesis, iron export and synaptic plasticity (Roberson et al. 2007; Hong et al. 2010; Lei et al. 2012; Frandemiche et al. 2014). This suggests that loss of tau function, which may also occur during hyperphosphorylation, could impact these roles. The lack of overt pathology in tau K/O mice is thought to be due to compensatory actions by other microtubule associated proteins (MAPs) such as MAP2, MAP1A and MAP1B (Harada et al. 1994). With hyperphosphorylated tau unbound from MTs, there is evidence this freely distributed form sequesters both normal tau and other MAPs, leading to disruption of MTs (Alonso et al. 1996; Alonso et al. 2001). Additionally, hyperphosphorylation of tau alters its association with key binding partners such as kinesis-associated protein JUN N-terminal kinase-interacting protein 1 (JIP1), impairing the formation of the kinesis complex (Ittner et al. 2009). Overall these changes compromise axonal trafficking of key cellular components such as the mitochondria, resulting in retrograde synapse degeneration and eventual neuronal loss (Mandelkow et al. 2003).

In addition to MT disruption, hyperphosphorylated tau may induce neurotoxicity through other mechanisms. It has been observed that hyperphosphorylation compromises normal truncation and degradation of tau protein. For example, tau phosphorylation at Ser262 or Ser356 alters recognition by the HSP70-interacting protein-heat shock protein 90 (CHIP-HSP90) complex, thus inhibiting degradation of tau and promoting aggregation instead (Dickey et al. 2007). Early in disease, tau hyperphosphorylation promotes relocalisation of tau from its predominantly axonal location, to the soma and dendrites. Hoover and

colleagues showed this phenomenon in Tg4510 transgenic tau mice, that express mutated (P301L) htau under the CAMKII promoter. (Santacruz et al. 2005). Synaptic dysfunction was observed through loss of AMPA and NMDA receptors (Hoover et al. 2010).

Another major characteristic of the tau pathology seen in neurodegenerative disease is protein aggregation. There is good evidence supporting phosphorylation as a preceding event to aggregation, as hyperphosphorylated tau isolated from human AD brains has the capacity to self-assemble into PHFs *in vitro* (Alonso et al. 2001). Additionally, tau hyperphosphorylation precedes aggregation in AD brains (Braak et al. 1994). In conclusion, it is thought that abnormally hyperphosphorylated tau and other sequestered components aggregate into NFTs consisting of PHFs, twisted ribbons and straight filaments (SFs) that are observed in late-stage pathology (Iqbal et al. 2008).

As has been described in the amyloid field, researchers now also believe that aberrantly aggregated species of tau do not represent the most toxic form of the protein. Firstly, tau aggregates are observed in aged but cognitively normal individuals with a condition known as primary age-related tauopathy (PART). Secondly, it was observed in the inducible Tg4510 mice, that cognitive deficits could be partially ameliorated when gene expression was suppressed. However, NFTs continued to accumulate, supporting the argument that these aggregations were not predominantly responsible for clinical phenotype (Santacruz et al. 2005). Finally, some researchers believe aggregation to be a protective mechanism to contain toxic tau species, as *in vitro* observations indicate that a tau phosphorylation stoichiometry of approximately 4 leads to sequestration while a stoichiometry above 10 results in self-aggregation (Alonso et al. 2004). However, eventually these larger aggregations will reach a point beyond which it is likely that their physical size disrupts normal cellular function and will lead to further neurodegeneration.

Tau can undergo a number of other equally important post-translational modifications such as glycosylation, acetylation, methylation and truncation, which are beyond the scope of the research performed in this thesis. There is evidence that these modifications impact tau hyperphosphorylation and researchers are beginning to investigate whether

any of these changes could represent viable therapeutic targets (for review see (Wang and Mandelkow 2015).

In summary, the hyperphosphorylation of tau is a dynamic phenomenon that occurs during normal brain development, hibernation and hypothermia. However, in chronic neurodegenerative disease, sustained tau hyperphosphorylation appears to induce toxicity in neurons through both a loss of physiological function and toxic gain of function (Fig 1.2). In addition, hyperphosphorylation of tau promotes aggregation of the protein into the late-stage pathology observed in disease. Many researchers suggest these aggregated forms of tau are inert and even a mechanism by which the cells remove toxic oligomers of tau, however, further investigation is required. In any case, the sustained hyperphosphorylation of tau represents an early event in the pathogenesis of neurodegenerative conditions such as AD.

1.3.4 Tauopathies

The tauopathies refer to a subset of neurodegenerative conditions characterised by the accumulation of misfolded and abnormally hyperphosphorylated tau (Goedert and Spillantini 2011). This heterogeneous group of diseases exhibit progressive neuronal loss resulting in a plethora of clinico-pathological phenotypes, often associated with dysfunction in motor (ataxia) and cognitive (dementia) function (Table 1.2).

There have been over 20 different tauopathies described thus far, either observed with tau as the primary pathology or in conjunction with other pathologies such as aggregations of Aβ, known as secondary tauopathies e.g. AD. For a number of years, there was little evidence tau was capable of directly causing etiology and pathogenesis of a neurodegenerative condition until the 1990s when a series of papers showed linkage between a set of diseases of chromosome 17 (Goedert and Spillantini 2000).

Later termed, FTDP-17 (Fronto-temporal dementia and parkinsonism linked to chromosome 17), these conditions showed filamentous pathology primarily consisting of hyperphosphorylated tau, but lacking in Aβ pathology (Goedert and Spillantini 2000). In addition to the fact that the tau gene maps to this region, tau was strongly implicated as a candidate for the FTDP-17 locus. To date 39 mutations in the tau gene have been found in

families with inherited fronto-temporal dementia, demonstrating that tau can be a causative factor in a neurodegenerative disease (Poorkaj et al. 1998; Spillantini et al. 1998; Goedert and Spillantini 2006). These mutations have since been utilised in generating transgenic models of tauopathy (for review see (Frank et al. 2007)).

It is reasonable to suggest that by understanding the mechanisms by which tau drives disease pathogenesis, common pathways and therapeutic opportunities may become apparent, however, the heterogeneity of these conditions and association with other pathologies, imply that this will not be a straightforward task.

1.3.5 Tau Pathology

Although all tauopathies exhibit hyperphosphorylated and insoluble tau aggregates, the precise spread of tau pathology and cells affected in the brain, varies between these diseases. AD is characterised by amyloid-containing plaques, which primarily consist of Aβ, and NFTs, formed largely of hyperphosphorylated tau protein (Fig 1.3). NFTs form intracellularly, filling the cytoplasm of neurons with filamentous tau in the form of PHFs and SFs. Characteristically these can be visualised with silver-staining, highlighting a distinctive 'flame' shape. Bundles of these PHFs and SFs, known as neuropil threads (NTs) also occupy the dendrites and displace much of the cytoskeleton (for review see (Cowan and Mudher 2013)). When a neuron occupied by an NFT has degenerated, extracellular bundles of the tau filaments remain, known as 'Ghost Tangles' (Cowan and Mudher 2013). In contrast to NFTs, these stain ubiquitin more readily than tau, suggesting ghost tangles are subject to considerable proteolysis. In addition to the extracellular diffuse and compact Aβ plaques found in AD, NTs and dystrophic neurites surround Aβ lesions forming neuritic or senile plaques in this disease (Fig 1.3) (Pensalfini et al. 2014).

Another tauopathy, Pick's Disease (PD), is characterised by spherical cytoplasmic inclusions, known as Pick bodies, which are rich in 3R tau and found in the hippocampus, basal ganglia and cortex (Fig 1.3) (Kovacs et al. 2013). Tau inclusions are additionally found in glial cells with tufted astrocytes and astrocytic plaques in progressive supranuclear palsy (PSP) and corticobasal degeneration (CBD) respectively (Yoshida

2014). The range of pathologies found in the tauopathies may partially account for the diverse set of clinical symptoms arising across these diseases.

Table 1.2:- Most prevalent tauopathies and secondary tauopathies. Pattern of dementia, movement disorder, 3R:4R tau isoform and associated genes of tauopathies (*) and secondary tauopathies associated with amyloid deposition (**). Table adapted from (Williams 2006).

Tauopathy	Pattern of Dementia	Movement Disorder	3R:4R	Associated Genes
* **Richardson's syndrome (RS)**	Frontal dysexecutive	Axial rigidity, postural instability, bradykinesia, ophthalmoplegia	1:2–4	MAPT H1
* **PSP parkinsonism (PSP-P) (Progressive Supranuclear Palsy (PSP))**	Late frontal dysexecutive	Asymmetric onset, axial rigidity, tremor, late falls	1:1–2	MAPT H1
* **Argyrophilic grain disease**	Limbic dementia	-	1:2	MAPT H1
* **Corticobasal degeneration (CBD)**	Parietal, frontal dysexecutive	Asymmetric parkinsonism, alien limb	1:2	MAPT H1
* **Pick's disease (PD)**	Frontal dysexecutive, PNFA, SD	Rare	3:1	None
* **FTDP-17**	Frontal behavioural	Symmetric rigidity and bradykinesia, ophthalmoplegia	1:2 1:1 2:1	Multiple mutations/deletions of MAPT
** **Alzheimer's disease**	Amnestic, cortical	Rare	1:1	APP, PS1, PS2
** **Down's syndrome**	Amnestic, cortical	No	1:1	Trisomy 21

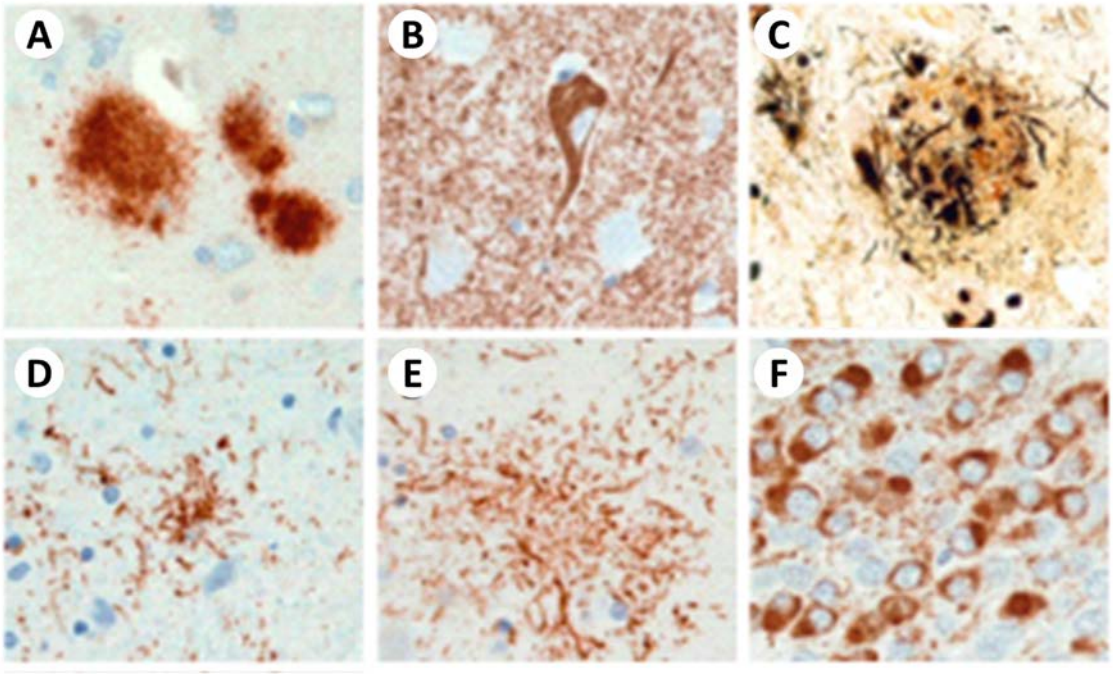

Fig 1.3:- Neuropathologic inclusions observed in tauopathies. Individuals with Alzheimer's Disease (AD) exhibit **(A)** extracellular Aβ plaques, **(B)** neurofibrillary tangles (NFT), composed of abnormal tau fibrils, and **(C)** neuritic (senile) plaques. Abnormal tau aggregates are seen in **(D)** tufted astrocytes from progressive supranuclear palsy (PSP) patients and **(E)** astrocytic plaques from individuals with corticobasal degeneration (CBD). Dense spherical and neuronal cytoplasmic tau inclusions, known as **(F)** Pick bodies, are observed in Pick's disease (PD). Figure adapted from (Murray et al. 2014).

In 1991, Heiko and Eva Braak characterised the spread of pathology in AD, utilising human post-mortem brain tissue. This gave rise to the 'Braak staging' of tau pathology progression (Braak and Braak 1991). Pathology begins with misfolded, hyperphosphorylated, silver-stain negative tau accumulating in the locus coeruleus of the brain stem. Stages 1 and 2, dictating very early symptomatic stages, highlight silver-stain positive tau aggregations confined in the upper layers of the transentorhinal cortex. Stages 3 and 4, clinically diagnosed as mild-cognitive impairment, show a significant involvement of the entorhinal and transentorhinal regions, with the beginnings of pathology evident in the hippocampus and subcortical nuclei. Finally, stages 5 and 6, where AD is in its most advanced phase, are characterised by a wide-spread formation of

tau aggregates stretching to neocortical regions and an exacerbated pathology in regions previously implicated.

Mechanisms responsible for this spread of pathology have been proposed and studies suggest tau may be acting in a prion capacity (for reviews see (Clavaguera et al. 2015; Wang and Mandelkow 2015)). The majority of evidence thus far would point towards a neuron-to-neuron transmission of propagation. For example, Clavaguera and colleagues demonstrated that tau filaments propagate along anatomically connected regions in tau transgenic mice expressing wild-type human tau (ALZ17), injected with brain homogenate from tau transgenic mice expressing mutant human tau (P301L) (Clavaguera et al. 2009). Additionally, it has been reported that tau is released from neurons in an activity-dependant manner and has been found in both interstitial (ISF) and cerebrospinal fluid (CSF) (Pooler et al. 2013; Yamada et al. 2014). However, another mechanism by which tau is thought to spread is through non-neuronal cells such as microglia. Utilising an adeno-associated virus based mouse model of tau spreading, Asai and colleagues demonstrated that microglia have the capacity to transfer tau via exosome secretion, and that depletion of microglia reduces propagation in this model (Asai et al. 2015).

Neuronal cell loss or atrophy is progressive in AD and, similarly to neurofibrillary pathology, the entorhinal cortex and hippocampus are the first to be afflicted (Braak and Braak 1991). Although NFTs are reported to correlate with cognitive decline in AD (Braak and Braak 1991), neuronal loss does exceed NFT numbers by at least one order of magnitude in a number of brain regions (Gómez-Isla et al. 1997). This supports earlier arguments that NFTs are not culpable for widespread neuronal loss, and in fact may be a protective mechanism.

Although the variation and composition in pathology may give clues as to the mechanism of dysfunction in these wide ranging tauopathies, therapeutic intervention must occur at the early stages of the disease before substantial neurodegeneration has taken place. As discussed, substantial evidence points toward tau hyperphosphorylation as one of these earliest events in pathological progression. It is therefore conceivable that the mechanisms determining this event are dysregulated in disease. In this case, investigating

kinase and phosphatase activity may provide the best chance of attenuating tau hyperphosphorylation and subsequent neurodegeneration.

1.3.6 Kinases

Tau phosphorylation is governed by a balance between kinase and phosphatase activity. Among the 85 potential phosphorylation sites, 31 are phosphorylated in physiological conditions, 28 are exclusively phosphorylated in AD brains and 15 are phosphorylated in both. Furthermore, there are an additional 10 putative sites, as yet without an identified kinase, which suggests that although challenging, there is likely to be considerable opportunity to uncover novel AD therapeutics targeting kinases and phosphatases (Martin et al. 2013).

Tau protein kinases can be subdivided in 3 classes (Martin et al. 2013):

1. PDPK (Proline-directed protein kinases):- Target serine or threonine preceding proline residue e.g. GSK3β, CDK5, MAPK, ERK1/2, JNK
2. Non-PDPK:- Target serine or threonine but do not require preceding proline residue e.g. TTBK1/2, CK1, MARK, PhK, PKA, PKB/AKT, PLC, DYRK1A/2, PKN, CamKII.
3. TPK (Tyrosine protein kinases):- 5 tyrosine sites on tau available for phosphorylation by TPKs e.g. SFK (Src), Lck, Syk, Fyn.

Despite several kinases having the capacity to phosphorylate tau, to date only a few have been demonstrated to play a role *in vivo* (Lucas et al. 2001; Noble et al. 2003). However, this is with the caveat that only a few have been thoroughly evaluated *in vivo.* Glycogen synthase kinase-3β (GSK3β) and cyclin-dependent Kinase 5 (CDK5) are highly expressed in the brain and have been observed associating with all stages of NFT development in AD (Pei et al. 1998; Pei et al. 1999). In addition, the Mitogen-activated protein kinases (MAPKs) P38, extracellular-signal-regulated-kinases (ERK) 1/2 and c-Jun-N-terminal kinases (JNK) 1/2/3 all have the capacity to phosphorylate tau and many of these sites are found in AD (for review see (Sergeant et al. 2008)).

Linked with numerous physiological functions such as cell proliferation, apoptosis and survival, these kinases sit within a number of cellular pathways including those related to inflammation (for review see (Medina and Wandosell 2011)). For example, the overexpression of IL-1β in a mouse model of AD has been shown to exacerbate tau phosphorylation, through aberrant activation of P38 and GSK3β (Kitazawa et al. 2011), while IL-6 drives p38 activity through the JAK-STAT signalling pathway (Spooren et al. 2011). Furthermore, GSK3β may provide a link between Aβ and tau hyperphosphorylation (Hooper et al. 2008). In vitro, Aβ peptides promote this latter effect with subsequent apoptotic death in rat hippocampal neurons (Takashima et al. 1996).

In contrast to the PDPKs, the majority of Non-PDPKs only phosphorylate tau at a comparatively small number of sites. However, these are no less important as many of these sites 'prime' the substrate for phosphorylation by other enzymes. This priming involves prior phosphorylation of the substrate at four AAs, C-terminal to the Thr or Ser being phosphorylated. For example, PKA can phosphorylate tau at Ser214, Ser217, Ser396/404 and at Ser416, which increases phosphorylation of tau by PDPKs such as GSK3β (Singh et al. 1995). This demonstrates that the phosphorylation of specific epitopes is likely to be crucial in bringing about an increased phosphorylation profile on tau.

TPKs represent the final class of kinases with the capacity to phosphorylate tau, in this instance targeting tyrosine residues. The kinase c-Abl, whose roles include regulation of apoptosis and cell proliferation, is found to be highly expressed early in NFT formation and its phosphorylation of tyrosine residues on tau may promote further phosphorylation (Tremblay et al. 2010). Hernandez and colleagues found that Aβ stimulated tau phosphorylation at Tyr18 through Fyn in vitro, suggesting a possible link between the two pathologies in AD (Hernandez et al. 2009).

1.3.7 Tau Therapeutics

Disappointing results from more than a decade of Aβ-targeted therapeutics have fuelled the search for alternative targets, and in accord, data from tau-targeted clinical trials are beginning to emerge. Although the precise mechanisms by which tau exerts its toxicity

are uncertain, the different potential possibilities have provided a number of feasible therapeutic strategies. These include targeted treatments to modulate/reduce hyperphosphorylation, protein cleavage, fibrillization and tau expression. Alternative targets include other post-translational modifications, stabilisation of MTs, tau degradation and immunotherapy (for review see (Khanna et al. 2016; Panza et al. 2016).

As discussed, substantial evidence points towards the hyperphosphorylation of the tau protein as a key step in the development of tauopathies. To inhibit this post-translational modification, early therapeutic efforts focussed on inhibition or enhancement of kinase and phosphatase activity respectively. Lithium, a treatment for bipolar disorder, and valproate both inhibit GSK3β and studies in tau transgenic mice have shown a positive reduction in tau pathology (Noble et al. 2005). However, both failed to show statistically positive outcomes when trialled in AD patients (Hampel et al. 2009; Tariot et al. 2011), with adverse side effects also reported in the latter study. Additionally, the GSK3β inhibitor, tideglusib demonstrated no cognitive improvements in a Phase IIb trial involving mild-to-moderate AD patients (Lovestone et al. 2015). CDK5 inhibitor peptide (CIP) has also been shown to be selective for CDK5 and previously demonstrated reduced tau and amyloid pathology, decreased neuroinflammation and a reversal in cognitive decline in transgenic mice (Sundaram et al. 2013). However, as of yet, no human trials are planned for tauopathy treatment.

As previously mentioned, tau undergoes numerous post-translational modifications including O-linked glycosylation. It is thought that this modification competes with phosphorylation on tau, and appears to lower the propensity for oligomers and fibrils to form (Lefebvre et al. 2003). Researchers have aimed to target the inhibition of the O-GlcNAcase (OGA), which removes GlcNAc groups from the tau protein. Preclinical data of ASN120290, suggested reduced tau phosphorylation and fewer paired helical filaments in the tau transgenic P301S mouse model. Phase I trials are underway for ASN120290 (Bowman-Rogers 2017).

The field of tau therapeutics has shown moderate promise with the aforementioned OGA inhibitor and immunotherapy treatments (for review and latest reports see (Panza et al. 2016; Bowman-Rogers 2017). However, many of these treatments suffer from specificity

issues and the complications arising from interference with widespread post-translational modification. Additionally, there were disappointing results reported for LMTX, a methylene blue derivative that inhibits fibrillization (Wischik et al. 1996). The primary endpoints of slowing cognitive and functional decline were not met in a Phase III trial involving patients with mild-to-moderate AD (Gauthier et al. 2016).

1.4 Inflammation

1.4.1 Genetic evidence linking inflammation and neurodegenerative disease

In the first descriptions of AD by Alois Alzheimer in 1907, it was not only the misfolded protein aggregates and neuronal death that were observed. Inflammation was additionally noted, translated as 'glia have produced abundant fibres; concurrently many glia show large fatty sacks' (Alzheimer 1907; Strassnig and Ganguli 2005).

Since then, our understanding of the nature of different glia cell, and what they do has changed dramatically (Heneka et al. 2015). Furthermore, the advances in imaging technology and immunocytochemistry cell staining has fuelled visualisation of neuroinflammation. In AD, resident innate immune cells, such as microglia and astrocytes, can be observed surrounding the proteinacious pathologies of the amyloid plaques and NFTs (Itagaki et al. 1989; Minett et al. 2016). The physiological functions of glia lie in maintaining homeostasis and clearing cellular debris in the brain, however these cells appear overwhelmed during neurodegenerative disease and many researchers believe their chronic activation contributes to pathology and further neuronal death.

Genetic studies have provided further evidence of a critical role for inflammation in neurodegenerative conditions, such as LOAD. Recent genome-wide association studies (GWAS) searching for single nucleotide polymorphisms, data from the LOAD consortium and whole genome sequencing have implicated numerous genes involved in inflammation and immune responses (Table 1.2) (for review see (Lopez Gonzalez et al. 2016)).

Table 1.3:- Examples of genes associated with increased risk of LOAD development and proposed involvement in inflammation (Rosenthal and Kamboh 2014; Malik et al. 2015; Lopez Gonzalez et al. 2016).

Risk gene	Involvement in Inflammation
ATP-bind cassette subfamily A member 7 *(ABCA7)*	Complement response
CD2 associated protein *(CD2AP)*	Transduces inhibitory signalling from ITIM-containing proteins
CD3 molecule *(CD33)*	Inhibits proinflammatory signalling
Clusterin *(CLU)*	Complement response
Complement component 3b/4b receptor 1 *(CR1)*	Complement response
EPH receptor 1 *(EPHA1)*	Regulation of T cell interactions through integrin pathway
Major histocompatibility complex, class II DR β5 *(HLA-DRB5)*	Presentation of immune-peptides
Inositol polyphosphate-5-phosphatase D *(INPP5D)*	Transduces inhibitory signalling from ITIM-containing proteins
Phosphatidylinositol binding clathrin assembly protein *(PICALM)*	Vascular receptor
Phospholipase D family, member 3 *(PLD3)*	Inhibition of Akt signalling
Sortilin-related receptor, L (DLR class) A repeats containing *(SORL1)*	Endocytic modulator of glial-derived neurotrophic factor
Triggering receptor expressed on myeloid cells 2 *(TREM2)*	Expressed on microglia and regulates cytokine production

Although there are still many unknowns as to the involvement of these genes in conditions such as LOAD, the location of the proteins they encode has been of significant interest. TREM2, CD33, CR1 and HLA-DRB5 (MHCII) are all found expressed on or within microglia (Ransohoff and El Khoury 2015). In the next section I will address the characteristics of this cell type and explore how these genes alter microglial function in neurodegenerative disease.

1.4.2 Microglia

Microglia are the resident phagocytic cells of the CNS, maintaining tissue homeostasis via removal of apoptotic bodies (Perry et al. 1985). Microglia represent 6-18% of the total cell population in the human brain parenchyma and 5-12% in mice, but density and morphology do vary between brain regions (Lawson et al. 1992; Mittelbronn et al. 2001). Additionally, human microglia density is higher in the white matter tracts while rodents show greater density in the grey matter (Carson et al. 2006). In the absence of stimulus, microglia exist in a resting state with ramified morphology, characterised by extending processes that survey the microenvironment around them for pathogens and cellular damage (Fig 1.4). Furthermore, this shape is maintained with little overlap between microglial processes (Nimmerjahn et al. 2005).

In comparison to other tissue macrophages, microglia express low levels of many molecules, with some absent altogether (Gautier et al. 2012). Recent transcriptomic studies in murine microglia suggest a unique signature with P2Y12, Hexb and Gpr34 only found in this subset of macrophage (Hickman et al. 2013; Butovsky et al. 2014). The tight regulation of microglia is owed to inhibitory signals sent from other cell types such as neurons. CD200R, C3XCR1 and CD33 are receptors which, when engaged by neural ligands, activate inhibitory pathways within the microglia (for review see (Ransohoff and Perry 2009)).

Microglia express numerous immune receptors which can affect their function. CD11b is an integrin that, together with CD18, comprises the complement receptor 3 (CR3/Mac-1) complex (Doens et al. 2014). Engagement of C3 with complement factor C3, promotes phagocytosis of pathogens. Additionally, the lysosomal marker CD68 is utilised to identify increased phagocytic activity of microglia.

Fc receptors (FcRs) bind the constant domain of immunoglobulins (Igs), with specific types existing for each isotype and sub-class of Ig e.g. FcγRs bind IgG (Swanson and Hoppe 2004; Nimmerjahn and Ravetch 2005). Activation occurs through crosslinkage of Ig in complex with an antigen, with the exception of FcγRI which can bind monomeric IgG. The microglial response induced is dependent on whether the receptor contains the activating immune-tyrosine activation motif (ITAM) domain e.g. FcγRI, or inhibitory immune-

tyrosine inhibitory motif (ITIM) domain e.g. FcγIIB. ITAM signalling results in cellular processes such as proliferation, cytokine release, phagocytosis and antigen presentation, while ITIM signalling is associated with the inhibition of these processes.

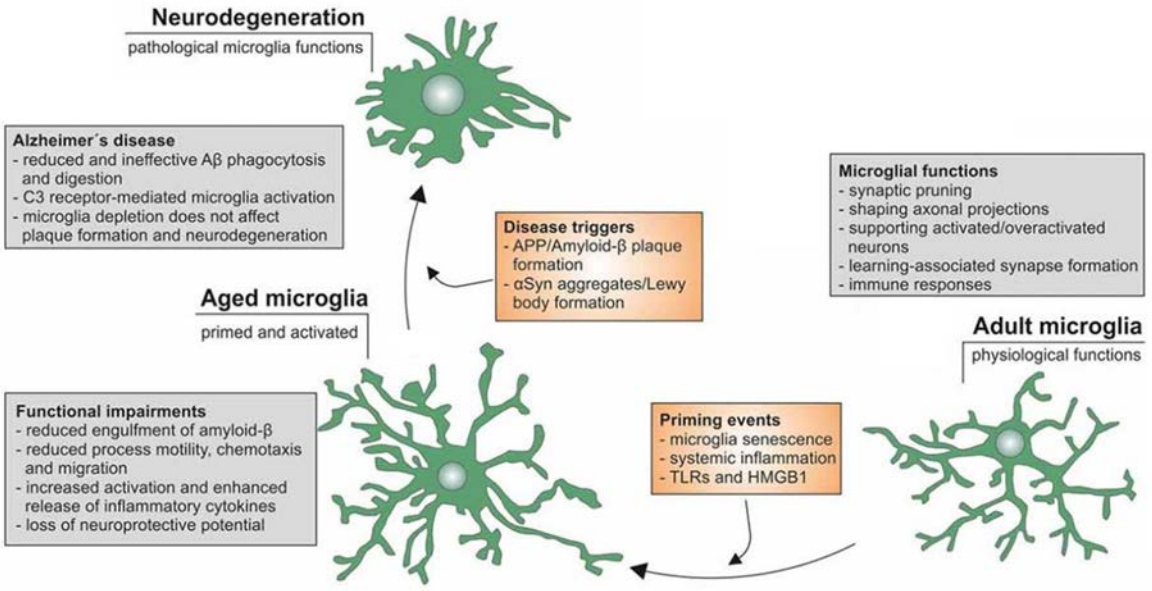

Fig 1.4:- Characteristics and triggers of microglial phenotypes in adulthood, ageing and neurodegeneration. There is evidence that microglia become primed and activated in ageing, with associated functional impairments. Factors such as Aβ deposition trigger a pathological microglial phenotype which is unable to phagocytose and clear plaques in AD. Schematic adapted from (Spittau 2017).

MHCII is associated with the presentation of antigenic peptides to other immune cells, thus facilitating the immune response. Microglia are thought to be the only cell type in the CNS to express MHCII, however there are suggestions it can also be expressed on astrocytes (Hamo et al. 2007). The upregulation of this marker, together with hypertrophic morphology, is considered a characteristic of activated microglia.

Toll-like receptors (TLRs) are a family of pattern-recognition receptors (PRRs) that recognise danger- and pathogen-associated molecular patterns (DAMPS and PAMPs) (Aravalli et al. 2007). There are 12 reported TLRs in mammals which act as the first line of immune defence, triggering an immune response consisting of proinflammatory

cytokines, nitric oxides (NOs) and reactive oxygen species (ROS). In the CNS, they are found upon microglia in addition to other cells types such as astrocytes. The receptors mentioned are only a sample of those reported to be found upon microglia (for more receptors see (Doens et al. 2014; Walker and Lue 2015; Korzhevskii and Kirik 2016)).

When activated, microglia were initially thought to exist in two phenotypic states, in a similar manner to other tissue macrophages. This included a classically activated state, M1, stimulated by exposure to proinflammatory cytokines including IFN-γ, and bacterial antigens such as lipopolysaccharide (LPS) (for review see (Orihuela et al. 2016)). In the early phases of the immune response, M1 polarized microglia secrete proinflammatory cytokines, such as TNFα and IL-1β, together with high expression of inducible NO (iNOS) and ROS. This phenotypic state is additionally characterised by an impaired phagocytic capacity (Gordon et al. 2014).

The alternative activation of microglia, termed M2, represents an anti-inflammatory phenotypic state. Upon exposure to IL-4 or IL-13, microglia produce anti-inflammatory cytokines, growth factors and have an increased phagocytic capacity (for review see (Orihuela et al. 2016)). This state is generally associated with tissue repair, clearance of cellular debris and resolution of the immune response. Further subtypes of the M2 phenotype have emerged with M2b polarisation triggered by FcγRs, TLRs and immune complexes (Anderson and Mosser 2002; Edwards et al. 2006). This results in downregulation of IL-12, increased IL-10 secretion and increased expression of MHCII, FcγRI and FcγRIIA. The M2c phenotypic state is induced by IL-10 or glucocorticoids, and results in increased expression of TGFβ, phingosine kinase (SPHK1) and CD163 (Mantovani et al. 2004). In reality, defining these polarised states has proved difficult as certain molecules, such as cytokines, are expressed in more than one phenotype (Carol A Colton et al. 2006).

1.4.3 Microglia ageing and priming

Ageing is the strongest risk factor for the majority of neurodegenerative diseases, including AD (Lindsay et al. 2002). However, while ageing itself is not considered a disease, the changes and decline that are associated with age put the individual at a much

greater risk of developing disease (Niccoli and Partridge 2012). The immune system undergoes a number of alterations, termed 'immunosenescence', that reduce the capacity to fight infection and increase susceptibility to other diseases (for review see (Gruver et al. 2007)). The decline in the adaptive branch of the immune system is characterised by increased antigenic stress, oxidative stress and incidence of autoimmunity. Changes occurring during immunosenescence include a decrease in naive T-cell population due to thymic diminution, while an increase in memory T-cell population is observed, particularly in the CD8+ T-cell compartment. Overall, these changes result in a loss of T-cell receptor (TCR) diversity and put the aged individual at risk from new infections. Additionally, T-helper type 2 cells (Th2) and T regulatory cells (T_{reg}) from the CD4+ T-cell compartment increase with age and further contribute to inadequate responses to new antigens.

Coupled with an innate immune system that remains largely functional during ageing, the decline of the adaptive branch results in a phenomenon known as 'inflammaging' (Franceschi et al. 2000; Franceschi and Campisi 2014). Inflammaging is characterised by a low-grade chronic proinflammatory state and is thought to develop through continuous antigenic stimulation in ageing (for review see (T Fulop et al. 2016)). These changes to the immune system are implicated in the development of age-related diseases such as diabetes type 2, atherosclerosis, chronic heart failure and neurodegenerative disease.

With regard to microglia, Hefendehl and colleagues showed a modest increase in density and a slower rate of movement when presented with tissue injury in aged mice (Hefendehl et al. 2014). Our lab and others have demonstrated that in ageing, microglia appear to shift to an activated baseline phenotype, characterised by region dependant increases in the expression of CD11b, CD68, F4/80 FcγRI and CD11c (Hart et al. 2012). Additionally, microglia found in the white matter show significantly increased expression of CD11c and FcγRI compared to the grey matter.

An important consequence of ageing on microglia, is the phenomenon of 'priming' (Fig 1.4). This refers to a state whereby microglia respond in an exaggerated manner to an inflammatory stimulus, compared to a microglia that is not primed (for reviews see (Perry and Teeling 2013; Perry 2014)). For example, Godbout and colleagues administered an

intraperitoneal (i.p.) injection of LPS, acting as a second stimulus, to young and aged naive mice and observed changes to cytokine levels and behaviour (Godbout et al. 2005). They found that levels of IL-1β and IL-6 in the aged mice demonstrated a greater increase 4 hours post LPS, than the younger mice. IL-6 remained elevated at 24 hours together with greater social depression and locomotor deficit.

Primed microglia are characterised by an increase in the expression of certain inflammatory markers such as CD11b and MHCII, which have been observed in aged rodents and humans (Streit and Sparks 1997; Frank, Wieseler-Frank, et al. 2006; VanGuilder et al. 2011). MHCII is a useful marker as it is seen to increase specifically on microglia in ageing and is associated with an exaggerated IL-1β response following activation with the inflammatory stimulus LPS (Henry et al. 2009). Additionally, morphological changes in microglia are observed in ageing, with a thickening and deramification of processes (Streit et al. 2004).

A recent meta-analysis of expression data from ageing mice revealed distinct differences from the M1/M2 polarisations produced following LPS and IL-4 stimulation respectively (Holtman et al. 2015). Networking implicated in microglial priming included those related to immune-, phagosome-, lysosome-, oxidative phosphorylation and antigen presentation signalling pathways. Interestingly, the ageing profile shares a significant overlap with a number of disease models including APP/PS1 and ME7 mice, modelling amyloid pathology and prion disease respectively. Therefore, it is reasonable to propose that microglial priming may one reason why age is a risk factor for neurodegenerative disease.

1.4.4 Microglia in neurodegenerative disease

Microglial activation is a hallmark of neurodegenerative conditions such as AD, with this cell type found clustered around Aβ plaques and NFTs (Itagaki et al. 1989; Perlmutter et al. 1992). Microglia have the capacity to bind and phagocytose soluble Aβ oligomers and fibrils through cell surface receptors such as SCARA1, CD36 and TLRs -2, -4, -6 and -9 (Paresce et al. 1996; Bamberger et al. 2003; Stewart et al. 2010). However, as the disease progresses there is continued secretion of proinflammatory mediators from activated microglia, which causes neurotoxicity (for review see (Lull and Block 2010)). Additionally,

these proinflammatory cytokines enhance the transcription of the β-secretase, BACE1, promoting further Aβ generation (Sastre et al. 2006). While microglia may be neuroprotective in the early stages of AD, there is evidence that their phagocytic capacity is reduced with ageing and disease progression (Fig 1.4), leading to the accumulation of Aβ plaques (Floden and Combs 2011; Njie et al. 2012). GWAS studies implicate receptors involved in phagocytosis such as CD33 and TREM2, offering further support to the importance of this process in disease progression (Lopez Gonzalez et al. 2016).

Neuroinflammation is explicitly implicated in the development of tauopathies. Using P301S mutant human tau transgenic mice, Yoshiyama and colleagues observed that microgliosis and synaptic pathology preceded NFT formation in these mice (Yoshiyama et al. 2007). Furthermore, inducing immunosuppression with FK506 attenuated tau pathology and increased the lifespan of these mice, therefore linking neuroinflammation with the early progression of tauopathies. Recent studies have additionally implicated microglia in the spread of tau pathology. Asai and colleagues developed an adeno-associated virus based model which exhibited tau propagation from the entorhinal cortex to the hippocampus in 4 weeks (Asai et al. 2015). They found that by depleting microglia, tau propagation was dramatically reduced. Further *in vitro* studies showed that exosome secretion from microglia was responsible for spreading in this model.

1.4.5 Astrocytes

Astrocytes are another class of glial cell derived from neural stem cells in the neuroepithelium of the CNS. They are characteristically of a ‘star’ shaped formation with processes extending approximately 100µm, making contacts at both the neuronal membrane and vasculature, with end-feet projections onto the endothelial cells and smooth muscle. At the blood-brain barrier (BBB), astrocytes create a physical barrier to the brain parenchyma known as the glia limitans, reducing the infiltration of a number of cells and supporting the reduced permeability of the BBB (Brightman 1991). Pericytes are contractile cells which wrap around the capillaries and venules to modulate blood flow through these structures and offer vital support to the BBB (Peppiatt et al. 2006). In addition to their role in the glia limitans, astrocytes provide metabolites to neurons,

modulate synaptic plasticity and control extracellular ions, neurotransmitters and fluids (for review see (Rossi 2015)).

When activated, astrocytes become reactive (undergo astrogliosis), a phenomenon often characterised by proliferation and up-regulation of Glial fibrillary acidic protein (GFAP) (Balasingam et al. 1994). The degree of this reaction is often dependent on the insult with minor threats quickly reverting back to a resting state with low levels of proliferation, while major insults invoke mass astrogliosis and the formation of a glial scar, with interwoven glial processes to limit further damage. Triggering of astrogliosis typically occurs from contact with proinflammatory cytokines, secreted from damaged cells, microglia, neurons, activated lymphocytes and other astrocytes. For example, TNF-α, in large concentrations, can disturb neural networks by influencing glutamate release (Santello et al. 2011). In a similar manner to microglia, astrocytes express a number of receptors including TLR-2, -3, -4, -5 and -9, who engagement elicits the release of numerous cytokines such as IL-1β, IL-6, IL-10, IFN-γ, TNF-α and TGF-β (for review see (Rossi 2015)).

In ageing, the numbers of astrocytes in human brains does not change (Pelvig et al. 2008; Fabricius et al. 2013), in contrast to rodents where they are reported to increase by 25-40% in the hippocampus and display hypertrophic morphology (Amenta et al. 1998; Mouton et al. 2002). Phenotypic changes include increased expression of GFAP and vimentin, usually associated with increased astrocyte motility and vesicle trafficking (Lepekhin et al. 2001; Cotrina and Nedergaard 2002; Adams et al. 2009; VanGuilder et al. 2011). Functionally, aged astrocytes display reduced neurotransmitter-induced Ca^{2+} signalling, which may impact further neuroactive substance release (Palygin et al. 2010; Lalo et al. 2014). Additionally, the reduced expression of the water channel aquaporin-4 with age may have impact on glymphatic drainage from the brain parenchyma to the CSF (Kress et al. 2014).

Akin to the microglial response in AD, astrocytes are usually found surrounding Aβ plaques, however, they can form their own clusters away from these protein deposits (Nagele et al. 2004; Simpson et al. 2010; Cai et al. 2017). Evidence suggests that alterations in astrocytic reactivity and atrophy occur before onset of symptoms and Aβ

plaque/NFT formation (Heneka et al. 2005; Owen et al. 2009; Carter et al. 2012), supporting the theory that neuroinflammation is an early phenomenon in AD development.

In vitro and *In situ* studies indicate that Aβ oligomers trigger abnormal calcium signalling in astrocytes (Alberdi et al. 2013), a feature observed in astrocytes surrounding amyloid plaques in APP/PS1 mice (Kuchibhotla et al. 2009). In mixed astrocyte-neuronal cultures Aβ-induced Ca^{2+} fluctuations were only observed in astrocytes but still resulted in neuronal death 24 hours after Aβ application (Abramov et al. 2003). Inhibition of Ca^{2+} influx into astrocytes halted these effects.

Dysfunction in astrocytic glutamate regulation is one of the earliest changes observed in AD (Masliah et al. 2000; Soni et al. 2014). In humans, astrocytic uptake of glutamate is mediated via glutamate transporters EAAT1/2 and deficits in these transporters result in overstimulation of neuronal glutamate receptors and excitotoxicity (Maragakis and Rothstein 2004).

Astrocytes also perform numerous and diverse roles in maintaining the homeostasis of the CNS, and creating an effective barrier to the rest of the body. It is therefore conceivable that the changes to this glial cell that occur during ageing, or in the course of a chronic neurodegenerative disease, will have a significant impact in accelerating the pathological processes. Although further investigation is required into the dysregulation of astrocytes in the aforementioned conditions, opportunities to therapeutically intervene may become apparent.

1.4.6 Cytokines and Chemokines

Cytokines are key inflammatory mediators and critical components in cellular communication (Heneka et al. 2015; Bagyinszky et al. 2017). In the CNS, the predominant sources of cytokines are the microglia and astrocytes, secreting proinflammatory cytokines in response to injury and anti-inflammatory cytokines during resolution of the neuroinflammatory response. In agreement with the inflammaging phenomenon, baseline brain proinflammatory cytokine levels such as IL-1β, TNF-α, IL-6, IFN-γ are reported to increase in rodent ageing (Prechel et al. 1996; Tha et al. 2000; Ye and Johnson

2001b; Frank, Barrientos, et al. 2006; Campuzano et al. 2009), while the opposite is observed with the levels of anti-inflammatory cytokines such as IL-10 (Ye and Johnson 2001a; Frank, Barrientos, et al. 2006).

In the 3xTg transgenic mouse strain, mutations in APP, PSEN-1 and MAPT result in the development of amyloid plaques and NFTs (Oddo et al. 2003). When these mice were crossed with IL-1β (XAT) mice, which exhibit sustained IL-1β overexpression, a 70-80% reduction in amyloid load was observed 1-3 months with an associated 4-6-fold increase in plaque-associated microglia (Ghosh et al. 2013). However, IL-1β induces elevated levels of hyperphosphorylated tau at pThr205, Thr231 (AT180) and Ser396/404 (PHF-1) epitopes with evidence of increased activity in the tau kinases GSK3β and p38 MAP kinase. This study highlights the fact that while the progression of neuroinflammatory processes aid the clearance of Aβ, perhaps through microglial phagocytosis, the side effect of chronic inflammation is the hyperphosphorylation of tau protein which may be driven through tau kinase activation. Additionally, despite early beneficial effects in facilitating plaque clearance, neuroinflammatory processes also upregulate the expression of the β-secretase BACE1, causing further Aβ generation (Sastre et al. 2008).

Studies investigating the effects of blocking proinflammatory cytokines, further support their detrimental role in neurodegenerative pathologies. Kitazawa and colleagues administered an IL-1 receptor (IL-1R) blocking antibody to 3xTg mice, finding a reduction in brain NF-κB activation, improved cognitive function, reduced fibrillary Aβ oligomers, reduction in IL-1β and TNF-α levels, and an attenuation in tau hyperphosphorylation (Kitazawa et al. 2011). Similar results have been observed in APP/PS1 mice treated with the TNF-α inhibitor Infliximab, where intracerebroventricular administration resulted in reduced levels of TNF-α, amyloid plaques and tau phosphorylation (Shi et al. 2011). However, when Montgomery and colleagues generated 3xTg mice lacking both TNF-α receptor 1 and 2 (TNF-RI/II), enhanced amyloid and tau-related pathology was observed when compared to age-matched 3xTg mice (Montgomery et al. 2011). Further *in vitro* studies indicated that TNF-α signalling was required in microglial-mediated uptake of Aβ. Similarly, crossing APP/PS1 mice with those deficient in the anti-inflammatory cytokine IL-10 had positive effects on synaptic integrity and cognitive deficit (Guillot-Sestier et al.

2015), demonstrating a complex relationship existing between cytokines and neurodegenerative disease.

1.5 Systemic Inflammation

1.5.1 Environmental evidence linking inflammation and neurodegenerative disease

As discussed previously, chronic neuroinflammation is a hallmark of neurodegenerative disease. Although there are strong indications that the inflammation observed is a reaction to the presence of other key pathologies i.e. Aβ plaques, Tau NFTs and dying neurons, there is also supportive evidence implicating inflammation as a causative factor. For example, GWAS studies consistently link polymorphisms in inflammatory genes to an increased risk of neurodegenerative disease (López-González et al. 2015). Additionally, *in vivo* animal studies reveal that neuroinflammatory changes occur before protein aggregation is observed (Heneka et al. 2005; Yoshiyama et al. 2007; Owen et al. 2009; Carter et al. 2012).

Some of the most persuasive arguments for inflammation's causative role in neurodegenerative disease pathogenesis come from studies of systemic inflammation. Conditions which characteristics include chronic low-grade systemic inflammation and compromised vascular function are often risk factors for neurodegenerative disease. Obesity (Miller and Spencer 2014)), atherosclerosis (Newman et al. 2005), diabetes (Biessels et al. 2006), rheumatoid arthritis (Wallin et al. 2012) and smoking (Anstey et al. 2007) are a few examples which increase the risk of neurodegenerative disease. It is of note that a number of these conditions are present during middle age or the years leading up this point, giving further support to systemic inflammation as a causative factor. Studies in animal models recapitulating these diseases demonstrate similar deleterious consequences to the CNS. For example, wild-type mice fed with a high-fat diet show evidence of increased proinflammatory signalling in the brain such as IBA-1 microglia, GFAP on astrocytes and TNF-α levels (for review see (Miller and Spencer 2014)). Additionally, deficits in learning ability, working memory and spatial memory are observed. In APP mice, high-fat diet caused further memory impairment and increased Aβ oligomer concentrations and deposition (Maesako et al. 2012).

Ageing is the strongest risk factor for neurodegenerative diseases such as AD (Lindsay et al. 2002), and one possible reason for this lies in the development of a chronic low-grade

proinflammatory state, termed inflammaging (Franceschi et al. 2000). The deleterious consequences of systemic inflammation associated with ageing, have been eloquently demonstrated using parabiosis, whereby a shared circulation is established between aged and young mice. Villeda and colleagues reported that young mice show a reduction in neurogenesis, increase in microglial reactivity and reduction in learning memory, while aged mice show the opposite effects (Villeda et al. 2011). Further analysis implicates the chemokine CCL11, which has a role in allergy and parasitic infection, as a prime causative factor in the neurogenesis and cognitive impairments observed. The MHCI component, β-2-microglobulin, is additionally found to be a pro-ageing factor in this context (Smith et al. 2015). In a follow-up study, aged mice were exchanged for APP mice to investigate the impact of young blood on a model of amyloid deposition. Here it was reported that a reversal of synaptophysin and calbindin loss (indicative of cognitive decline) and an improvement in working memory was observed in the APP mice (Middeldorp et al. 2016).

In addition to previous examples, numerous infections over a 4-year period have been shown to double the risk of AD development (Dunn et al. 2005). Furthermore, in a cohort of AD patients, those that were reported to have 1 or more systemic inflammatory events, had a higher rate of cognitive decline (ADAS-COG) with associated increases in serum TNF-α levels (Holmes et al. 2009). Preliminary data suggests AD patients with *Helicobacter pylori* (*H*. pylori) infection have a lower MMSE score, increased plasma proinflammatory cytokine levels and increased phosphorylated-tau levels in the CSF (Roubaud-Baudron et al. 2012).

Periodontitis is a common gum infection that can caused by numerous pathogens including the gram-negative bacteria *Porphyromonas gingivalis* (*P*. gingivalis) (Albandar and Rams 2002). Recently it was reported that in a small study involving individuals with mild-to-moderate AD, those that tested positive for antibodies against *P*. gingivalis, had an increase in cognitive decline (ADAS-cog) over a 6 month follow-up period, independent to baseline cognitive state (Ide et al. 2016). It has been shown that bacterial pathogens such as *P*. gingivalis, promote a systemic proinflammatory state with elevations in factors such TNF-α and C-reactive protein (CRP) (Farhad et al. 2014). Elevations in these inflammatory markers are associated with the development of neurodegenerative disease. For example, increased serum levels of the acute phase protein, CRP, at middle-

age, is associated with heightened risk of dementia (Schmidt et al. 2002; Komulainen et al. 2007).

The benefits of targeting systemic inflammation therapeutically became apparent through early epidemiological studies in the 1990s. McGeer, Rogers and colleagues observed that patients taking non-steroidal anti-inflammatory drugs (NSAIDs) for arthritis, were at half the risk of developing AD compared to the general population (McGeer et al. 1996). Population studies that followed suggested if an individual was older than 55 and showed no signs of dementia, that 2 years of NSAID treatment could cut the risk of developing AD by up to 80% (in 't Veld et al. 2001). Unfortunately, despite these encouraging observations, clinical trials in AD patients presented little clinical benefit (Arvanitakis et al. 2008). Reasons for this have been debated (for review see (Sastre and Gentleman 2010)). One of these may be related to time of intervention, with NSAIDs administered too late in disease progression for clinical benefit. Furthermore, the Alzheimer's Disease Anti-Inflammatory Prevention Trial (ADAPT) studies, have highlighted that the beneficial effects of NSAIDs can differ depending on the type of NSAID and pre-clinical profile, eluding to a dynamic inflammatory landscape (Breitner et al. 2011). Therefore, targeting specific immune pathways may prove more efficacious in the future (Calsolaro and Edison 2016).

1.5.2 The inflammation hypothesis of Alzheimer's Disease

Since the early 1990s, the Amyloid-Cascade Hypothesis (ACH) has dominated as the leading theory on the pathogenesis of AD (Hardy and Higgins 1992). Indeed, as the majority of familial cases of AD are driven by mutations in the processing of the APP gene, the idea that Aβ is a leading event in pathogenesis, is an attractive one. However, conflict arises when trying to fit this hypothesis to the late-onset sporadic form of AD (LOAD). Firstly, numerous elderly individuals show a high plaque burden without any dementia reported (Lue et al. 1996). Secondly, these individuals are reported to have higher brain levels of the proposed toxic form of Aβ, Aβ42, than aged-matched patients with AD (Maarouf et al. 2011). Furthermore, transgenic animal models expressing mutated forms of APP and PS1 do not develop AD-like phenotype (Guo et al. 2012), only recapitulating aspects due to strong expression promoters and combinations of mutations absent from

human disease (Schwab et al. 2004; Simón et al. 2009). Although the ACH has uncovered aspects of AD disease mechanism, particularly in the familial form of the disease, it appears to have also diverted attention away from other key characteristics and pathologies of the disease.

The 'inflammation hypothesis of AD', has been proposed by Dimitrije Krstic and Irene Knuesel as an alternative explanation to the pathogenesis of LOAD. It positions chronic inflammation, aberrant tau and axonal dysfunction as the leading causes of AD (Krstic and Knuesel 2012). The hypothesis developed from theirs and others work demonstrates that systemic administration of the viral mimic PolyI:C to wild-type mice during late gestation, results in the expression of inflammatory cytokines in the foetal brain (Meyer et al. 2006), a reduction in adult neurogenesis with accompanying impairment in working memory (Meyer et al. 2008), and accelerated deposition of aggregated proteins, such as amyloid plaques, in the brains of aged offspring (Knuesel et al. 2009). Furthermore, a second systemic PolyI:C challenge in 12-month old wild-type offspring, is reported to exacerbate phenotype with deposition of APP, Tau aggregation, microglial activation (CD68) and reactive gliosis (GFAP) (Krstic et al. 2012), supporting the previously outlined 'priming' phenomenon. Further evidence for a central role of chronic inflammation in AD development comes from PET imaging of AD patients showing inverse correlation between cognitive status and microglial activation, rather than Aβ load (Edison et al. 2008).

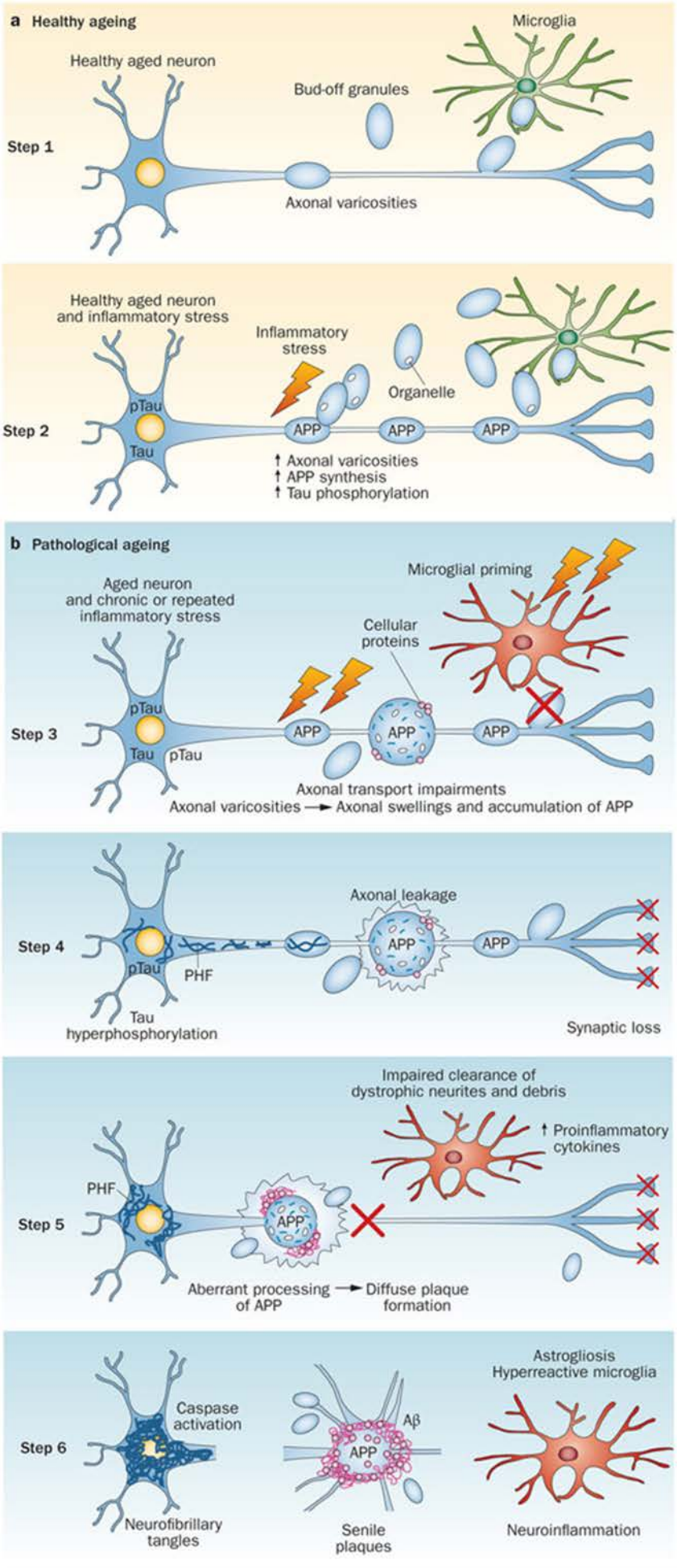
a Healthy ageing
Microglia
Healthy aged neuron
Bud-off granules
Step 1
Axonal varicosities
Healthy aged neuron
and inflammatory stress
Inflammatory
stress
Organelle
pTau
Step 2
APP
APP
APP
Tau
↑ Axonal varicosities
↑ APP synthesis
↑ Tau phosphorylation
b Pathological ageing
Microglial priming
Aged neuron
and chronic or repeated
inflammatory stress
Cellular
proteins
pTau
Step 3
APP
APP
APP
Tau
pTau
Axonal transport impairments
Axonal varicosities → Axonal swellings and accumulation of APP
Axonal leakage
Step 4
APP
APP
pTau
PHF
Tau
hyperphosphorylation
Synaptic loss
Impaired clearance of
dystrophic neurites and debris
↑ Proinflammatory
cytokines
PHF
Step 5
APP
Aberrant processing → Diffuse plaque
of APP
formation
Astrogliosis
Hyperreactive microglia
Caspase
activation
Aβ
Step 6
APP
Neurofibrillary
tangles
Senile
plaques
Neuroinflammation

Fig 1.5:- The inflammation hypothesis of late-onset Alzheimer disease. (1) During healthy ageing, neurons release misfolded or damaged proteins via a 'budding' mechanism, observed as axonal varicosities. (2) Cellular stress and inflammation accelerate this process, while the resulting granules produced are phagocytosed and removed by microglia. (3) In pathological ageing, chronic inflammation induces tau phosphorylation and missorting, destabilising axonal transport and impairing the functional budding mechanism. In parallel, microglial priming and extensive astrogliosis are observed. Additionally, chronic inflammation increases levels of APP which contributes to protein accumulation in the axons. (4) Disturbed energy metabolism and axonal transport facilitates PHF tau formation and these events result in loss of synaptic contacts. (5) Axonal leakage exposes cellular proteins to lysosomal proteinases, promoting formation of neurotoxic peptides. Recruited to remove cellular debris from axons, hyper-activated microglia instead cause additional damage to neurons through release of proinflammatory cytokines and mediators. Senile Aβ plaques begin to form. (6) Caspase activation, resulting from neuritic degeneration, promotes the formation of NFTs. Figure adapted from (Krstic and Knuesel 2012).

Contrary to the toxic role of Aβ outlined in the ACH, Krstic, Knuesel and other researchers believe this protein and APP have physiological and protective functions in responding to neuronal insults (Krstic and Knuesel 2013). Indeed, Aβ has been reported to depress synaptic activity following NMDA receptor activation (Lesne et al. 2005) – perhaps serving to inhibit excitotoxicity, capture metal ions which can reduce oxidative stress (Atwood et al. 2003), and have both anti-inflammatory (Kurnellas et al. 2013) and antimicrobial functions (Soscia et al. 2010). Similarly, APP levels are increased in response to traumatic brain injury, systemic inflammation and IL-1β (Krstic and Knuesel 2013) while APP K/O mice are vulnerable to kainic acid-induced epilepsy and cerebral ischemia (Steinbach et al. 1998; Koike et al. 2012). Therefore, these studies make an argument for APP and Aβ protecting and responding to brain insults respectively. If these insults were sustained, such as in the case of chronic inflammation, or if there were mutations in the processing of APP i.e. familial AD, these protective functions may be lost and neurodegeneration facilitated. The steps of the proposed model are outlined above (Fig 1.5), and evidence for the events can be found in the accompanying review.

In summary, this hypothesis positions chronic inflammation as a causative factor in LOAD, and tau phosphorylation as an early event in its pathogenesis. Indeed, Heiko Braak and

colleagues observed tau-related neuronal changes appearing considerably earlier than amyloid deposition in post-mortem human brains, with half of cases showing abnormal tau protein without the presence of amyloid deposits (Braak et al. 2013). If inflammation-induced tau hyperphosphorylation is an early event in LOAD pathogenesis, identification of the mechanisms involved may be crucial in developing disease-modifying treatments.

1.5.3 Immune-to-brain crosstalk

The theory that the immune system was separate from the CNS, making the latter an immune 'privileged' site, was supported from work in tissue grafts. It was observed that tissue grafts in the brain or eye were maintained longer than other regions of the body, seemingly owing to their avoidance of immune mechanisms (Medawar 1948; Ridley and Cavanagh 1969). This work was supported by differences in features between the CNS and the rest of the body, particularly the discovery of the blood-brain barrier (BBB) (Goldmann 1913).

The BBB is formed from endothelial cells that line the cerebral microvessels, providing optimal chemical conditions for CNS function (for review see (Abbott et al. 2010)). The endothelial cells are joined by tight and gap junctions, and supported by a collagen, fibronectin and laminin-rich basement membrane. Pericytes are embedded within this membrane, and act to regulate microvascular blood flow and angiogenesis among other roles (for review see (Trost et al. 2016)). Astrocytic end-feet surround the endothelial cells, completing the barrier and maintaining homeostasis in nearby cells. Endothelial cells of the BBB contain proportionally more mitochondria compared to other epithelium and are polarised into luminal (blood) and abluminal (brain) sides. These features restrict movement into the CNS and support the concept that a barrier exists between the immune system and the CNS.

Further evidence for the immune privilege theory was the apparent lack of lymphatic vessels draining antigen and immune cells from the brain parenchyma into the peripheral lymph nodes, and the paucity of dendritic cells, limiting antigen presentation in the lymphatic system (Galea et al. 2007). Despite MHCI molecules being expressed on almost all nucleated cells of the body, this appeared to be lacking on immune cells of the eye or

brain (Niederkorn 2006). Cells such as CD8+ T-cells are therefore unable to recognise antigens presented by these cells.

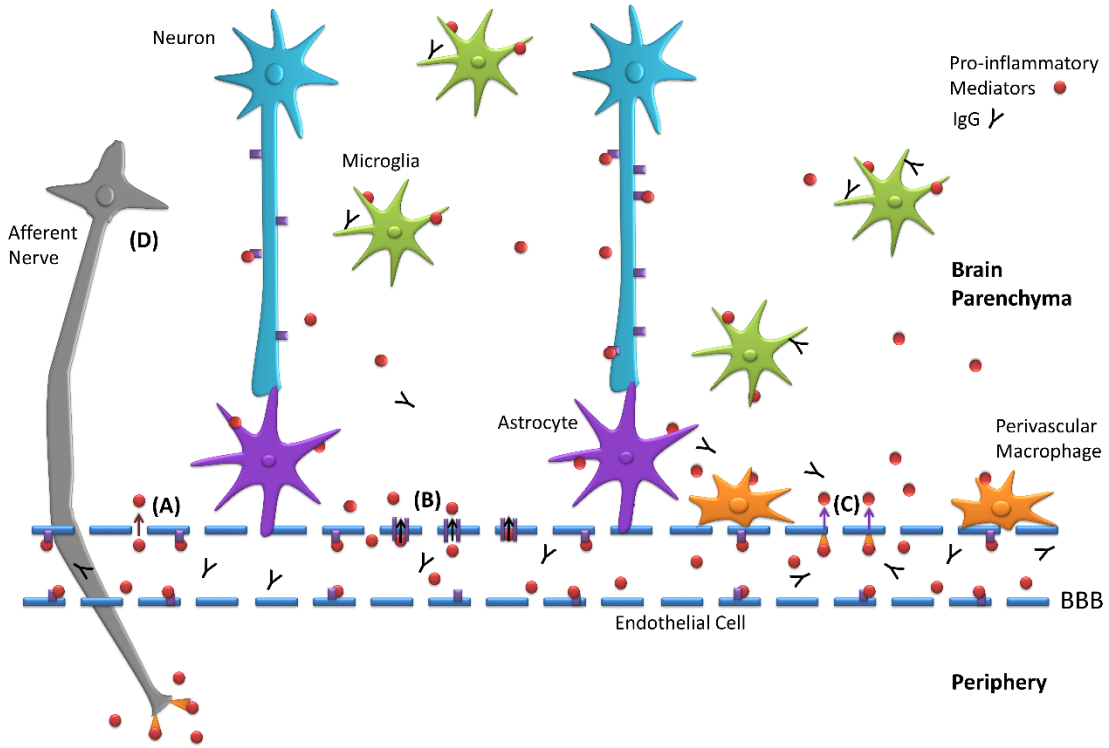

Fig 1.6:- Immune-to-brain communication pathways. (A) Passive diffusion of cytokines across circumventricular organs. (B) Transporters facilitate cytokine movement across the BBB. (C) Direct stimulation of cells of the BBB such as the endothelium cells, resulting in secretion of proinflammatory mediators from this cell type. (D) Activation of afferent nerves in the periphery (e.g. vagus nerve) leading into the CNS. Cells such as microglia, astrocytes and perivascular macrophages propagate inflammatory signals across the brain parenchyma. Figure adapted from (Seruga et al. 2008).

However, evidence has emerged indicating that the CNS is partially, rather than absolutely, isolated from the rest of the immune system (Fig 1.6). Firstly, the BBB cannot be considered impermeable as, in addition to passive diffusion of lipids and the presence of solute carriers, transporters on the endothelium actively transport cytokines such as TNF-α, IL-1α, IL-1β and IL-6 (Banks et al. 1995) along with IgG via neonatal FcγR-mediated endocytosis (neonatal Fc receptor) (for review see (Xiao and Gan 2013)).

The movement of leukocytes across the BBB is complicated and not fully established but it appears as though cells of the immune system can access three anatomical compartments; CSF, meninges and brain parenchyma (for reviews see (Bechmann et al. 2007; Wilson et al. 2010)), with trafficking enhanced in CNS injury and inflammation. Leukocytes access the CSF via the choroid plexus (CP) into the subarachnoid space where it is contained. Migration from the blood directly into the parenchyma requires transport across the BBB and through the perivascular space (Virchow-Robin Space (VRS)).

As pathogens have the capacity to infect the CNS, surveillance is required from the periphery. This monitoring of the CSF occurs at the CP which contains fenestrations and lacks tight junctions within its endothelium. Therefore, it places less restriction on diapedesis of leukocytes. Memory T-cells are at a proportionally greater concentration in the CSF to the blood and activated T-cells have upregulated adhesion molecules facilitating their transport. Access to the brain parenchyma appears to occur preferentially at the post-capillary venules where two neuroinflammatory steps occur to allow leukocyte access (Bechmann et al. 2007). Systemic Inflammation induces upregulation of adhesion molecules such as ICAM-1 on endothelial cells facilitating diapedesis where leukocytes will then reside within the VRS. Expression of CXCL12 on the surface of endothelial cells is responsible for recruiting CXCR4+ T-cells (McCandless et al. 2006). The second step involves movement across the glia limitans, consisting of astrocyte end-feet processes, which may be aided by the presence of macrophages (Babcock et al. 2003). Circumventricular organs (CVOs), which the CP may be classified under, additionally lack the distinctive BBB and permit immune cell trafficking under inflammatory conditions (Schulz and Engelhardt 2005).

An additional route of communication between the periphery and the CNS, relies on direct inflammatory stimulation of the endothelial cells (Fig 1.6). LPS and cytokines trigger intracellular cascades in endothelial cells and perivascular macrophages, which lead to an increase in COX-2 expression and subsequent prostaglandin (PG) release, which propagates neuroinflammation. Experimentally, LPS administration to the periphery of mice has been shown to induce memory deficits and fever, which can be ameliorated with COX-2 inhibition (Jain et al. 2002; Zhang et al. 2003).

LPS and cytokines have also been shown to have direct effects on microglia and perivascular macrophages, stimulating TNF-α release from these cells types (Breder et al. 1994). These inflammatory mediators gain access via passive diffusion through the CVOs, for example the median eminence. TNF-α may then be responsible for increased expression of the LPS co-receptor CD14, propagating a proinflammatory profile across the brain parenchyma (Nadeau and Rivest 2000).

The final means of communication arises from stimulation of the nerves in the periphery (Fig 1.6). Initial findings reported that efferent sympathetic nerve fibres have the capacity to innervate lymphoid organs, with lymphocytes found associating with the nerve terminals (Felten et al. 1985). Later it was shown that this relationship was bidirectional. Systemic LPS and IL-1β administration has been shown to induce sickness behaviours, through what is thought to be afferent vagal nerve stimulation in the periphery, which causes immunological changes in the CNS (Bluthé, Walter, et al. 1994; Bret-Dibat et al. 1995). Subsequently it has been demonstrated that fever induced in this experimental setup is only seen following low and not high dose LPS, suggesting that other pathways discussed, are involved in partially mediating this effect. Since then, a number of other afferent nerves have been implicated in this communication (Roth and De Souza 2001), and further understanding of efferent signalling has emerged from the discovery that efferent vagal nerve stimulation has an anti-inflammatory action, via a cholinergic pathway (Wang et al. 2003). Either directly or indirectly, IL-1 within the CNS is chiefly implicated as the resulting effector from afferent stimulation, as studies have shown that LPS induces IL-1 mRNA expression in locations such as the CVOs and CP (Quan et al. 1998). At the sensory end, IL-1β and PGE2 are implicated in interactions with the vagal afferents and mediating LPS effects (Goehler et al. 1999).

In addition to the sympathetic nerve innervation that can influence the peripheral immune state, the humoral Hypothalamic-pituitary-adrenal (HPA) axis exerts its presence with recruitment of the endocrine system. The pathway follows that initial neuronal activation of the hypothalamus from non-pathological neuroinflammation, results in the release of corticotrophin-releasing hormone (CRH). CRH stimulates adrenocorticotrophic hormone (ACTH) secretion from the pituitary gland into the circulation together with glucocorticoids from stimulation of the adrenal gland. Glucocorticoids have important

anti-inflammatory and immunosuppressive feed-back properties and are exploited as treatment in diseases such as rheumatoid arthritis and multiple sclerosis, characterised by a proinflammatory state. One mechanism suggests transrepression of proinflammatory genes, whereby glucocorticoid receptor engagement inhibits activity of NF-κB and AP-1 (for review see (Coutinho and Chapman 2011)). However, long-term use of glucocorticoids is itself associated with inflammatory-like disease development (Wei et al. 2004), and a number of studies have shown that the more immune cells that become glucocorticoid insensitive, the less sensitive the periphery is to anti-inflammatory feedback and an amplified inflammatory response is observed following peripheral immune activation (Kinsey et al. 2008; Sorrells and Sapolsky 2010). Increased glucocorticoid production occurs from hyper-activation of the HPA axis, and this may occur during neuroinflammation where proinflammatory cytokine levels, such as IL-1β, are increased (Anforth et al. 1998).

1.5.4 Sickness behaviours

Whilst there is substantial evidence that chronic neuroinflammation is detrimental to the CNS, transient forms are considered a beneficial effect associated with induction of fever and 'sickness behaviours' (for review see (Dantzer 2001)). Fever is an adaptive homeostatic mechanism whereby the body's temperature set-point is raised in order to promote immune cell proliferation and attenuate pathogen growth. A 'sickness behaviour' describes a change in motivational state whereby priorities and subsequent behaviours alter to cope with the present infection. These behaviours include lethargy, social withdrawal and reduced food and water intake which may act to disrupt spreading of pathogen between hosts and possibly reduce iron consumption, therefore limiting bacterial replication (Kluger and Rothenburg 1979). The signals for these behavioural changes are mediated by proinflammatory cytokines such as IL-1β, IL-6 and TNF-α which first signal a rapid response through afferent neurons and subsequent slow response through diffusible mechanisms discussed previously. Experimentally this has been seen when IL-1β and TNF-α are injected into the periphery of mice, resulting in decreased social exploration (Bluthé, Pawlowski, et al. 1994).

1.5.5 Immune-to-brain crosstalk in ageing and neurodegeneration

With barriers discussed restricting communication between the CNS and the periphery during life, there is evidence that their integrity is lost with ageing. Observations at the BBB include focal necrosis of the cerebral endothelium, decreased endothelial mitochondrial density, increased pinocytotic vesicles, accumulation of extracellular matrix components in the BBB basement membrane, alterations to astrocytic end-feet, disruption to tight junctions and loss of elasticity associated with vessel wall stiffening (for review see (Gorlé et al. 2016)). Additionally, it has shown that pericytes begin to degenerate and further contribute to the compromised BBB. MRI scans indicate that signs of BBB breakdown in humans, occur first in the hippocampus (Montagne et al. 2015), while mice show increased IgG extravasation in the cortex and hippocampus (Elahy et al. 2015). Age driven changes also occur at the blood-cerebrospinal fluid barrier (BCSFB), an area formed by epithelial cells of the CP. Here, studies have shown an increase in cellular atrophy, shortening of microvilli and the formation of intracellular neurofibrillary inclusions known as Biondi rings (for review see (Serot et al. 2003)).

Disruption of these brain barriers are thought to contribute to the onset and development of neurodegenerative disease. The age-related changes, described previously, are reported to be enhanced in AD patients, with microvascular reduction and neurovascular dysfunction observed (Marchesi 2011). Using Evans blue and albumin assays, it has been shown that APP mice have increased BBB permeability, even before the onset of amyloid plaque deposition (Ujiie et al. 2003). Together with inflammation, it appears a compromised cerebral vasculature is one of the earliest changes in a diseases like AD.

The link between these vascular deficits and AD development, may lie in one of the proteinacious pathologies, Aβ. Firstly, one of the primary roles of CSF is the clearance of toxic entities. A dramatic reduction of CSF turnover is observed in human ageing, and therefore this may contribute to inefficient clearance of Aβ from the brain (Silverberg et al. 2003; González-Marrero et al. 2015). Additionally, BBB expression of Aβ efflux receptors such as LRP1 is reduced during ageing, while the opposite is true for influx receptors such as RAGE (Silverberg et al. 2010). Overall, an increase in parenchymal Aβ

levels contribute to Aβ plaque deposition and cerebral amyloid angiopathy (CAA), while also further damaging brain barriers, as has been reported both in endothelial cell culture and at the BCSFB in mice receiving an intracerebroventricular injection of Aβ42 oligomers (Suhara et al. 2002; Brkic et al. 2015).

As discussed previously, the appearance of amyloid plaques elicits a strong glial response characterised by the secretion of proinflammatory cytokines. *In vitro* modelling of endothelium, demonstrates that cytokines such as TNF-α and IL-6 increase the permeability of this cellular layer with associated decreases in tight junction protein expression (Rochfort et al. 2014). Additionally, soluble and cell-associated forms of these cytokines are reported to be upregulated in isolated brain microvessels from AD patients (Grammas and Ovase 2001).

The barrier deterioration observed in neurodegenerative disease, leaves the CNS vulnerable to systemic inflammation. Takeda and colleagues reported that APP mice, given an i.p. injection of LPS, have elevated levels of proinflammatory cytokines, such as IL-6, in their brain interstitial fluid (Takeda et al. 2013). Additionally, greater sickness behaviours including decreased social interaction and food intake were experienced, compared to wild-type mice. A FITC-labelled albumin permeability assay suggested LPS had caused greater BBB breakdown in the APP mice, compared to wild-type animals, providing evidence that AD pathology leaves this barrier more susceptible to the deleterious effects of systemic inflammation.

An evolution of thought has occurred regarding the crosstalk between the peripheral immune system and the CNS, leading us to a point where we now know they are not separate entities and therefore must be considered together when investigating all aspects of inflammation. The brain is crucial in regulating and providing feedback on peripheral inflammation while the periphery exerts its own influences on the inflammatory state of the CNS. Additionally, both ageing and neurodegenerative compromise the barriers between these two compartments leaving the CNS vulnerable to systemic inflammation. Elucidating the main mechanisms responsible for this deterioration, may provide targets with which to therapeutically intervene.

1.6 Models of Systemic Inflammation

1.6.1 Lipopolysaccharide (LPS)

Lipopolysaccharide (LPS) is the major component of the outer wall of gram-negative bacteria. It consists of an oligosaccharide side chain, providing water solubility, bound to an inner core linker and the main toxic and immuno-modulating component, Lipid A (Raetz and Whitfield 2002). LPS administration provides a useful means of stimulating the innate immune response and investigating the consequences this has to both the periphery and CNS.

LPS, like other bacterial components and pathogens, exerts its immuno-stimulatory effect through structural motifs known as the Toll-like receptors (TLRs), present on cells of the innate immune system (Poltorak et al. 1998). Specifically, LPS acts on TLR-4 along with other known agonists such as respiratory syncytial virus (RSV) and endogenous β-defensin 2 (Lu et al. 2008). Ultimately TLR signalling leads to the production of proinflammatory cytokines and maturation in function of antigen-presenting cells (APCs) (Akira et al. 2006).

Oligomerisation of TLR-4 occurs after recognition of an LPS molecule, leading to recruitment of downstream adapters through the Toll-interleukin-1 receptor (TIR) domains of TLR-4. Two pathways are then engaged, either myeloid differentiation primary response gene 88 (MyD88) –dependent or –independent (for review see (Lu et al. 2008)).

Firstly, the resulting MyD88-dependant signalling leads to the activation of MAPKs mitogen-activated protein kinase (MAPKs) such as JUN N-terminal kinase (JNK), p38 and extracellular-signal-regulated kinases (ERKs). These in turn promote transcription factors such as AP-1, CREB and NF-κB to switch on genes responsible for the production of proinflammatory cytokines such as IL-1β, IL-6 and TNF-α. In contrast, MyD88-independent or TRIF-based signalling results from endocytosis of the TLR-4/LPS complex into endosomes. The resultant signalling produces such factors as type I interferon IFN-β and the anti-inflammatory cytokine IL-10, in addition to late NF-κB activation.

The immune response to systemic LPS has been well characterised in both the periphery and the CNS. A systematic review conducted by Marie-Christine Pardon, found a single peripheral injection of LPS caused elevations of proinflammatory serum cytokines, such as IL-1β, IL-6 and TNF-α, which peaked between 2-6 hours in a dose-dependent manner (Pardon 2015). This was accompanied by acute phase proteins such as CRP, and was closely followed by anti-inflammatory cytokine feedback, with elevations in IL-4 and IL-10 observed. The majority of studies demonstrated that peripheral cytokine levels were back to baseline by 24 hours. Investigations into the neuroinflammatory consequences of peripheral LPS are complicated by the measure of both mRNA and protein at a limited range of time points. Erickson and colleagues measured protein levels of numerous cytokines in both the serum and a hemibrain from wild-type mice, following a single i.p. injection of LPS (Erickson and Banks 2011). It was found that cytokine levels in the serum and brain did not uniformly follow any pattern of upregulation following immune stimulus. For example, IL-6 and mKC followed a similar pattern in both compartments, peaking at 16 hours post injection, whereas IL-1β and TNF-α levels were highest in the brain at the 28 hour time point when serum levels had returned to baseline. This illustrates the differing and dynamic signalling pathways translating immune response from the periphery to the brain.

In attempts to mimic chronic systemic inflammation, researchers have utilised a multiple LPS protocol. Repeated injections of LPS have given mixed results in relation to an immune response in the periphery and brain following subsequent stimuli. High LPS doses (>1mg/kg) or short dosing regimens (4-6 hours) have reported elevated cytokine levels (Erickson and Banks 2011). In contrast, our lab has shown that subsequent LPS administration during the anti-inflammatory phase, at a lower dose (0.5/mg/kg), causes an attenuated cytokine response in the periphery (Püntener et al. 2012). This latter response is indicative of the development of endotoxin tolerance (ET) or hyporesponsiveness, whereby, upon exposure to LPS, a transcriptional shift is observed, primarily in monocytes and macrophages (for review see (Biswas and Lopez-Collazo 2009)). Subsequent challenges of LPS elicit an attenuated immune response compared to initial stimulus, in order to protect the organism from tissue-damaging inflammation.

Whether ET occurs in the brain as well as the periphery, is still unclear. In a similar trend to the periphery, subsequent stimuli in a high LPS dose regimen have been reported to result in an exacerbated cytokine response (Erickson and Banks 2011), while milder doses display the opposite (del Rey et al. 2009). As with ageing and neurodegenerative pathology, there is a suggestion that LPS primes cells in the brain, however further investigation is required, particularly with regard to dosing regimens and time points (Püntener et al. 2012; Pardon 2015).

1.6.2 LPS and Aβ pathology

With strong evidence of systemic inflammation altering neuroinflammatory processes, researchers are curious to ascertain what consequences this may have to the development of neurodegenerative disease. In line with the Amyloid-Cascade hypothesis, some of earliest experiments investigated the effect of LPS on Aβ plaque pathology. In two mouse models of amyloid deposition, APP/PS1 and Tg2576 (Hsiao et al. 1996; Holcomb et al. 1998), it was shown that intracranial (i.c.) injection of LPS caused the clearance of diffuse, but not compact, plaques, 1 week post stimulus (DiCarlo et al. 2001; Herber et al. 2007). This plaque removal was accompanied by microglia activation, as visualised by increases in CD45, CR3, CD68 and MHCII, and all LPS-induced effects were attenuated with systemic administration of the glucocorticoid dexamethasone, used to block microglial activation.

However, other studies have shown the opposite effects of LPS treatment of amyloid pathology. Qiao and colleague administered intracerebroventricular LPS, daily for 2 weeks, to APP mice with the V171F Indiana mutation (Games et al. 1995). This resulted in localised microglial activation and increased amyloid plaques deposition (Qiao et al. 2001). Additionally, weekly administration of i.p. LPS for 12 weeks, to APP^{swe} mice (Borchelt et al. 1997), caused an increase in Aβ+ and APP+ neurons with an associated rise in the number of F4/80+ microglia (Sheng et al. 1996). There is evidence that increases in Aβ pathology from LPS treatment are driven by increased activity of a β-secretase (BACE1) that cleaves and processes APP (Lee et al. 2008). With differences in transgenic model used, route of administration and chronicity of treatment, it is difficult to fully determine the effects of LPS on Aβ. These studies alone suggest acute LPS results

in Aβ plaque clearance while prolonged LPS is responsible for exacerbation of previous pathology, in keeping with evidence implicating chronic inflammation in neurodegenerative disease progression.

1.6.3 LPS and tau phosphorylation

With the link between inflammation and Aβ still unclear and the disappointing clinical trial outcomes from Aβ-targeted treatments, researchers have begun to turn their attention to another pathological hallmark of many neurodegenerative disease, tau. Additionally, this shift has driven investigation into the relationship between inflammation and the development of tau pathology. The first *In vitro* investigations led by Li and colleagues, showed that tau phosphorylation at the Ser202/Thr205 (AT8) epitope was significantly increased in primary rat neocortical neurons co-cultured with microglia, which had previously been activated with LPS (Li et al. 2003). Interleukin-1β and p38 MAP kinase were additionally implicated in these findings, supported by the evidence that inhibitors of these entities attenuated the induced tau phosphorylation. This was one of the first studies to identify a clear sequence of events, starting with microglial activation, microglial cytokine secretion, neuronal tau kinase activation and subsequent tau phosphorylation.

Further *in vivo* studies, conducted in Tg4510 mice, demonstrated that an intracranial injection of LPS exacerbated microglial activation (CD45) and increased phosphorylation at the Ser202/Thr205 (AT8) and Ser396/404 (PHF-1) epitopes of tau, 1 week post administration (Lee et al. 2010). Although phosphorylation of tau had increased, the number of silver-positive neurons, a marker of pre- and mature tangles, had not been significantly altered. This may have been due to the short 1 week time frame between LPS injection and tissue harvesting.

Given that systemic inflammation is a risk factor for neurodegenerative disease, researchers are keen to explore the relationship between peripheral inflammation and tau phosphorylation. Bhaskar and colleagues utilised the htau strain of tau transgenic mice, which are knock-out for mouse tau and knock-in for all 6 isoforms of human tau (Andorfer et al. 2003). These mice demonstrate tau phosphorylation at 3 months, tau

aggregates at 9 months and neuronal loss by 15 months. Intraperitoneal injection of LPS into 2-month old htau mouse induced tau phosphorylation at the Thr231 (TG3) and Ser202/Thr205 (AT8) epitopes (Bhaskar et al. 2010). The role of microglia in tau phosphorylation was demonstrated by crossing htau mice with mice deficient in CXC3CR1. This fractalkine receptor has been shown to play a role in restraining microglial activation and providing neuroprotection. Disruption to this signalling with ageing or neuronal loss is postulated to enhance the microglial activation observed in neurodegenerative disease, although detrimental effects are dependent on disease context (for review see (Lauro et al. 2015)). The crossing of htau and CX3CR1 K/O lines is reported to increase microglial activation, p38 MAP kinase activation and hippocampal tau phosphorylation at numerous epitopes, when compared to age-matched 6-month old htau mice alone. Furthermore, later studies have shown that overexpression of CX3CL1, the CX3CR1 ligand, reduces tau pathology, microglial activation and neurodegeneration in the Tg4510 tau transgenic model (Nash et al. 2013).

The role of chronic systemic inflammation has been modelled using multiple-LPS protocols. In one instance, Kitazawa and colleague utilised the 3xTg transgenic model, which develops both amyloid and tau pathology (Kitazawa et al. 2005). Six weeks of biweekly i.p. LPS to 4-month animals caused elevations in IL-1β, increased numbers of activated microglia (CD45), and exacerbated tau phosphorylation at the Ser202/Thr205 (AT8) epitope. Increased levels of p25, the CDK5 regulator, were additionally observed and subsequent inhibition of this kinase with roscovitine, attenuated the increases in tau phosphorylation. This study implicates CDK5 as a possible transducer of inflammatory mediated tau phosphorylation, however, with multiple doses and observations made long after first insult, other kinase activity cannot be discounted at earlier time points. The same protocol used in 12-month old 3xTg mice showed an interesting shift to a GSK3β mediated increase in tau phosphorylation which could be attenuated with a lithium rich diet (Sy et al. 2011). Tau was also seen to be increased in insoluble fractions following LPS treatment, suggesting that onset of aggregation and pathology was accelerated along with behavioural deficits. These effects were also reversed with a GSK3β inhibitor. These studies are interesting in highlighting that different kinases may dominate tau phosphorylation as disease pathology and/or perhaps ageing progresses. Therefore,

therapeutic intervention may have to be tailored to the staging of neurodegenerative disease.

Furthermore, in both these studies, the multiple LPS protocol did not alter levels of detergent –soluble or –insoluble Aβ, and plaque counts were not altered in the 12-month old mice (Kitazawa et al. 2005; Sy et al. 2011). While the effects of LPS-induced inflammation on Aβ pathology remain unclear, there is growing evidence that inflammation has a detrimental role in the progression of tau hyperphosphorylation and pathology, and may be the driving force in disease progression.

These previous studies suggest LPS-induced systemic inflammation has the capacity to drive tau phosphorylation in transgenic models which are genetically predisposed to develop tau pathology. However, as treatments targeting the later stages of neurodegenerative disease have failed, interest has intensified in earlier intervention and investigations are beginning to explore whether inflammation has the capacity to induce tau phosphorylation, as well as drive it.

Using wild-type mice, it has been demonstrated that acute low-dose LPS (0.1mg/kg) causes transient hippocampal tau phosphorylation at the epitopes Ser396/404 (PHF-1), Ser202/Thr205 (AT8) and Ser422, 20 minutes post injection (Roe et al. 2011). This effect persists at Ser396/404 (PHF-1) for 240 minutes when the final time point was taken. Additionally, increased phosphorylation of tau has been observed at the Ser396 epitope, 12 hours post LPS injection (1mg/kg), with associated activation in the tau kinase CDK5 (Czapski et al. 2016). Studies taken at later time points, report tau phosphorylation occurring 24 hours post injection at the Ser396 and Thr205 epitopes, using high doses of systemic LPS (10mg/kg (Bhaskar et al. 2010), 15mg/kg (Liu et al. 2016)). This set of studies would suggest LPS-induced systemic inflammation has the capacity cause tau phosphorylation, in a dose-dependent manner.

Two studies have investigated tau phosphorylation following multiple LPS challenge in wild-type mice. Kitazawa and colleagues observed increases in tau phosphorylation at the Ser202/Thr205 (AT8) epitope following biweekly injections of LPS (0.5mg/kg) for 6 weeks (Kitazawa et al. 2005), while Gardner et al showed increases at the Thr235 epitope following daily injections of LPS (0.25mg/kg) for 1 week (Gardner et al. 2016).

Both the acute and chronic studies presented here, suggest LPS has the capacity to both induce and drive tau phosphorylation. Mechanistic experiments implicate microglial activation, proinflammatory cytokines and kinase activation as possible mediators in this process and therefore present as promising therapeutic targets.

1.6.4 *Salmonella* Typhimurium

Although LPS protocols provide a practical and reproducible means to investigate the effects of inflammation, this bacterial mimetic largely engages the innate and not the adaptive branch of the immune system. This raises questions as to how well LPS mimics the inflammatory time course of an infection and its translation into human medicine. SL3261 is an example of an attenuated strain of *Salmonella enterica* subsp. *Enterica* serovar Typhimurium (*S.* Typhimurium) (Hoiseth and Stocker 1981). In mice, this serovar induces symptoms similar to human typhoid fever (Santos et al. 2001). However, the insertion of a transposon in the AroA gene restricts virulence and produces a milder disease time course, facilitating experimental investigation in this model (Hoiseth and Stocker 1981).

S. Typhimurium usually invades the body through specialised epithelial cells (microfold cells) found on the luminal side of the intestinal wall. The intracellular bacteria will subsequently infect phagocytic cells such as macrophages and dendritic cells, before escaping apoptosis and entering the circulation (for review see (Mittrucker and Kaufmann 2000)). If injected through the peritoneum, bacteria bypass gut infiltration and begin to colonise organs with large phagocytic populations such as the spleen and liver.

During these first few days of infection, the innate immune system is stimulated, resulting in elevations of proinflammatory cytokines. We, and others have shown the SL3261 strain of *S.* Typhimurium induces a strong peripheral inflammatory response for at least 3 weeks with elevations of IFN-γ, IL-1β and IL-12 observed in the spleen and serum of C57BL/6 wild-type mice (Püntener et al. 2012). This initial response facilitates clearance of bacteria from the blood by phagocytes in the spleen and liver (Dunlap et al. 1991). Macrophages phagocytose the bacteria, aided by antibodies and complement, while the *S.* Typhimurium itself forces uptake to ensure intracellular survival of the pathogen (Muniz-

Junqueira et al. 1997; Ramos-Morales and Francisco 2012). While antigens found on the surface of the bacteria, such as LPS, induce a strong inflammatory response as demonstrated by increases in IL-1β and IL-6, the early production of IFN-γ and TNF-α are crucial in inducing bactericidal mechanisms in macrophages (Nauciel and Espinasse-Maes 1992).

Both *In vitro* and *in vivo* studies support evidence that S. Typhimurium ligands engage numerous TLRs such as lipoprotein (TLR-1/2/6), LPS (TLR-4), flagellin FLiC (TLR-5), CpG-rich repetitive elements in S. Typhimurium DNA (TLR-9) and CsgA (TLR-2), a subunit that forms the biofilm matrix (Broz 2012). Furthermore, once established in the Salmonella-containing Vacuole (SCV) in a cell, NOD-like receptors (NLRs), such as NOD 1/2, interact with RIP2 kinase, a potent activator of NF-κB. Other NLRs, such as NLRC4 and NLRP3, induce the assembly of the inflammasome, a large multiprotein complex ultimately leading to the production of IL-1β and IL-18.

Although, the innate response is paramount in restricting initial growth of *S.* Typhimurium, the adaptive branch is required for elimination. Studies in mice lacking certain components of the adaptive immune system, suggest that Th1-polarised CD4+ T-cells are critical in the clearance of *S.* Typhimurium, while CD8+ T-cells and B-cells play a more modest role (for review see (Pham and McSorley 2015)). By approximately 40 days post infection, the consensus suggests that *S.* Typhimurium is no longer detectable in the spleen and liver (McSorley and Jenkins 2000; Cunningham et al. 2007).

With the SL3261 strain providing a model of prolonged systemic inflammation through engagement of numerous immune pathways, our lab was interested in the consequences this has to the CNS (Püntener et al. 2012). Behavioural testing in C57BL/6 mice demonstrated an acute deficit in burrowing 1-3 hours post infection, however, this returned to baseline by 24 hours, suggesting the effects observed were a consequence of initial endotoxin exposure. With the elevations in serum and spleen proinflammatory cytokines at 1 week, cells present in the cerebral vasculature began to express significant levels of MHCI and MHCII which were maintained for the full 3 week protocol. Vascular cell adhesion molecules V-CAM1 and ICAM-1 additionally showed peak expression at 1 week following infection with SL3261, while evidence of CD68 expression in microglia was

also apparent. The expression of proinflammatory cytokines IL-1β and IL-12, were significantly elevated 3 weeks following infection, suggesting a delayed response when compared to the periphery. In summary, SL3261 infection demonstrates robust inflammation in both the periphery and CNS compartments for at least 3 weeks post stimulus. Interestingly, an additional intracerebral challenge of LPS, 4 weeks post infection with *S.* Typhimurium caused significant increases in brain CD11c and MHCII expression compared to similarly challenged naive mice. This suggests that infections, in addition to ageing and neurodegeneration, may have the capacity to prime immune cells in the brain.

1.6.5 Infections and Aβ pathology

Despite accumulating evidence of infections as risk factors for neurodegenerative disease, experimental studies are limited. The intracellular, gram-negative bacteria *Chlamydia* pneumonia (*C*. pneumonia) has been shown to induce Aβ deposition in the brains of wild-type mice, 3 months following intranasal infection (Little et al. 2004). Additionally, intracranial injections of *S.* Typhimurium have been reported to induce widespread Aβ deposition before plaques are usually observed in the 5xFAD APP/PS1 mouse model (Oakley et al. 2006; Kumar et al. 2016). These two studies suggest that Aβ has antimicrobial functions, and that intriguingly, infections may trigger Aβ deposition in neurodegenerative disease.

Another gram-negative bacteria *Helicobacter* pylori (*H*. pylori), found to reside in the digestive tract, has also been utilised to assess the deleterious effects of systemic inflammation resulting from bacterial infection. Animal studies have shown that wild-type rats, given an i.p. injection of *H*. pylori filtrate, have increased concentrations of Aβ42 in the hippocampus, with associated memory deficits and impairment in spatial learning (Wang et al. 2014). However, Aβ deposition was not demonstrated in wild-type mice (Roubaud-Baudron et al. 2015) using a similar protocol, and further studies are required in AD models.

1.6.6 Infections and Tau pathology

In 2011, Sy and colleagues injected a neuro-adapted strain of mouse hepatitis virus (MHV) into the hippocampus of 11-13 month old 3xTg transgenic mice (Sy et al. 2011). Four weeks post infection, they reported activation of microglia and infiltration of macrophages and t-cells. Furthermore, increased activity of GSK3β was observed together with increased numbers of Ser202/Thr205 (AT8) positive neurons. No changes to Aβ pathology were reported.

Although this study suggests viral infections in the brain have the capacity to drive tau pathology, no studies, as of yet, have assessed whether the systemic inflammation from any bacterial infection is sufficient. The use of LPS to mimic systemic inflammation, has revealed that inflammation arising from the periphery has the capacity to influence tau phosphorylation. However, as LPS poorly replicates the chronic inflammation observed during the time course of an infection, further studies utilising models such as SL3261 (*S.* Typhimurium) would be beneficial for elucidating whether these effects are observed in real-life scenarios.

1.7 Hypothesis and Aims

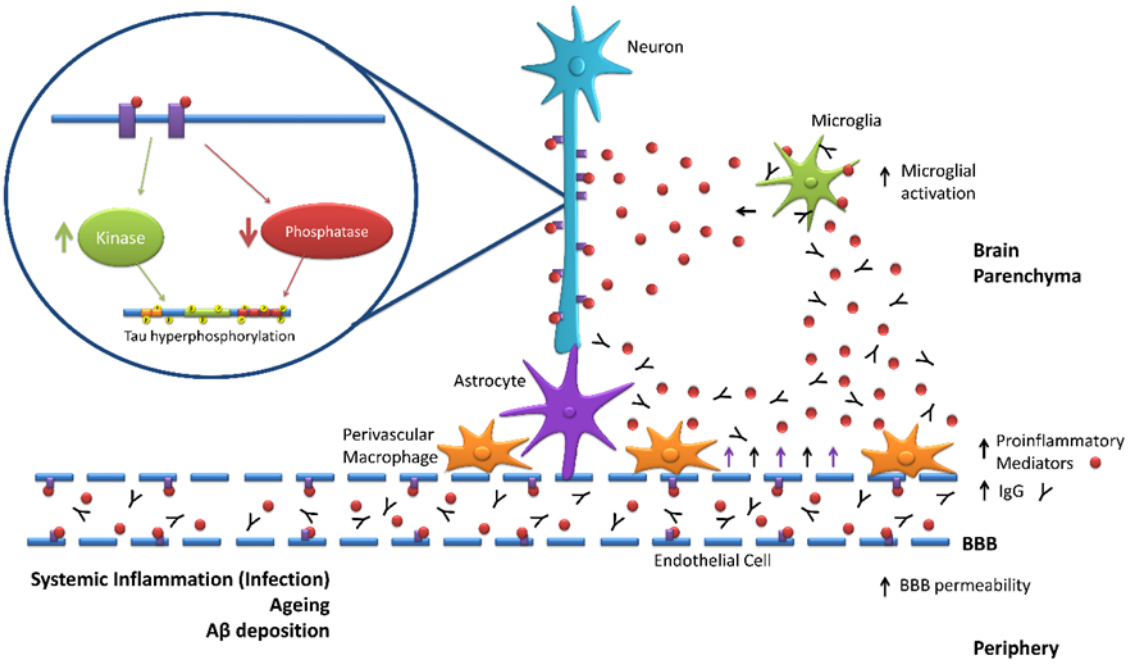

Fig 1.7:- Hypothesis schematic. During systemic inflammation, the levels of circulating inflammatory mediators are elevated and gain access to the brain parenchyma through routes such as the CVOs, transient opening of the BBB and/or *de novo* generation from stimulated endothelial cells. Subsequently, these inflammatory mediators activate innate immune cells of the brain such as the perivascular macrophages, astrocytes and microglia, which themselves propagate proinflammatory signals onto adjacent neurons. Inflammatory pathways in neurons are activated, driving increased and decreased activation of kinases and phosphatases respectively. This imbalance in activity induces tau hyperphoshorylation. Additional risk factors such as ageing and Aβ deposition exaggerate the consequences of this immune-to-brain communication with compromisation of the BBB and 'priming' of the innate immune cells. Therefore, greater tau hyperphosphorylation is observed under these conditions.

There is good evidence that systemic inflammation is a risk for neurodegenerative diseases like AD, but the reasons for this remain unclear. Experimental studies using LPS suggest that inflammatory processes drive tau phosphorylation that could precede tau aggregation and neurodegeneration. One commonly outlined pathway suggests systemic inflammation elicits neuroinflammation through crosstalk mechanisms, such as activation of cells at the BBB. In turn, this inflammation is propagated via activation of microglia and

secretion of proinflammatory cytokines. Due to increased inflammatory mediators and stress, intracellular cascades within neurons drive activation of numerous tau kinases, which subsequently promote the hyperphosphorylation of tau (Fig 1.7). Chronic activation of these signalling pathways eventually leads to the loss of neurons.

Aim 1:- Confirm previous studies suggesting LPS has the capacity to induce tau phosphorylation in adult wild-type mice. Using both single and multiple intraperitoneal (i.p.) injections of LPS, I will ascertain whether acute and/or chronic systemic inflammation in this model increases the levels of tau phosphorylation in the brain. Additionally, I will measure the changes in microglial phenotype and cytokine levels to determine neuroinflammatory signalling that may be responsible.

Our lab has previously shown that LPS protocols poorly replicates the inflammatory time course generated from an infection. As LPS predominately signals through TLR-4 and the innate immune system, numerous inflammatory pathways including those in the adaptive branch are not stimulated. Therefore, there is a need to address the role of real-life bacterial infection in the induction of tau phosphorylation.

Aim 2:- Utilise the SL3261 attenuated strain of *S*. Typhimurium to determine whether systemic inflammation elicited from this bacterium, has the capacity to induce tau phosphorylation in the brain of adult wild-type mice. This will be performed at time points during the peak of the infection and after resolution to determine long term consequences to the brain. Additionally, I will measure systemic and brain cytokine levels, and microglial phenotype changes to elucidate the neuroinflammatory pathways responsible.

The literature suggests neurodegeneration occurs decades before clinical symptoms become apparent. Studies have shown that immune cells of the brain, such as microglia, become ‘primed’ during ageing, whereby a secondary immune stimulus elicits an exaggerated inflammatory response. Furthermore, there is evidence of increased crosstalk between the periphery and CNS in ageing, with possible breakdown of the BBB. I hypothesize that microglial priming during ageing triggers greater microglia activation, proinflammatory cytokine secretion and subsequent tau hyperphosphorylation that is

observed at the earliest stages of neurodegenerative disease. This is facilitated by greater periphery-to-brain communication at middle-age.

Aim 3:- Compare multiple LPS challenge with *S*. Typhimurium infection in middle-aged wild-type mice, to determine whether immune cells in the brain are primed to an immune stimulus. Furthermore, I will investigate whether this phenomenon has the capacity to induce tau hyperphosphorylation at middle-age. I will also measure phenotypic changes of cells at the BBB to ascertain whether increased crosstalk may be contributing to the inflammatory responses observed in the brain.

In AD where Aβ pathology is a hallmark feature, the Amyloid-Cascade Hypothesis positions Aβ dysfunction as an early event in this condition, and perhaps the trigger for pathogenesis. One possible mechanism by which Aβ drives AD, is thought to be through priming of immune cells in the brain. Furthermore, Aβ pathology has been shown to disrupt the structure and function of the BBB, leaving it vulnerable to peripheral inflammation. Therefore, I hypothesize that an immune stimulus, provided by an infection, will gain greater access to the CNS compartment through a compromised BBB. Subsequently this will drive an exacerbated inflammatory response from Aβ-primed CNS immune cells, such as the microglia, promote neuronal stress and stimulate tau hyperphosphorylation.

Aim 4:- Infect a transgenic APP mouse strain, Tg2576, with *S*. Typhimurium to determine whether Aβ deposition evokes an exacerbated response from immune cells such as microglia. Next, I will investigate whether this heightened inflammation drives tau phosphorylation that could be an early event in neurodegeneration. Additionally, I will examine whether Aβ pathology in this model, disrupts the integrity of the BBB which may facilitate deleterious crosstalk between the periphery and CNS.

In conclusion, I aim to show that systemic inflammation, resulting from infection, has the capacity to drive tau phosphorylation in the brain. I believe that additional factors such as ageing and Aβ pathology will lower the threshold for this occur and may represent causative factors in AD (Fig 1.7). By elucidating the predominant mechanisms, I aim to identify signalling pathways to therapeutically target before neurodegeneration has taken place.

Chapter 2: Materials and Methods

2.1 *In vivo*

2.1.1 Animals

Mice were housed in plastic cages with sawdust bedding in groups of 5 to 10. The housing room was temperature controlled (19-23°C) with a light-dark cycle (12h:12h with light on at 0700 h). Food (standard chow, RM1, SDS, UK) and water were available *ad libitum* during housing. All procedures were performed in accordance with the United Kingdom Home Office Licensing Inspectorate and after local ethical approval. Home office project license 30/3057 was used for all in house experiments. C57BL/6 mice were obtained from Charles River (Margate, UK) and bred in house. Adult (3-4 month old) female C57BL/6 mice were used in chapters 3-5. Middle-aged (11-12 month old) female C57BL/6 mice were used in chapter 5. Aged (16-17 month old) female and male Tg2576 mice were used in chapter 6 (Hsiao et al. 1996). For the breeding of the Tg2576 mice, hemizygous male transgenic mice were purchased from Taconic (US) and shipped to the Southampton biomedical research facility. The mice were re-derived into a clean animal facility and male offspring bearing the APP transgene were selected. Transgenic male mice were bred with wild-type SJL females producing offspring with a 50% chance of possessing the transgene. Next, transgenic male offspring were bred with gamma-chain deficient females on a BALB/c background (Murinello et al. 2014). Heterozygous gamma-chain deficient offspring with (transgenic mice) and without (non-transgenic mice) the APP transgene present were used in chapter 6 experiments. All breeding was carried out by BRF staff and genotyping was performed by Dr. James Fuller. Brain tissue from 12 month old transgenic Tg4510 tau mice (Santacruz et al. 2005) was kindly provided by Dr. Ayodeji Asuni at Lundbeck for optimisation of tau antibodies.

2.1.2 Intraperitoneal injection of lipopolysaccharide (LPS)

Mice were challenged with i.p. injections of Lipopolysaccharide (LPS, 0.5mg/kg) derived from *Salmonella abortus equi* (L5886, Lot:034M4022V, 3000000 EU/mg, Sigma, Poole

UK). This dose was selected to best replicate methods used by Kitazawa and colleagues (Kitazawa et al. 2005). Control animals received an intraperitoneal (i.p.) injection of 200µl sterile saline (Southampton General Hospital, Hampshire, UK). In chapter 3, mice challenged with single LPS received 1 i.p. injection of LPS (0.5mg/kg) and were sacrificed 24 hours later. In chapter 3, mice received 16 i.p. injections of LPS (0.5mg/kg) or 200µl sterile saline, over an 8 week period. In chapter 5, mice received 8 i.p. injections of LPS (0.5mg/kg) or 200µl sterile saline, over a 4 week period. In chapter 5, an additional group, termed 'single LPS', received 1 i.p. injection of LPS followed by 7 i.p. injections of 200µl sterile saline, over a 4 week period. Mice were injected at 11am every Monday and Thursday. Body weight was recorded both before and 24 hours post injection. Mice were sacrificed 24 hours after the final injection.

2.1.3 Infection with *Salmonella* Typhimurium

Mice were randomly assigned to one of two groups, saline or *S*. Typhimurium and relocated into a Containment Level 2 (CL2) facility, 3 days before infection, for acclimatisation. Mice were housed in plastic cages with sawdust bedding in groups of 5. The housing room was temperature controlled (19-23°C) with a light-dark cycle (12h:12h with light on at 0700 h). Food (standard chow, RM1, SDS, UK) and water were available *ad libitum* during housing. Mice were injected with 200µl of sterile saline (Fannin, UK) or $1x10^6$ CFU of the aroA attenuated strain *Salmonella enterica* subsp. *enterica* serovar Typhimurium (*S.* Typhimurium*,* SL3261) (Hoiseth and Stocker 1981). Body weight was recorded daily for 1 week after infection, weekly for a total of 4 weeks, and monthly thereafter for 8 and 24 weeks, before sacrifice and tissue collection.

2.1.4 Nesting behaviour

Nesting protocol and scoring was performed as described previously (Deacon 2006). Mice were moved into individual cages 1 hour before the beginning of the dark cycle, 1 day prior to sacrifice. Cages consisted of a 0.5cm covering of sawdust and centred 5cm x 5cm square of cotton wadding (nestlet, LBS Biotech, Horley, UK). No other environmental enrichment was present, however food and water were available *ad libitum*. During dark

cycle, mice tore up nestlet to construct nest. The nests were assigned scores the next day based on the following criteria.

1. Nestlet more than 90% intact.
2. Nestlet partially torn (50-90% intact), no nest site.
3. Nestlet mostly torn (greater than 50%), no nest site.
4. Nestlet mostly shredded, and there is a defined nest site in one quarter of the cage. Nest walls are lower than a mouse laying on its side in more than 50% of total nest circumference.
5. A near perfect nest using >90% of the nestlet and positioned in one corner of the cage. Nest walls are as tall as a mouse laying on its side for more than 50% of total nest circumference.

Nests exhibiting characteristics of two scores were awarded marks of 0.5. Assessor was blinded to experimental groups.

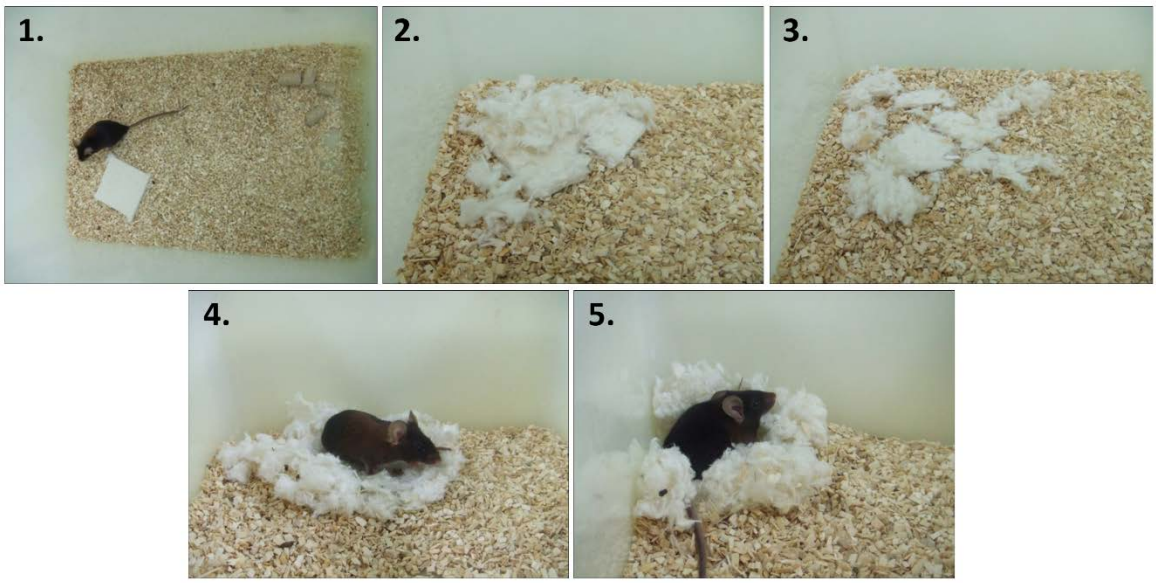

Fig 2.1:- Example nests and scores. Image adapted from (Deacon 2012).

2.2 Tissue harvesting

2.2.1 Perfusion

Mice were terminally anaesthetised with an 0.5ml i.p. injection of 2,2,2'-tribromoethanol crystals (25g) in tertiary amyl alcohol (15.5ml) (Tribromoethanol (*Avertin*) for Rat). The thoracic cavity was opened, an incision was made in the right atrium and blood was collected (0.5-1ml) for later analysis of serum. Next, transcardial perfusion with 5U/ml heparin (Southampton General Hospital Pharmacy) in 0.9% saline, was performed.

2.2.2 Brain dissection

Brain tissue was immediately dissected post perfusion and separated at the midline with a sagittal incision. The right hemisphere was embedded in optimal cutting temperature (OCT, medium Fischer Scientific, UK) and frozen on isopentane (Thermofisher, Leicestershire, UK) for later immunohistochemistry studies. A hippocampal punch was taken from the left hemisphere for enrichment of this brain region, before being frozen in liquid nitrogen for later biochemical (western blot, immunoassay) analysis.

2.3 Immunohistochemistry

2.3.1 Immunohistochemistry

Frozen hippocampal sections were cut in a coronal plane at 10µm on a cryostat (Leica 3050S) and mounted on APES-coated (3-aminopropyltriethoxysilane) slides before storage at -20°C. Sections were dried and post fixed in absolute alcohol (4°C) for 15 minutes, before quenching endogenous peroxidase activity with 1% H_2O_2 (Sigma, Dorset, UK) in 1X Phosphate-buffered saline (PBS) for 10 minutes. Blocking of non-specific binding of antibodies occurred in 1X PBS containing 2% Bovine Serum Albumin (BSA, Thermofisher, Leicestershire, UK) and 10% normal animal serum (dependent on species of secondary antibody host) for 1 hour at room temperature. Sections were incubated with primary antibody (Table 2.1) overnight (18 hours, 4°C). The following day, sections were incubated at room temperature (RT) for 1 hour with biotinylated secondary antibody (Table 2.2) before incubation with Avidin-Biotin Peroxidase complex (ABC, Vector Labs, Peterborough, UK) according to manufacturer's instructions. Briefly, 1 drop of reagent A (Avidin DH) and reagent B (biotinylated horseradish peroxidase H) was added to 5ml of 1X PBS, vortexed for 1 minute and allowed to stand at RT for 30 minutes before application to tissue sections for 30 minutes. Binding of antibody was detected using DAB (3,3'-diamobenzidine) as the chromogen (Sigma, Dorset, UK), catalysed by 0.015% H_2O_2 and made in 0.1M Phosphate-Buffer. Sections were counterstained with haematoxylin, dehydrated and coverslipped.

2.3.2 Immunofluorescence protocol

Frozen hippocampal sections were cut in a coronal plane at 10µm on a cryostat (Leica 3050S) and mounted on APES-coated (3-aminopropyltriethoxysilane) slides before storage at -20°C. Sections were dried and post fixed in absolute alcohol (4°C) for 15 minutes, before blocking of non-specific binding of antibodies with 2% Bovine Serum Albumin (BSA, Fisher Scientific, Loughborough, UK) in 1X PBS, and 10% normal animal serum (dependent on species of secondary antibody host) for 1 hour at room temperature. Sections were incubated with primary antibody (Table 2.1) overnight (18 hours, 4°C). The following day, sections were incubated in darkness at RT for 1 hour with

fluorescently conjugated secondary antibody (Table 2.2). Sections were incubated with 4',6-diamidino-2-phenylindole (DAPI (1 in 2000), D9542, Sigma, Dorset, UK) diluted in 1X PBS for 5 minutes. Slides were coverslipped with Mowiol 4-88 (81381, Sigma, Dorset, UK) containing 2.5% DABCO (1,4-diazabicyclo(2.2.2)octane, Sigma, Dorset, UK) for fluorescence enhancement.

Table 2.1:- Primary antibodies used for immunohistochemistry, immunofluorescence and western blot.

Primary Antibody	Antibody Details	Clone (Catalogue No.)	Distributor	Optimal Concentration / Method
FcγRI	Rat α mouse mAB	AT152-9	Cancer Sciences, Southampton, General Hospital, UK	1:500 (IHC/IF)
CD68	Rat α mouse mAB	FA-11 (MCA1957)	Bio-Rad (formerly AbD Serotec, Oxford, UK)	1:500 (IHC/IF)
CD11b	Rat α mouse mAB	5C6 (MCA711)	Bio-Rad (formerly AbD Serotec, Oxford, UK)	1:500 (IHC/IF)
MHCII	Rat α mouse mAB	M5 (114.15.2)	eBioscience (Thermofisher, Leicestershire, UK)	1:500 (IHC/IF)
Aβ	Mouse α human mAB	3D6 (recombinant IgG2a)	In house (Made by Dr. James Fuller)	1:1000 (IF)
Laminin	Rabbit α mouse mAB	L9393	Sigma (Dorset, UK)	1:2000 (IF)
pSer396	Rabbit α mouse pAB	Poly8074 (807401)	Biolegend (California, US)	1:2000 (WB)
pThr205	Rabbit α mouse pAB	Poly8069 (806901)	Biolegend (California, US)	1:1000 (WB)
Total tau	Rabbit α mouse pAB	K9JA (A0024)	Dako (California, US)	1:10,000 (WB)

Table 2.2:- Secondary antibodies used for immunohistochemistry, immunofluorescence and western blot.

Secondary Antibody	Antibody Details	Catalogue Number	Distributor	Optimal Concentration
Rabbit anti-rat IgG	Biotinylated	BA-4000	Vector Laboratories (Peterborough, UK)	1:100 (IHC)
Goat anti-rabbit IgG	Alexa Fluor 488	A-11008	Thermofisher (Leicestershire,UK)	1:500 (IF)
Donkey anti-rat IgG	Alexa Fluor 488	A-21208	Thermofisher (Leicestershire,UK)	1:500 (IF)
Goat anti-rabbit IgG	Alexa Fluor 568	A-11010	Thermofisher (Leicestershire,UK)	1:500 (IF)
Goat anti-rat IgG	Alexa Fluor 568	A-11077	Thermofisher (Leicestershire,UK)	1:500 (IF)
Sheep anti-mouse IgG	$F(ab')_2$ fragment-FITC	F2266	Sigma (Dorset, UK)	1:500 (IF)
Goat anti-rabbit IgG	IRDye 800CW	926-32211	LI-COR (Lincoln, UK)	1:10,000 (WB)
Goat anti-mouse IgG	IRDYE 680RD	926-68070	LI-COR (Lincoln, UK)	1:20,000 (WB)

2.3.3 Quantification of Immunohistochemistry

Coronal hemi-brain sections stained using the DAB protocol were scanned with a 10x objective using an Olympus VS-110 slide scanner and Olympus VS-ASW-2.9 acquisition software. The hippocampus was selected freehand using the freeware ImageJ, as pictured in Fig 2.2. The images were de-convoluted using HDAB RGB values, allowing separation of DAB and haematoxylin channels. The DAB staining was converted into a binary image and a specific marker threshold was set, that best represented staining observed in the images. Four sections from throughout the hippocampus were quantified for each sample. Mean area fraction (% staining of total area) was then calculated. Quantification was performed using an automated macro. Fluorescent and representative images were

taken with a 10x and 40x objective on a Leica DM5000 microscope, using LasAF software. For fluorescent quantification, images were converted into binary and a specific marker threshold was set, that best represented staining observed in the images. Area fraction (% staining of total area) was then calculated. To ensure impartiality, quantification was performed blinded to experimental groups.

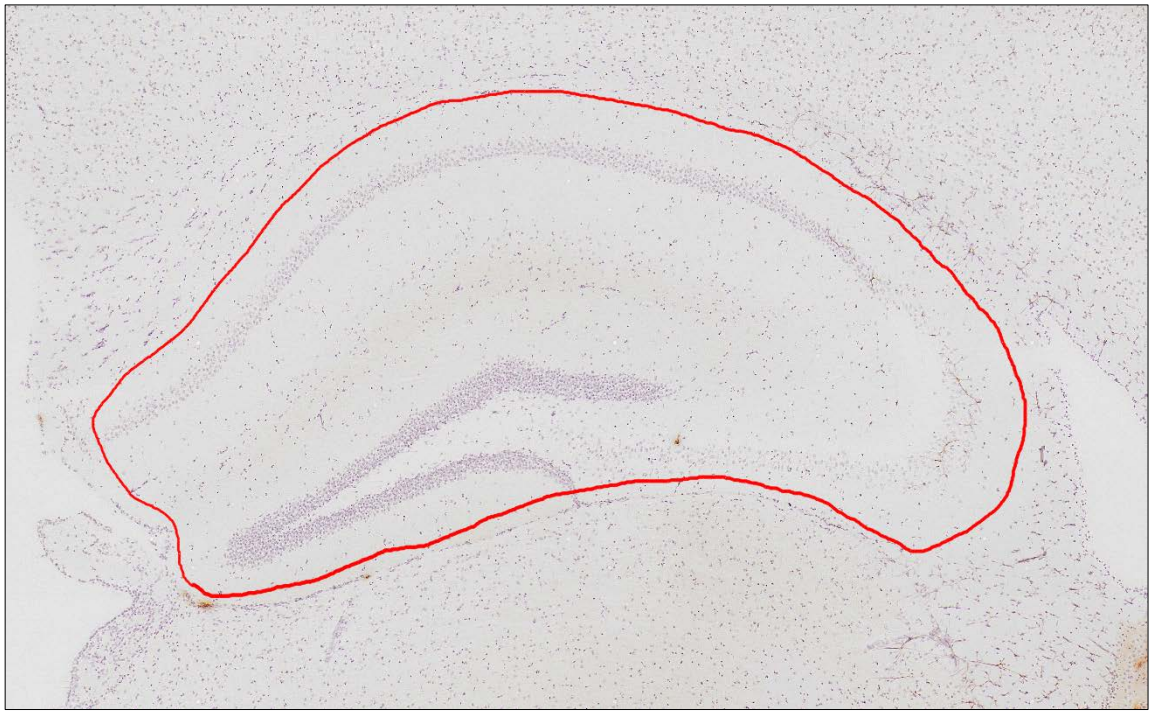

Fig 2.2:- Quantification area of the hippocampus.

2.4 10-plex Immunoassay

2.4.1 Protein extraction

Frozen hippocampal-enriched homogenates were weighed and placed in a 20% w/v buffer containing 150mM NaCl, 25nM TRIS, 1% triton x-100, complete mini protease inhibitor tablet (Roche, West Sussex, UK) and phosSTOP mini phosphatase inhibitor tablet (Roche, West Sussex, UK) (1 tablet per 10ml lysis buffer). Tissue was homogenised at 30,000 rpm for 30 seconds using a polytron homogeniser. Homogenates were incubated on ice for 15 minutes before centrifugation at 20,000G for 30 minutes (4°C). The supernatants generated were frozen into aliquots for immunoassay and western blot. In the case of the Tg2576 mice, pellets were re-suspended in 70% formic acid and incubated for 15 minutes, in order to solubilise aggregated forms of Aβ. This suspension was neutralised in 20 volumes of pH8 TRIS, and centrifuged at 20,000G for 1 hour. The resulting supernatant was utilised to measure the formic acid soluble Aβ fraction, using immunoassay. Total proteins levels were calculated using BCA protein assay (Pierce, Illinois, US), following manufacturer's instructions. Briefly, 25µl of diluted (1:10) protein homogenate was plated onto a 96-well plate in triplicate. Reagent A was combined with Reagent B (50:1) and 200µl was added to each sample well. The plate was incubated at 37°C for 30 minutes and read using an Infinite 200 Pro plate reader. Protein values were calculated against a bovine serum albumin (BSA) standard protein curve.

2.4.2 10-plex Immunoassay protocol

Proinflammatory cytokines (V-PLEX plus proinflammatory panel 1 (mouse), K15048G-1) and Aβ levels (V-PLEX Aβ peptide panel 1 (4G8), K15199E-1) were measured using multispot ELISAs (Mesoscale Discovery, Maryland, US), as per manufacturer's instructions. Briefly, hippocampal-enriched tissue homogenates were diluted (1:2) with supplied diluent and, together with calibrators, loaded onto 96 well mesoscale plates. Formic acid soluble Aβ fractions were diluted 1:10. Plates were incubated for 2 hours on a microplate shaker (700 rpm), before 3 wash steps in 1X PBS. Sulfotag linked antibodies were added to each well and a further incubation of 2 hours took place. Plates were washed 3 times

and Read Buffer T added for analysis on a Sector PR400 plate reader. Cytokine levels were normalised to total protein concentration, as measured by BCA protein assay.

2.5 Western blot

2.5.1 Protein Extraction

Protein extraction was carried out as outlined in the immunoassay protocol. Only triton-soluble fractions were used.

2.5.2 SDS-PAGE

Hippocampal-enriched homogenates were diluted with ddH_2O and 4X sample buffer (Sigma, Dorset, UK) to a 1mg/ml concentration and denatured at 95°C for 5 minutes, before brief vortexing and centrifugation at 300G for 1 minute.

The Bio-Rad mini protein II gel system (Bio-Rad, Oxford, UK) was used for casting and running SDS-Poly-Acrylamide gel electrophoresis (PAGE) gels. All gels were run with a resolving (10%) and stacking layer (2.5%) (Table 2.3). The resolving gels were poured and overlaid with isopropanol (Thermofisher, Leicestershire, UK), until the acrylamide (Sigma, Dorset, UK) had polymerised. The isopropanol was then removed, washed with 1X TBS, stacking gel poured, lane comb inserted and gels left to polymerise. Bio-Rad short plates and back plates were used to cast the gels producing a gel thickness of 1.5mm. Samples were loaded (20µl) in separate lanes with Kaleidoscope 250KDa ladder (161-0375, Bio-Rad, Oxford, UK). Gels were placed in a chamber surrounded by 1X laemmli buffer (Table 2.4) and placed on ice. Gels were run at 100V for approximately 2 hours.

2.5.3 Protein Transfer

Proteins were transferred from SDS-Poly-Acrylamide gel to Polyvinylidene difluoride (PVDF) membrane (Bio-Rad, Oxford, UK). A stack was constructed consisting of a sponge pre-soaked in transfer buffer (1X laemmli buffer containing 20% v/v methanol), 2 sheets of filter paper (Whatman, 3mm chromatography paper, pre-soaked as above), the gel, a sheet of pre-soaked PVDF, 2 sheets of filter paper and an additional pre-soaked sponge. N.B. PVDF was charged in 100% methanol for 2 minutes prior to soaking in 1X transfer buffer. This was placed into a mini blotting tank with transfer buffer. Proteins were electro-transferred overnight (18 hours) in a cold room (4°C), at 30V.

2.5.4 Antibody labelling of protein

Post-transfer, the stack was disassembled and PVDF washed with 1X TBS for 2 minutes. The membranes were incubated in BSA (5%) block for 60 minutes, before being transferred to a 50 ml falcon tube containing 4ml of BSA (5%) solution and primary antibody. Membranes were incubated on a test tube roller (50 rpm) overnight (18 hours) in a cold room (4°C). The following day, the membranes were washed (3 x 5 minutes) in 1X TBS (0.05% tween). Membranes were subsequently incubated in darkness, on a test tube roller (RT) for 1 hour in BSA (5%) solution containing infrared fluorescent secondary antibodies. The membranes were washed (3 x 5 minutes) in 1X TBS (0.05% tween), before being left in 1XTBS until imaging the same day on a LICOR Odyssey scanner.

Table 2.3:- Resolving and stacking gel components.

Component	Stock	Resolving Gel (10%) (volume for 1 gel)	Stacking Gel (2.5%) (volume for 1 gel)
Acrylamide	30%	4.0ml	0.52ml
Tris pH 8.8	1.5M	3.0ml	-
Tris pH 6.8	0.5M	-	1.0ml
APS	10%	120µl	40µl
ddH_2O	-	5.0ml	2.5ml
TEMED	>99%	12µl	4µl

Table 2.4:- 10X laemmli buffer components.

Component	Amount added
Tris base	30g
Glycine	144g
SDS	10g
Made up in 1 litre ddH_2O and adjusted to pH 8.3	

2.6 Statistics

Statistical analysis was performed using GraphPad Prism 7 software (California, US) with the exception of body weight data which was analysed using a 3-way analysis of variance (ANOVA) and 3-way repeated measure ANOVA in SPSS, in chapters 5 and 6. For experiments with a single independent variable and two groups, two tailed *t*-tests were used. Data sets were tested for normality using Shapiro-Wilk Test and equal variances using Bartlett's test. Failure of these tests, resulted in transformation of the data using the functions: Y=logY or Y=log(Y+1). To reduce likelihood of type I statistical errors, experiments with 3 or more groups were tested by 1, 2 or 3-way ANOVA, depending on the number of independent variables, and significant results were followed up by Tukey post-hoc testing. If transformed data was not normally distributed, the original data sets were analysed using appropriate non-parametric test (i.e. Mann Whitney U test and Kruskal Wallis test). Graphs were constructed using GraphPad Prism 7 software, displaying mean and standard deviation.

Chapter 3: Characterisation of single and multiple LPS challenge in adult wild-type mice

3.1 Introduction

Systemic inflammation caused by infections has been implicated in the development of many neurodegenerative conditions such as Alzheimer's Disease (Dunn et al. 2005; Holmes et al. 2009). Although the CNS is thought to be immune privileged, this is considered relative, with numerous routes of crosstalk between this compartment and the periphery. These include activation of cells such as the endothelium at the cerebral vasculature and circumventricular organs, in addition to stimulation of the vagal nerve and transport of cytokines across the blood-brain barrier (BBB) (for review see Holmes 2013). Subsequently, there is evidence that crosstalk resulting from systemic inflammation drives proinflammatory processes in the brain and predisposes or exacerbates pathology associated with neurodegeneration (Kitazawa et al. 2005). To investigate the phenomenon experimentally, researchers have turned to models of systemic inflammation in animals. The most widely adopted model utilises a bacterial endotoxin, also known as lipopolysaccharide (LPS).

LPS is the major membrane component of the outer coat of gram-negative bacteria and a potent stimulant of the innate immune system. This occurs through engagement with pattern recognition receptors (PRRs), in particular Toll-like receptor 4 (TLR4) (Barichello et al. 2015). This receptor is found in many tissues throughout the body, particularly, but not selectively, upon immune cells. Binding of LPS induces a cascade of signalling events within the cell, ultimately leading to the production of proinflammatory cytokines such IL-1β, IL-6 and TNF-α, and prompting the innate immune response (Alexander and Rietschel 2001).

An intraperitoneal (i.p.) injection of LPS into a rodent is a commonly utilised model of systemic inflammation (Pardon 2015), causing innate immune cell activation, elevations in peripheral pro- and anti-inflammatory cytokines, including IL-1β, IL-6 and IL-10 (Erickson and Banks 2011; Biesmans et al. 2013), and associated sickness behaviours, such

as fever, social withdrawal and a reduction in food intake (Dantzer 2009). Although differences in dose, time points and strain/species contribute to discrepancies observed between studies, a single acute dose of LPS is generally considered to result in elevated levels of cytokines in the brain and activation of immune cells such as microglia, with resolution occurring between 24-72 hours post injection (Hoogland et al. 2015; Catorce and Gevorkian 2016). However, to mimic the longer term inflammation resulting from chronic infection, a multiple challenge protocol has been adopted (Pardon 2015).

Despite increased interest over the past decade into the relationship between inflammation, including systemic inflammation, and neurodegeneration, it is still unclear what pathways may be linking these two processes (Krstic and Knuesel 2012; Doty et al. 2015; Chen et al. 2016). One possible connection may lie in the microtubule-associated protein tau, which becomes hyperphosphorylated and aggregated over the course of neurodegenerative disorders such as AD. Using the multiple LPS model in transgenic mice (3xTg) exhibiting extensive amyloid and tau pathology, Kitazawa et al found that above from basal levels during early pathology, there was increased tau hyperphosphorylation, but not amyloid pathology (Kitazawa et al. 2005). This was in part attributed to an increase in CD45+ microglia and activation of the tau kinase CDK5. Tau hyperphosphorylation was additionally detected in non-transgenic mice, used as controls, supporting a role of systemic inflammation in tau phosphorylation, independent of underlying neuropathology.

To confirm this finding and further investigate the possible underlying mechanism leading to tau phosphorylation, in response to systemic LPS challenge, adult (3-4 month old) C57BL/6 mice received single or multiple i.p. injections of LPS or saline. A dose of LPS (0.5mg/kg) was selected, based on previously published work from our group showing a robust neuroinflammatory response (Teeling et al. 2007; Püntener et al. 2012). In the multiple LPS protocol, mice received bi-weekly LPS for 8 weeks to mimic inflammation resulting from chronic infection. Tissue was taken 24 hours after the final LPS injection as elevated cytokines levels and microglial activation are reported at this time point (Hoogland et al. 2015). Tissue was additionally harvested from mice at 24 hours following a single dose of LPS or saline, to compare the effects of single v.s. multiple LPS injections.

Given the body of evidence from previous literature (Lim et al. 2015; Catorce and Gevorkian 2016), I expect that inflammation induced in the periphery propagates to the brain and causes the activation of immune cells such as the microglia. To substantiate this, I have analysed the expression of receptors found on this cell type, FcγRI and CD11b. I hypothesize that the activation of microglia and other immune cells, results in the release of inflammatory cytokines in the brain parenchyma, and the subsequent phosphorylation of the tau protein in neurons. Phosphorylation of two tau epitopes implicated in pathology were assessed using western blot. This study focussed on the hippocampus, an area where early tau pathology is observed in AD (Braak and Braak 1991).

3.2 Materials and Methods

3.2.1 Study Design

Single and Multiple LPS

Adult (3-4 months old) C57BL/6 wild-type mice were randomly assigned to one of four groups (n=8, female), single saline, single LPS, multiple saline or multiple LPS. Mice receiving multiple challenges were injected 16X (i.p.) with 200µl of saline or LPS (0.5mg/kg) over the course of 8 weeks. Mice receiving a single challenge were injected once (i.p.) with 200µl of saline or LPS (0.5mg/kg). Mice were weighed on the day of injection and 24 hours post injection throughout the experiment. Mice were given an overdose of anaesthetic (Tribromoethanol (*Avertin*) for Rat) 24 hours after the final LPS or saline injection, prior to the collection of blood. The mice were transcardially perfused with saline, with the brain taken for bioanalysis. Further details of methods used for tissue analysis are outlined in chapter 2.

3.3 Results

3.3.1 Metabolic response in adult wild-type mice challenged with single and multiple LPS injections

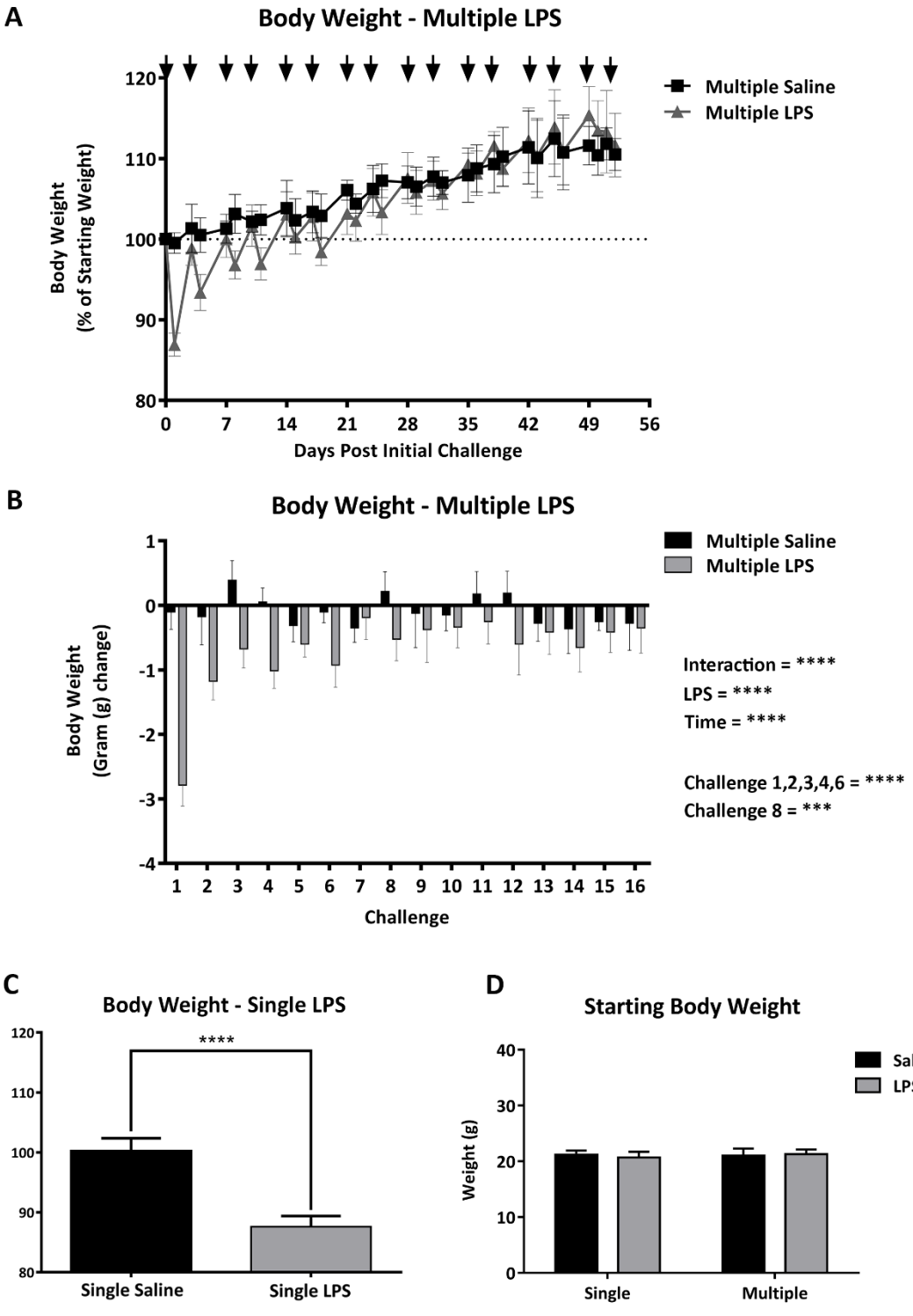

Fig 3.1:- Body weight from adult wild-type mice challenged with single and multiple LPS injections. Mice were weighed prior to and 24 hours after, each LPS (0.5mg/kg) or saline injection throughout the experiment. Body weight ((A) % of starting weight), (B) gram (g) change) of adult wild-type mice challenged with multiple (16X) LPS or saline injections. Data was analysed by 2-way ANOVA and Tukey post hoc test (n=8), and displayed as mean + SD. (B) Body weight (% of starting weight) of adult wild-type mice, 24 hours post injection with LPS or saline. Data was analysed by two tailed T-test (n=8), and displayed as mean + SD. (C) Starting body weight (grams) of adult wild-type mice. Data was analysed by 2-way ANOVA and Tukey post hoc test (n=8), and displayed as mean + SD.

In mice receiving a single LPS injection, a mean weight loss of 12% (2.6g) was observed from starting weight, 24 hours post injection (Fig 3.1C). In comparison saline-injected mice showed no mean change over this time period.

In line with this finding, mice receiving multiple LPS injections demonstrated a mean weight loss of 13% (2.8g) from starting weight, 24 hours post initial challenge (Fig 3.1A,B). Subsequent to this initial LPS challenge, a mean weight loss of 1.2g, 0.7g, 1.0g, 0.6g and 0.9g was observed following the 2^{nd}, 3^{rd}, 4^{th}, 5^{th} and 6^{th} challenges respectively (Fig 3.1B). Additionally, mice receiving multiple LPS challenges had recovered to above starting weight by the 4^{th} injection (Fig 3.1A). Analysis indicated a significant effect of time ($p \leq 0.0001$) and LPS ($p \leq 0.0001$) over the duration of the experiment. Additionally, an interaction ($p \leq 0.0001$) was observed demonstrating that LPS caused a significantly greater body weight decrease compared to saline-injected mice, following the 1^{st}, 2^{nd}, 3^{rd}, 4^{th}, 6^{th} ($p \leq 0.0001$) and 8^{th} ($p \leq 0.001$) challenges (Fig 3.1B). Mice receiving multiple saline injections, did not gain or lose weight above a mean of 0.4g, following any of the challenges (Fig 3.1B). On the day of the final injection, a mean body weight of 111% and 113% from starting body weight was observed in mice receiving multiple challenges of saline and LPS respectively (Fig 3.1A).

Initial weight data demonstrated no significant difference in starting body weight between groups (Fig 3.1D).

3.3.2 Neuroinflammatory response in adult wild-type mice challenged with single and multiple LPS injection

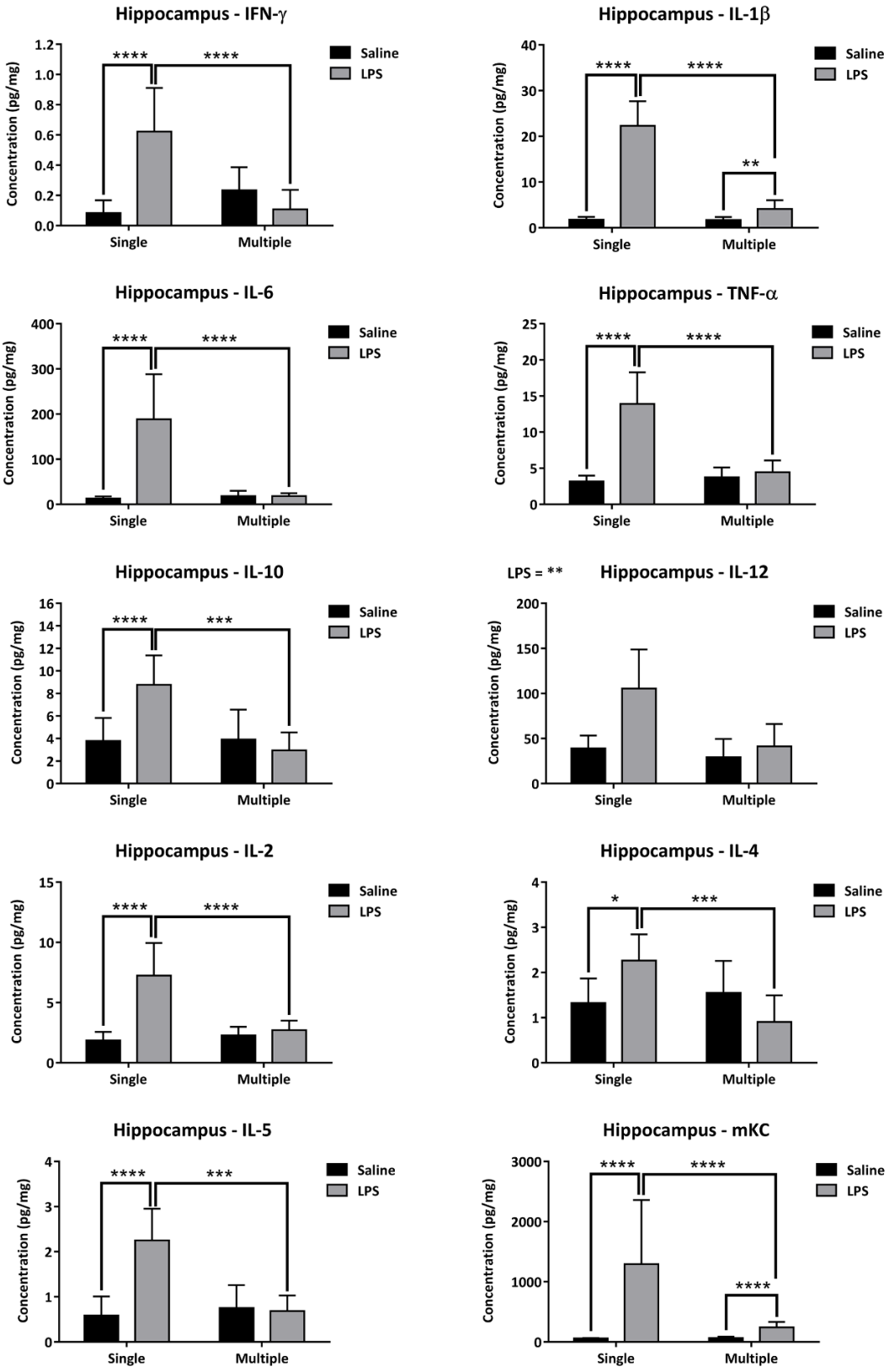

Fig 3.2:- Cytokine expression levels in hippocampal-enriched tissue from adult wild-type mice challenged with single and multiple LPS injections. Cytokine levels (pg/mg of total protein) in hippocampal-enriched tissue homogenate from adult wild-type mice following single (1X) or multiple (16X) injections of LPS or saline. Tissue was taken 24 hours post final injection. Data was analysed by 2-way ANOVA and Tukey post hoc test (n=8), and displayed as mean + SD.

Levels of brain cytokines were measured in hippocampal-enriched tissue homogenate using a 10-plex immunoassay (Fig 3.2).

Twenty-four hours after a single challenge of LPS, significant elevations in the cytokines IFN-γ (7-fold, $p \leq 0.0001$), IL-1β (13-fold, $p \leq 0.0001$), IL-6 (15-fold, $p \leq 0.0001$), TNF-α (4-fold, $p \leq 0.0001$), IL-10 (2-fold, $p \leq 0.0001$), IL-2 (4-fold, $p \leq 0.0001$), IL-4 (2-fold, $p \leq 0.05$), IL-5 (4-fold, $p \leq 0.0001$) and mKC (22-fold, $p \leq 0.0001$) were observed, compared to mice that received a single challenge of saline.

Multiple LPS challenges caused significant elevations in IL-1β (2-fold, $p \leq 0.01$) and mKC (4-fold, $p \leq 0.0001$) compared to mice receiving multiple injections of saline. A combined LPS effect was demonstrated with increased levels of IL-12 (2-fold, $p \leq 0.01$) compared to saline-injected control mice. Despite these findings, it should be noted that all cytokines measured were mostly unchanged from mice receiving multiple saline injections.

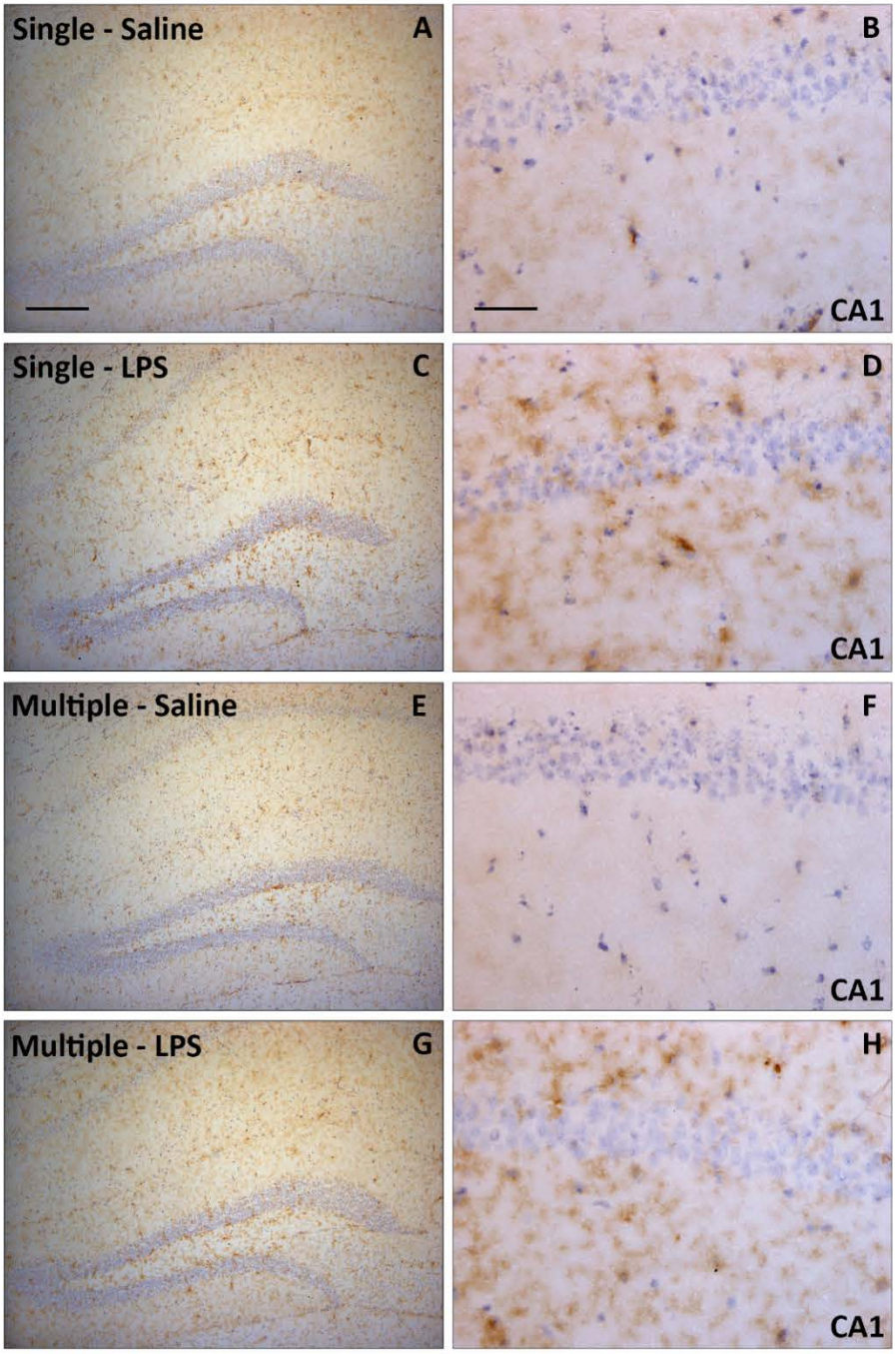
Single - Saline
A
B
CA1
Single - LPS
C
D
CA1
Multiple - Saline
E
F
CA1
Multiple - LPS
G
H
CA1

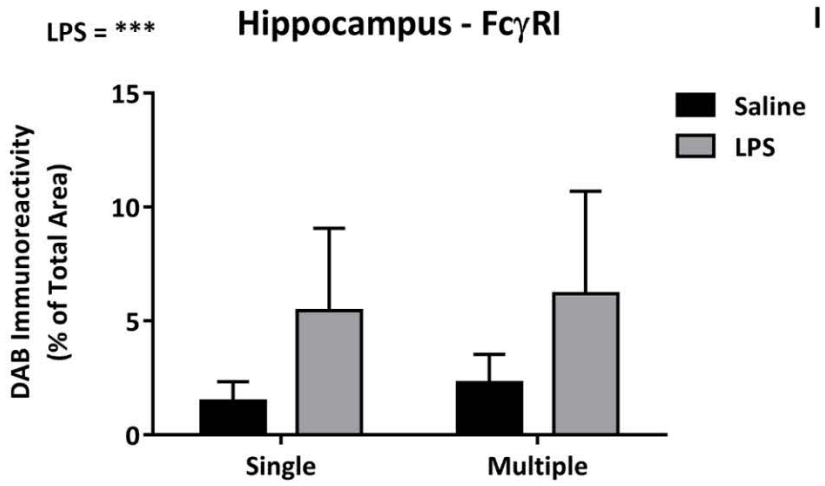
LPS = ***
Hippocampus - FcγRI
I
DAB Immunoreactivity (% of Total Area)
15
10
5
0
Saline
LPS
Single
Multiple

Fig 3.3:- FcγRI expression in the hippocampus of adult wild-type mice challenged with single or multiple LPS injections. Overview of FcγRI expression in adult wild-type mice following a single (1X) injection of LPS (C) or saline (A), or multiple (16X) injections of LPS (G) or saline (E). Scale bar = 200µm. Tissue was taken 24 hours post final injection. (B,D,F,H) Higher magnification images of CA1 region derived from overview of hippocampus. Scale bar = 50µm. (I) Quantification of FcγRI expression (DAB immunoreactivity (% of total area)) from entirety of hippocampus. Data was analysed by 2-way ANOVA and Tukey post hoc test (n=8), and displayed as mean + SD.

To investigate the cellular response to single or multiple challenges of LPS, FcγRI expression on myeloid cells, such as microglia, was assessed by immunohistochemistry (Fig 3.3).

Quantification of FcγRI expression in the hippocampus indicated a significant increase following single and multiple LPS challenges compared to saline-injected control mice (3-fold, $p \leq 0.001$) (Fig 3.3I). No significant difference between single and multiple challenges of LPS was observed. LPS challenge caused a widespread increase in FcγRI expression on microglia, in addition to increases in localised staining, particularly in the hippocampal fissure (Fig 3.3C,G).

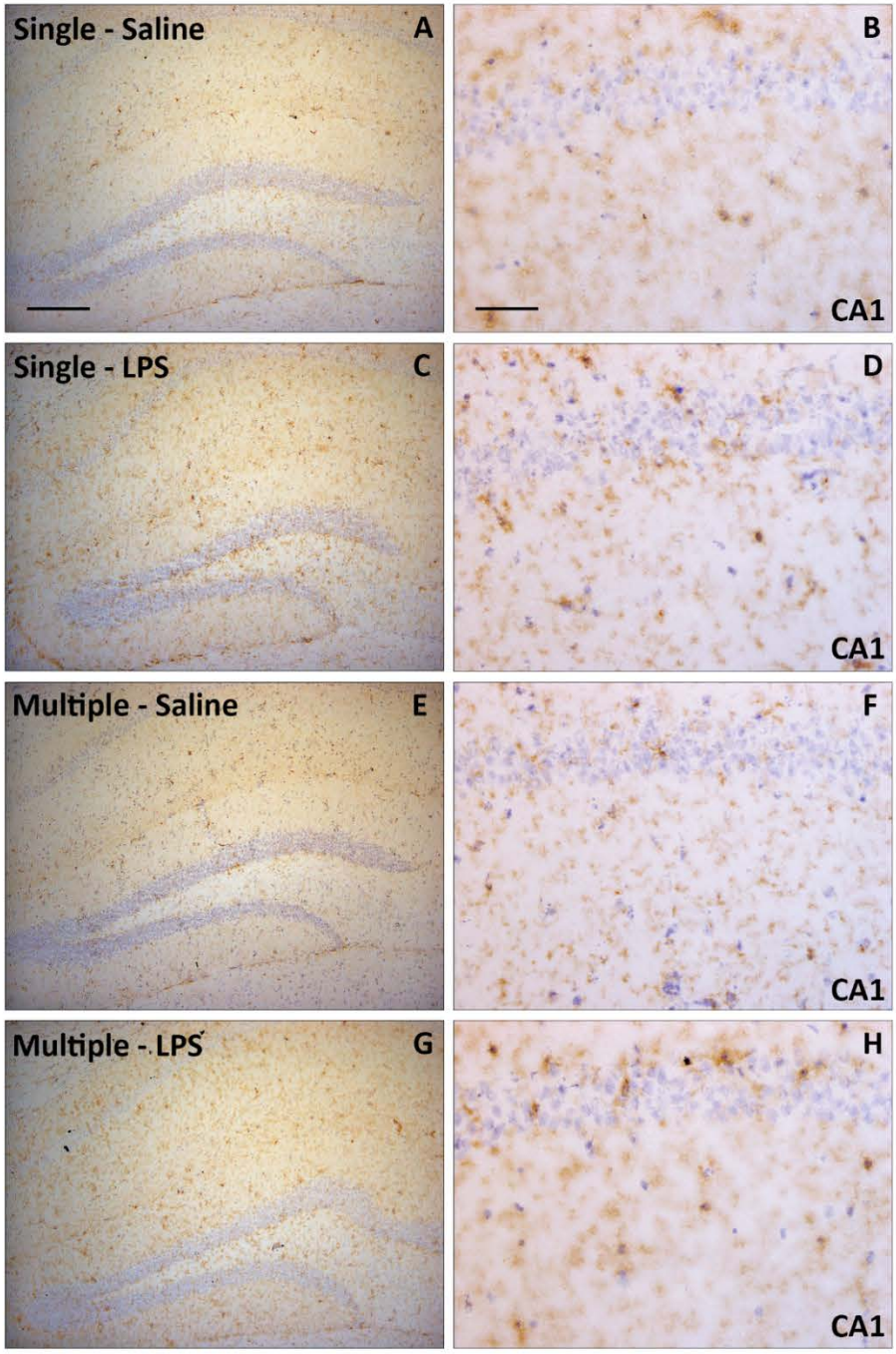
Single - Saline
A
B
CA1
Single - LPS
C
D
CA1
Multiple - Saline
E
F
CA1
Multiple - LPS
G
H
CA1

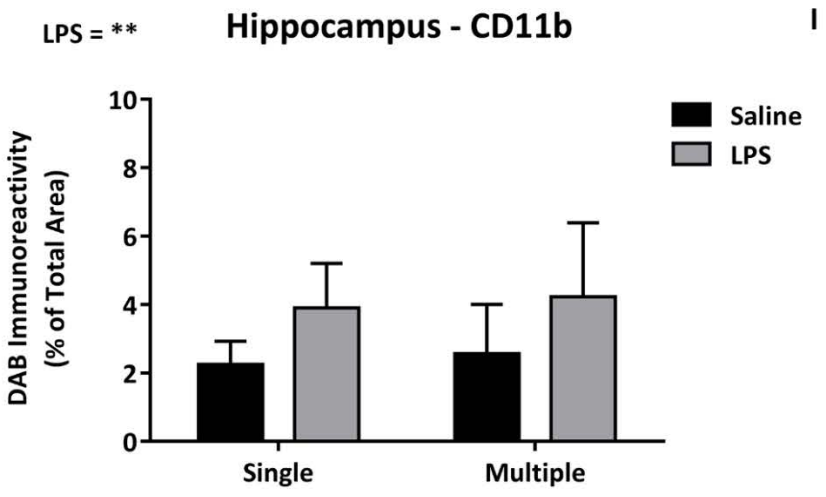
LPS = **
Hippocampus - CD11b
I
DAB Immunoreactivity (% of Total Area)
10
8
6
4
2
0
Saline
LPS
Single
Multiple

Fig 3.4:- CD11b expression in the hippocampus of adult wild-type mice challenged with single or multiple LPS injections. Overview of CD11b expression in adult wild-type mice following a single (1X) injection of LPS (C) or saline (A), or multiple (16X) injections of LPS (G) or saline (E). Scale bar = 200µm. Tissue was taken 24 hours post final injection. (B,D,F,H) Higher magnification images of CA1 region derived from overview of hippocampus. Scale bar = 50µm. (I) Quantification of CD11b expression (DAB immunoreactivity (% of total area)) from entirety of the hippocampus. Data was analysed by 2-way ANOVA and Tukey post hoc test (n=8), and displayed as mean + SD.

To investigate the cellular response to single or multiple challenges of LPS, CD11b expression on myeloid cells, such as microglia, was assessed by immunohistochemistry (Fig 3.4).

Quantification of CD11b expression in the hippocampus indicated a significant increase following single and multiple LPS challenges compared to saline-injected control mice (2-fold, $p \leq 0.01$) (Fig 3.4I). No significant difference between single and multiple challenges of LPS was observed. LPS challenge caused a widespread increase in CD11b expression on microglia, in addition to increases in localised staining, particularly in the hippocampal fissure (Fig 3.4C,G).

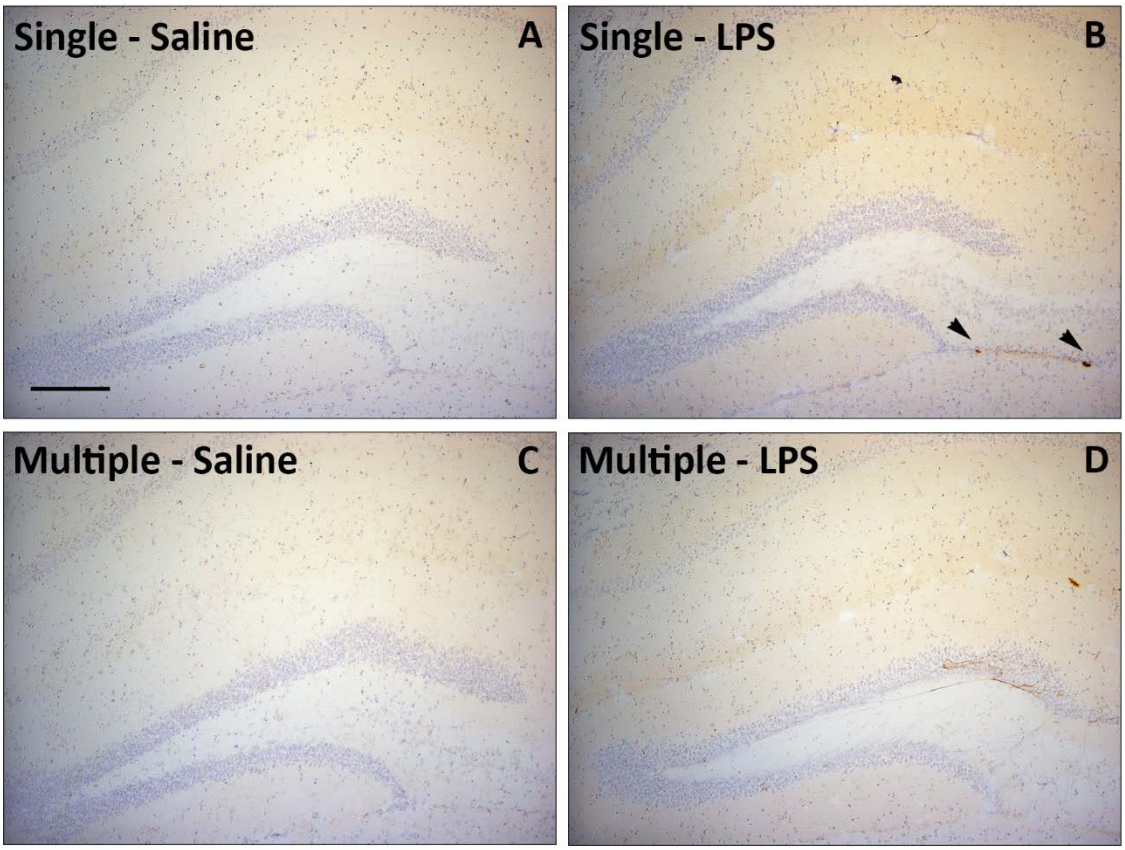

Fig 3.5:- MHCII expression in the hippocampus of adult wild-type mice challenged with single or multiple LPS injections. Overview of MHCII expression in adult wild-type mice following a single (1X) injection of LPS (B) or saline (A), or multiple (16X) injections of LPS (D) or saline (C). Tissue was taken 24 hours post final injection. Black arrows indicate MHCII+ cells. Scale bar = 200µm.

To investigate the cellular response to single or multiple challenges of LPS, MHCII expression on myeloid cells, such as microglia, was assessed by immunohistochemistry (Fig 3.5).

MHCII+ cells were largely absent from the hippocampus of all experimental groups, with the exception of a small number of round cells localised around the pial membrane and ventricles (black arrows). For this reason, quantification was not performed.

3.3.3 Neurochemistry in adult wild-type mice challenged with single and multiple LPS challenges

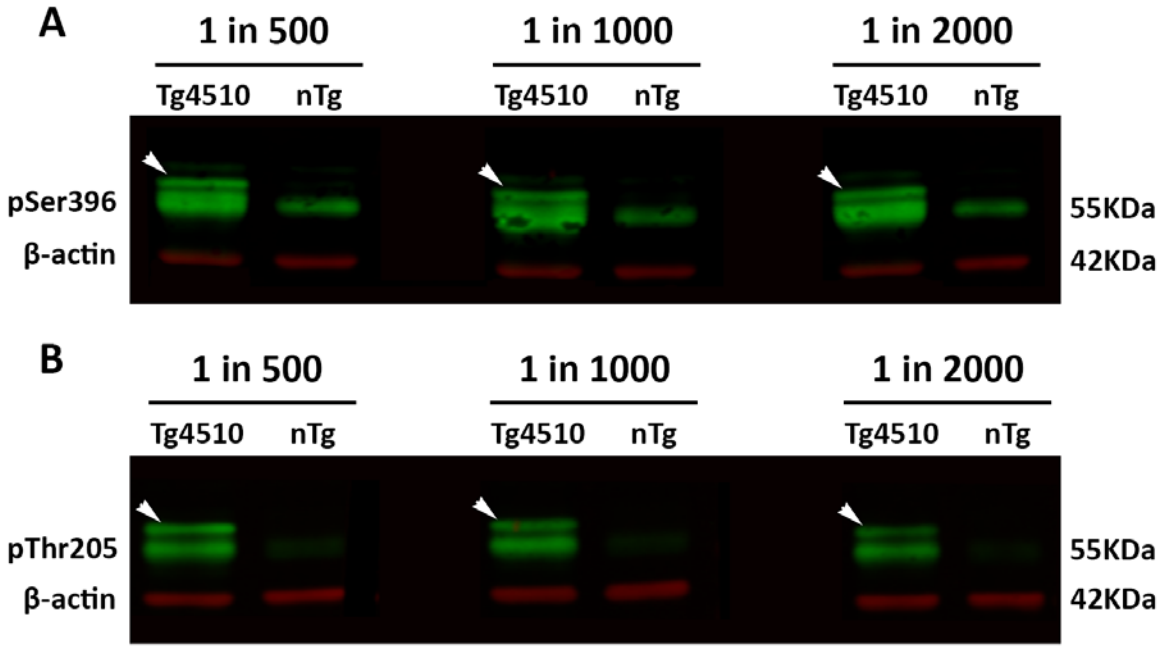

Fig 3.6:- Optimisation of phosphorylated-tau antibodies. Tg4510 and non-transgenic (tTA) brain tissue homogenate blotted with dilutions (1 in 500, 1000, 2000) of (A) pSer396 and (B) pThr205 in green. β-actin (red) was used for normalisation of protein loading. White arrows indicate a 64KDa hyperphosphorylated and insoluble form of 4R0N tau.

Methods for detection of phosphorylated-tau antibodies were optimised using brain tissue homogenate from 12 month old tau transgenic Tg4510 mice and non-transgenic littermates (Fig 3.6).

The Tg4510 strain incorporates a human tau transgene, under the CAMKII promoter, containing the P301L mutation. These mice demonstrate enhanced phosphorylation of endogenous tau at 12 months old, that migrates at 55KDa, with a hyperphosphorylated and insoluble form of 4R0N tau migrating at 64KDa (Santacruz et al. 2005). The phosphorylated-tau antibodies pSer396 and pThr205 were diluted 1 in 500, 1000 and 2000. For pSer396, 1 in 2000 was selected as a strong signal was still observed at this dilution and the non-tau transgenic mice used in these experiments were expected to

have a lower level of tau phosphorylation. For pThr205, 1 in 1000 was selected for these same reasons.

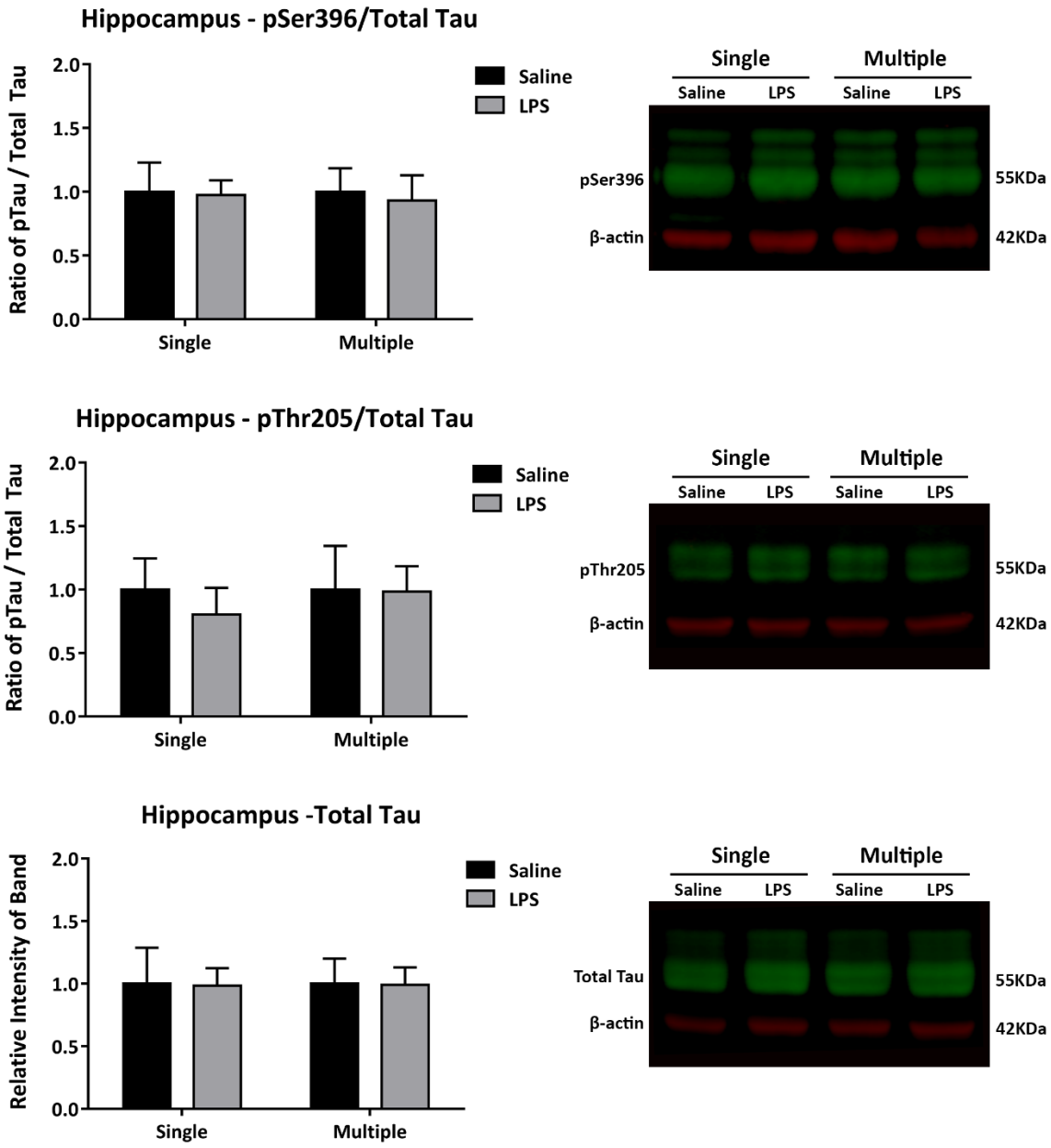

Fig 3.7:- Phosphorylated- and total tau expression levels in hippocampal-enriched tissue from adult wild-type mice challenged with single or multiple LPS injections. Expression of pSer396 and pThr205 (ratio of ptau/total tau), and total tau levels (relative intensity) in hippocampal-enriched homogenate from adult wild-type mice following single (1X) or multiple (16X) injections of LPS or saline. Representative western blots showing tau (green) and β-actin (red) immunoreactivity, with the latter used for normalisation of protein loading. Tissue was taken 24 hours post final injection. Data was analysed by 2-way ANOVA and Tukey post hoc test (n=8), and displayed as mean + SD.

To investigate the impact of single and multiple LPS challenges on tau-related neurochemistry in the brain, total and phosphorylated-tau levels were measured in hippocampal-enriched tissue homogenate by western blot (Fig 3.7).

Quantification of tau-related immunoreactive bands obtained from western blot demonstrated no significant change following single or multiple LPS challenges, with respect to pSer396, pThr205 or total tau levels.

3.4 Discussion

Systemic inflammation is implicated in the development of neurodegenerative diseases, however the mechanisms that elicit this process are not fully understood (Hoogland et al. 2015; Bueno et al. 2016). Researchers have turned to *in vivo* animal models to investigate the mechanism behind this relationship, and commonly utilise the endotoxin; LPS as a potent stimulant of the innate immune system. Systemic inflammation can be induced in mice by administering i.p. injections of LPS, either as a single dose, to mimic acute inflammation, or as multiple challenges to model inflammation resulting from a chronic infection in the periphery. The literature suggests that the latter paradigm has the capacity to drive the hyperphosphorylation of tau in transgenic models, where a mutated form of the human tau is expressed, supporting the hypothesis that inflammation can exacerbate pre-existing tau pathology (Kitazawa et al. 2005). However, there is limited evidence that inflammation can induce phosphorylation of mouse tau in non-transgenic mice (Bhaskar et al. 2010). Hence it is uncertain whether tau phosphorylation is causative to neurodegeneration or an early event in the degenerative process. Therefore, in this chapter I have administered single or multiple injections of LPS to adult wild-type mice, in order to investigate whether LPS-induced systemic inflammation has the capacity to cause phosphorylation of mouse tau. Microglial phenotype changes and cytokine response in the brain have additionally been analysed as a measure of neuroinflammation, to help explain whether mechanisms they elicit are responsible for this relationship.

Systemic inflammation elicits numerous sickness behaviours including a reduced motivation for food and fluids (Hart 1988; Pardon 2015). This can be measured as a decrease in weight and tracked throughout the experimental protocol as a useful readout of metabolic response. As predicted, a single LPS injection caused a mean weight loss of approximately 12% (2.6g), 24 hours post injection. In line with this finding, the group of mice receiving multiple LPS injections demonstrated a similar mean body weight decrease after initial challenge. However, subsequent injections of LPS showed an attenuated response with smaller body weight losses. This is likely due to the development of endotoxin tolerance (ET) in the multiple LPS model.

Endotoxin tolerance or hyporesponsiveness refers to a state whereby, upon exposure to LPS, a transcriptional shift is observed, primarily in monocytes and macrophages (for review see (Biswas and Lopez-Collazo 2009)). Subsequent challenges of LPS elicit a dampened proinflammatory response compared to initial exposure, in order to protect the organism from tissue-damaging inflammation. This response is characterised by a reduction in proinflammatory cytokine release, particularly TNF-α and IFN-γ, increase in anti-inflammatory cytokine release, such as IL-10, increased anti-microbial and phagocytic function and lowered antigen presentation capacity, possibly regulated by epigenetic modulation.

When determining neuroinflammatory changes, the data presented here demonstrates a robust inflammatory response in the hippocampus of mice exposed to a single i.p. injection of LPS, with large increases observed in the proinflammatory cytokines IFN-γ, IL-1β, IL-6 and TNF-α. Additionally, elevations of anti-inflammatory cytokines such as IL-10, IL-2 and IL-4 are demonstrated.

There are conflicting reports in the literature as to whether cytokines are still elevated in the brain at 24 hours post i.p LPS injection. Biesmans et al found no significant changes in protein levels of TNF-α, IL-1β, IL-6 and IL-10 at 24 hours post injection with LPS (2mg/kg) in male outbred NMRI mice (Biesmans et al. 2013). However, two studies conducted by Erickson et al and Cazareth et al, using CD-1 (3mg/kg LPS) and C57BL/6 (2mg/kg LPS) respectively, found elevations of these cytokines at the 24 hour time point (Erickson and Banks 2011; Cazareth et al. 2014). Overall, despite discrepancies caused by mouse strain and possible strength of LPS strain used in the study, the cytokine response in the brain appears to be in the later stages of resolving by the 24 hour time point. Therefore based on previous literature I predict that larger increases would have been observed between 6-12 hours post injection (Pardon 2015).

By comparing single v.s. multiple challenges of LPS in this study, it has been observed that multiple injections of LPS elicit an attenuated cytokine response in the hippocampus. Characteristic of ET, only moderate elevations in IL-1β and mKC were seen following subsequent injections of LPS. Erickson et al found decreases in protein IL-1β, and increases in IL-6 and TNF-α following 3 injections of LPS (3mg/kg) compared to a single

dose of LPS (Erickson and Banks 2011). The high dose of LPS, differing strain of mouse and relatively shorter injection and sacrifice time points may account for the differences observed with the data presented here.

Our lab has previously shown C57BL/6 mice adminstered with 3 LPS i.p. injections (0.5mg/kg) every 24 hours, exhibit increases in hippocampal IL-1β after the second challenge (Püntener et al. 2012). However, as tissue was taken 4 hours after each injection, the increase observed may be a result of the first injection, equivalent to 28 hours post initial challenge. At 4 hours post initial injection, protein levels may still be low and therefore do not show an increase. As levels of IL-1β are back to baseline by the third injection, these results would fit with the data presented in this chapter, highlighting an attenuation of cytokine response in the brain, following multiple challenges of LPS.

Schaafsma and colleagues have investigated the mechanism behind endotoxin tolerance in microglia, finding the NF-κB subunit ReIB is critical in binding and repressing cytokine promoters such as that of IL-1β (Schaafsma et al. 2015). This resulted in a suppressed, but not ablated expression of IL-1β following susbequent LPS challenges, both *in vitro* and *in vivo*, and in accordance with the results presented here. Additionally, primary microglia preconditioned with LPS, show greater phagocytic capacity and secretion of iNOS and NO, supporting partial but not full inhibition of immune response during ET.

Interestingly, in contrast to the levels of cytokines, increased expression of FcγRI and CD11b was observed to similar levels in mice receiving single or multiple challenges of LPS, when compared to saline-injected control mice. FcγRI has a higher affinity for monomeric IgG and upon binding can lead to phagocytosis, cytokine release, proliferation and antigen presentation (Swanson and Hoppe 2004; Nimmerjahn and Ravetch 2005). CD11b is an integrin that, when paired to CD18, forms the complement receptor 3 (CR3) complex. CR3 interacts with pathogens opsonized with complement factor C3b/iC3b and facilitates uptake into the cell (von Bernhardi et al. 2015). In this study, it appears both cells associated with the vasculature, such as perivascular macrophages, and microglia have increased expression of these receptors in response to LPS, indicative of a more activated state.

In a systematic review of studies utilising single and multiple LPS challenges, Marie Christine Pardon concluded that microglia were activated 6 hours following a single LPS, peaking from 8 hours to 2 days and returning to basal resting state after 7 days, in line with the findings presented here (Pardon 2015). Studies utilising multiple LPS challenges have shown mixed results, most likely due to differences in species of animal, strain of animal, sex of animal, doses of LPS, time of dosing and tissue harvesting, route of administration, brain region examined and bacterial source of LPS. Frank-Cannon et al followed a similar protocol to the one presented here, injecting C57BL/6 mice bi-weekly with LPS (0.1mg/kg, i.p.) from *E. coli*, finding no evidence of microglial activation (CD45) after 8 weeks in the midbrain (Frank-Cannon et al. 2008). The smaller dose, source of LPS, differing brain region and use of CD68 as a marker of microglial activation may explain the differences seen with this study.

The results presented here suggest microglial phenotype changes, as measured by FcγRI and CD11b expression, are increased in the brain, despite the ET that appears to have developed after multiple challenges of LPS . Sustained microglial phenotype changes in the hippocampus has been reported in rats exposed to multiple i.p. LPS challenges (Borges et al. 2012), supporting these findings. One explanation for microglia not developing ET may lie in exposure to the LPS directly. Results from studies which have assessed whether LPS enters the brain parenchyma following single or multiple doses of LPS, are highly variable and often dependant on method variables previously discussed (Varatharaj and Galea 2017). Without exposure to LPS, activation of microglia may be TLR-4 independent and therefore ET is not observed.

Alternatively, microglial phenotype changes observed at 4 weeks post LPS injection, are a long lasting effect from the initial exposure to LPS seen after a single dose of LPS. This theory may explain why microglia still express elevated levels of FcγRI and CD11b while still being in an endotoxin tolerant state. In support of the microglial tolerance observed by Schaafsma and collegues (Schaafsma et al. 2015), recent studies have shown that this is governed by the release of macrophage colony-stimulating factor (M-CSF) from astrocytes and neurons (Chu et al. 2016).

There are conflicting reports as to whether LPS crosses the BBB (Banks et al. 2015; Varatharaj and Galea 2017). However, LPS does stimulate cells that make up the BBB, such as the endothelium, which have the capacity to produce and release cytokines, such as IL-6 and TNF-α, into the brain parenchyma (Verma et al. 2006). Additionally, systemic inflammation has been reported to induce upregulation of transporters for cytokines, such as TNF-α, and facilitate modification of tight junctions, allowing influx of cytokines into the brain (Varatharaj and Galea 2017). Therefore, the predominant source of cytokines may come from cells composing the BBB or from the circulation itself. While it is still unclear whether endothelial cells develop ET (Ogawa et al. 2003; Wang et al. 2011; Stark et al. 2016), fewer circulating cytokines may explain the attentuation in brain cytokine levels observed following multiple LPS challenges. Additionally, a peripheral source for the changes in brain cytokines may clarify why microglial phenotype does not mirror these alterations.

With evidence of neuroinflammation in both models of systemic LPS, the next line of investigation assessed whether this was sufficient to cause changes to neurons, in the form of tau hyperphosphorylation. Systemic inflammation has been shown to increase tau phosphorylation and exacerbate pre-existing tau pathology, in transgenic mice expressing a mutated human form of the tau protein (Kitazawa et al. 2005; Sy et al. 2011). However, studies investigating whether systemic inflammation has to capacity to induce tau phosphorylation in wild-type models are limited.

Roe et al demonstrated that a single, acute low dose of LPS i.p. (0.1mg/kg) caused increased tau phosphorylation at the epitopes Ser396, Ser202/Thr205 (AT8) and Ser422, 20 minutes post injection (Roe et al. 2011). This effect persisted at Ser396 for 240 minutes when the final time point was taken, however, the lack of saline-injected control in this experiment does bring into question whether the stress of injection contributed to the transient tau phosphorylation observed. Additionally, increased phosphorylation of tau has been seen at the Ser396 epitope, 12 hours post injection (1mg/kg), with associated activation in the tau kinase CDK5 (Czapski et al. 2016). There are two reports of tau phosphorylation occuring 24 hours post injection at the Ser396 and Thr205 epitopes, using high doses of systemic LPS (10mg/kg (Bhaskar et al. 2010), 15mg/kg (Liu et al. 2016)).

The data presented in this chapter suggests a single injection of LPS (0.5mg/kg) is not sufficient to induce tau phosphorylation in wild-type mice. Although the previous studies were carried out in adult (2-6 month old) C57BL/6 mice, it is likely that higher doses of LPS are required to induce phosphorylation at later time points such as 24 hours post injection. In agreement with this, Bhaskar et al did not observe tau phosphorylation at 24 hours using a 1mg/kg dose of LPS (Bhaskar et al. 2010). Administration of LPS doses above 1mg/kg are considered to simulate sepsis (Barron et al. 2016), and therefore it is difficult to translate these findings when studying infection as a risk factor for AD.

Two studies have investigated multiple LPS challenge in adult (4-6 month old) C57BL/6 mice, with regard to the induction of tau phosphorylation. Kitazawa and collegues found increases in tau phosphorylation at the Ser202/Thr205 (AT8) epitope following bi-weekly injections of LPS (0.5mg/kg) for 6 weeks (Kitazawa et al. 2005), while Gardner et al observed increases at the Thr235 epitope following daily injections of LPS (0.25mg/kg) for 1 week (Gardner et al. 2016). Both studies analysed tissue 24 hours post final injection, in line with the protocol utilised in this chapter. The discrepancy with the data presented here may arise from differing epitopes or detection antibodies as there are numerous epitopes on which tau can be phosphorylated. The latter study also detected increases in total tau levels which may account for the changes observed in levels of phosphorylation. Additionally, neuroinflammatory changes in these models were not investigated and therefore it unclear whether the development of ET occurred.

If ET has developed in these studies and an increase in tau phosphorylation is observed, the attenuated but still significantly elevated levels of IL-1β may be responsible. IL-1β has been heavily implicated in tau phosphorylation both *in vitro* (Li et al. 2003) and *in vivo* (Kitazawa et al. 2005), through activation of the tau kinases P38, CDK5 and GSK3β. If the mechanism linking inflammation and tau phosphorylation acts through IL-1β signalling, there may be opportunity in which to theraputically intervene.

In summary, the data presented in this chapter demonstrates that a single systemic injection of LPS results in a robust neuroinflammatory reponse as illustrated with significant increases in pro- and anti-inflammatory cytokines in the hippocampus of wild-type mice. This response is attenuated in mice receiving multiple challenges of LPS, with

only moderate increases in IL-1β and mKC remaining, indicative of ET development. However, microglial phenotype changes are observed 24 hours following both paradigms. It stands to reason that if microglia are primarily responsible for the changes in brain cytokine levels, then their phenotypic expression of receptors would reflect this and a difference would have been observed following single and multiple LPS challenges. As discussed, there may be numerous explanations for this. Phenotypic markers expression such as, FcγRI and CD11b, may not reflect functional changes including cytokine production, and therefore these markers may not be good indictors of ET development. Alternatively, the source of the changes in brain cytokine levels may be peripheral and therefore as tolerance develops in this compartment, a central attenuation is also observed. Therefore, future studies would benefit from analysis of the peripheral immune response e.g. serum cytokines levels and alterations of the BBB.

The neuroinflammatory changes in mice receiving single or repeated injections of LPS, do not induce tau phosphorylation in the hippocampus, measured 24 hours after final challenge. This is in contrast to previous reports, which do observe positive tau phosphorylation following both single and multiple LPS protocols. However, the experiments reported in this chapter were powered (n=8), in comparison to the discussed articles which report n=4. Additionally, increases in tau phosphorylation following a single challenge of LPS are dose-dependent. Although higher doses may result in increase tau phosphorylation, they also simulate sepsis and not the inflammation resulting from a common bacterial infection.

Chapter 4: Characterisation of salmonella infection in adult wild-type mice

4.1 Introduction

In chapter 3, it was shown that an acute single challenge of systemic LPS results in a robust neuroinflammatory response, measured at 24 hours post injection, characterised by elevations in pro- and anti-inflammatory cytokines and microglial phenotype changes. When multiple LPS insults were administered, this cytokine response was attenuated with only mild elevations of hippocampal IL-1β and mKC observed, indicative of ET. This calls into question how successful multiple LPS challenges replicate the inflammatory time course of a systemic infection and translate into human medicine (Püntener et al. 2012). Additionally, neither single nor multiple LPS challenge had the capacity to induce tau phosphorylation in adult wild-type mice, contrary to previous reports (Kitazawa et al. 2005; Bhaskar et al. 2010; Roe et al. 2011; Czapski et al. 2016; Gardner et al. 2016; Liu et al. 2016).

To address these issues, I have characterised the peripheral and central inflammatory response following infection with an attenuated bacterial strain of *Salmonella enterica* subsp. *enterica* serovar Typhimurium (*S.* Typhimurium*,* SL3261). In mice, this serovar induces symptoms similar to human typhoid fever (Santos et al. 2001). However, the insertion of a transposon in the AroA gene restricts virulence and produces a milder disease time course, facilitating experimental investigation in this model (Hoiseth and Stocker 1981).

S. Typhimurium induces a robust peripheral inflammatory response for 3 weeks post infection, with elevations of the proinflammatory cytokines IFN-γ, IL-1β and IL-12 in the blood and spleen (Püntener et al. 2012). Significant increases in brain IL-1β and IL-12 are additionally described at this time point. In this chapter, the *S.* Typhimurium model has been utilised to investigate whether the inflammation following a bacterial infection has the capacity to induce tau phosphorylation in adult wild-type mice. With the engagement of both the innate and adaptive branches of the immune system, *S.* Typhimurium may

provide the chronic and diverse inflammatory response required to elicit the phosphorylation of the tau protein.

Adult (3-4 month old) C57BL/6 wild-type mice were infected with *S.* Typhimurium. Tissue was taken at acute time points of 1 and 4 weeks, when inflammation is at its highest, and at later time points of 8 and 24 weeks post infection, when the bacteria is reported to have already been cleared (McSorley and Jenkins 2000; Mittrucker and Kaufmann 2000; Cunningham et al. 2007). Although an acute cytokine elevation in the brain may be sufficient for inducing tau phosphorylation, chronic exposure to this inflammation may additionally be important and separate the effects between bacterial infection and the multiple LPS model.

The hypothesis for this chapter mirrors that of the previous chapter using multiple LPS, whereby inflammation induced in the periphery propagates to the brain and causes the activation of immune cells such as the microglia. I hypothesize that the activation of this cell type and others, results in the release of inflammatory cytokines in the brain parenchyma, and the subsequent phosphorylation of the tau protein in neurons. However, I believe the prolonged and diverse nature of the inflammation resulting from *S.* Typhimurium will provide the difference in triggering this final step.

4.2 Materials and Methods

4.2.1 Study Design

S. Typhimurium Infection

Three days before infection, adult (3-4 months old) C57BL/6 wild-type mice were randomly assigned to one of eight groups (n=8, female) and relocated into the CL2 facility for acclimatisation. Mice in these groups received saline or *S.* Typhimurium and tissue was collected 1 week, 4 weeks, 8 weeks or 24 weeks post infection. Mice were injected (i.p.) with 200µl of saline or $1x10^6$ CFU S. *Typhimurium* (SL3261, (Hoiseth and Stocker 1981)). Mice were weighed daily after infection, or saline injection, for one week, once weekly for 4 weeks and once monthly thereafter. At indicated time points, mice received an overdose of anaesthetic (Rat Avertin) prior to the collection of blood. The thoracic cavity was exposed, an incision made in the right atrium and blood was collected (0.5-1ml) for later analysis of serum, followed by transcardial perfusion with 0.9% heparinised saline. Brain and spleen were taken for bioanalysis. Further details of methods used for tissue analysis are outlined in chapter 2.

4.3 Results

4.3.1 Metabolic and peripheral immune response in adult wild-type mice infected with *S.* Typhimurium

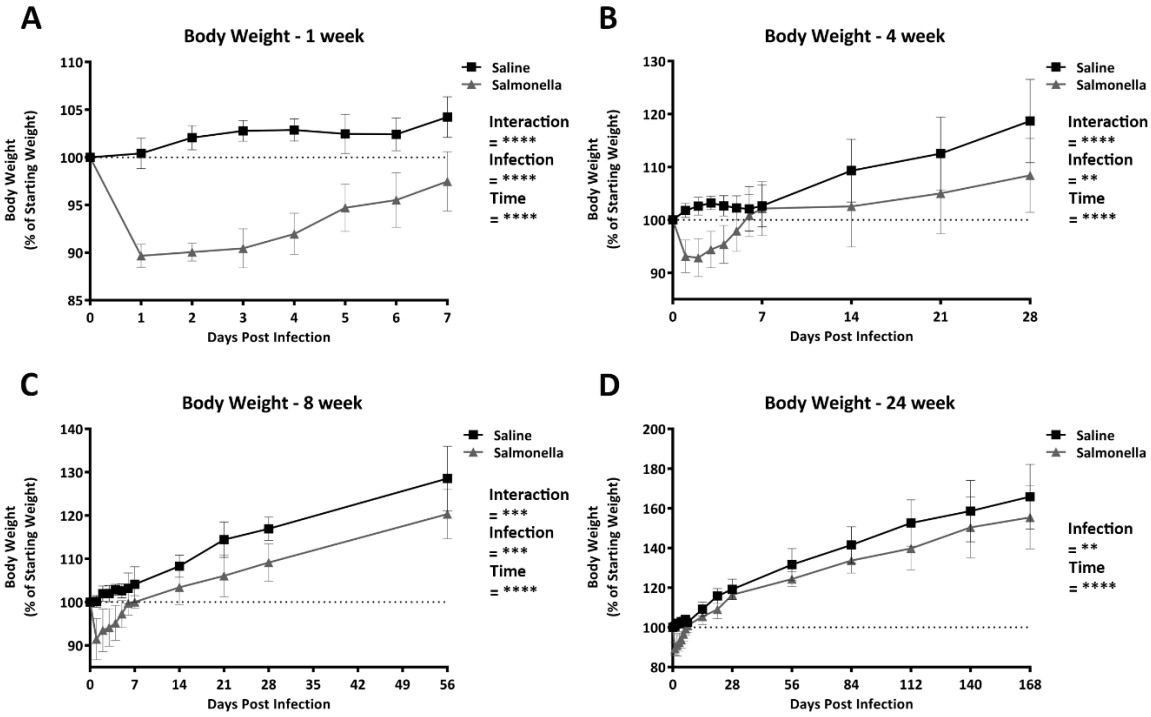

E

Body Weight Experiment	****	***	**	*
1 week	Day 1,2,3,4,5,6,7			
4 week		Day 2,28	Day 1,3	Day 4,14,21
8 week	Day 1,2	Day 3,4,21,28,56		Day 5
24 week	-	-	-	-

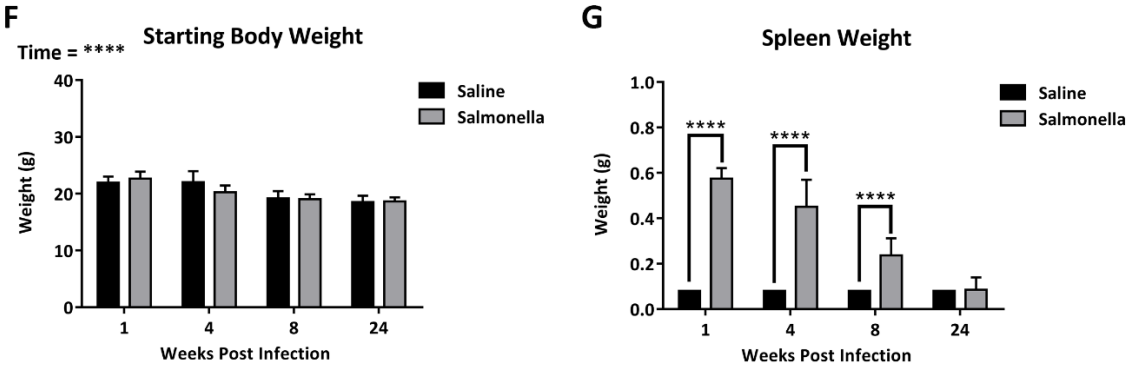

Fig 4.1:- Body and spleen weight from adult wild-type mice infected with S. Typhimurium. Mice were weighed daily after infection, or saline injection, for one week, once weekly for 4 weeks and once monthly thereafter. (A) Body weight (% of starting weight) of adult wild-type mice infected with *S.* Typhimurium for 1 week (A), 4 weeks (B), 8 weeks (C) or 24 weeks (D). (E) Table of post hoc statistics from adult wild-type mice infected with *S.* Typhimurium for 1 week, 4 weeks, 8 weeks or 24 weeks. (F) Starting body weights (grams) of adult wild-type mice. (G) Spleen weight (grams) of adult wild-type mice at sacrifice. Data was analysed by 2-way ANOVA and Tukey post hoc test (n=8), and displayed as mean + SD.

One day post infection, mice administered with *S.* Typhimurium displayed a mean weight loss of 9% (1.8g) across all groups, in comparison to a 1% (0.2g) increase observed in saline-injected control groups (Fig 4.1A,B,C,D). Analysis indicated a significant effect of time ($p \leq 0.0001$) and infection (1wk: $p \leq 0.0001$, 8wk: $p \leq 0.001$, 4 and 24wk: $p \leq 0.01$) over the duration of all experiments. Additionally, an interaction between these factors was observed in the 1, 4 and 8 week groups. Post hoc analysis indicated a statistical difference between saline and S. Typhimurium for at least 4 days in these groups, before mice infected with S. Typhimurium regained weight after this initial loss (Fig 4.1E). In the 4 and 8 week groups, the weights between mice receiving saline or S. Typhimurium converged at approximately 7 days, before diverging again with a significant difference seen at days 14, 21, 28 and 56. Although weights remained lower in S. Typhimurium groups, a similar rate of increase was observed from 7 days onwards.

A significant effect of time was observed in the starting body weight of groups analysed (Fig 4.1F). The mean starting body weights of the 1, 4, 8 and 24 weeks groups were 22.3g, 21.1g, 19.1g and 18.6g respectively. Upon sacrifice, a significantly higher spleen weight was seen 1 (7-fold), 4 (6-fold) and 8 (3-fold) weeks post infection with *S.* Typhimurium compared to those injected with saline ($p \leq 0.0001$) (Fig 4.1G).

Serum - IFN-γ

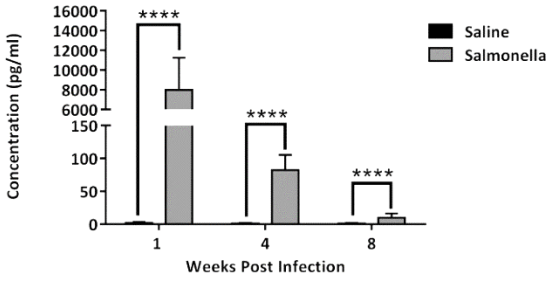

Serum - IL-1β

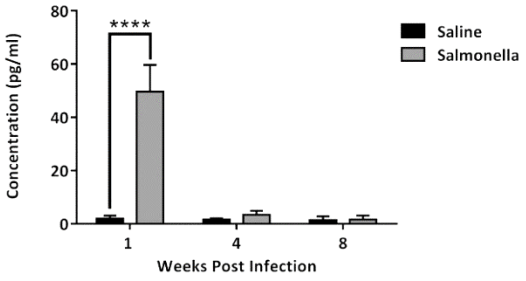

Serum - IL-6

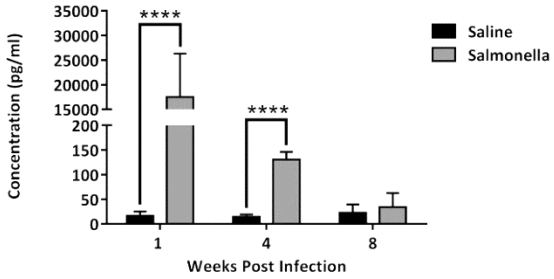

Serum - TNF-α

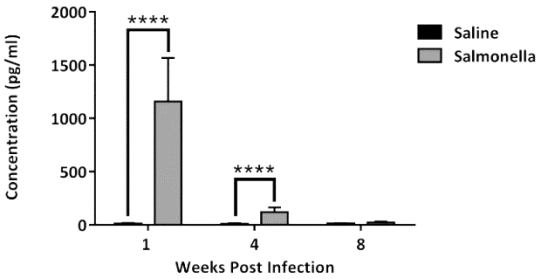

Serum - IL-10

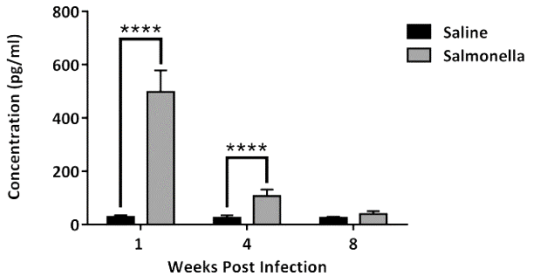

Serum - IL-12

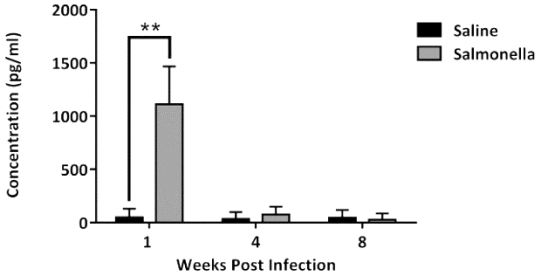

Serum - IL-2

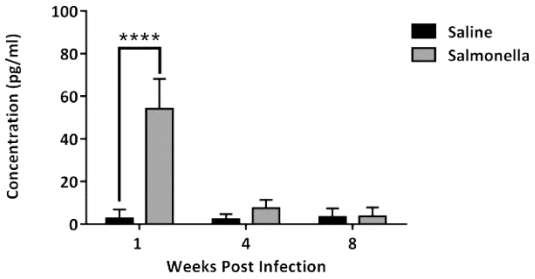

Serum - IL-4

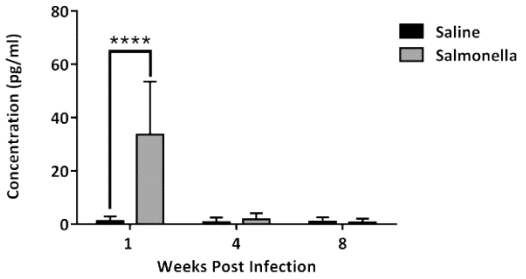

Serum - IL-5

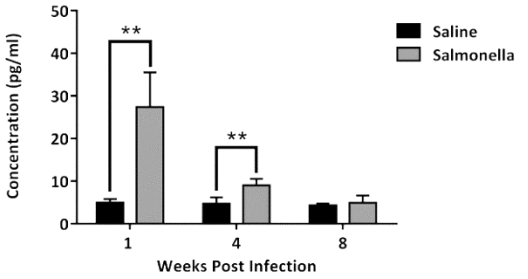

Serum - mKC

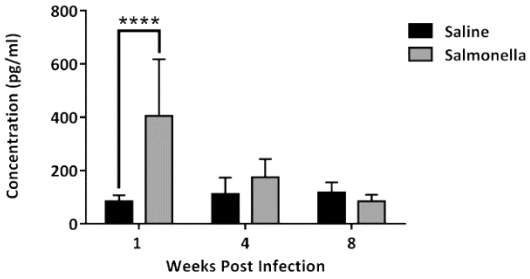

Fig 4.2:- Cytokine expression levels in serum from adult wild-type mice infected with S. Typhimurium. Cytokine levels (pg/ml) in serum from adult wild-type mice 1, 4 or 8 weeks post infection with S. Typhimurium, or injection with saline. Data was analysed by 2-way ANOVA and Tukey post hoc test (n=6), and displayed as mean + SD.

Circulating levels of cytokines were measured in serum samples using a 10-plex immunoassay (Fig 4.2).

One week post infection, S. Typhimurium induced a significant increase in the inflammatory cytokines IFN-γ (4834-fold, $p \leq 0.0001$), IL-1β (23-fold, $p \leq 0.0001$), IL-6 (1153-fold, $p \leq 0.0001$), TNF-α (98-fold, $p \leq 0.0001$), IL-10 (23-fold, $p \leq 0.0001$), IL-12 (11-fold, $p \leq 0.01$), IL-2 (12-fold, $p \leq 0.0001$), IL-4 (14-fold, $p \leq 0.0001$), IL-5 (6-fold, $p \leq 0.01$) and mKC (5-fold, $p \leq 0.0001$) compared to saline-injected control mice.

Four weeks post infection, S. Typhimurium induced a significant increase in the inflammatory cytokines IFN-γ (74-fold, $p \leq 0.0001$), IL-6 (9-fold, $p \leq 0.0001$), TNF-α (11-fold, $p \leq 0.0001$), IL-10 (4-fold, $p \leq 0.0001$) and IL-5 (1.9-fold, $p \leq 0.01$) compared to saline-injected control mice.

Eight weeks post infection, S. Typhimurium induced a significant increase in the proinflammatory cytokine IFN-γ (8-fold, $p \leq 0.0001$) compared to saline-injected control mice. As the majority of cytokines were back to baseline by 8 weeks, serum cytokines at 24 weeks post infection were not analysed.

4.3.2 Neuroinflammatory response in adult wild-type mice infected with S. Typhimurium

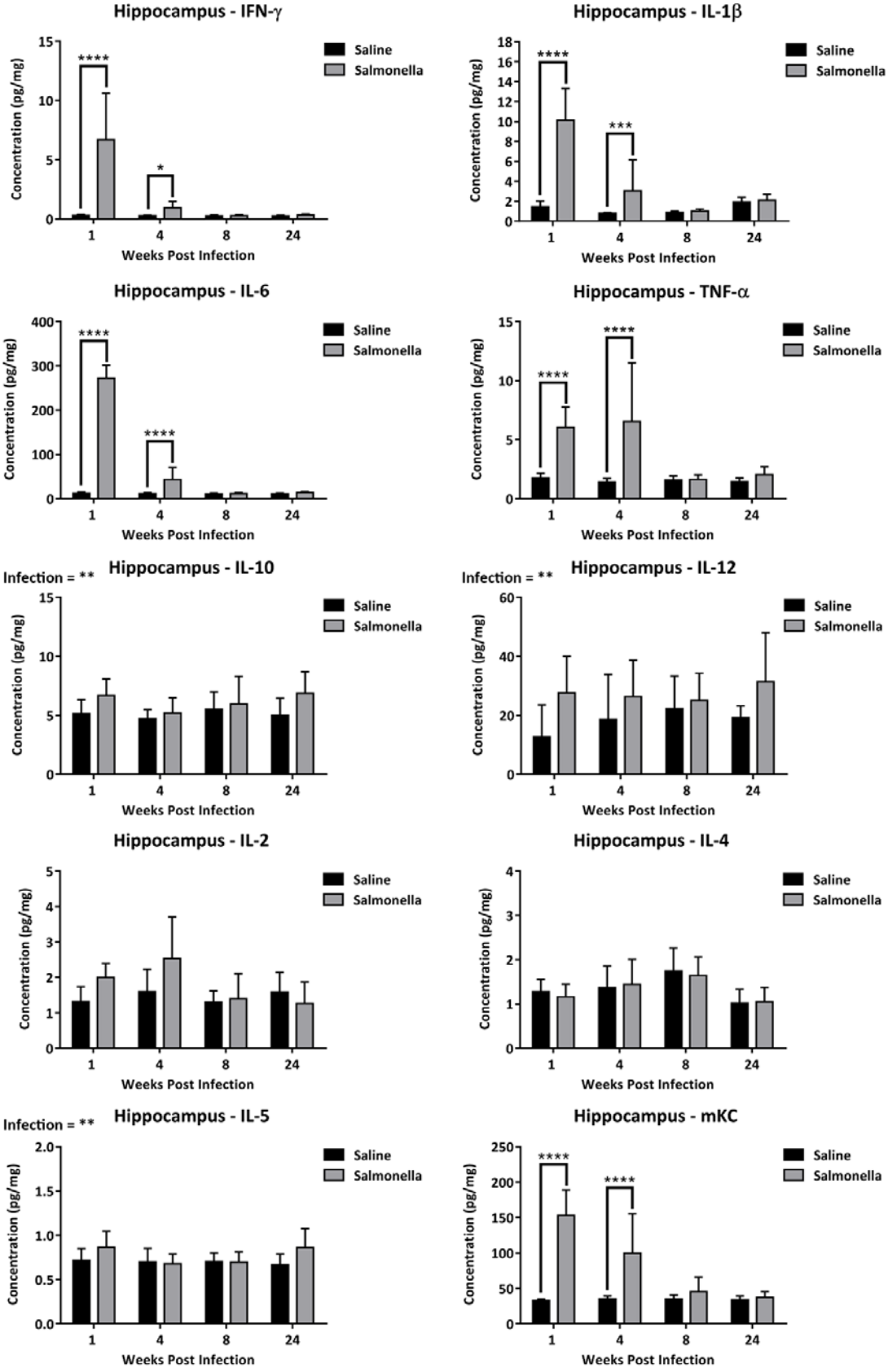

Fig 4.3:- Cytokine expression levels in hippocampal-enriched tissue from adult wild-type mice infected with S. Typhimurium. Cytokine levels (pg/mg of total protein) in hippocampal-enriched tissue homogenate from adult wild-type mice 1, 4, 8 or 24 weeks post infection with S. Typhimurium, or injection with saline. Data was analysed by 2-way ANOVA and Tukey post hoc test (n=6-8), and displayed as mean + SD.

Levels of brain cytokines were measured in hippocampal-enriched tissue homogenate using a 10-plex immunoassay (Fig 4.3).

One week post infection, S. Typhimurium induced a significant increase in the proinflammatory cytokines IFN-γ (23-fold, $p \leq 0.0001$), IL-1β (7-fold, $p \leq 0.0001$), IL-6 (22-fold, $p \leq 0.0001$), TNF-α (3-fold, $p \leq 0.0001$) and mKC (5-fold, $p \leq 0.0001$) compared to saline-injected control mice.

Four weeks post infection, S. Typhimurium induced a significant increase in the proinflammatory cytokines IFN-γ (3-fold, $p \leq 0.05$), IL-1β (4-fold, $p \leq 0.001$), IL-6 (4-fold, $p \leq 0.0001$), TNF-α (5-fold, $p \leq 0.0001$) and mKC (3-fold, $p \leq 0.0001$) compared to saline-injected control mice.

No significant changes were observed at the 8 and 24 week time points, in any of the cytokines assessed.

4.3.3 Neurochemistry in adult wild-type mice infected with *S*. Typhimurium

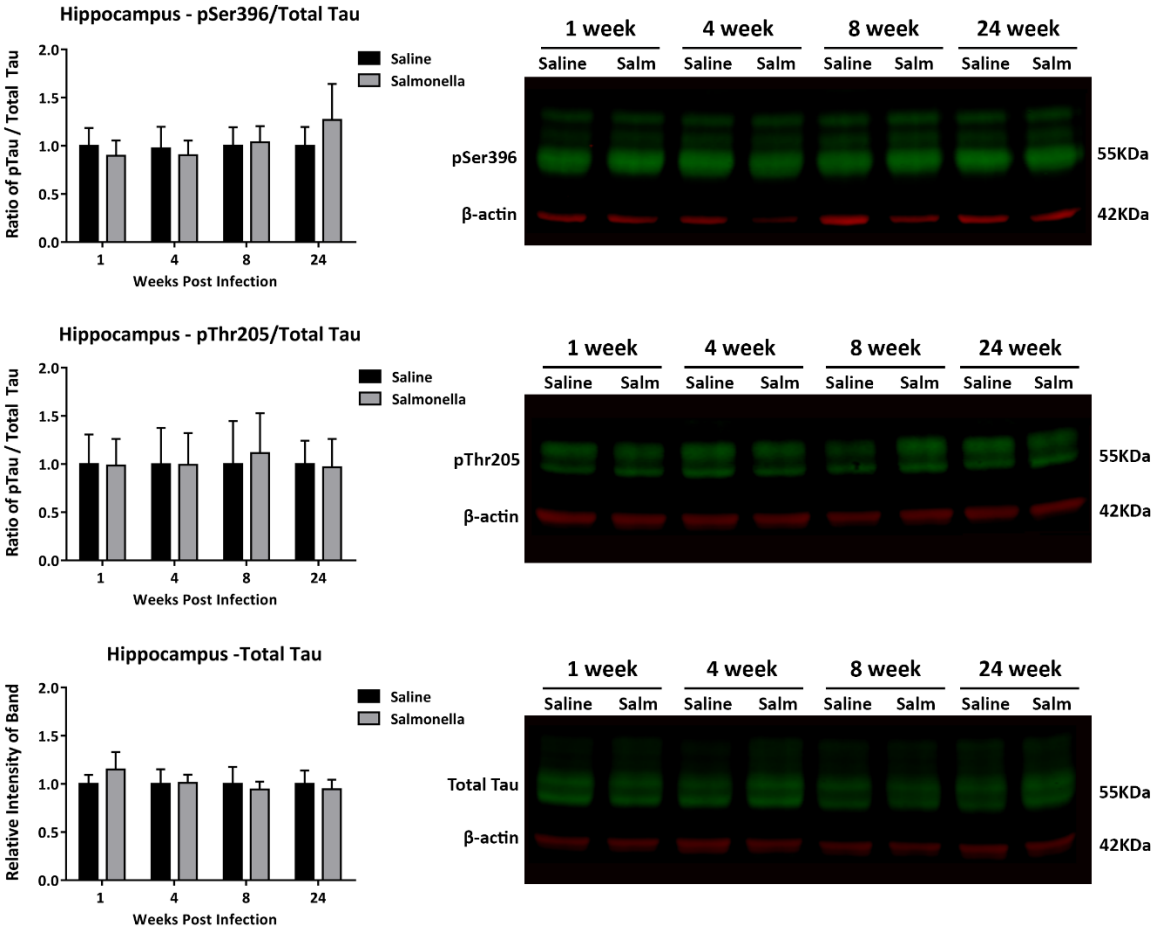

Fig 4.4:- Phosphorylated- and total tau expression levels in hippocampal-enriched tissue from adult wild-type mice infected with S. Typhimurium. Expression of pSer396 and pThr205 (ratio of ptau/total tau), and total tau levels (relative intensity) in hippocampal-enriched homogenate from adult wild-type mice 1, 4, 8 or 24 weeks post infection with S. Typhimurium, or injection with saline. Representative western blot membranes showing tau (green) and β-actin (red) immunoreactivity, with the latter used for normalisation of protein loading. Data was analysed by 2-way ANOVA and Tukey post hoc test (n=8), and displayed as mean + SD.

To investigate the impact of S. Typhimurium infection on tau-related neurochemistry in the brain, total and phosphorylated-tau levels were measured in hippocampal-enriched tissue homogenate by western blot (Fig 4.4).

Quantification of the tau-related immunoreactive bands obtained from western blot showed no significant change following S. Typhimurium infection, with respect to pSer396, pThr205 or total tau levels.

4.4 Discussion

There is evidence that infections, and resulting systemic inflammation, are a risk factor for the development of neurodegenerative diseases such as AD (Barichello et al. 2015; Lim et al. 2015; McManus and Heneka 2017). In the previous chapter, a multiple systemic LPS model was utilised to mimic aspects of a bacterial infection and investigate consequences to the CNS. Despite robust neuroinflammation observed following a single challenge, multiple injections resulted in an attenuated inflammatory response in the brain suggesting the development of ET. Furthermore, neither single nor multiple LPS paradigms elicited tau phosphorylation in these wild-type models. Reasoning that multiple LPS challenges may poorly replicate the effects of a bacterial infection; in this chapter, an attenuated bacterial strain of *S.* Typhimurium was utilised to address this issue. In addition to the characterisation of short- and long-term central and peripheral inflammatory effects, investigation was undertaken into whether this model of systemic inflammation has the capacity to induce tau phosphorylation in wild-type mice.

Systemic inflammation elicits numerous sickness behaviours including a reduced motivation for food and fluids (Hart 1988; Pardon 2015). This can be measured as a decrease in weight and tracked throughout the experimental protocol as a useful readout of metabolic response. Mice infected with *S.* Typhimurium displayed an initial mean weight loss of 9% from starting body weight, perhaps reflective of initial sickness behaviours triggered by LPS found on *S.* Typhimurium. Following this initial decrease, weight was regained over a 1 week duration, as previously described (Püntener et al. 2012), likely due to compensatory mechanisms governed by the hypothalamus (Perry and Wang 2012). Splenomegaly was demonstrated in infected mice with significantly increased spleen weight at 1, 4 and 8 weeks post infection with *S.* Typhimurium. Commonly this increase is attributed to recruitment and expansion of phagocyte and lymphocyte populations, although large increases in the numbers of immature red blood cells are additionally reported (Jackson et al. 2010).

Furthermore, serum cytokines were analysed to investigate the peripheral response to *S.* Typhimurium. All cytokines assessed were significantly increased 1 week following infection. After i.p administration of *S.* Typhimurium, the initial stages of innate immune

response allow clearance of bacteria from the blood by phagocytes in the spleen and liver (Dunlap et al. 1991). Macrophages phagocytose the bacteria, facilitated by antibodies and complement, while the *S.* Typhimurium itself forces its own uptake into the cell, ensuring intracellular survival of the pathogen (Muniz-Junqueira et al. 1997; Ramos-Morales and Francisco 2012). While antigens found on the surface of the bacteria, such as LPS, induce a strong inflammatory response as demonstrated by increases in IL-1β and IL-6, the early production of IFN-γ and TNF-α are crucial in inducing bactericidal mechanisms within macrophages (Nauciel and Espinasse-Maes 1992). During these initial stages, a number of cell populations such as macrophages, B cells and NK cells produce IFN-γ, enhanced by other cytokines such as IL-12. This crucially results in Th1 polarisation of T-cells, a critical step in elimination of the *S.* Typhimurium (Mizuno et al. 2003). Of particular relevance to this study, is the ongoing systemic inflammation in this model, demonstrated by the elevated levels of IFN-γ, IL-6, TNF-α, IL-10 and IL-5 observed at the 4 week time point. Furthermore, IFN-γ levels are increased in the serum 8 weeks following infection, and are thought to be produced by *S.* Typhimurium-specific Th1 cells in these later stages (VanCott et al. 1998). Overall, the data presented here demonstrates *S.* Typhimurium infection in the susceptible C57BL/6 strain causes a prolonged systemic inflammatory response. Evidence from the previous literature suggests engagement with a diverse range of cell types including macrophages, NK cells, dendritic cells, B-cells and T-cells, for eventual elimination of the bacteria by 40 days (for review see (Mittrucker and Kaufmann 2000)).

Next, cytokines levels in the hippocampus were investigated to establish the neuroinflammatory consequences of the *S.* Typhimurium infection. In comparison to the serum profile, changes in cytokine levels in the hippocampus were relatively restricted with the increase favouring a proinflammatory profile, including IFN-γ, IL-1β, IL-6, TNF-α and mKC. The levels of these cytokines peaked at 1 week but did show sustained expression up to the 4 week time point. The source of these cytokines was not explored in the context of these studies, and represents a critical area for further investigation. However, in the case of IFN-γ, IL-6 and TNF-α, there is a possibility that the elevations in brain cytokines are a result of increased circulating peripheral levels, as it has been shown cytokines can gain access to the brain parenchyma through cytokine transport systems in

the BBB (Banks et al. 1996; Pan et al. 1997). On the other hand, IL-1β and mKC serum cytokine levels are low at the 4 week time point, while hippocampal cytokine levels remain high. This may suggest that these particular mediators are being produced locally, by cells such as the endothelia, perivascular macrophages, astrocytes and microglia (Shaftel et al. 2008).

Our group has previously characterised the central and peripheral effects of *S.* Typhimurium infection on the periphery and brain, at 1 day, 1 week, 2 weeks and 3 weeks post infection (Püntener et al. 2012). The study reported a delayed neuroinflammatory response when compared to the periphery, with regard to elevation of cytokines. The data presented here shows the majority of cytokine levels in the brain peak at 1 week and are reduced by 4 weeks post infection. Therefore, although delayed local production of brain cytokines cannot be ruled out, intermediate time points are required to determine whether elevations continue between 1 and 4 weeks. Immunohistochemical analysis of cell activation revealed a modest upregulation of CD11b and CD68 on perivascular macrophages and microglia, in addition to high expression of MHCI, MHCII, VCAM-1 and ICAM-1 on the brain vasculature at 1 week post infection (Püntener et al. 2012). Therefore, it is reasonable to speculate that numerous cell types are responsible for the elevations in cytokines observed following infection, including microglia and cells associated with the vasculature such as perivascular macrophages and endothelial cells.

After gathering evidence of a prolonged exposure to elevated proinflammatory cytokines in the brain, hyperphosphorylation of tau protein was investigated. Despite evidence of neuroinflammation at 1 week and 4 weeks post infection, no significant changes in tau phosphorylation were observed at these time points. Additionally, no changes were observed at the later time points of 8 and 24 weeks post infection. Increased tau phosphorylation has previously been observed in studies utilising neurotrophic viruses such as mouse hepatitis virus (MHV) and herpes simplex virus type 1 (HSV-1), and in transgenic rats demonstrating characteristics of human immunodeficiency virus (HIV-1) (Sy et al. 2011; Álvarez et al. 2012; Cho et al. 2017). Additionally, Gasparotto and colleagues demonstrated increased tau phosphorylation at the Ser396 epitope, in the cortex of BALB/c mice, 16 weeks following infection with the parasite L. *amazonensis* (Gasparotto et al. 2015). Interestingly, no changes were reported in protein levels of TNF-

α and IL-1β in the cortex and phosphorylation was reduced in these mice using an antioxidant therapy (NAC). This may indicate that, although the induction of tau phosphorylation by proinflammatory cytokines is well established (Zilka et al. 2012), other mechanisms such as oxidative stress, may be critical in certain circumstances.

In conclusion, mice infected with *S.* Typhimurium provide a model of systemic inflammation characterised by peripheral and central inflammation for at least 4 weeks. This model has an advantage over commonly utilised multiple LPS protocols which are subject to the rapid development of ET and subsequent attenuation of the inflammatory response. Although not investigated in this study, previous reports suggest the engagement of numerous immune pathways and cell types in both the periphery and the brain (Mittrucker and Kaufmann 2000; Püntener et al. 2012), allowing greater insight into the time course and effects of infection encountered in a real world scenario. With elevated brain cytokine levels observed following infection, this study would benefit from examination of central and peripheral sources in order to decipher the contributions of each cell type.

Despite evidence of neuroinflammation, induction of tau phosphorylation was not observed, analogous to results obtained in the multiple LPS study. Other mechanisms, such as increased oxidative stress, may be more critical in tau phosphorylation induction than the elevations of certain proinflammatory cytokines in the brain. In addition to alternative mechanisms, the circumstance under which systemic inflammation is encountered, may be imperative. The mice infected with *S.* Typhimurium or subjected to multiple LPS challenges, were 3-4 months old, an age equivalent to a young human adult (Dutta and Sengupta 2016). Neurodegenerative conditions, such as LOAD, do not develop until advanced age (Kukull et al. 2002). It is likely that the mechanisms in place to resolve inflammation in a healthy manner are fully functional in adults (Serhan and Petasis 2011), and therefore pathological tau phosphorylation is not observed in these models of systemic inflammation.

Chapter 5: Multiple LPS challenge and salmonella infection in middle-aged and adult wild-type mice

5.1 Introduction

In chapter 3, it was demonstrated that multiple challenges of LPS, result in a moderate peripheral and central immune response. This model generates an attenuated cytokine response that likely differs from infections encountered in a real-world scenario. To address this issue in chapter 4, the level of peripheral and central inflammation was assessed following infection with an attenuated strain of the bacteria of *S*. Typhimurium. However, despite evidence of neuroinflammation in both models of systemic inflammation, alterations in tau phosphorylation were not observed in adult wild-type mice. This may suggest that additional factors are required, in order for systemic inflammation to have a deleterious influence on tau phosphorylation.

One possible pre-requisite to the induction of tau phosphorylation is ageing, the single biggest risk factor for AD (Niccoli and Partridge 2012). Numerous changes occur to the immune system as a result of age-induced immune senescence (Dorshkind and Swain 2009). These include a functional decline in the adaptive branch, while the innate immune response is maintained resulting in a heightened inflammatory state termed inflammaging (Tamas Fulop et al. 2016). This is characterised by increases in oxidative stress and levels of proinflammatory cytokines, such as IL-6, in both serum and CSF (Guest et al. 2014; Tegeler et al. 2016).

A consequence of inflammaging is thought to be an increased sensitisation of certain immune cells, such as microglia, known as priming (Perry and Teeling 2013). Microglia upregulate cell surface markers, such as MHCII, in a primed state, and are capable of producing an exaggerated response to an inflammatory stimulus. For example, Godbout et al showed that systemic inflammation, induced by i.p. administration of LPS (10ug/mouse), administered to aged (20-24 month old) wild-type mice, resulted in exaggerated cortical levels of IL-1β mRNA compared to adult (3-4 month old) animals (Godbout et al. 2005). However, studies using real infections are lacking, and therefore I

set out in this chapter to address this issue by utilising *S*. Typhimurium infection in a model of ageing, and comparing the effects on neuroinflammation and tau pathology to multiple challenges of LPS.

Although extensive pathological and inflammatory changes to the brain occur in the later stages of AD, there is evidence that these alterations begin decades before symptoms arise (Reiman et al. 2012; Rodriguez-Vieitez et al. 2016). Additionally, research shows elevated serum levels of the acute phase protein C-reactive protein (CRP) at middle-age are associated with heightened risk of the development of dementia (Schmidt et al. 2002; Komulainen et al. 2007). Therefore, investigating the middle-age time window may be beneficial in identifying the earliest causes in AD.

In this study, middle-aged (11-12 month old) and adult (3-4 month old) wild-type mice were exposed to two models of systemic inflammation. Firstly, mice were challenged with multiple injections of LPS (0.5mg/kg) or saline over the course of 4 weeks. Additionally, one group of adult mice received a single injection of LPS followed by saline challenges to assess whether the changes observed in the multiple LPS group, were a result of this chronic set of insults or a lasting effect of the first LPS injection. Secondly, mice were infected with *S*. Typhimurium and tissue taken 4 weeks later. This time point was chosen as I have previously shown in chapter 4, that inflammation still persists in the brain while the infection is in the later stages of resolution. Additionally, this allows for comparison between the two models.

Measurements of serum and brain cytokine levels were taken and immune cell marker expression assessed, to investigate the activation of peripheral and central immune cells respectively. The resulting changes may also indicate whether an exaggerated immune response occurs, firstly, in middle-aged mice and, secondly, following each model of systemic inflammation. Finally, tau phosphorylation was analysed to evaluate whether systemic inflammation elicits pathology aligned with the earliest stages of a neurodegenerative disorder.

I hypothesize that inflammaging, as well as priming of immune cells, occurs at middle age and will result in an exaggerated peripheral and central immune response as measured by proinflammatory cytokine levels and immune cell receptor expression. In turn, the

increased activation of inflammatory pathways in the brain will elicit tau phosphorylation. The studies described herein aim to substantiate this hypothesis.

5.2 Materials and Methods

5.2.1 Study Design

Multiple LPS

Middle-aged (11-12 month old) and adult (3-4 month old) wild-type mice were randomly assigned to one of two groups (n=6-8, female), saline or LPS. Mice were injected 8x (i.p.) with 200µl of saline or LPS (0.5mg/kg) over the course of 4 weeks, and referred to as saline and multiple LPS respectively. A third group of adult mice (3-4 months old), referred to as single LPS, received 1 injection of LPS (0.5mg/kg) followed by 7 injections of saline (200µl), over the course of 4 weeks. Mice were weighed on the day of injection and 24 hours post injection throughout the experiment. Mice were given an overdose of anaesthetic (Rat Avertin) prior to the collection of blood. An incision was made in the right atrium and blood was collected (0.5-1ml) for later analysis of serum, followed by transcardial perfusion with 0.9% heparinised saline. Brain and spleen were taken for bioanalysis. Further details of methods used for tissue analysis are outlined in chapter 2.

***S*. Typhimurium Infection**

Three days before infection, middle-aged (11-12 month old) and adult (3-4 month old) wild-type mice were randomly assigned to one of two groups (n=6-8, female), saline or *S*. Typhimurium and relocated into the CL2 facility for acclimatisation. Mice were injected (i.p.) with 200µl of saline or $1x10^6$ CFU *S*. Typhimurium. Mice were weighed daily for 1 week and weekly thereafter. Mice were given an overdose of anaesthetic (Rat Avertin) prior to the collection of blood. An incision was made in the right atrium and blood was collected (0.5-1ml) for later analysis of serum, followed by transcardial perfusion with 0.9% heparinised saline. Brain and spleen were taken for bioanalysis. Further details of methods used for tissue analysis are outlined in chapter 2.

5.3 Results

5.3.1 Metabolic and peripheral immune response following multiple LPS challenge and *S*. Typhimurium infection in middle-aged and adult wild-type mice

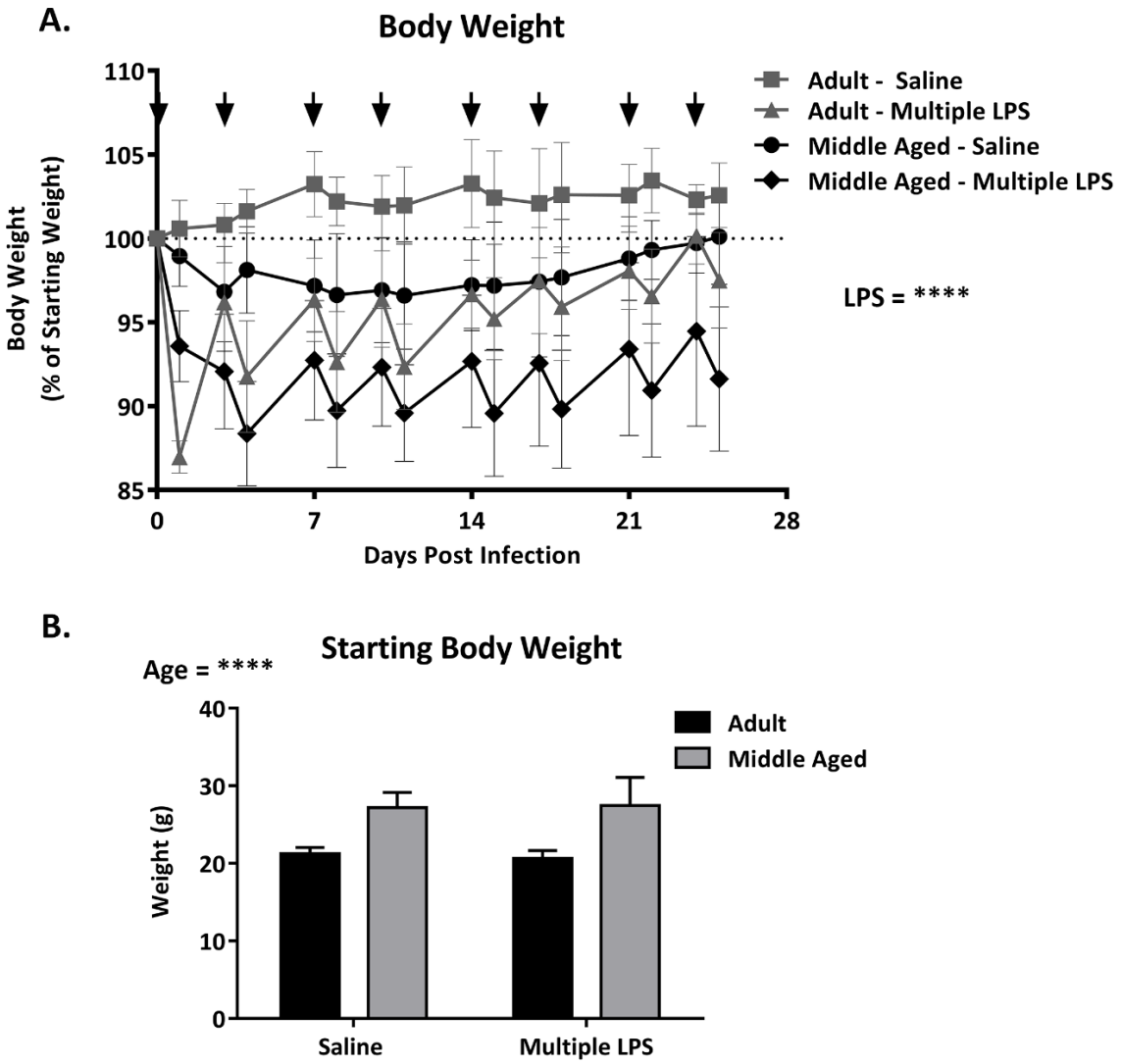

Fig 5.1:- Body and spleen weight from middle-aged and adult wild-type mice challenged with multiple LPS injections. Mice were weighed on the day of and 24 hours after each LPS (0.5mg/kg) or saline injection throughout the experiment (A) Body weight (% of starting weight) of middle-aged and adult wild-type mice challenged with multiple LPS or saline injections. Data was analysed using 3-way ANOVA with repeated measure (n=6-8), and displayed as mean ± SD. (B) Starting body weights (grams) of middle-aged and adult wild-type mice. Data was analysed by 2-way ANOVA and Tukey post hoc test (n=6-8), and displayed as mean + SD.

One day following the first LPS injection, mice displayed a weight loss of approximately 6% (1.8g) and 13% (2.8g) from starting weight, in middle-aged and adult mice respectively (Fig 5.1A). Analysis indicated a significant difference in body weight throughout the 4 week period between mice challenged with multiple LPS injections and those receiving saline as control ($p \leq 0.0001$). Adult mice administered with LPS injections recovered to approximately 5% below starting weight on the day of the second injection and subsequently lost 5% body weight upon second LPS challenge. These mice recovered to starting weight by day 24 (8^{th} injection). In contrast, middle-aged mice administered with LPS injections lost additional weight by the second day of LPS injection and subsequently lost a further 4% body weight upon second LPS challenge. These mice maintained body weight at approximately 7% below starting weight for the duration of the experiment.

Weight data demonstrate middle-aged mice had a significantly higher starting body weight compared to adults ($p \leq 0.0001$), of approximately 7 grams (Fig 5.1B).

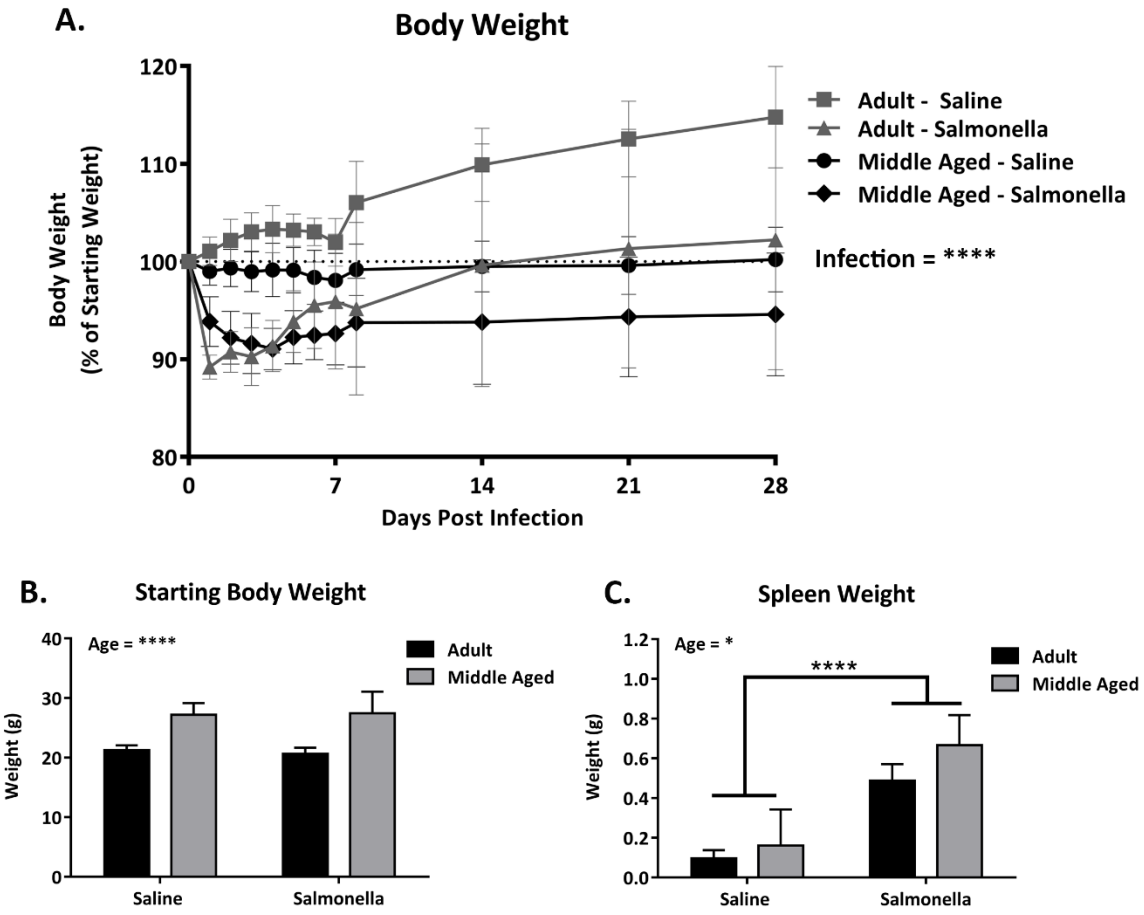

Fig 5.2:- Body and spleen weight from middle-aged and adult wild-type mice infected with S. Typhimurium. Mice were weighed daily after infection, or saline injection, for one week, and then once weekly thereafter. (A) Body weight (% of starting weight) of middle-aged and adult wild-type mice infected with S. Typhimurium. Data was analysed using 3-way ANOVA with repeated measures (n=6-8), and displayed as mean ± SD. (B) Starting body weight (grams) of middle-aged and adult wild-type mice. (C) Spleen weight (grams) of middle-aged and adult wild-type mice at sacrifice. Data was analysed by 2-way ANOVA and Tukey post hoc test (n=6-8), and displayed as mean + SD.

One day post infection, mice administered with *S*. Typhimurium displayed a weight loss of approximately 6% (1.6g) and 10% (2.2g) from starting weight, in middle-aged and adult mice respectively (Fig 5.2A). Analysis indicated a significant difference in body weight throughout the 4 week period between mice infected with *S*. Typhimurium and those receiving saline as control ($p \leq 0.0001$). Additionally, a trend towards differences in age was observed but did not reach statistical significance ($p=0.058$). At 14 days, adult mice infected with *S*. Typhimurium regained weight up to starting body weight. In contrast, middle-aged mice receiving *S*. Typhimurium maintained weight 5% below starting body weight for the duration of the 4 weeks.

Weight data demonstrate middle-aged mice had a significantly higher starting body weight compared to adults ($p \leq 0.0001$), of approximately 6 grams (Fig 5.2B). Upon sacrifice at 28 days post infection, a significantly higher spleen weight was observed in mice infected with *S*. Typhimurium compared to those injected with saline ($p \leq 0.0001$) (Fig 5.2C). Additionally, middle-aged mice had a greater spleen weight than the adult wild types, of approximately 0.08 grams ($p \leq 0.05$).

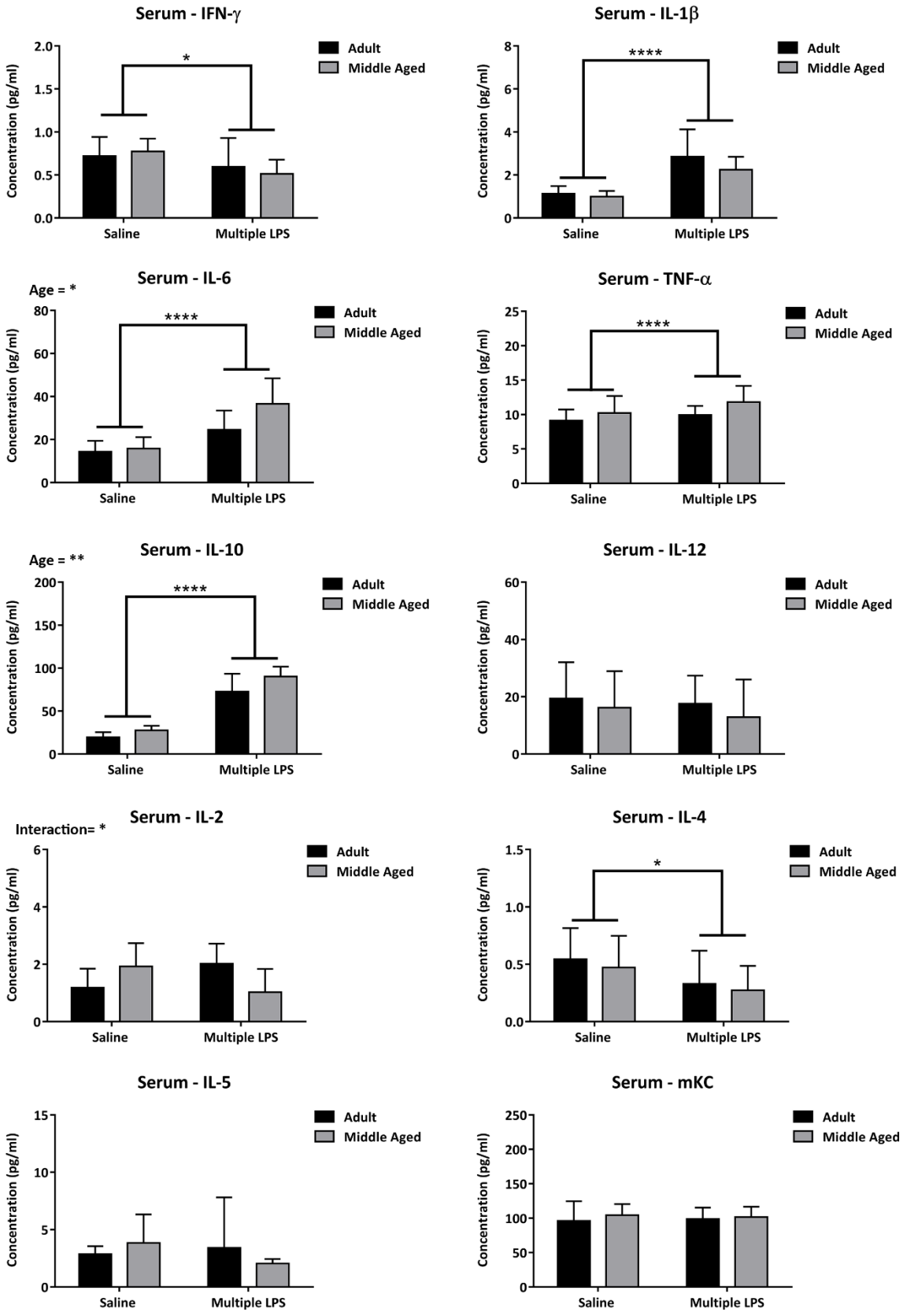
Serum - IFN-γ
Concentration (pg/ml)
2.0
1.5
1.0
0.5
0.0
*
Saline
Multiple LPS
Adult
Middle Aged
Serum - IL-1β
Concentration (pg/ml)
8
6
4
2
0
****
Saline
Multiple LPS
Adult
Middle Aged
Serum - IL-6
Age = *
Concentration (pg/ml)
80
60
40
20
0
****
Saline
Multiple LPS
Adult
Middle Aged
Serum - TNF-α
Concentration (pg/ml)
25
20
15
10
5
0
****
Saline
Multiple LPS
Adult
Middle Aged
Serum - IL-10
Age = **
Concentration (pg/ml)
200
150
100
50
0
****
Saline
Multiple LPS
Adult
Middle Aged
Serum - IL-12
Concentration (pg/ml)
60
40
20
0
Saline
Multiple LPS
Adult
Middle Aged
Serum - IL-2
Interaction= *
Concentration (pg/ml)
6
4
2
0
Saline
Multiple LPS
Adult
Middle Aged
Serum - IL-4
Concentration (pg/ml)
1.5
1.0
0.5
0.0
*
Saline
Multiple LPS
Adult
Middle Aged
Serum - IL-5
Concentration (pg/ml)
15
10
5
0
Saline
Multiple LPS
Adult
Middle Aged
Serum - mKC
Concentration (pg/ml)
250
200
150
100
50
0
Saline
Multiple LPS
Adult
Middle Aged

Fig 5.3:- Cytokine expression levels in serum from middle-aged and adult wild-type mice challenged with multiple LPS injections. Cytokine levels (pg/ml) in serum from middle-aged or adult wild-type mice following 8 injections of LPS or saline. Data was analysed by 2-way ANOVA and Tukey post hoc test (n=6-8), and displayed as mean + SD

Circulating levels of cytokines were measured in serum samples using a 10-plex immunoassay (Fig 5.3).

Multiple challenges of LPS induced a significant increase in the proinflammatory cytokines IL-1β (3-fold, $p \leq 0.0001$), IL-6 (2-fold, $p \leq 0.05$), TNF-α (1.1-fold, $p \leq 0.01$) and IL-10 (3-fold, $p \leq 0.01$), and a significant decrease in IFN-γ (1.3-fold, $p \leq 0.01$) and IL-4 (2-fold, $p \leq 0.01$), compared to saline-injected control mice. Additionally, middle-aged mice had increased levels of IL-6 (1.3-fold, $p \leq 0.05$) and IL-10 (1.2-fold, $p \leq 0.01$) compared to adult wild types. An interaction was observed in IL-2 ($p \leq 0.05$) suggesting while adult mice increase levels of this cytokine in response to multiple LPS, middle-aged mice show the opposite effect. This data suggests a moderate proinflammatory response is still elicited in the periphery of both middle-aged and adult wild-type mice, in response to multiple challenges of LPS.

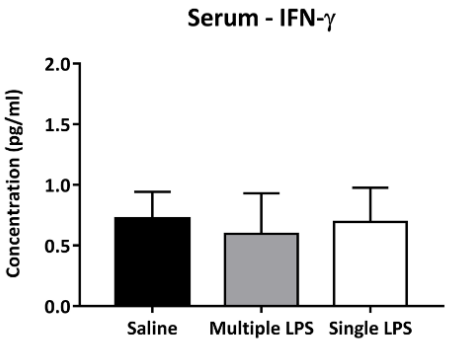
Serum - IFN-γ
Concentration (pg/ml)
2.0
1.5
1.0
0.5
0.0
Saline
Multiple LPS
Single LPS

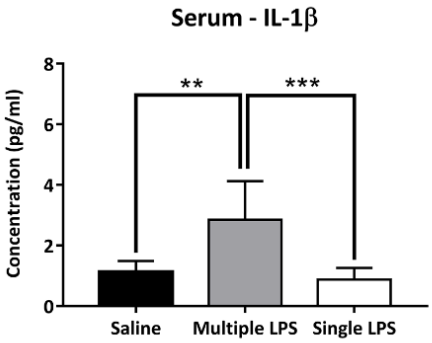
Serum - IL-1β
Concentration (pg/ml)
8
6
4
2
0
**
***
Saline
Multiple LPS
Single LPS

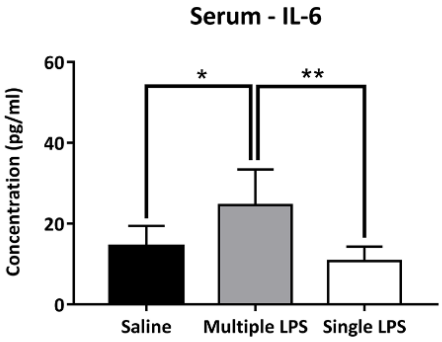
Serum - IL-6
Concentration (pg/ml)
60
40
20
0
*
**
Saline
Multiple LPS
Single LPS

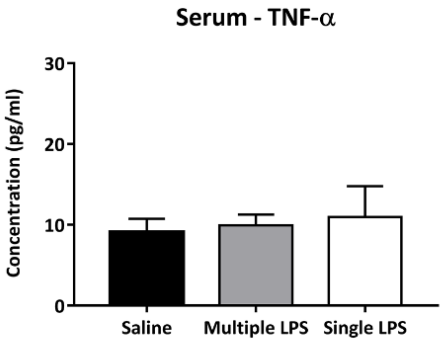
Serum - TNF-α
Concentration (pg/ml)
30
20
10
0
Saline
Multiple LPS
Single LPS

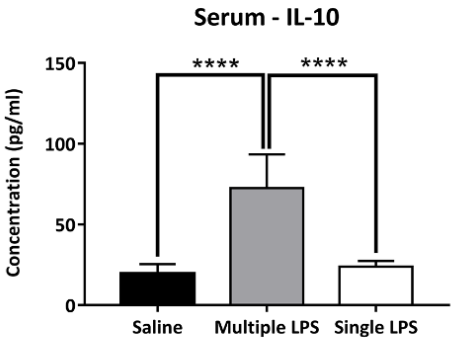
Serum - IL-10
Concentration (pg/ml)
150
100
50
0
****
****
Saline
Multiple LPS
Single LPS

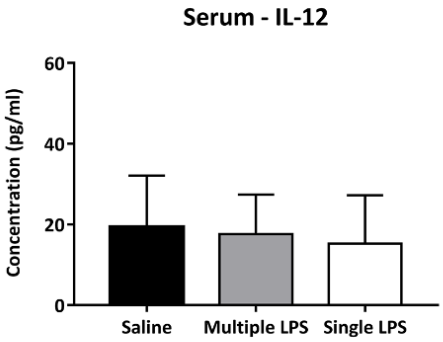
Serum - IL-12
Concentration (pg/ml)
60
40
20
0
Saline
Multiple LPS
Single LPS

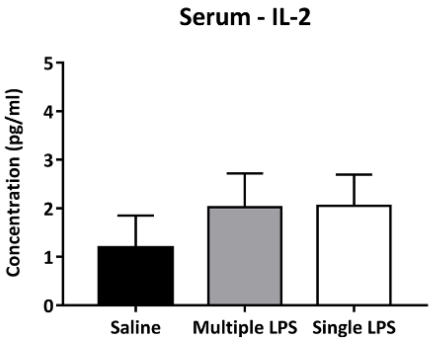
Serum - IL-2
Concentration (pg/ml)
5
4
3
2
1
0
Saline
Multiple LPS
Single LPS

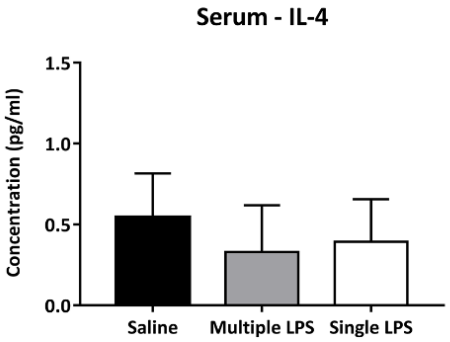
Serum - IL-4
Concentration (pg/ml)
1.5
1.0
0.5
0.0
Saline
Multiple LPS
Single LPS

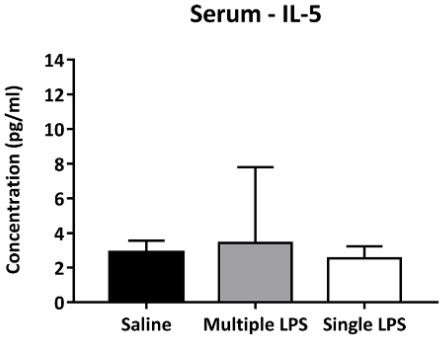
Serum - IL-5
Concentration (pg/ml)
14
12
10
8
6
4
2
0
Saline
Multiple LPS
Single LPS

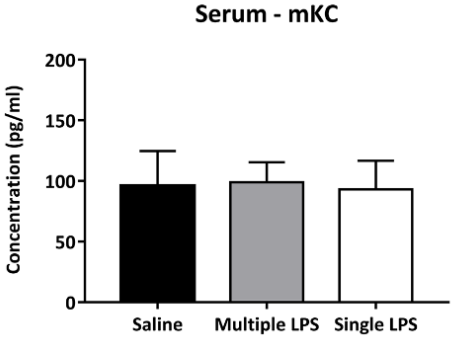
Serum - mKC
Concentration (pg/ml)
200
150
100
50
0
Saline
Multiple LPS
Single LPS

Fig 5.4:- Cytokine expression levels in serum from adult wild-type mice challenged with single or multiple LPS injections. Cytokine levels (pg/ml) in serum from adult wild-type mice, 24 hours post sacrifice, following injections of multiple LPS (8X), single LPS (1 x LPS, 7 x saline) or saline alone (8X). Data was analysed by 1-way ANOVA and Tukey post hoc test (n=6-8), and displayed as mean + SD.

Circulating levels of cytokines were measured in serum samples using a 10-plex immunoassay to compare differences between single and multiple challenges of LPS (Fig 5.4).

Multiple LPS challenges induced a significant increase in proinflammatory cytokines compared to single LPS challenge (IL-1β (3-fold, $p \leq 0.001$), IL-6 (2-fold, $p \leq 0.01$), IL-10 (3-fold, $p \leq 0.0001$)) and saline-injected control mice (IL-1β (3-fold, $p \leq 0.01$), IL-6 (2-fold, $p \leq 0.05$), IL-10 (4-fold, $p \leq 0.0001$)). This data suggests IL-1β, IL-6 and IL-10 elevations observed in the periphery, following multiple challenges of LPS, are not a lasting result of the first LPS injection, but due to the chronic application of this insult.

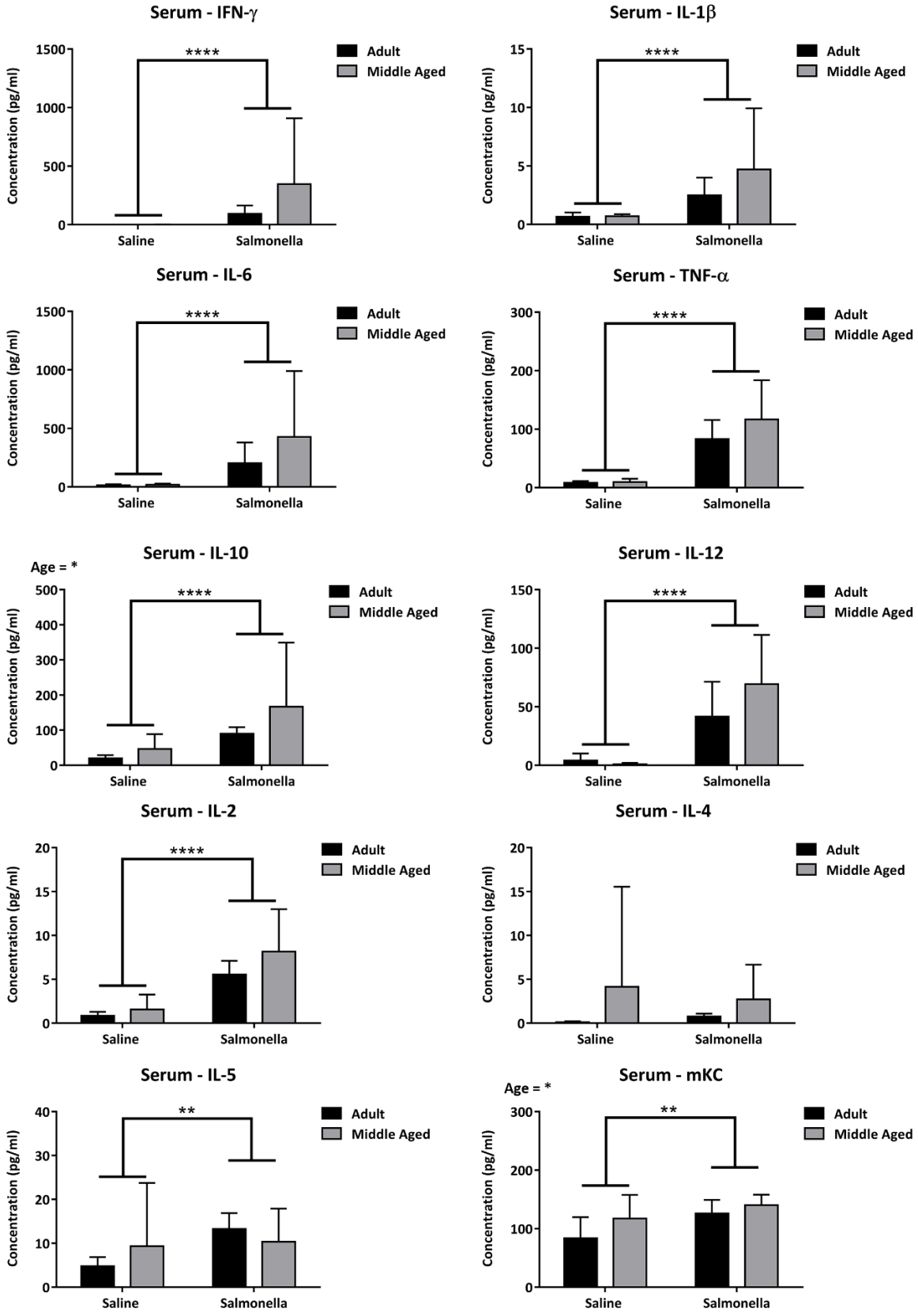
Serum - IFN-γ
Concentration (pg/ml)
1500
1000
500
0
****
Adult
Middle Aged
Saline
Salmonella
Serum - IL-1β
Concentration (pg/ml)
15
10
5
0
****
Adult
Middle Aged
Saline
Salmonella
Serum - IL-6
Concentration (pg/ml)
1500
1000
500
0
****
Adult
Middle Aged
Saline
Salmonella
Serum - TNF-α
Concentration (pg/ml)
300
200
100
0
****
Adult
Middle Aged
Saline
Salmonella
Serum - IL-10
Age = *
Concentration (pg/ml)
500
400
300
200
100
0
****
Adult
Middle Aged
Saline
Salmonella
Serum - IL-12
Concentration (pg/ml)
150
100
50
0
****
Adult
Middle Aged
Saline
Salmonella
Serum - IL-2
Concentration (pg/ml)
20
15
10
5
0
****
Adult
Middle Aged
Saline
Salmonella
Serum - IL-4
Concentration (pg/ml)
20
15
10
5
0
Adult
Middle Aged
Saline
Salmonella
Serum - IL-5
Concentration (pg/ml)
40
30
20
10
0
**
Adult
Middle Aged
Saline
Salmonella
Serum - mKC
Age = *
Concentration (pg/ml)
300
200
100
0
**
Adult
Middle Aged
Saline
Salmonella

Fig 5.5:- Cytokine expression levels in serum from middle-aged and adult wild-type mice infected with S. Typhimurium. Cytokine levels (pg/ml) in serum from middle-aged or adult wild-type mice 4 weeks post infection with S. Typhimurium, or injection with saline. Data was analysed by 2-way ANOVA and Tukey post hoc test (n=6-8), and displayed as mean + SD.

Circulating levels of cytokines were measured in serum samples using a 10-plex immunoassay (Fig 5.5).

Infection with *S*. Typhimurium induced a significant increase in the proinflammatory cytokines IFN-γ (309-fold, p≤0.0001), IL-1β (5-fold, p≤0.0001), IL-6 (19-fold, p≤0.0001), TNF-α (11-fold, p≤0.0001), IL-10 (4-fold, p≤0.0001), IL-12 (22-fold, p≤0.0001), IL-2 (6-fold, p≤0.0001), IL-5 (2-fold, p≤0.01) and mKC (1.3-fold, p≤0.01) compared to saline-injected control mice. Additionally, middle-aged mice had increased levels of IL-10 (1.8-fold, p≤0.05) and mKC (1.2-fold, p≤0.05) compared to adult wild types. Although there were trends towards greater IFN-γ, IL-1β, IL-6, TNF-α, IL-10, IL-12 and IL-2 elevations in the middle-aged mice, no statistical differences with the adult mice were observed following *S*. Typhimurium infection. This data suggests a prolonged proinflammatory response in the periphery of both middle-aged and adult wild-type mice in response to *S*. Typhimurium, 4 weeks post infection.

5.3.2 Neuroinflammatory response following multiple LPS challenge and *S.* Typhimurium infection in middle-aged and adult wild-type mice

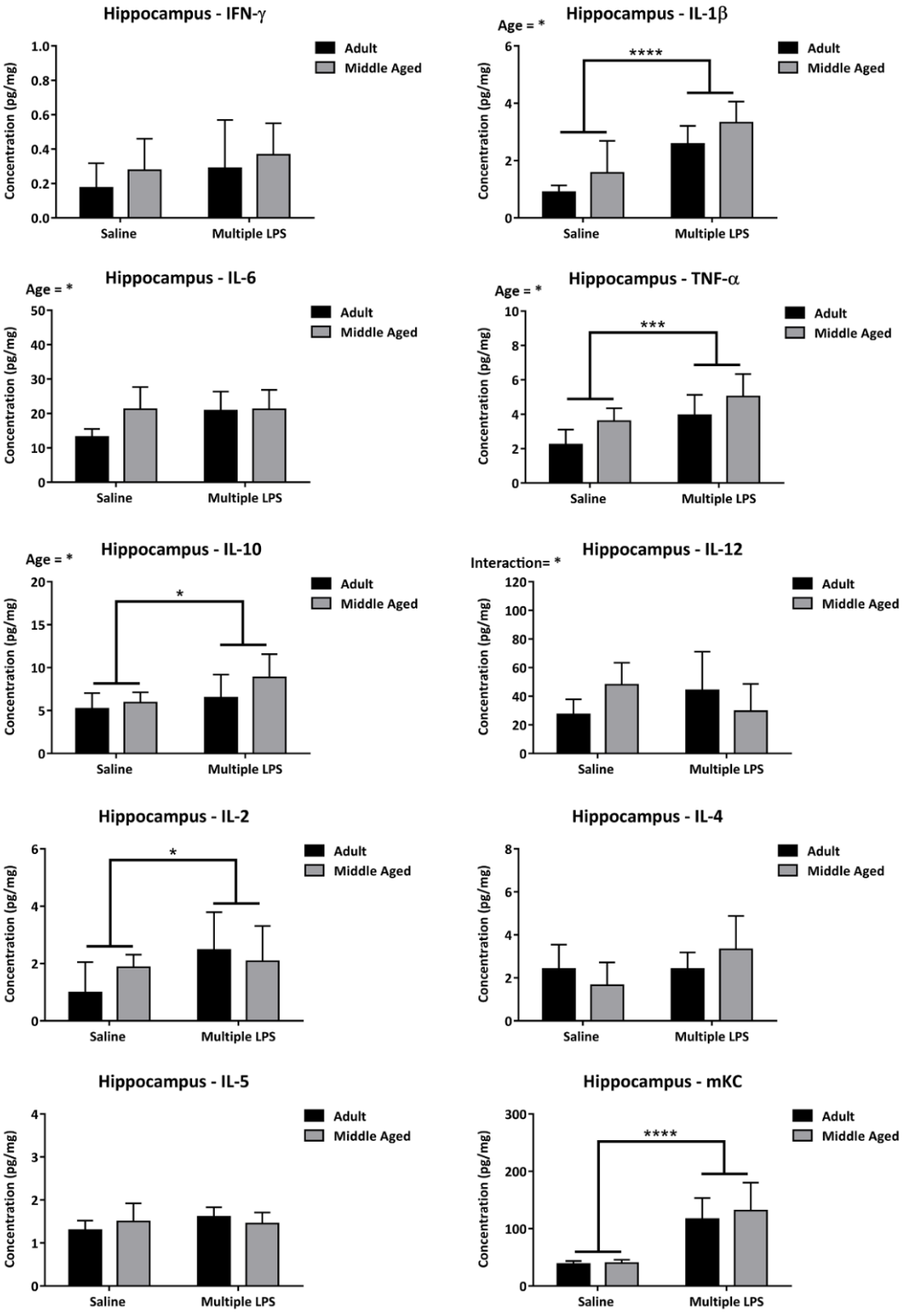

Fig 5.6:- Cytokine expression levels in hippocampal-enriched tissue from middle-aged and adult wild-type mice challenged with multiple LPS injections. Cytokine levels (pg/mg of total protein) in hippocampal-enriched tissue homogenate from middle-aged or adult wild-type mice following 8 injections of LPS or saline. Data was analysed by 2-way ANOVA and Tukey post hoc test (n=6-8), and displayed as mean + SD.

Levels of brain cytokines were measured in hippocampal-enriched tissue homogenate using a 10-plex immunoassay (Fig 5.6).

Multiple challenges of LPS induced a significant increase in the proinflammatory cytokines IL-1β (2-fold, $p \leq 0.0001$), TNF-α (2-fold, $p \leq 0.001$), IL-10 (1.3-fold, $p \leq 0.05$), IL-2 (2-fold, $p \leq 0.05$) and mKC (3-fold, $p \leq 0.0001$) compared to saline-injected control mice. Additionally, middle-aged mice had elevated levels of IL-1β (1.3-fold, $p \leq 0.05$), IL-6 (1.2-fold, $p \leq 0.05$), TNF-α (1.4-fold, $p \leq 0.05$) and IL-10 (1.2-fold, $p \leq 0.05$) compared to adult wild types. An interaction was observed in the levels of IL-12 ($p \leq 0.05$), meaning adult mice produced increased levels of this cytokine in response to multiple LPS challenges while middle-aged mice demonstrate the opposite effect. Although there were trends towards greater IL-1β, TNF-α and IL-10 elevations in the middle-aged mice, no statistical differences with the adult mice were observed following LPS challenges. This data suggests a moderate proinflammatory response in the hippocampus of both middle-aged and adult wild-type mice in response to multiple challenges of LPS.

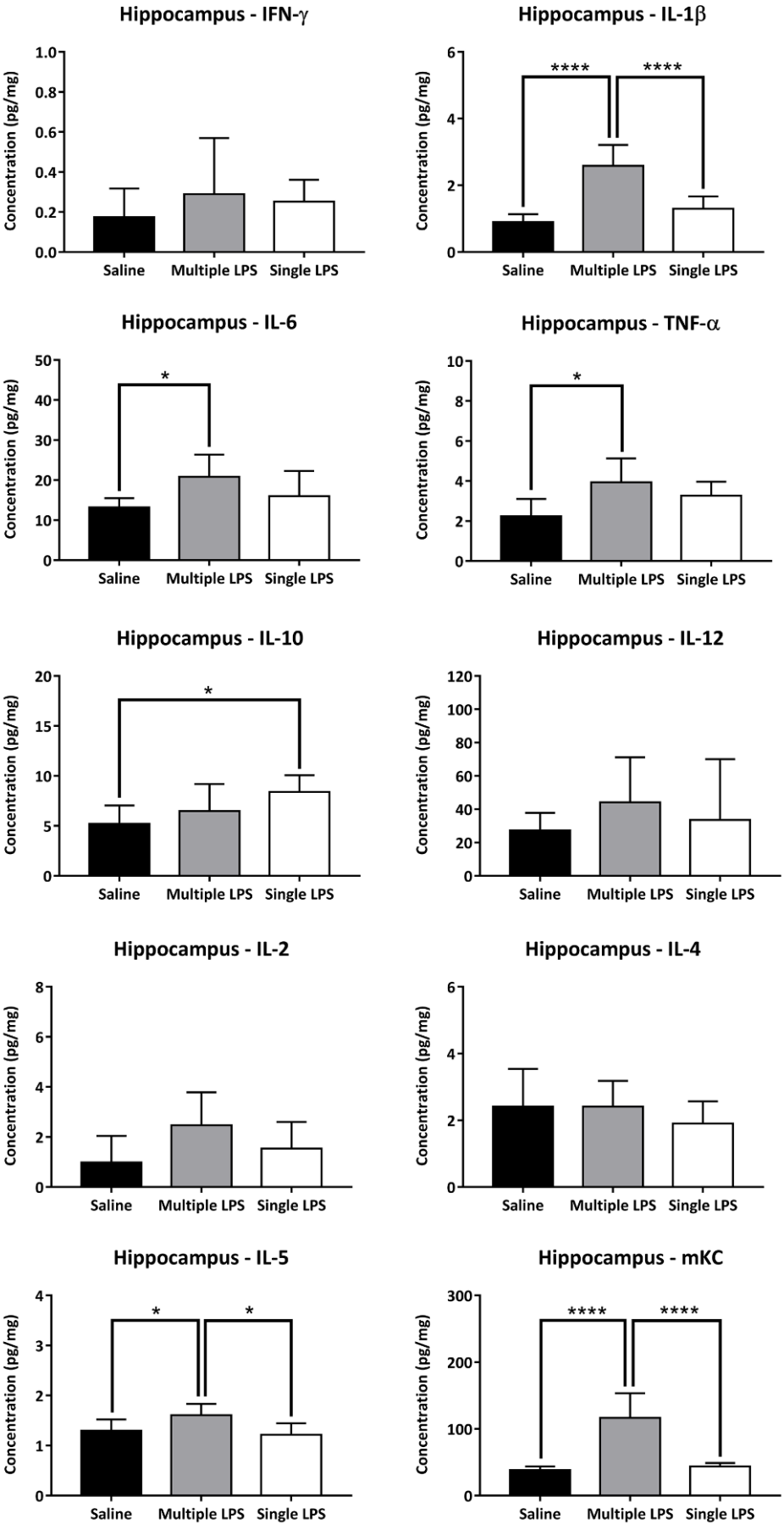
Hippocampus - IFN-γ
Concentration (pg/mg)
1.0
0.8
0.6
0.4
0.2
0.0
Saline
Multiple LPS
Single LPS
Hippocampus - IL-1β
Concentration (pg/mg)
6
4
2
0
****
****
Saline
Multiple LPS
Single LPS
Hippocampus - IL-6
Concentration (pg/mg)
50
40
30
20
10
0
*
Saline
Multiple LPS
Single LPS
Hippocampus - TNF-α
Concentration (pg/mg)
10
8
6
4
2
0
*
Saline
Multiple LPS
Single LPS
Hippocampus - IL-10
Concentration (pg/mg)
20
15
10
5
0
*
Saline
Multiple LPS
Single LPS
Hippocampus - IL-12
Concentration (pg/mg)
120
100
80
60
40
20
0
Saline
Multiple LPS
Single LPS
Hippocampus - IL-2
Concentration (pg/mg)
8
6
4
2
0
Saline
Multiple LPS
Single LPS
Hippocampus - IL-4
Concentration (pg/mg)
6
4
2
0
Saline
Multiple LPS
Single LPS
Hippocampus - IL-5
Concentration (pg/mg)
4
3
2
1
0
*
*
Saline
Multiple LPS
Single LPS
Hippocampus - mKC
Concentration (pg/mg)
300
200
100
0
****
****
Saline
Multiple LPS
Single LPS

Fig 5.7:- Cytokine expression levels in hippocampal-enriched tissue from adult wild-type mice challenged with single or multiple LPS injections. Cytokine levels (pg/mg of total protein) in hippocampal-enriched tissue homogenate from adult wild-type mice following injections of multiple LPS (8 x LPS), single LPS (1 x LPS, 7 x saline) or saline alone (8X). Data was analysed by 1-way ANOVA and Tukey post hoc test (n=6-8), and displayed as mean + SD.

Levels of brain cytokines were measured in hippocampal-enriched tissue homogenate using a 10-plex immunoassay to compare differences between single and multiple challenges of LPS (Fig 5.7).

Multiple LPS challenges induced a significant increase in proinflammatory cytokines compared to single LPS challenge (IL-1β (2-fold, $p \leq 0.0001$), IL-5 (1.2-fold, $p \leq 0.05$), mKC (3-fold, $p \leq 0.0001$)) and saline-injected control mice (IL-1β (3-fold, $p \leq 0.0001$), IL-6 (2-fold, $p \leq 0.05$), TNF-α (2-fold, $p \leq 0.05$), IL-5 (1.2-fold, $p \leq 0.05$), mKC (3-fold, $p \leq 0.0001$). Additionally, single LPS challenge induced a significant increase in IL-10 (1.6-fold, $p \leq 0.0001$) compared to saline-injected control mice. This data suggests IL-1β, IL-5 and mKC elevations observed in the hippocampus, following multiple challenges of LPS, are not a lasting result of the first LPS injection, but due to the repeated application of this insult.

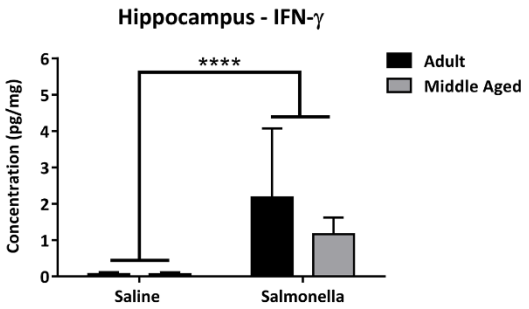
Hippocampus - IFN-γ
Concentration (pg/mg)
****
Adult
Middle Aged
Saline
Salmonella

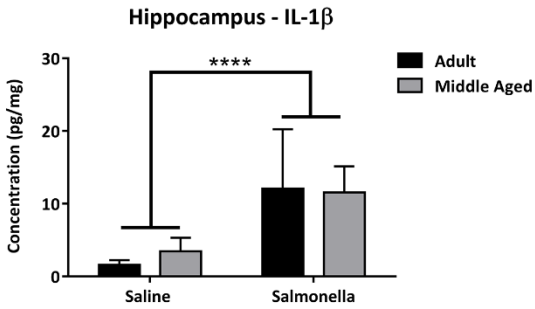
Hippocampus - IL-1β
Concentration (pg/mg)
****
Adult
Middle Aged
Saline
Salmonella

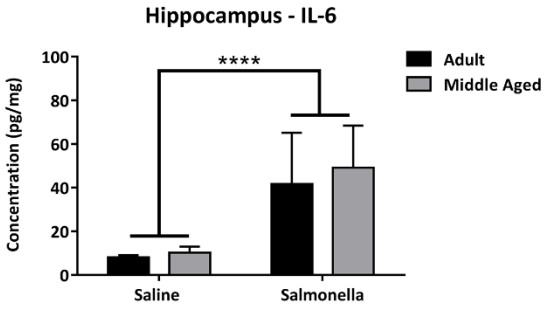
Hippocampus - IL-6
Concentration (pg/mg)
****
Adult
Middle Aged
Saline
Salmonella

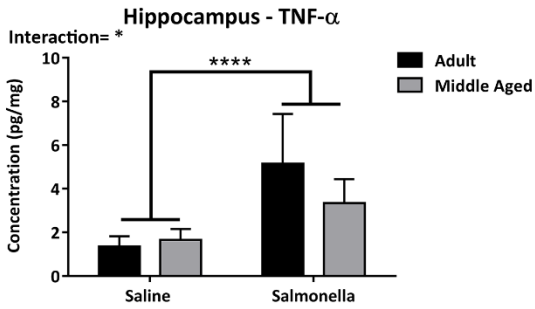
Hippocampus - TNF-α
Interaction= *
Concentration (pg/mg)
****
Adult
Middle Aged
Saline
Salmonella

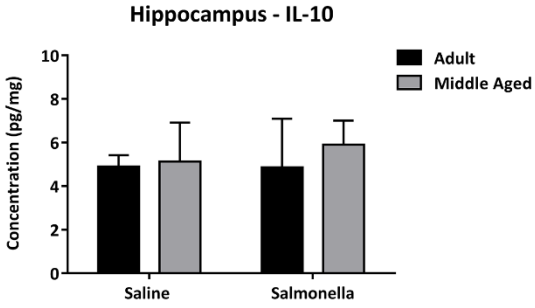
Hippocampus - IL-10
Concentration (pg/mg)
Adult
Middle Aged
Saline
Salmonella

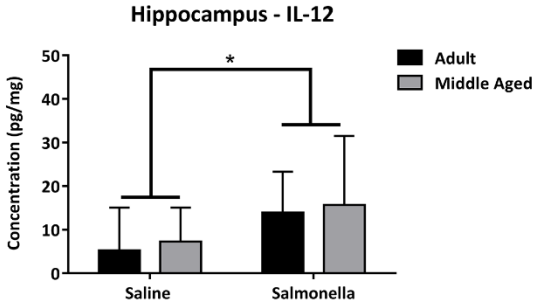
Hippocampus - IL-12
Concentration (pg/mg)
*
Adult
Middle Aged
Saline
Salmonella

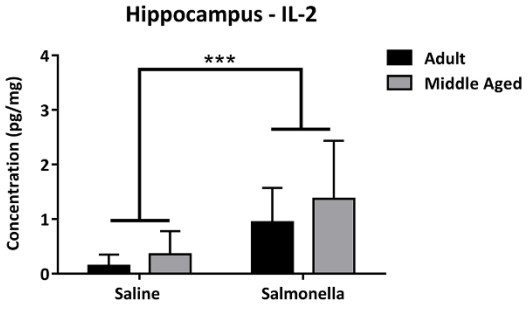
Hippocampus - IL-2
Concentration (pg/mg)
***
Adult
Middle Aged
Saline
Salmonella

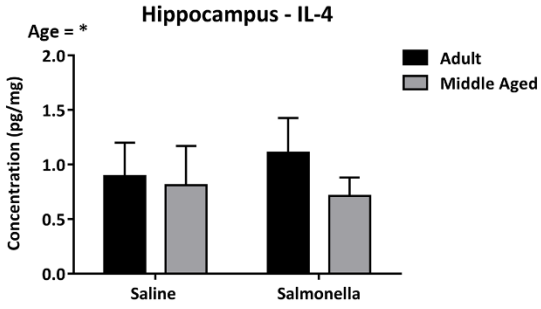
Hippocampus - IL-4
Age = *
Concentration (pg/mg)
Adult
Middle Aged
Saline
Salmonella

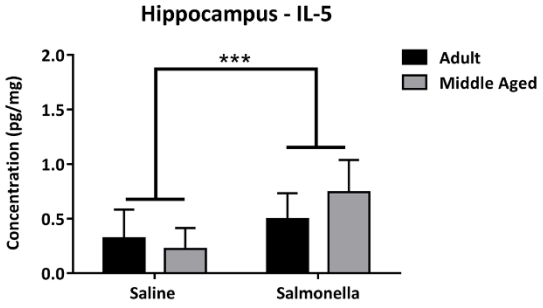
Hippocampus - IL-5
Concentration (pg/mg)
***
Adult
Middle Aged
Saline
Salmonella

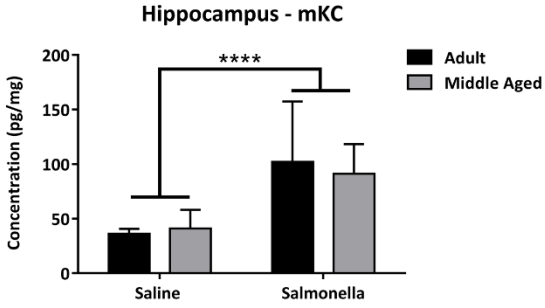
Hippocampus - mKC
Concentration (pg/mg)
****
Adult
Middle Aged
Saline
Salmonella

Fig 5.8:- Cytokine expression levels in hippocampal-enriched tissue from middle-aged and adult wild-type mice infected with S. Typhimurium. Cytokine levels (pg/mg of total protein) in hippocampal-enriched tissue homogenate from middle-aged or adult wild-type mice 4 weeks post infection with S. Typhimurium, or injection with saline. Data was analysed by 2-way ANOVA and Tukey post hoc test (n=6-8), and displayed as mean + SD.

Levels of brain cytokines were measured in hippocampal-enriched tissue homogenate using a 10-plex immunoassay (Fig 5.8).

Infection with *S*. Typhimurium induced a significant increase in the proinflammatory cytokines IFN-γ (26-fold, p≤0.0001), IL-1β (5-fold, p≤0.0001), IL-6 (5-fold, p≤0.001), TNF-α (3-fold, p≤0.0001), IL-12 (22-fold, p≤0.05), IL-2 (5-fold, p≤0.001), IL-5 (2-fold, p≤0.01) and mKC (3-fold, p≤0.0001) compared to saline-injected control mice. Additionally, middle-aged mice had reduced levels of IL-4 (1.3-fold, p≤0.05) compared to adult wild types. An interaction was observed in the levels of TNF-α, meaning adult mice produce a stronger response to *S*. Typhimurium than middle-aged wild types. This data suggests a prolonged proinflammatory response in the hippocampus of both middle-aged and adult wild-type mice in response to *S*. Typhimurium, 4 weeks post infection.

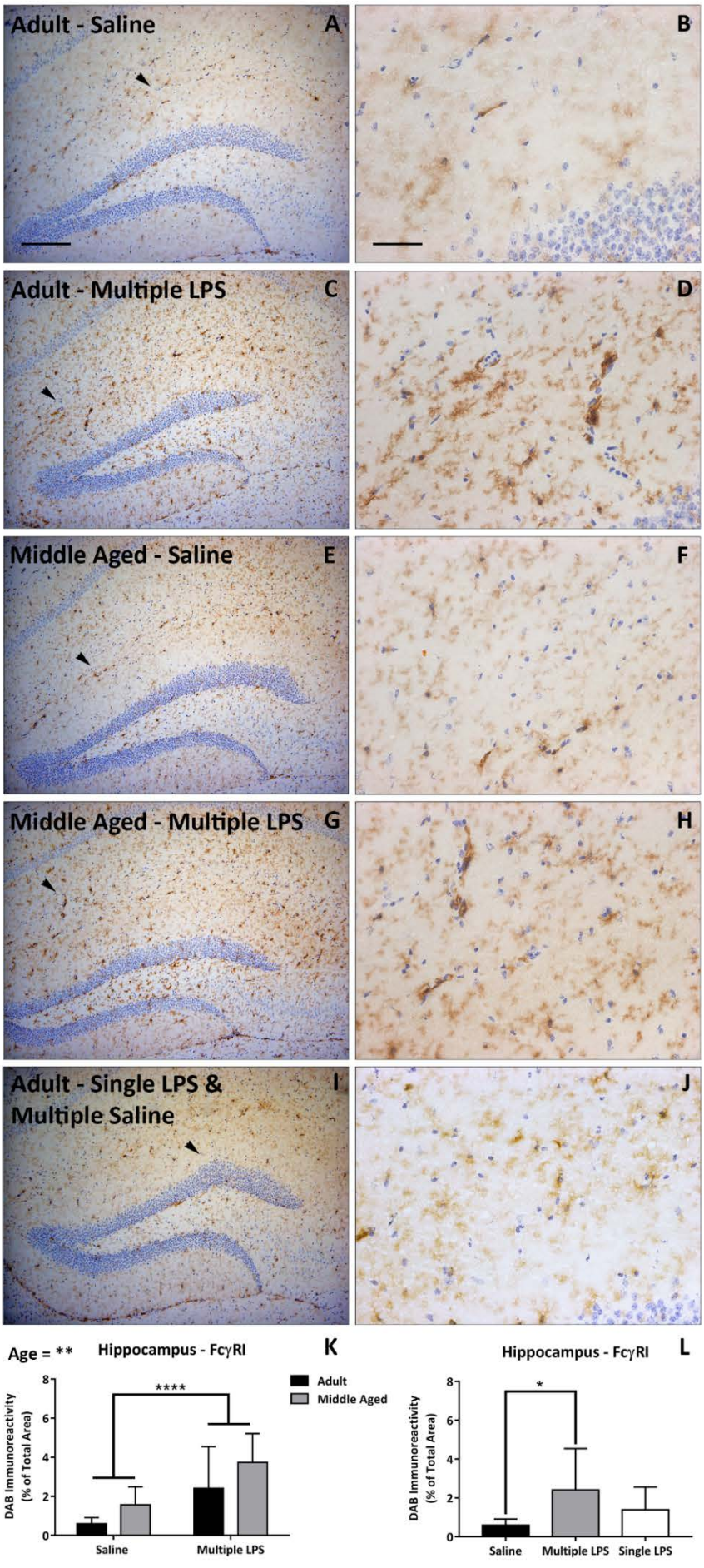
Adult - Saline
A
B
Adult - Multiple LPS
C
D
Middle Aged - Saline
E
F
Middle Aged - Multiple LPS
G
H
Adult - Single LPS &
Multiple Saline
I
J
Age = **
Hippocampus - FcγRI
K
Adult
Middle Aged
DAB Immunoreactivity
(% of Total Area)
****
Saline
Multiple LPS
Hippocampus - FcγRI
L
*
Saline
Multiple LPS
Single LPS

Fig 5.9:- FcγRI expression in the hippocampus of middle-aged and adult wild-type mice challenged with single or multiple LPS injections. Overview of FcγRI expression in middle-aged (E,G) or adult wild-type mice (A,C,I) following multiple LPS (8X) (C,G), a single injection of LPS (1 x LPS, 7 x saline) (I), or saline alone (8X) (A,E). Scale bar = 200µm. Higher magnification images derived from overview of hippocampus and indicated with black arrows. Scale bar = 50µm. (K,L) Quantification of FcγRI expression (DAB immunoreactivity (% of total area)) from entirety of hippocampus. Data was analysed by 1- (L) or 2- (K) way ANOVA and Tukey post hoc test (n=6-8), and displayed as mean + SD.

To investigate the cellular response to single or multiple injections of LPS, FcγRI expression on myeloid cells, such as microglia, was assessed by immunohistochemistry (Fig 5.9).

Quantification of FcγRI expression in the hippocampus indicated a significant increase following multiple LPS challenge, in both middle-aged and adult wild types, compared to saline-injected control mice (3-fold, $p \leq 0.0001$) (Fig 5.9K). Additionally, middle-aged mice demonstrated elevated FcγRI expression compared to adult wild-types (1.6-fold, $p \leq 0.01$) (Fig 5.9K). Multiple challenges of LPS caused a widespread increase in FcγRI expression on microglia, in addition to increases in localised staining, particularly in the hippocampal fissure (Fig 5.9). Multiple, but not single, challenge of LPS resulted in elevated FcγRI expression in adult wild-type mice suggesting this observation is not solely attributed to the first LPS insult.

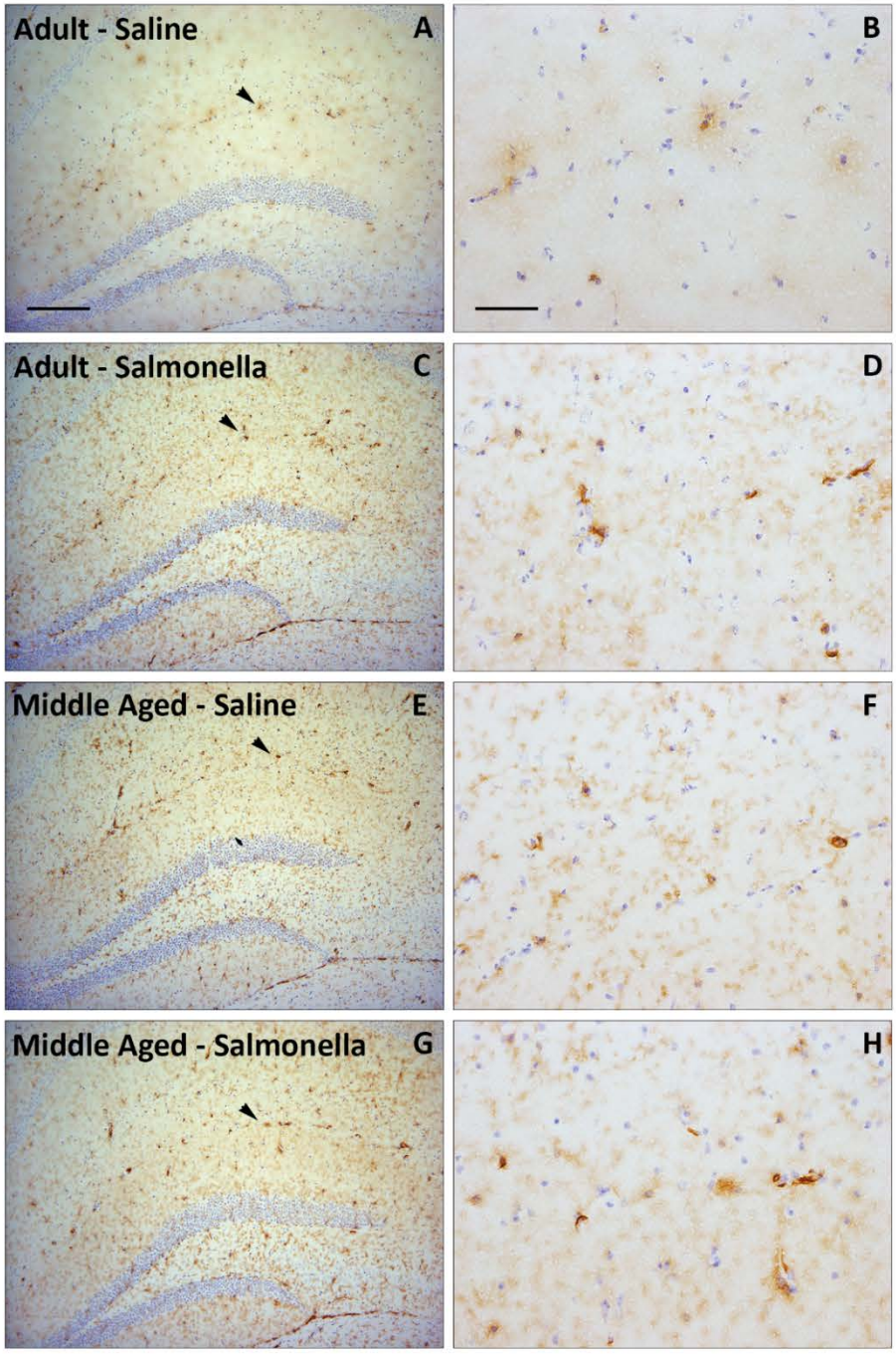
Adult - Saline
A
B
Adult - Salmonella
C
D
Middle Aged - Saline
E
F
Middle Aged - Salmonella
G
H

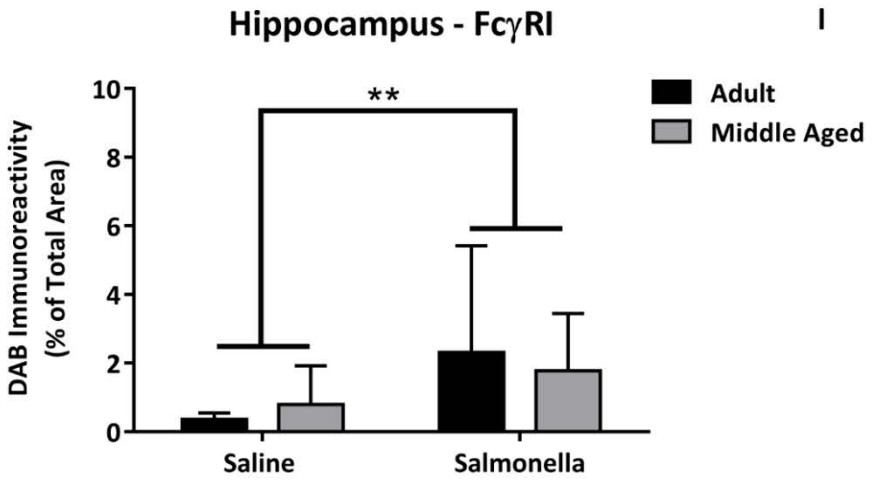
Hippocampus - FcγRI
I
DAB Immunoreactivity (% of Total Area)
10
8
6
4
2
0
**
Adult
Middle Aged
Saline
Salmonella

Fig 5.10:- FcγRI expression in the hippocampus of middle-aged and adult wild-type mice infected with S. Typhimurium. Overview of FcγRI expression in middle-aged (E,G) or adult wild-type mice (A,C) 4 weeks post infection with S. Typhimurium (C,G), or injection with saline (A,E). Scale bar = 200μm. Higher magnification images derived from overview of hippocampus and indicated with black arrows. Scale bar = 50μm. (I) Quantification of FcγRI expression (DAB immunoreactivity (% of total area)) from entirety of hippocampus. Data was analysed by 2-way ANOVA and Tukey post hoc test (n=6-8), and displayed as mean + SD.

To investigate the cellular response to *S*. Typhimurium infection, FcγRI expression on myeloid cells, such as microglia, was assessed by immunohistochemistry (Fig 5.10).

Quantification of FcγRI expression in the hippocampus indicated a significant increase following *S*. Typhimurium infection, in both middle-aged and adult wild types, compared to saline-injected control mice (4-fold, $p \leq 0.01$) (Fig 5.10I). *S*. Typhimurium infection caused a widespread increase in FcγRI expression on microglia, in addition to increases in localised staining, particularly in the hippocampal fissure (Fig 5.10D).

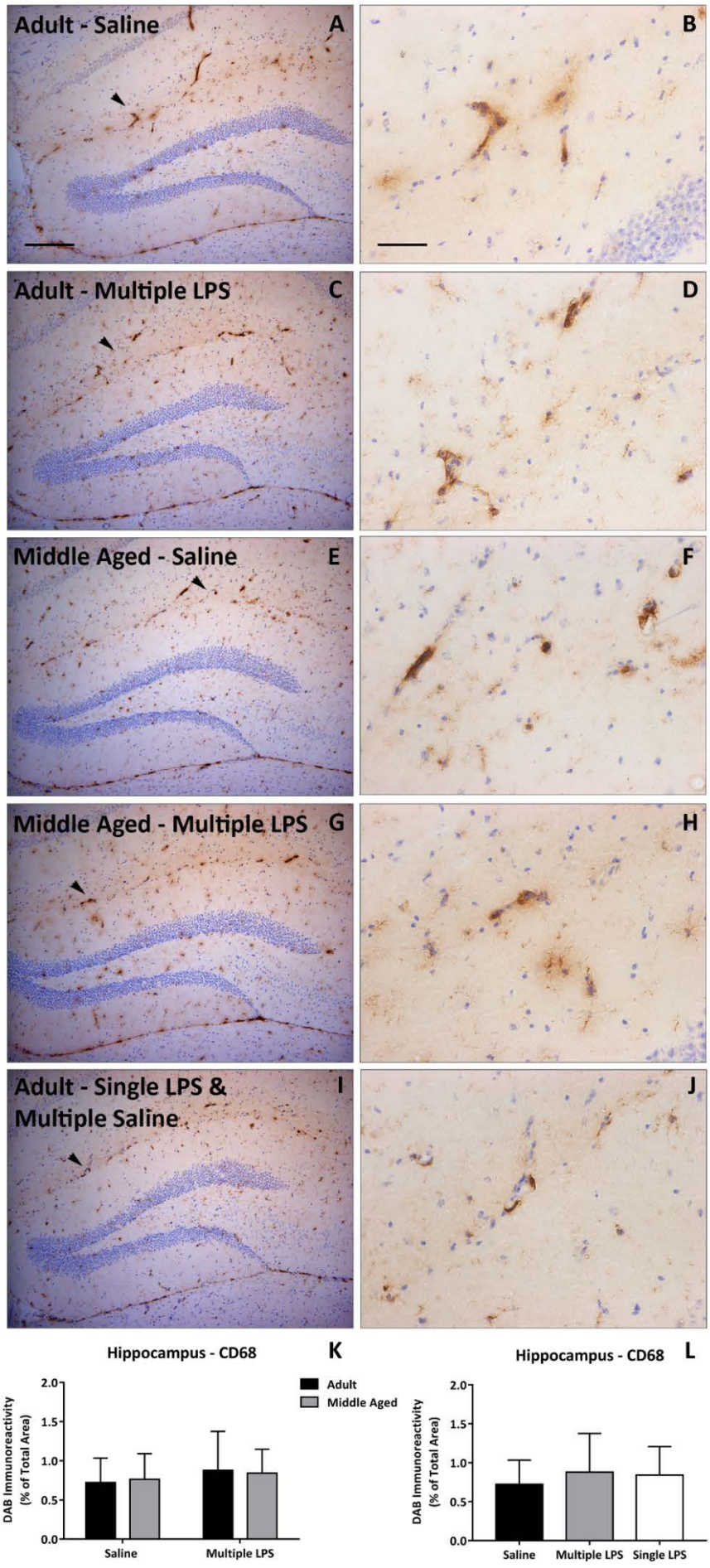
Adult - Saline
A
B
Adult - Multiple LPS
C
D
Middle Aged - Saline
E
F
Middle Aged - Multiple LPS
G
H
Adult - Single LPS &
Multiple Saline
I
J
Hippocampus - CD68
K
DAB Immunoreactivity
(% of Total Area)
2.0
1.5
1.0
0.5
0.0
Saline
Multiple LPS
Adult
Middle Aged
Hippocampus - CD68
L
DAB Immunoreactivity
(% of Total Area)
2.0
1.5
1.0
0.5
0.0
Saline
Multiple LPS
Single LPS

Fig 5.11:- CD68 expression in the hippocampus of middle-aged and adult wild-type mice challenged with single or multiple LPS injections. Overview of CD68 expression in middle-aged (E,G) or adult wild-type mice (A,C,I) following multiple LPS (8X) (C,G), a single injection of LPS (1 x LPS, 7 x saline) (I), or saline alone (8X) (A,E). Scale bar = 200µm. Higher magnification images derived from overview of hippocampus and indicated with black arrows. Scale bar = 50µm. (K,L) Quantification of CD68 expression (DAB immunoreactivity (% of total area)) from entirety of hippocampus. Data was analysed by 1- (L) or 2- (K) way ANOVA and Tukey post hoc test (n=6-8), and displayed as mean + SD.

To investigate the cellular response to single or multiple injections of LPS, CD68 expression in myeloid cells, such as microglia, was assessed by immunohistochemistry (Fig 5.11).

Quantification of CD68 expression in the hippocampus indicated no significant change following multiple challenges of LPS, in both middle-aged and adult wild types, compared to saline-injected control mice (Fig 5.11K). The pattern of CD68 expression appeared widespread within microglia, in addition to localised staining, particularly in the hippocampal fissure (Fig 5.11B,D,F,H). Additionally, there was no significant difference in CD68 expression between single and multiple challenges of LPS (Fig 5.11L).

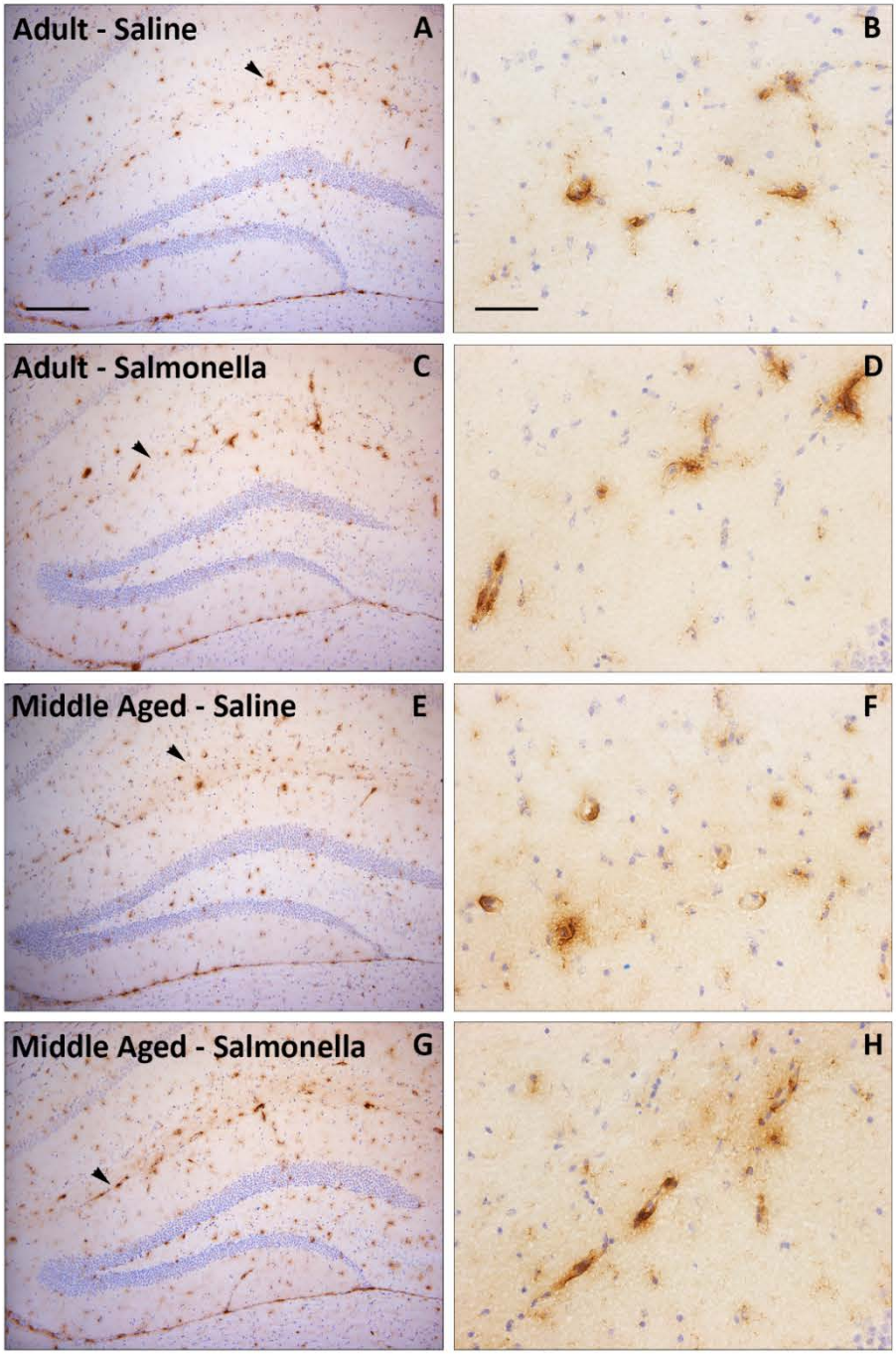
Adult - Saline
A
B
Adult - Salmonella
C
D
Middle Aged - Saline
E
F
Middle Aged - Salmonella
G
H

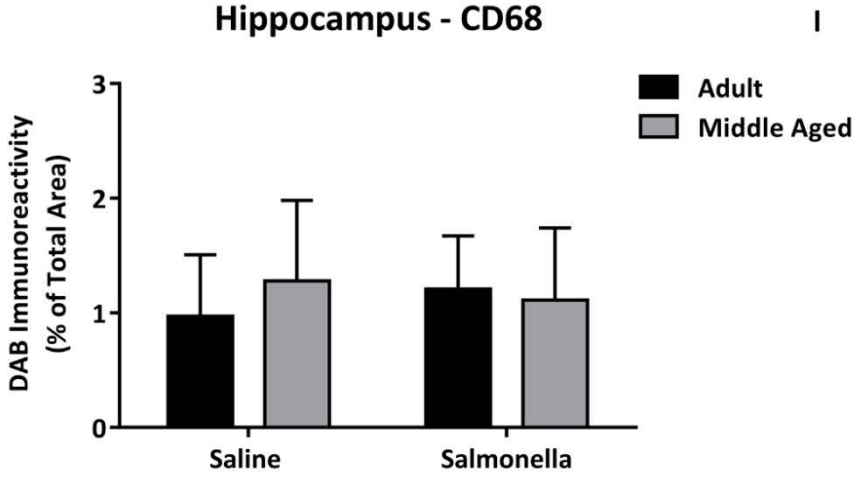
Hippocampus - CD68
I
Adult
Middle Aged
DAB Immunoreactivity
(% of Total Area)
3
2
1
0
Saline
Salmonella

Fig 5.12:- CD68 expression in the hippocampus of middle-aged and adult wild-type mice infected with *S*. Typhimurium. Overview of CD68 expression in middle-aged (E,G) or adult wild-type mice (A,C) 4 weeks post infection with *S*. Typhimurium (C,G), or injection with saline (A,E). Scale bar = 200µm. Higher magnification images derived from overview of hippocampus and indicated with black arrows. Scale bar = 50µm. (I) Quantification of CD68 expression (DAB immunoreactivity (% of total area)) from entirety of hippocampus. Data was analysed by 2-way ANOVA and Tukey post hoc test (n=6-8), and displayed as mean + SD.

To investigate the cellular response to *S*. Typhimurium infection, CD68 expression in myeloid cells, such as microglia, was assessed by immunohistochemistry (Fig 5.12).

Quantification of CD68 expression in the hippocampus indicated no significant change following *S*. Typhimurium infection, in both middle-aged and adult wild types, compared to saline-injected control mice (Fig 5.12I). The pattern of CD68 expression appeared widespread within microglia, in addition to localised staining, particularly in the hippocampal fissure (Fig 5.12B,D,F,H).

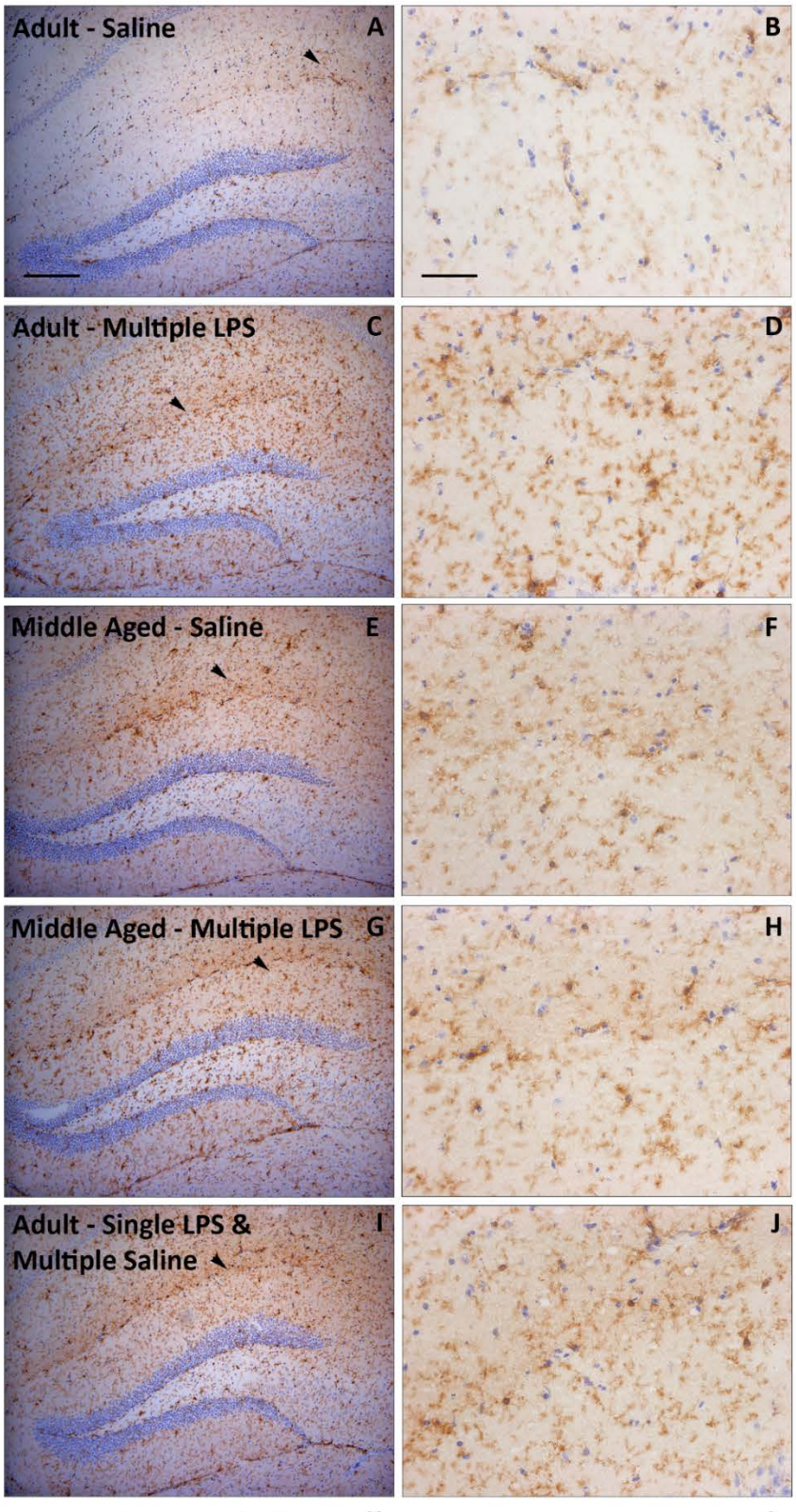
Adult - Saline
A
B
Adult - Multiple LPS
C
D
Middle Aged - Saline
E
F
Middle Aged - Multiple LPS
G
H
Adult - Single LPS &
Multiple Saline
I
J
Hippocampus - CD11b
K
Adult
Middle Aged
DAB Immunoreactivity
(% of Total Area)
****
Saline
Multiple LPS
Hippocampus - CD11b
L
***
**
Saline
Multiple LPS
Single LPS

Fig 5.13:- CD11b expression in the hippocampus of middle-aged and adult wild-type mice challenged with single or multiple LPS injections. Overview of CD11b expression in middle-aged (E,G) or adult wild-type mice (A,C,I) following multiple LPS (8X) (C,G), a single injection of LPS (1 x LPS, 7 x saline) (I), or saline alone (8X) (A,E). Scale bar = 200µm. Higher magnification images derived from overview of hippocampus and indicated with black arrows. Scale bar = 50µm. (K,L) Quantification of CD11b expression (DAB immunoreactivity (% of total area)) from entirety of hippocampus. Data was analysed by 1- (L) or 2- (K) way ANOVA and Tukey post hoc test (n=6-8), and displayed as mean + SD.

To investigate the cellular response to single or multiple injections of LPS, CD11b expression on myeloid cells, such as microglia, was assessed by immunohistochemistry (Fig 5.13).

Quantification of CD11b expression in the hippocampus indicated a significant increase following multiple LPS challenge, in both middle-aged and adult wild types, compared to saline-injected control mice (3-fold, $p \leq 0.0001$) (Fig 5.13K). The pattern of CD11b expression appeared widespread on microglia, in addition to localised staining, particularly in the hippocampal fissure (Fig 5.13B,D,F,H). Both multiple and single challenge of LPS resulted in elevated CD11b expression in adult wild-type mice suggesting this observation may be a lasting effect from the first LPS injection (Fig 5.13L).

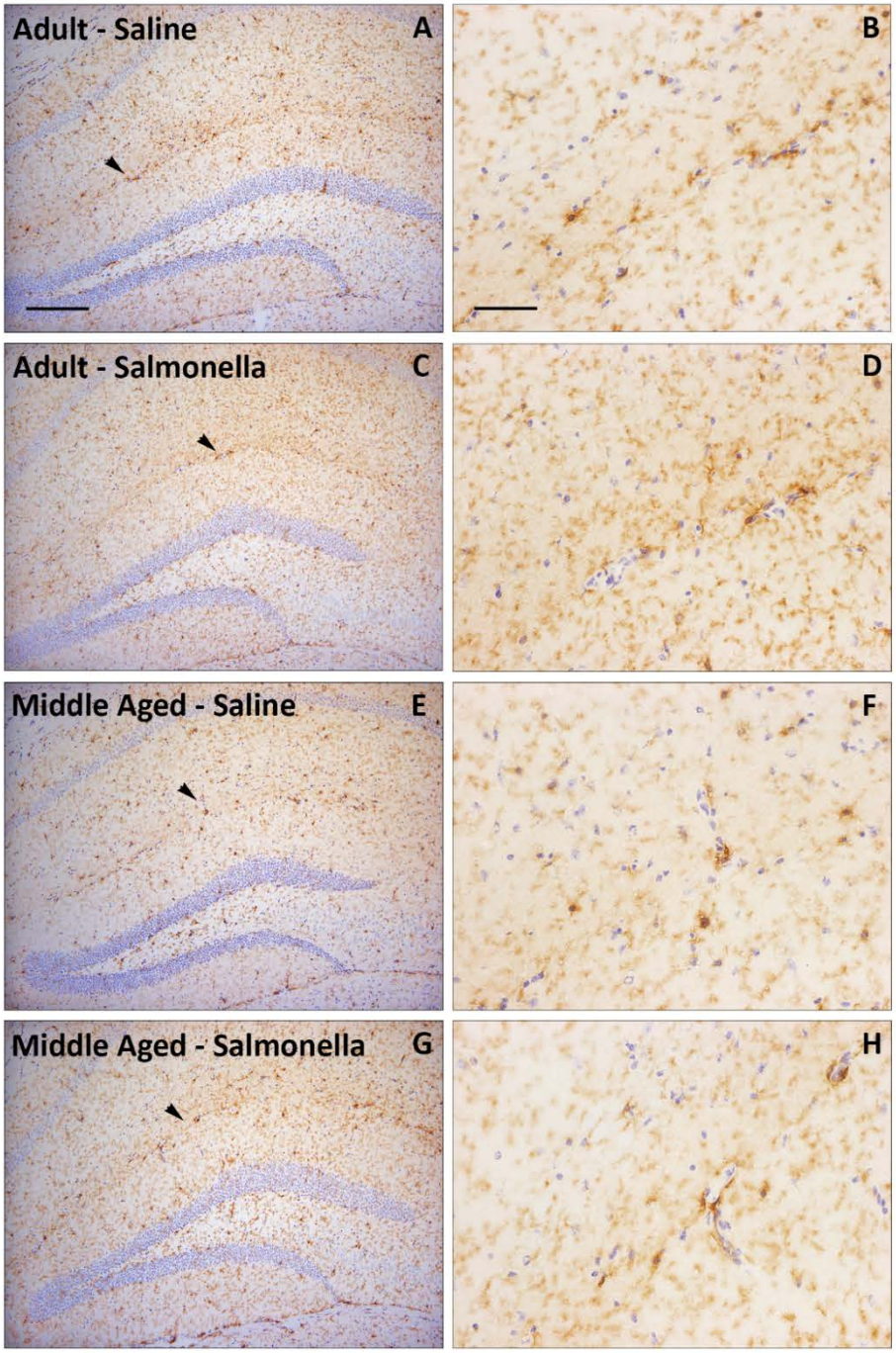
Adult - Saline
A
B
Adult - Salmonella
C
D
Middle Aged - Saline
E
F
Middle Aged - Salmonella
G
H

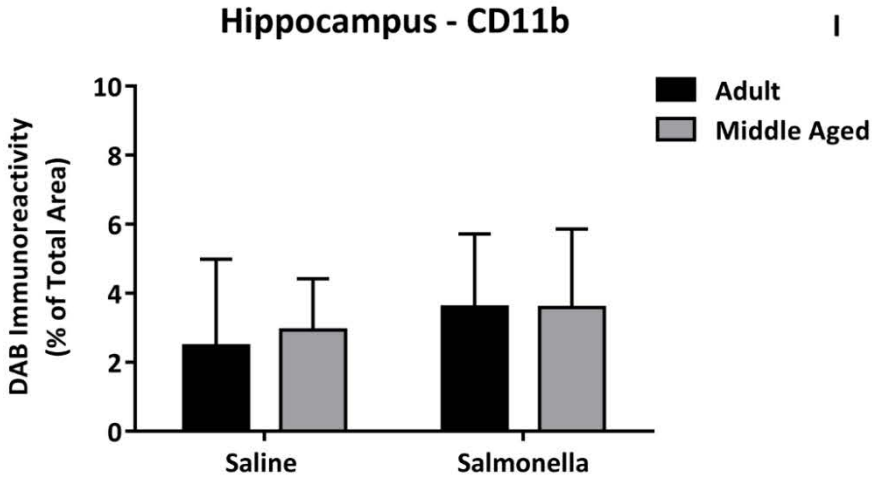
Hippocampus - CD11b
I
Adult
Middle Aged
DAB Immunoreactivity
(% of Total Area)
10
8
6
4
2
0
Saline
Salmonella

Fig 5.14:- CD11b expression in the hippocampus of middle-aged and adult wild-type mice infected with *S*. Typhimurium. Overview of CD11b expression in middle-aged (E,G) or adult wild-type mice (A,C) 4 weeks post infection with *S*. Typhimurium (C,G), or injection with saline (A,E). Scale bar = 200µm. Higher magnification images derived from overview of hippocampus and indicated with black arrows. Scale bar = 50µm. (I) Quantification of CD11b expression (DAB immunoreactivity (% of total area)) from entirety of hippocampus. Data was analysed by 2-way ANOVA and Tukey post hoc test (n=6-8), and displayed as mean + SD.

To investigate the cellular response to *S*. Typhimurium infection, CD11b expression on myeloid cells, such as microglia, was assessed by immunohistochemistry (Fig 5.14).

Quantification of CD11b expression in the hippocampus indicated no significant change following *S*. Typhimurium infection, in both middle-aged and adult wild types, compared to saline-injected control mice (Fig 5.14I). The pattern of CD11b expression appeared widespread on microglia, in addition to localised staining, particularly in the hippocampal fissure (Fig 5.14B,D,F,H).

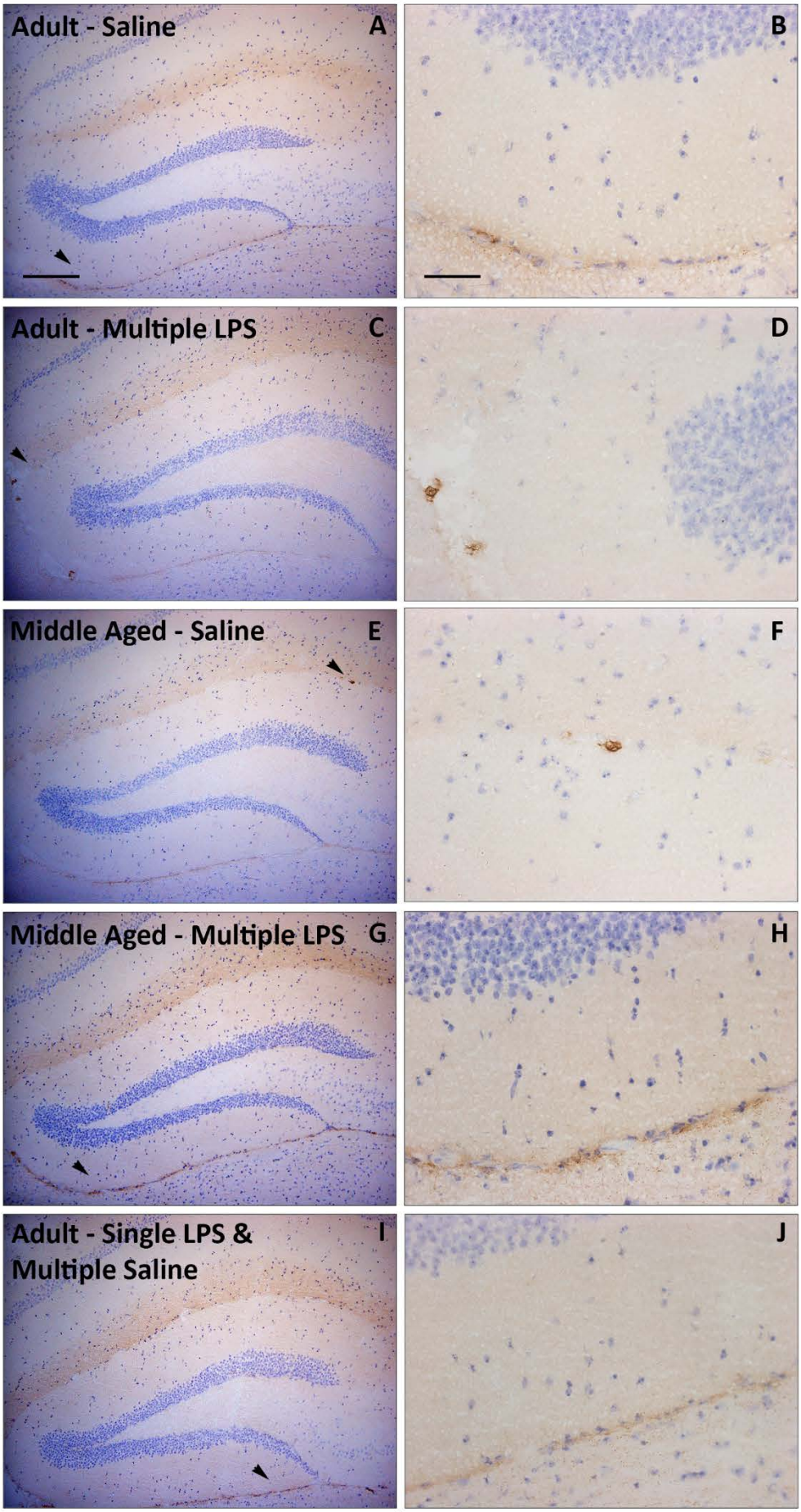
Adult - Saline
A
B
Adult - Multiple LPS
C
D
Middle Aged - Saline
E
F
Middle Aged - Multiple LPS
G
H
Adult - Single LPS &
Multiple Saline
I
J

Figure 5.15:- MHCII expression in the hippocampus of middle-aged and adult wild-type mice challenged with single or multiple LPS injections. Overview of MHCII expression in middle-aged (E,G) or adult wild-type mice (A,C,I) following multiple LPS (8X) (C,G), a single injection of LPS (1 x LPS, 7 x saline) (I), or saline alone (8X) (A,E). (B,D,F,H) Higher magnification images derived from overview of hippocampus and indicated with black arrows. Scale bar = 50µm.

To investigate the cellular response to single or multiple injections of LPS, MHCII expression on myeloid cells, such as microglia, was assessed by immunohistochemistry (Fig 5.15).

MHCII+ cells were largely absent from the hippocampus of all groups, with the exception of a small number of round cells localised around the pial membrane and ventricles. For this reason, quantification was not performed.

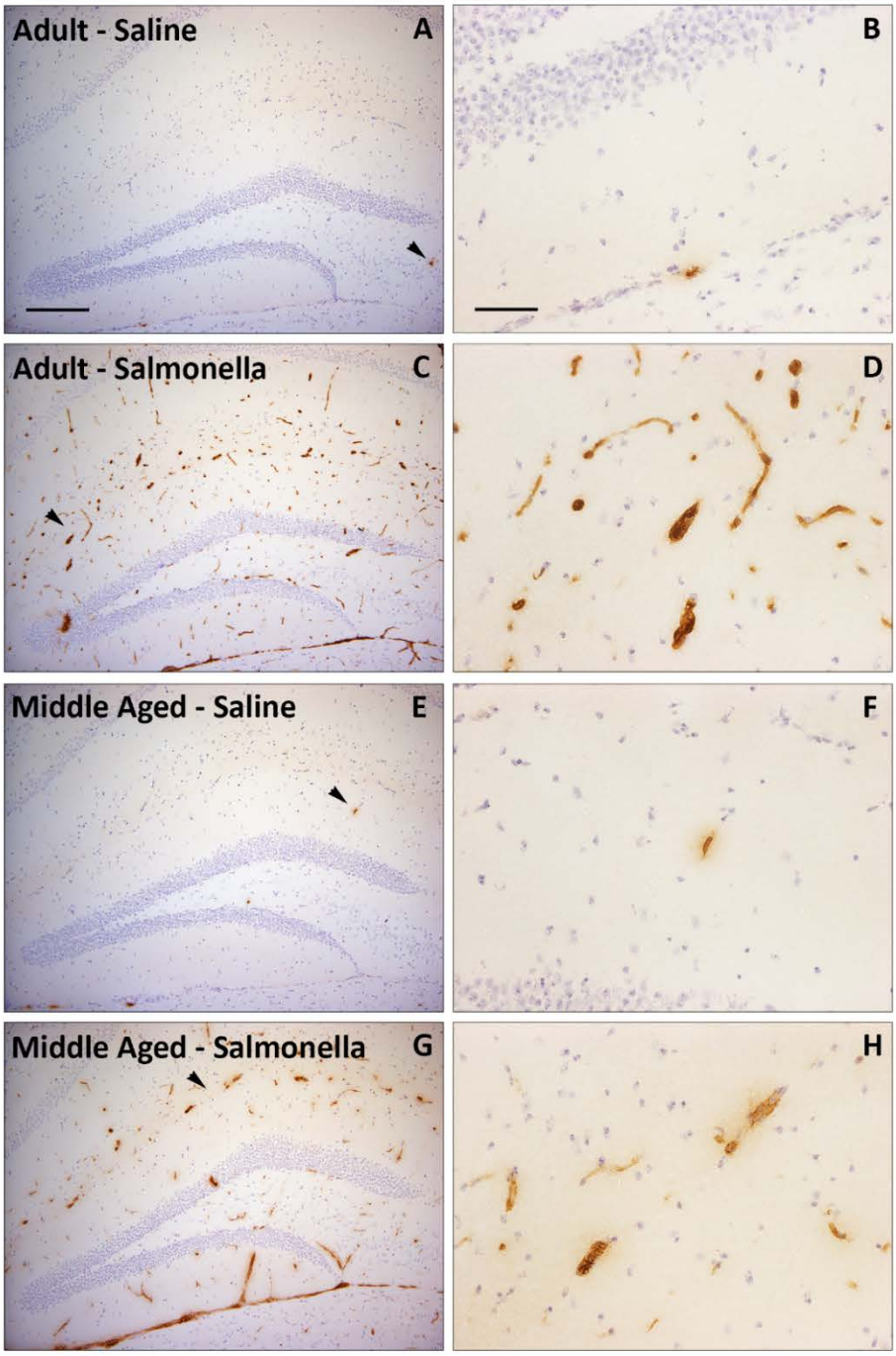
Adult - Saline
A
B
Adult - Salmonella
C
D
Middle Aged - Saline
E
F
Middle Aged - Salmonella
G
H

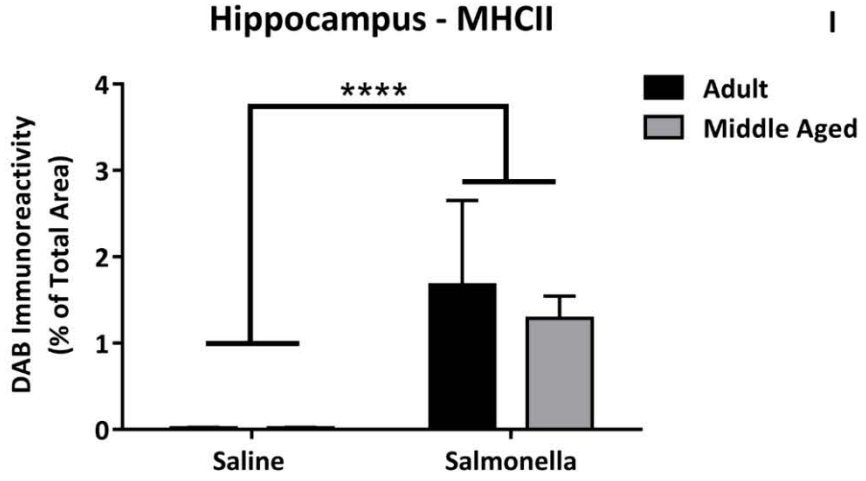
Hippocampus - MHCII
I
DAB Immunoreactivity (% of Total Area)
4
3
2
1
0
****
Adult
Middle Aged
Saline
Salmonella

Fig 5.16:- MHCII expression in the hippocampus of middle-aged and adult wild-type mice infected with *S*. Typhimurium. Overview of MHCII expression in middle-aged (E,G) or adult wild-type mice (A,C) 4 weeks post infection with *S*. Typhimurium (C,G), or injection with saline (A,E). Scale bar = 200µm. (B,D,F,H) Higher magnification images derived from overview of hippocampus and indicated with black arrows. Scale bar = 50µm. (I) Quantification of MHCII expression (DAB immunoreactivity (% of total area)) from entirety of hippocampus. Data was analysed by 2-way ANOVA and Tukey post hoc test (n=6-8), and displayed as mean + SD.

To investigate the cellular response to *S*. Typhimurium infection, MHCII expression on myeloid cells, such as microglia, was assessed by immunohistochemistry (Fig 5.16).

Quantification of MHCII expression in the hippocampus indicated a significant increase following *S*. Typhimurium infection, in both middle-aged and adult wild types, compared to saline-injected control mice (87-fold, $p \leq 0.0001$) (Fig 5.16I). In contrast to FcγRI, CD68 and CD11b, the pattern of MHCII expression is indicative of cells associated with blood vessels exclusively. This is most apparent along the pial membrane at the bottom of the hippocampal images (Fig 5.16A,C,E,G). Co-staining with blood vessels markers may further elucidate the pattern of this MHCII expression.

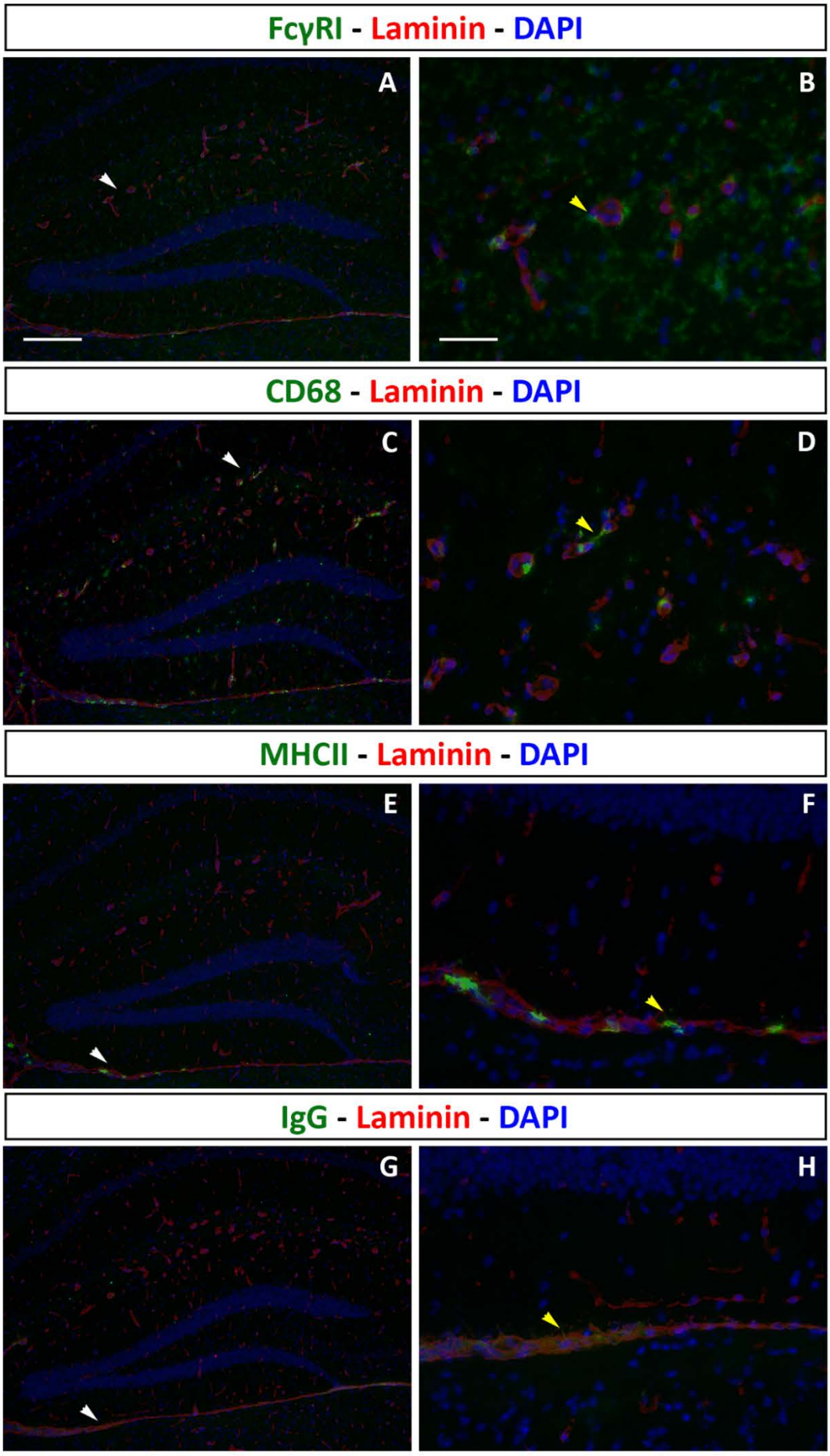
FcγRI - Laminin - DAPI
A
B
CD68 - Laminin - DAPI
C
D
MHCII - Laminin - DAPI
E
F
IgG - Laminin - DAPI
G
H

Fig 5.17:- Association of FcγRI, CD68, MHCII and IgG with laminin in the hippocampus of middle-aged wild-type mice challenged with multiple LPS injections. (A,C,E,G) Overview of FcγRI+, CD68+ or MHCII+ cells (green) and endogenous IgG (green) with laminin (red) and DAPI (blue), from the hippocampus of a middle-aged mouse challenged with multiple LPS injections. Scale bar = 200µm. (B,D,F,H) Higher magnification images derived from overview of hippocampus and indicated with white arrows. Scale bar = 50µm**.** Yellow arrows indicate FcγRI+, CD68+ or MHCII+ cells (green) and endogenous IgG (green) associated with laminin (red).

To further explore the localisation of FcγRI+, CD68+ or MHCII+ cells and endogenous IgG, co-staining with laminin was performed, highlighting blood vessel association using immunofluorescence (Fig 5.17).

Co-staining with laminin confirmed FcγRI+ and CD68+ cells associated with the basement membranes of the vasculature. In alignment with studies using DAB (Fig 5.9), expression of FcγRI was observed across microglia in the brain parenchyma in addition to the basement membranes (Fig 5.17A,B).

In contrast, CD68 expression was largely limited to the basement membranes of the blood vessels with few examples of luminal staining. There appears to be partial staining on microglia of the brain parenchyma which, as quantified in DAB (Fig 5.11), does not alter following multiple challenges of LPS (Fig 5.17C,D).

The small number of MHCII-positive cells were found to largely associate with the pial membrane and ventricles (Fig 5.17E,F), as observed in DAB staining (Fig 5.15). Microglia of the brain parenchyma were not found to express MHCII on their cell surface, even following multiple LPS challenge.

Endogenous IgG immunoreactivity was rare and localised within the vasculature of the pial membrane vessel, in all experimental groups, suggesting the BBB is intact (Fig 5.17G,H).

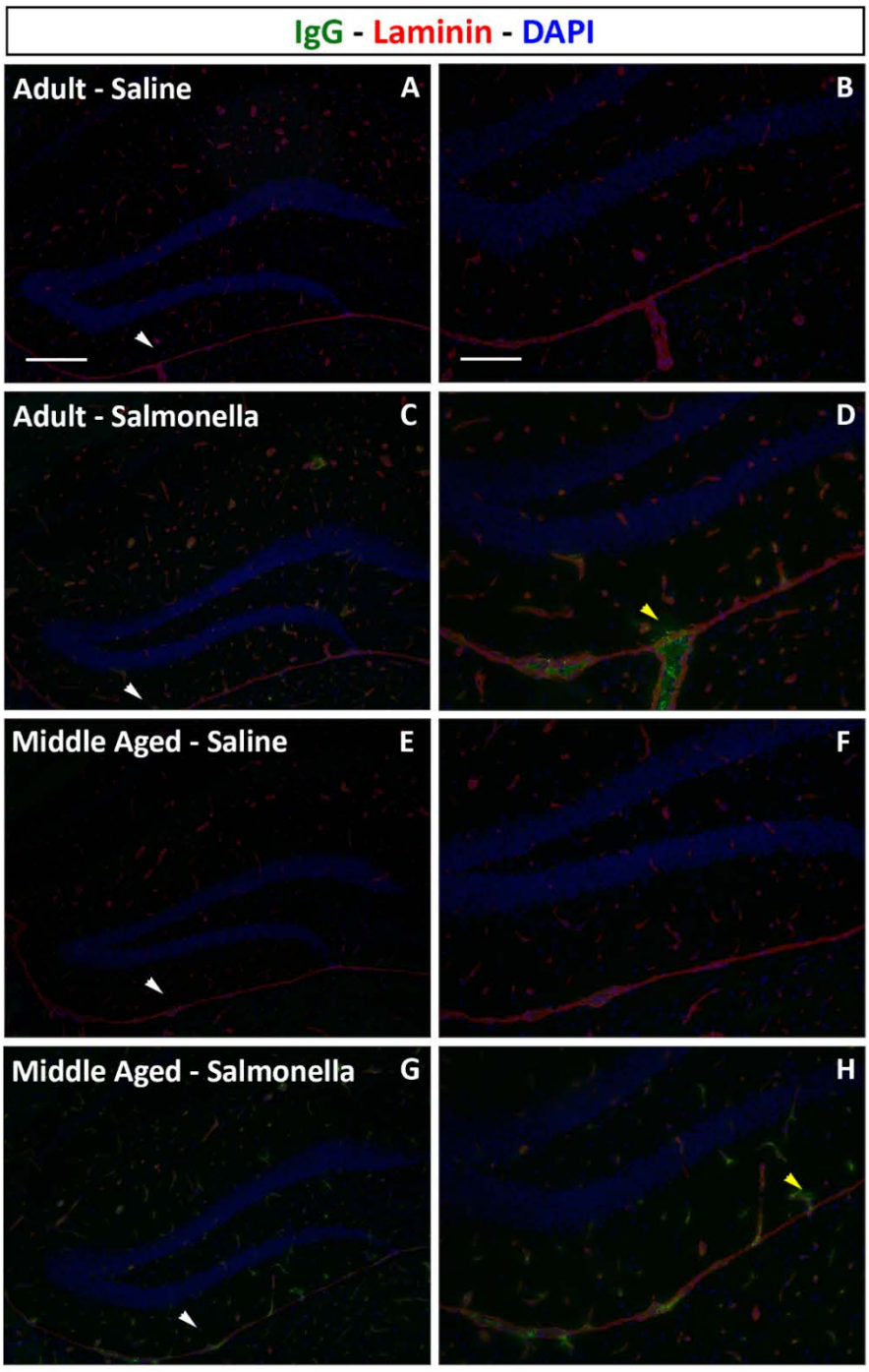
IgG - Laminin - DAPI
Adult - Saline
A
B
Adult - Salmonella
C
D
Middle Aged - Saline
E
F
Middle Aged - Salmonella
G
H

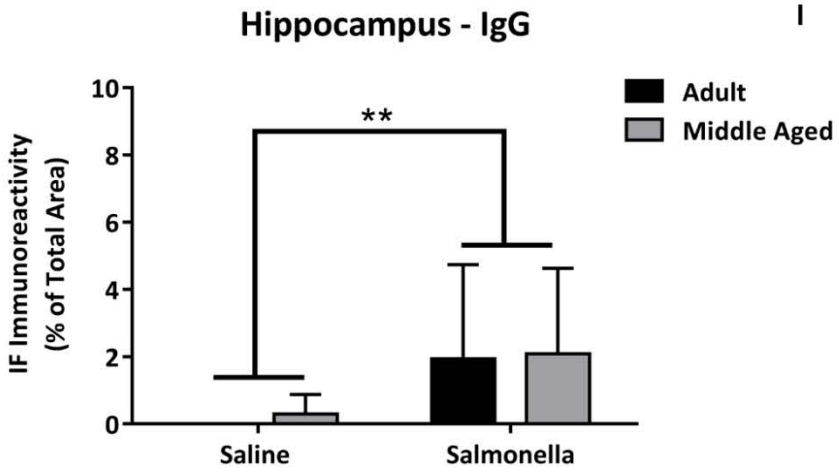
Hippocampus - IgG
I
IF Immunoreactivity (% of Total Area)
10
8
6
4
2
0
**
Adult
Middle Aged
Saline
Salmonella

Fig 5.18:- IgG immunoreactivity in the hippocampus of middle-aged and adult wild-type mice infected with *S*. Typhimurium. Overview of endogenous IgG immunoreactivity in middle-aged (E,G) or adult wild-type mice (A,C) 4 weeks post infection with *S*. Typhimurium (C,G), or injection with saline (A,E). Scale bar = 100µm. (B,D,F,H) Higher magnification images derived from overview of hippocampus and indicated with white arrows. Scale bar = 200µm. Yellow arrows indicate IgG infiltration into brain parenchyma (I) Quantification of IgG immunoreactivity (Immunofluorescence immunoreactivity (% of total area)) from entirety of hippocampus. Data was analysed by 2-way ANOVA and Tukey post hoc test (n=6-8), and displayed as mean + SD.

To investigate the infiltration of plasma proteins following *S*. Typhimurium infection, endogenous IgG immunoreactivity was assessed using immunofluorescence (Fig 5.18).

Quantification of IgG immunoreactivity in the hippocampus indicated a significant increase following *S*. Typhimurium infection, in both middle-aged and adult wild types, compared to saline-injected control mice (13-fold, $p \leq 0.01$) (Fig 5.18I). Co-staining with laminin demonstrated endogenous IgG is found within the blood vessels suggesting systemic immune response is still evident 4 weeks post-infection (Fig 5.18B,D). However, there appears to be infiltration into the brain parenchyma, as indicated by yellow arrows, in both the middle-aged and adult wild-type mice, following infection with *S*. Typhimurium (Fig 5.18D,H).

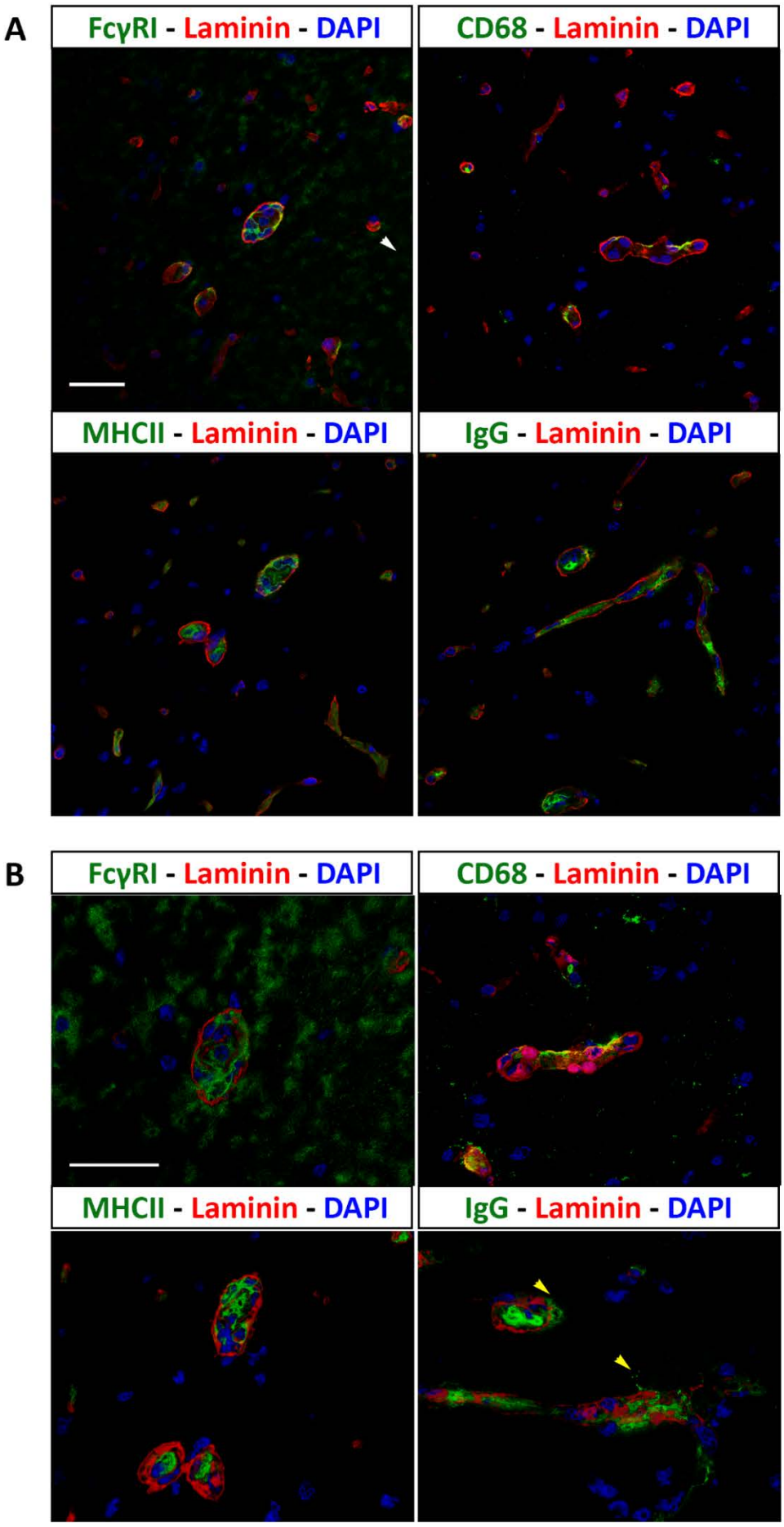
A
FcγRI - Laminin - DAPI
CD68 - Laminin - DAPI
MHCII - Laminin - DAPI
IgG - Laminin - DAPI
B
FcγRI - Laminin - DAPI
CD68 - Laminin - DAPI
MHCII - Laminin - DAPI
IgG - Laminin - DAPI

Fig 5.19:- Association of FcγRI, CD68, MHCII and IgG with laminin in the hippocampus of middle-aged wild-type mice infected with S. Typhimurium. (A) Representative high magnification confocal images of FcγRI+, CD68+ or MHCII+ cells (green) and endogenous IgG (green) with laminin (red) and DAPI (blue), from the hippocampus of a middle-aged mouse following infection with S. Typhimurium. (B) Representative high magnification 3D confocal images FcγRI+, CD68+ or MHCII+ cells (green) and endogenous IgG (green) with laminin (red) and DAPI (blue), from the hippocampus of a middle-aged mouse following infection with S. Typhimurium. Yellow arrows indicate IgG infiltration into brain parenchyma. Scale bar = 25µm.

To further explore the localisation of FcγRI+, CD68+ or MHCII+ cells and endogenous IgG, co-staining with laminin was performed, highlighting blood vessel association using confocal microscopy (Fig 5.19).

Co-staining with laminin confirmed FcγRI+ and CD68+ cells associated with the basement membranes of the vasculature. In alignment with studies using DAB (Fig 5.10), expression of FcγRI was observed across microglia in the brain parenchyma in addition to the basement membranes (Fig 5.19).

In contrast, CD68 expression was limited to the basement membranes of the blood vessels with few examples of luminal staining. There appears to be partial staining on microglia of the brain parenchyma which, as quantified in DAB (Fig 5.12), does not change following S. *Typhimurium* infection (Fig 5.19).

MHCII-positive cells were found exclusively associated with basement membranes of the vasculature (Fig 5.19). The pattern of staining suggests luminal localisation dissimilar to FcγRI and CD68 expression observed previously. Microglia of the brain parenchyma were not found to express MHCII on their cell surface, even following S. *Typhimurium* infection.

The majority of endogenous IgG appears to be localised within the lumen of blood vessels, however, leaking of this plasma protein into the surrounding parenchyma is observed and indicated by yellow arrows (Fig 5.19).

5.3.3 Neurochemistry following multiple LPS challenge and *S*. Typhimurium infection in middle-aged and adult wild-type mice

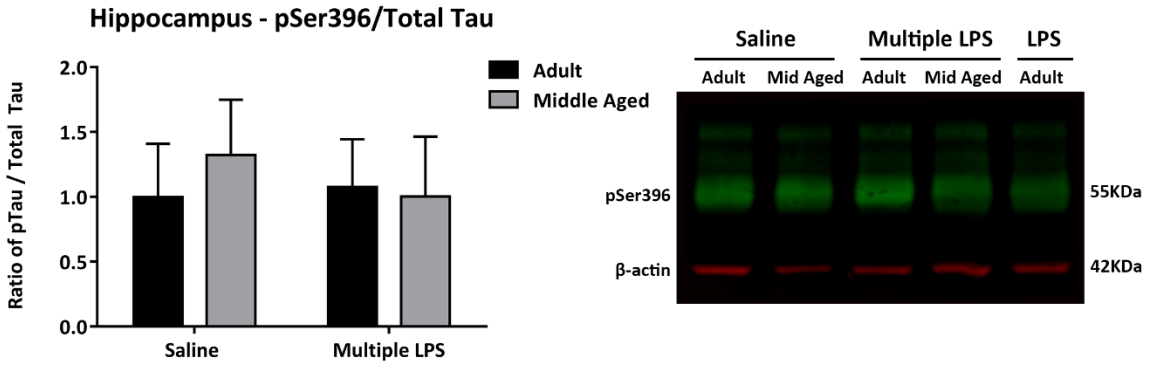

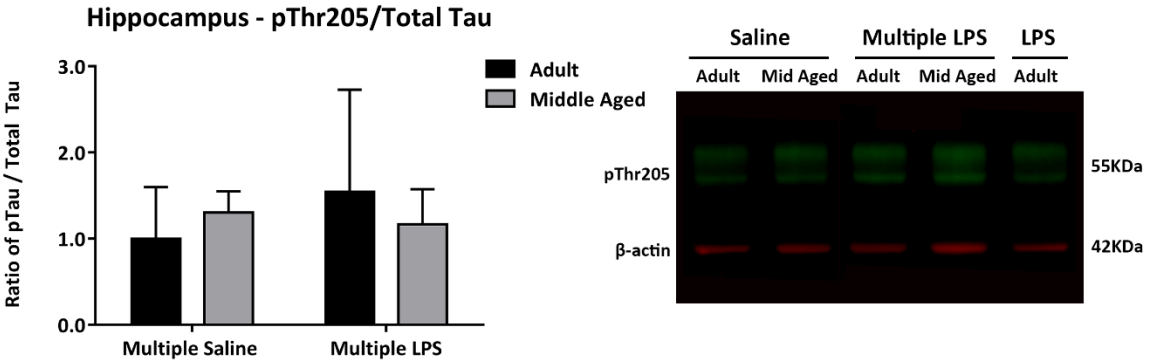

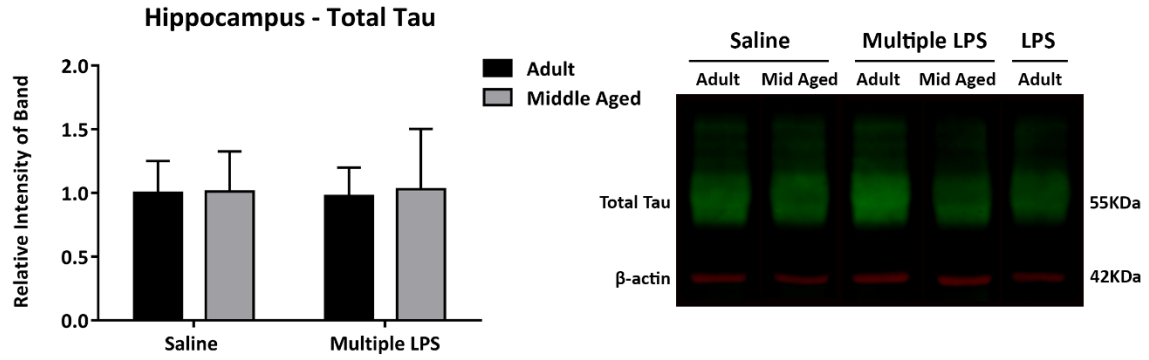

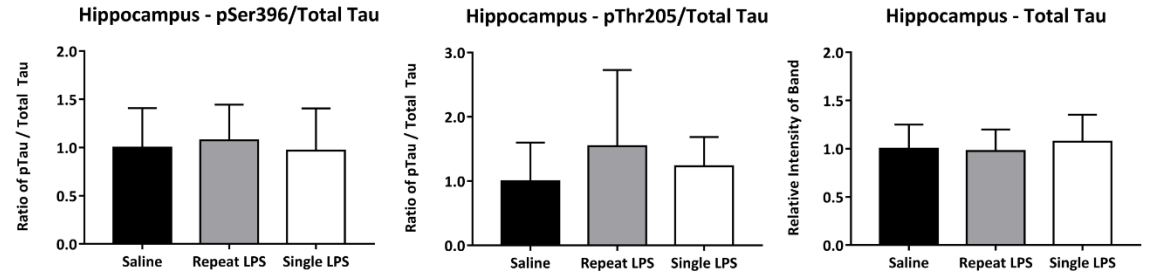

Fig 5.20:- Phosphorylated- and total tau expression levels in hippocampal-enriched tissue from middle-aged and adult wild-type mice challenged with single or multiple LPS injections.
Expression of pSer396 and pThr205 (ratio of ptau/total tau), and total tau levels (relative intensity) in hippocampal-enriched homogenate from middle-aged or adult wild-type mice following injections of multiple LPS (8X), single LPS (1 x LPS, 7 x saline) or saline alone (8X). Representative western blot membranes demonstrating tau (green) and β-actin (red) immunoreactivity, with the latter used for normalisation of protein loading. Data was analysed by 1- or 2-way ANOVA and Tukey post hoc test (n=6-8), and displayed as mean + SD.

To investigate the impact of single and multiple LPS challenges on tau-related neurochemistry in the brain, total and phosphorylated-tau levels were measured in hippocampal-enriched tissue homogenate by western blot (Fig 5.20).

Quantification of the tau-related immunoreactive bands obtained from western blot showed no significant change following multiple LPS challenge or between ages, with respect to pSer396, pThr205 or total tau levels. Additionally, there was no difference in tau phosphorylation or total tau levels following either single or multiple LPS challenge.

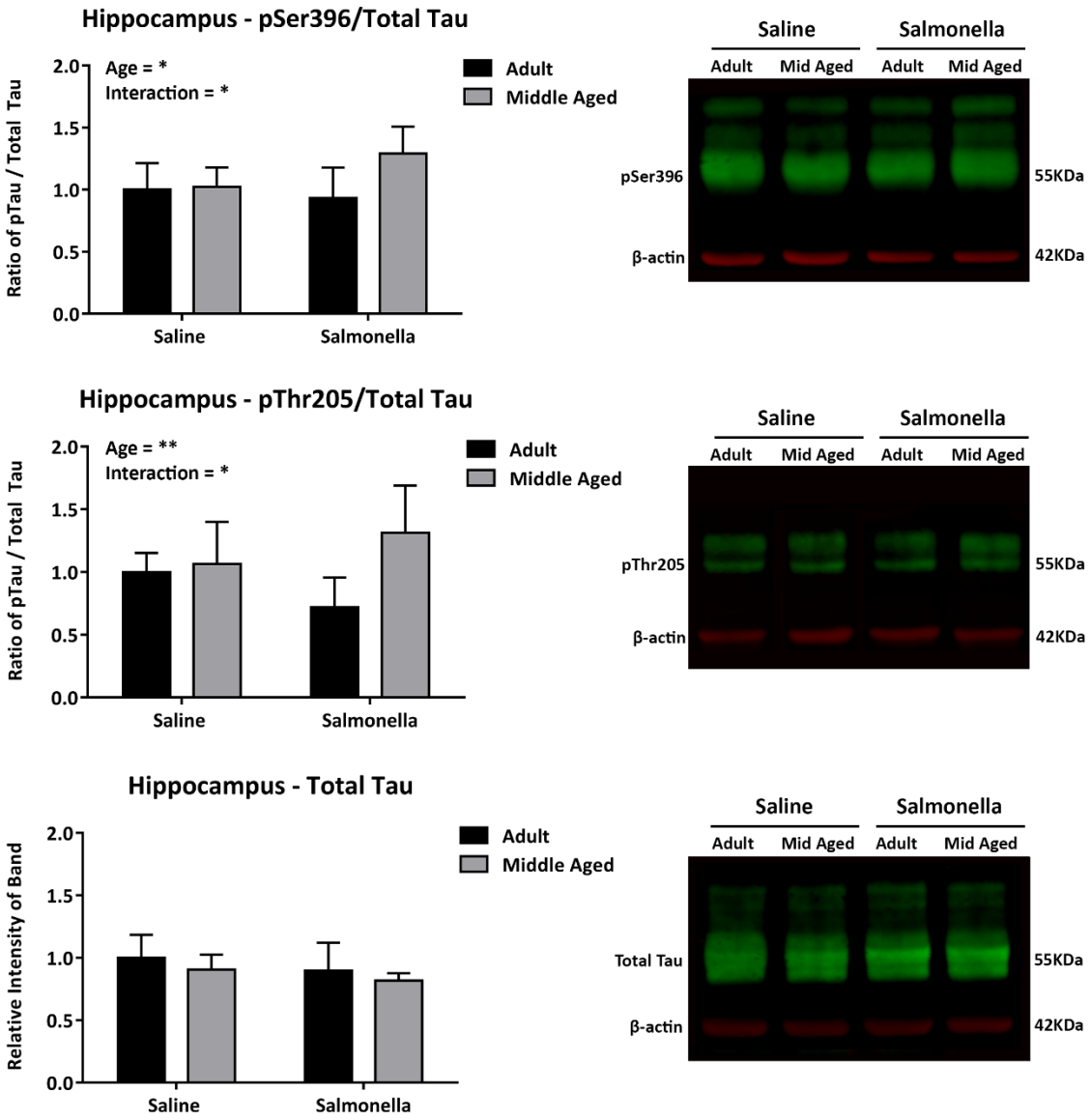

Fig 5.21:- Phosphorylated- and total tau expression levels in hippocampal-enriched tissue from middle-aged and adult wild-type mice infected with S. Typhimurium. Expression of pSer396 and pThr205 (ratio of ptau/total tau), and total tau levels (relative intensity) in hippocampal-enriched homogenate from middle-aged or adult wild-type mice 4 weeks post infection with S. Typhimurium, or injection with saline. Representative western blot membranes demonstrating tau (green) and β-actin (red) immunoreactivity, with the latter used for normalisation of protein loading. Data was analysed by 2-way ANOVA and Tukey post hoc test (n=6-8), and displayed as mean + SD.

To investigate the impact of S. *Typhimurium* infection on tau-related neurochemistry in the brain, total and phosphorylated-tau levels were measured in hippocampal-enriched tissue homogenate by western blot (Fig 5.21).

Quantification of the tau-related immunoreactive bands obtained from western blot demonstrated a significant interaction between age and S. *Typhimurium* infection for both the pSer396 and pThr205 epitopes ($p \leq 0.01$); post hoc tests revealed, however, that S. *Typhimurium* infection did not cause a significant change in middle-aged or adult wild-type mice with respect to the age-matched saline-injected controls. This suggests that 4 weeks post infection with S. *Typhimurium*, adult mice show a trend towards reduced phosphorylation at tau phospho-epitopes, while middle-aged mice demonstrate a trend towards increased phosphorylation. Additionally, middle-aged mice had elevated phosphorylation at both tau phospho-epitopes (pSer396 (1.2-fold, ($p \leq 0.05$), pThr205 (1.4-fold, ($p \leq 0.01$)), compared to adult wild types. No differences were observed in total tau levels between groups.

5.4 Discussion

The process of ageing is the single biggest risk factor for the development of neurodegenerative disease (Niccoli and Partridge 2012). It is proposed that throughout life, the challenges to an individual's immune system contribute to this by promoting a proinflammatory environment in the CNS. Clinical evidence supports this theory, as patients displaying greater peripheral inflammation at middle-age have an increased risk of developing dementia and cognitive deficits (Schmidt et al. 2002; Komulainen et al. 2007; Singh-Manoux et al. 2014). Using inflammatory mimetics, such as LPS, it is unclear experimentally whether middle-age is sufficient for a significantly altered response to systemic inflammation (Deng et al. 2006; Nikodemova et al. 2016). However, as pathological and inflammatory changes are thought to occur decades before symptoms of dementia arise (Dubois et al. 2014), it is critical to understand at what stage of life these inflammatory challenges are having a deleterious impact. Therefore, I have taken the novel approach of utilising an attenuated strain of the bacterium *S*. Typhimurium to infect middle-aged (11-12 month old) wild-type mice, to replicate an inflammatory challenge more akin to that experienced by humans. In an additional experiment, the commonly utilised model of systemic inflammation, multiple LPS challenge, was employed for comparison.

Analysis of weight data suggests adult mice lost more weight than their middle-aged counterparts following the first challenge with LPS. A similar trend was observed in the mice receiving *S*. Typhimurium. Additionally, adult mice receiving multiple LPS challenges or *S*. Typhimurium, recovered to starting weight by 24 and 14 days respectively following initial insult. Middle-aged mice, on the other hand, maintained a weight at approximately 5% below starting weight in both experiments. The explanation for this latter finding may lie in the starting body weights before infection, as middle-aged mice are significantly heavier than the adult wild types. It has been previously shown that middle-aged mice gain weight at a slower rate than adults and therefore may be unable to regain weight following infection (Fahlström et al. 2011).

The peripheral immune response was assessed by calculating spleen weight and levels of serum cytokines. Results indicate adult and middle-aged mice have a significantly greater

spleen weight following *S*. Typhimurium infection, compared to saline-injected control mice. However, despite middle-aged mice having heavier spleens generally, there was no difference in enlargement following *S*. Typhimurium infection, between the ages. The spleens of mice receiving multiple LPS challenges did not change at time of sacrifice (data not shown), likely due to lack of immune cell proliferation in this organ.

Levels of serum cytokines support the notion that the peripheral immune response in the middle-aged mice is similar to the adults. Multiple LPS challenge induced moderate elevations in IL-1β, IL-6, TNF-α and IL-10 at both ages in the periphery. In chapter 3, the development of tolerance was proposed using this model and differences between the ages, following LPS, may only be seen acutely after a single dose. In support of this, Mouton et al observed an exaggerated response to LPS (0.3mg/kg) in middle-aged (14-16 month old) C57BL/6 mice compared to adult (6 month old) counterparts (Mouton et al. 2012). This manifested as elevated circulating levels of IL-1β and IL-6 between LPS groups of middle-aged and adult mice, however the greater age of these mice and 2 hour sacrifice time point may explain some of these findings. Significant differences in the serum levels of IL-1β, IL-6 and IL-10 between multiple LPS and single LPS challenge, suggest the initial LPS insult is not solely responsible for the elevations in these cytokines.

Infection with *S*. Typhimurium elicited a robust and significant increase in both pro- and anti-inflammatory serum cytokines, independent of age and in line with observations from chapter 4. Significant elevations of IFN-γ, IL-1β, IL-6, TNF-α, IL-10, IL-12, IL-2, IL-5 and mKC were detected, further demonstrating the broad range of immune response elicited. Most notably, IFN-γ levels increased by 309-fold, which may be a result of T-cell involvement in the resolution of the *S*. Typhimurium infection (Mizuno et al. 2003). In contrast, multiple LPS challenges caused a small reduction in the levels of this cytokine.

Moderately higher baseline levels of IL-6, IL-10 and mKC were observed in middle-aged mice compared to adults, between both experiments. There is limited research on the baseline levels of these in middle-aged mice, however, no alterations at this time point have been reported previously (Kang et al. 2004; Shan et al. 2013). Overall, the similar peripheral response would suggest cytokine-induced sickness behaviours were not responsible for differences in initial weight loss following infection, between ages.

Additionally, these findings suggest a lack of peripheral priming in middle-aged mice as effects were not significantly additive with either model of systemic inflammation. However, acute time points would need to be assessed to comprehensively determine whether priming has occurred.

As advanced ageing is reported to be a prerequisite for priming in the brain (Godbout et al. 2005), neuroinflammation was investigated in middle-aged mice to identify if an exaggerated immune response was observed following multiple LPS challenges or infection with *S*. Typhimurium. Microglia are heavily implicated in this response from a second stimulus in ageing (Sierra et al. 2007), as minocycline has been shown to inhibit sickness behaviours and the generation of proinflammatory cytokines IL-1β and IL-6 following systemic administration of LPS (Henry et al. 2008).

The results presented here demonstrate a significant increase in the expression of FcγRI following both multiple LPS challenge and *S*. Typhimurium*,* in both adult and middle-aged wild-type mice. Similarly, neither challenges demonstrated any changes in CD68 expression in the hippocampus. However, this was not observed with the expression of CD11b, whereby multiple LPS, but not *S*. Typhimurium infection, caused a significant increase. Baseline FcγRI expression was elevated in middle-aged mice from the multiple LPS experiment, however, this was not seen in groups from the *S*. Typhimurium experiment. It has previously been reported that the expression of markers, such as CD11b, FcγRI, CD68, CD11c and F4/80, increase with age in both mice and rats (Perry et al. 1993; Hart et al. 2012), while a mediator of microglial repression, CX_3CL1, is found downregulated (Wynne et al. 2010).

My results support previous research in male C57BL/6 mice, demonstrating that markers associated with microglia, such as F4/80 and CD11b, are unaltered by the middle-age time point (Deng et al. 2006). Interestingly, our lab and others have shown that microglial marker expression, such as CD11b and CD68, is not dramatically altered following systemic inflammation in ageing conditions and therefore may not best represent the functional state of this cell type (Henry et al. 2009; Wynne et al. 2010; Hart et al. 2012). Alternatively, our lab has identified that changes to microglial marker expression with age are usually found in the white matter and therefore the focus on the hippocampus in this

study would not reveal this (Hart et al. 2012). Comparison of single and multiple LPS challenge, revealed the latter induced significant changes in FcγRI expression while a single challenge, although increased, demonstrated a smaller effect. This suggests the lasting effect of this initial LPS insult is not solely responsible for the elevations in FcγRI. In contrast, CD11b expression is marginally higher following single LPS challenge compared to multiple injections. Therefore, there appears to be a prolonged upregulation of CD11b in the hippocampus following a single LPS challenge.

In conclusion, this comparative study supports that while FcγRI demonstrates a shared change between the two models, alterations to the expression of CD11b is unique to an LPS protocol, and not found following infection with *S*. Typhimurium.

There is substantial evidence that an exaggerated microglial response to a second insult, as measured by levels of cytokines, is observed in a diverse range of models exhibiting advanced age (Xie et al. 2003; Godbout et al. 2005; Barrientos et al. 2006; Chen et al. 2008; Henry et al. 2008; Henry et al. 2009; Wynne et al. 2010). Multiple LPS challenge induced moderate elevations in brain expression of IL-1β, TNF-α, IL-10 at both ages. Additionally, IL-2 and mKC demonstrated significant increases, while IL-6 remained unchanged. Interestingly, no interaction was seen with infection and age, with the exception of IL-12 which showed increased levels in adult mice upon stimulation with LPS, while the opposite trend is seen at middle age. Studies previously carried out in middle-aged (9-10 month old) ICR/CD1 mice injected with systemic LPS (5mg/kg) i.p. have shown significantly elevated mRNA levels of IL-1β, TNF-α, IL-10 and IL-6 in middle-aged mice, 3 hours following systemic LPS, in comparison to adults (Nikodemova et al. 2016). However, these levels had returned to baseline by 24 hours and this additive effect was not observed after a second challenge of LPS. Comparison of single and multiple LPS challenge, suggests IL-1β, IL-5 and mKC are uniquely upregulated in the latter protocol.

The hippocampal cytokine profile from mice infected with *S*. Typhimurium mirrors changes seen in the serum, albeit to a lesser degree. Increases in the levels of IFN-γ, IL-1β, IL-6, TNF-α, IL-12, IL-2, IL-5 and mKC were observed. Akin to multiple LPS challenge, no interaction was seen with infection and age, with the exception of TNF-α levels which were higher in adult mice following infection.

Interestingly, lower levels of IL-4 were observed in middle-aged mice, independent of *S*. Typhimurium infection. This has been demonstrated before in the hippocampus of aged rats (Maher et al. 2005; Nolan et al. 2005), together with reports of reduced IL-4R and sensitivity (Fenn et al. 2012). Coupled with unaltered levels of IL-10 seen here, microglia may be lacking factors required to switch to an anti-inflammatory M2 phenotype.

It is difficult to directly compare the results from previous studies with those presented here, as different strains of mice, source and doses of LPS and injection protocols are utilised. However, these data support that while *S*. Typhimurium induces an inflammatory response with greater change and diversity than multiple LPS challenge at the 4 week time point, neither model produces an exaggerated effect in middle-aged animals. While acute inflammatory stimuli are required to fully test priming, the models of chronic inflammation utilised here do not support the hypothesis that it occurs in the brain of middle-aged mice.

An important marker of microglial priming, that is observed to increase with ageing, is MHCII (Perry et al. 1993; Sheffield and Berman 1998; Godbout et al. 2005). Following infection with *S*. Typhimurium, MHCII+ cells associated with the vasculature rather than microglia in the parenchyma, in adult and middle-aged mice. Confocal microscopy suggests these cells line the inside of the blood vessel lumen and therefore may be endothelial in identity. Endothelial cells are important contributors in the immune response to a foreign pathogen, with the ability to generate and secrete proinflammatory cytokines into the brain parenchyma (Mai et al. 2013). MHCII is induced through circulating IFN-γ (Etienne et al. 1999), which is observed in both aged and middle-aged mice following infection. Given the minimal phenotypic alterations to microglia in this model, further investigation into the contribution of endothelial cells to cytokines changes would be warranted.

Additionally, a significant increase in endogenous IgG immunoreactivity was observed following infection with *S*. Typhimurium, in both adult and middle-aged mice. Confocal microscopy suggests IgG enters the parenchyma from blood vessels and therefore may be communicating with immune cells, such as microglia. Monomeric IgG has the capacity to bind FcγRI, induce ITAM signalling and drive a signalling cascade including the activation

of Syk kinases, PKC and elevation of intracellular Ca^{2+} (Swanson and Hoppe 2004; Nimmerjahn and Ravetch 2005). This results in further activation of the MAP kinase family, NF-κB and the transcription of proinflammatory cytokines including IL-1β, IL-6 and TNF-α (Bournazos et al. 2016). Given the increases observed in IgG, FcγRI and proinflammatory cytokines, this pathway may be a critical route in transducing the inflammatory response from the periphery to the CNS following *S*. Typhimurium infection. As there was no difference in IgG immunoreactivity between middle-aged and adult mice, this stage in the ageing process may not demonstrate any decline in BBB integrity. However, given the strong effect of *S*. Typhimurium on BBB permeability, any subtle changes with age may be eclipsed. FcγRI+ and CD68+ cells were also observed in association with the vasculature. Whether these are perivascular macrophages or microglia, they may also have a role to play in transducing inflammation from the periphery to the CNS.

Middle-aged and adult mice challenged with multiple LPS demonstrated a similar association of FcγRI+ and CD68+ cells with the vasculature. However, there was a lack of MHCII upregulation on the vasculature and no change in levels of endogenous IgG. The absence of these changes at the BBB may explain the relatively smaller increases in hippocampal cytokine levels observed in this model, in comparison to infection with *S*. Typhimurium.

Finally, the impact of these inflammatory changes on tau-related neurochemistry was assessed by investigating phosphorylation of two tau epitopes. The data generated shows that a significantly higher ptau/total tau ratio was observed at both epitopes in middle-aged mice compared to adults. Shan et al showed a similar trend at these epitopes in middle-aged male C57BL/6 mice (Shan et al. 2016), while human post-mortem data suggests phosphorylation of Ser396 is closely related to early tau pathological events in AD (Mondragón-Rodríguez et al. 2014).

Interestingly, middle-aged and adult wild-type mice showed the opposite responses to infection with *S*. Typhimurium, with regard to phosphorylation of tau. An interaction was observed in both the ratios of pThr205/total tau and pSer396/total tau, suggesting an increase in tau phosphorylation occurs in middle-aged mice while the converse is true for

adult wild-types. Information on the impact of infection on tau phosphorylation in middle-aged mice is limited to non-transgenic controls in studies utilising tau transgenic mice. For example, Sy et al infected 3xTg (11-13 month old) mice with mouse hepatitis virus (MHV), directly into the brain, and found exacerbated tau pathology in the transgenic mice, 2 and 4 weeks following infection. However, MHV-infected non-transgenic mice did not develop any tau pathology in the hippocampus. Therefore, to the best of my knowledge, the results presented in this chapter are the first to report differences in tau phosphorylation between middle-aged and adult wild-type mice following infection. Although modest, this response may provide one reason why ageing is the biggest risk factor for neurodegenerative diseases like AD, and provide evidence that tau phosphorylation, resulting from systemic inflammation, may be one of the earliest events in their development.

Interestingly, mice from the multiple LPS experiment, did not show increases in tau phosphorylation at middle-age. Together with the lack of tau phosphorylation induced at either epitope, following challenge with multiple LPS, this data suggests the increases observed in middle-aged mice from the *S*. Typhimurium are a consequence of both infection and age.

In summary, this chapter has demonstrated the inflammatory response provoked in the periphery and brain, differs in both intensity and diversity between multiple LPS challenge and infection with *S*. Typhimurium over a 4 week time course. However, in each of these models of systemic inflammation, middle-aged and adult mice show a similar response. While others have previously observed an exaggerated response from immune cells such as microglia at this age, the data provided here would not support those findings. On the contrary, a reduced TNF-α response in the brains of middle-aged mice following *S*. Typhimurium infection, would imply impairment. However, this was not observed for the rest of the cytokines assessed. It is difficult to compare publications on microglial priming in middle age, as animals used are often differing in species, strain and sex. The time point following insult and model of systemic inflammation used may also differ, thereby contributing to conflicting results (Niraula et al. 2016).

An additional separation between the models lies in relation to the vasculature. This is evidenced by infiltration of endogenous IgG and upregulation of MHCII on cells associated with the vasculature, following infection with *S*. Typhimurium. The absence of similar changes in the multiple LPS model, may contribute to the relatively weaker inflammatory response observed in the hippocampus. Crosstalk at the BBB, including cytokine and plasma protein infiltration, may provide a crucial step in propagating systemic inflammation into the CNS.

Changes in tau phosphorylation were only observed following infection with *S*. Typhimurium. The interaction would suggest an increase in phosphorylation is seen in middle-aged mice while the converse is true for the adults. Two conclusions may be drawn from these findings. Firstly, changes in tau phosphorylation are observed following *S*. Typhimurium infection, and not in the multiple LPS model, as there is a differing peripheral inflammatory profile, alteration of the BBB and a larger inflammatory response in the brain. Secondly, as there is a difference in tau phosphorylation between adult and middle-aged mice following infection with *S*. Typhimurium, but similar cytokine elevations are observed, ageing may have predisposed cells of the brain such as neurons to react differently to a cellular stress. Middle-aged mice have been shown to have increased oxidative stress in the brain (Liu et al. 2003), and therefore the addition of neuroinflammation may result in the increases in tau phosphorylation shown in this study.

Other signalling pathways not assessed here could provide further information as to the differences observed. In the 3xTg model, multiple systemic LPS elicited greater tau phosphorylation in both adult and middle aged mice, however the predominant kinase responsible had switched from CDK5 to GSK3β (Kitazawa et al. 2005; Sy et al. 2011). This demonstrates that the reaction to neuroinflammation had changed in middle-aged mice, however, further work is necessary to determine whether this occurs in wild-type mice.

Chapter 6: Salmonella infection in Tg2576 APP^{SWE} mice

6.1 Introduction

In the previous chapters, it has been shown that two models of systemic inflammation, multiple i.p. injections of LPS or infection with the bacterial strain *S*. Typhimurium, result in distinct neuroinflammatory profiles, characterised by changes in brain cytokine expression levels and microglial phenotype. In middle-aged mice (11-12 month old), the data trend suggested that infection with *S*. Typhimurium caused increased tau phosphorylation, but not in adults (3-4 month old). Although these moderate changes would imply that a deleterious response to systemic inflammation is only occurring at middle-age, more significant alterations may require a change in the susceptibility of the brain environment, associated with risk factors for neurodegenerative diseases.

The Amyloid Cascade Hypothesis (ACH) postulated that the abnormal processing of APP, production of, and subsequent deposition of Aβ were leading events in AD pathogenesis (Hardy and Higgins 1992), followed by aberrant tau phosphorylation and aggregation, leading to eventual neuronal death. Over the past couple of decades, this hypothesis has evolved to incorporate parallel factors such as lipid metabolism, innate immune function and endosomal vesicle recycling, however, the notion that aberrant Aβ processing precedes alterations in tau remains a core aspect to the hypothesis (Selkoe and Hardy 2016).

Numerous *in vitro* and *in vivo* studies have substantiated this theory, although the predominant molecular mechanisms involved remain unclear (for review see Lloret et al. 2015). Application of soluble Aβ42 dimers, isolated from the cortex of an AD patient, to primary rat hippocampal neurons, have been shown to induce tau phosphorylation at AD-relevant epitopes and cytoskeletal disruption (Jin et al. 2011). Additionally, when mice expressing the Swedish mutation in the APP gene (Tg2576) are crossed with mice expressing mutated P301L human tau (JNPL3), increased numbers of NFTs are observed compared to mutant human tau only control mice (Lewis et al. 2001), supporting the theory that Aβ has the potential to exacerbate tau pathology.

Proposed mechanisms linking Aβ and tau include activation of tau kinases such as GSK3β, via NMDA receptors (Shipton et al. 2011). Although this may offer a direct connection between the two pathologies, an intriguing indirect mechanism may lie in the capacity of Aβ to induce neuroinflammation. Post-mortem AD brains consistently show evidence of gliosis occurring around Aβ plaque pathology (Itagaki et al. 1989), a feature recapitulated to varying extents in transgenic APP mouse models (Duyckaerts et al. 2008). In relation to my hypothesis that inflammation drives tau phosphorylation and pathology, Aβ may be acting as a facilitator to this process.

To explore what effect Aβ may have in the relationship between systemic inflammation and tau phosphorylation, I have chosen to use a well characterised murine model of amyloid deposition, the APP transgenic Tg2576 strain (Hsiao et al. 1996). These mice possess a transgene coding for human APP (hAPP) with the Swedish mutation (K670N, M671L) downstream of the hamster prion promoter, resulting in overexpression of hAPP and production and deposition of increased levels of Aβ40 and Aβ42. Diffuse and congophillic plaques are seen in the cortex by 7-8 and 12-15 months respectively (Kawarabayashi et al. 2001), however limited deposition of Aβ is also reported in the hippocampus by at least 12 months of age (Hsiao et al. 1996). In this study, I have chosen to use mice at 16-17 months of age. As ageing is the biggest risk factor for a neurodegenerative disease like AD, this time point offers an additional risk factor as the mice are of an advanced age compared to previous chapters.

It has been previously shown by Sly et al that systemic inflammation mediated by i.v. administration of LPS (25μg/mouse) to Tg2576 mice (16 month old), results in elevated cortical levels of IL-1β mRNA and Aβ42 as early as 2 hours following delivery, compared to non-transgenic littermates (Sly et al. 2001). This exaggerated response is thought to represent microglial cell priming in amyloid models (Yin et al. 2017), and therefore the addition of systemic inflammation will drive further neuroinflammation and pathology. As infection with *S*. Typhimurium has been shown to alter tau phosphorylation in the previous chapter, I have utilised it here as a novel approach to explore if an exaggerated immune response is observed in the Tg2576 model.

I hypothesise that amyloid deposition in the hippocampus of aged Tg2576 mice (16-17 month old) will prime immune cells, such as microglia, and result in an enhanced neuroinflammatory response, 4 weeks following systemic infection with *S*. Typhimurium. In turn, this will drive further amyloid deposition and induce pathological tau phosphorylation. As in previous chapters, samples were taken 4 weeks post infection and analysed for changes in neuroinflammatory markers and tau phosphorylation. Additionally Aβ isoform levels were measured to explore indirect mechanisms, and nesting behaviours assessed to examine phenotypic behaviours and changes to activities of daily living (ADL) (Deacon 2012).

6.2 Materials and Methods

6.2.1 Study Design

Three days before infection, aged transgenic (Tg2576) and non-transgenic littermate mice (16-17 month old) were randomly assigned to one of two groups (n=4-6, mixed gender), saline or *S*. Typhimurium and relocated into the CL2 facility for acclimatisation. Mice were injected (i.p.) with 200µl of saline or 1x10^6 CFU *S*. Typhimurium and provided with water soaked high-energy food pellets for 24 hours post infection to counter excessive weight loss. Mice were weighed daily for 1 week and approximately weekly thereafter. One day prior to sacrifice, mice were moved to individual cages for nesting behaviour assessment, performed by Mr Paul Ibbett. Blinded assessment was carried out the following day. Mice were given an overdose of anaesthetic (Rat Avertin) prior to the collection of blood. An incision was made in the right atrium and blood was collected (0.5-1ml) for later analysis of serum, followed by transcardial perfusion with 0.9% heparinised saline. Brain and spleen were taken for bioanalysis. Further details of methods used for tissue analysis are outlined in chapter 2.

6.2.2 Nesting behaviour

Nesting protocol and scoring was performed as described previously (Deacon 2006). Further detail can be found in chapter 2. The scoring system is as follows:–

1. Nestlet more than 90% intact.
2. Nestlet partially torn (50-90% intact), no nest site.
3. Nestlet mostly torn (greater than 50%), no nest site.
4. Nestlet mostly shredded, and there is a defined nest site in one quarter of the cage. Nest walls are lower than a mouse laying on its side in more than 50% of total nest circumference.
5. A near perfect nest using >90% of the nestlet and positioned in one corner of the cage. Nest walls are as tall as a mouse laying on its side for more than 50% of total nest circumference.

Nests exhibiting characteristics of two scores were awarded marks of 0.5.

6.3 Results

6.3.1 Metabolic and peripheral immune response in Tg2576 mice and non-transgenic littermates infected with *S*. Typhimurium

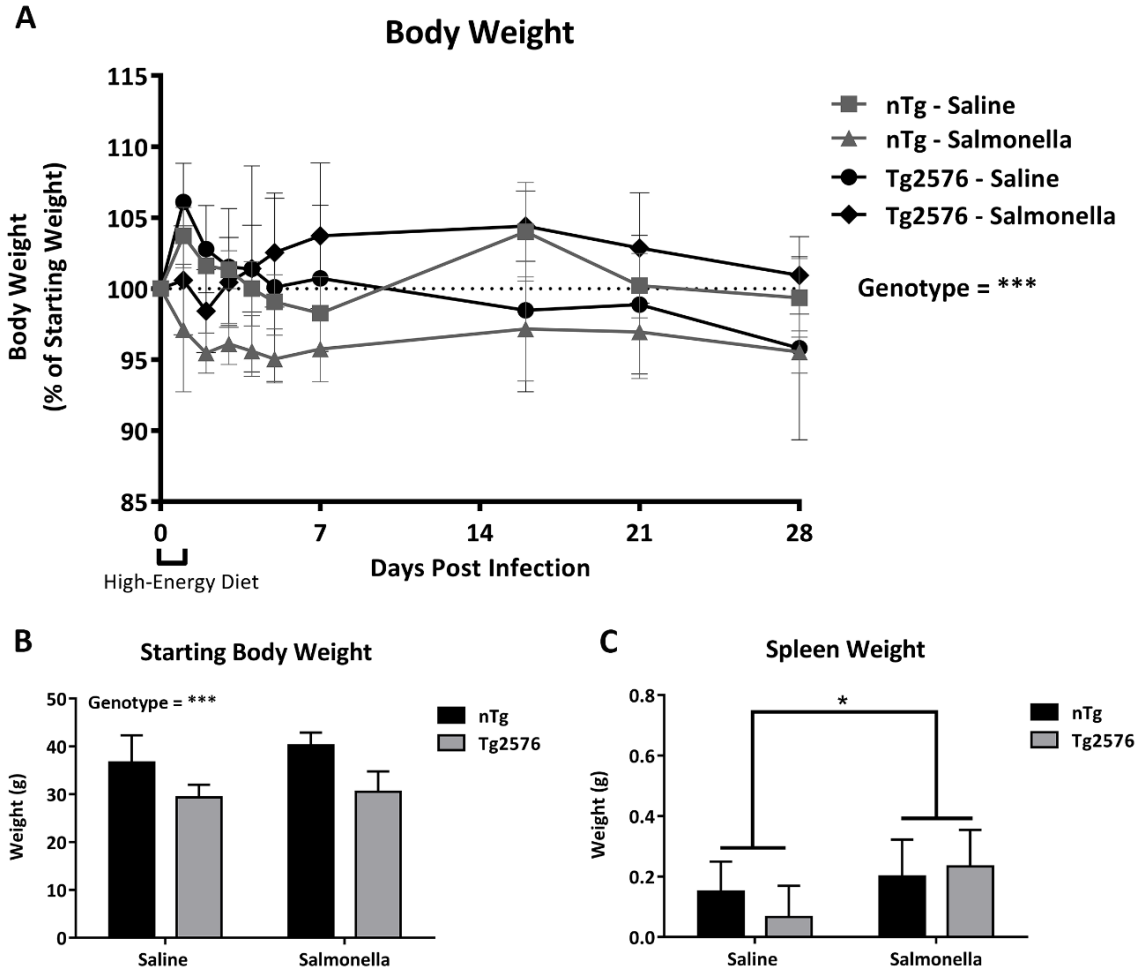

Fig 6.1:- Body and spleen weight from Tg2576 transgenic mice and non-transgenic littermates infected with *S*. Typhimurium. Mice were weighed daily after infection, or saline injection, for one week, and then approximately once weekly thereafter. All mice were given a high-energy diet for 1 day post infection to counter risk of excessive weight loss. (A) Body weight (% of starting weight) of Tg2576 transgenic mice and non-transgenic littermates infected with *S*. Typhimurium. Data was analysed using 3-way ANOVA with repeated measure (n=4-6), and displayed as mean ± SD. (B) Starting body weight (grams) of Tg2576 transgenic mice and non-transgenic littermates. (C) Spleen weight (grams) of Tg2576 transgenic mice and non-transgenic littermates at sacrifice. Data was analysed by 2-way ANOVA and Tukey post hoc test (n=4-6), and displayed as mean ± SD.

One day post infection, mice adminstered with *S*. Typhimurium and fed a high-energy diet displayed a weight change of approximately +0.6% (+0.3g) and -2.9% (-1.2g) from starting weight, in Tg2576 and non-transgenic mice respectively (Fig 6.1A). Mice administered with a saline injection and fed a high-energy diet displayed a weight change of approximately +6.1% (+1.8g) and +3.7% (+1.3g) from starting weight, in Tg2576 and non-transgenic mice respectively (Fig 6.1A). Analysis indicated a significant difference in body weight throughout the 4 week period between Tg2576 mice and non-transgenic littermates ($p \leq 0.001$). There was no significant difference in body weight between mice infected with *S*. Typhimurium or those receiving a saline injection.

Tg2576 mice displayed a significantly lower starting body weight compared to non-transgenic littermates ($p \leq 0.001$), of approximately 9 grams (Fig 6.1B). Upon sacrifice at 28 days post infection, there was a significantly higher spleen weight in mice infected with *S*. Typhimurium compared to those injected with saline ($p \leq 0.05$), independent of genotype (Fig 6.1C).

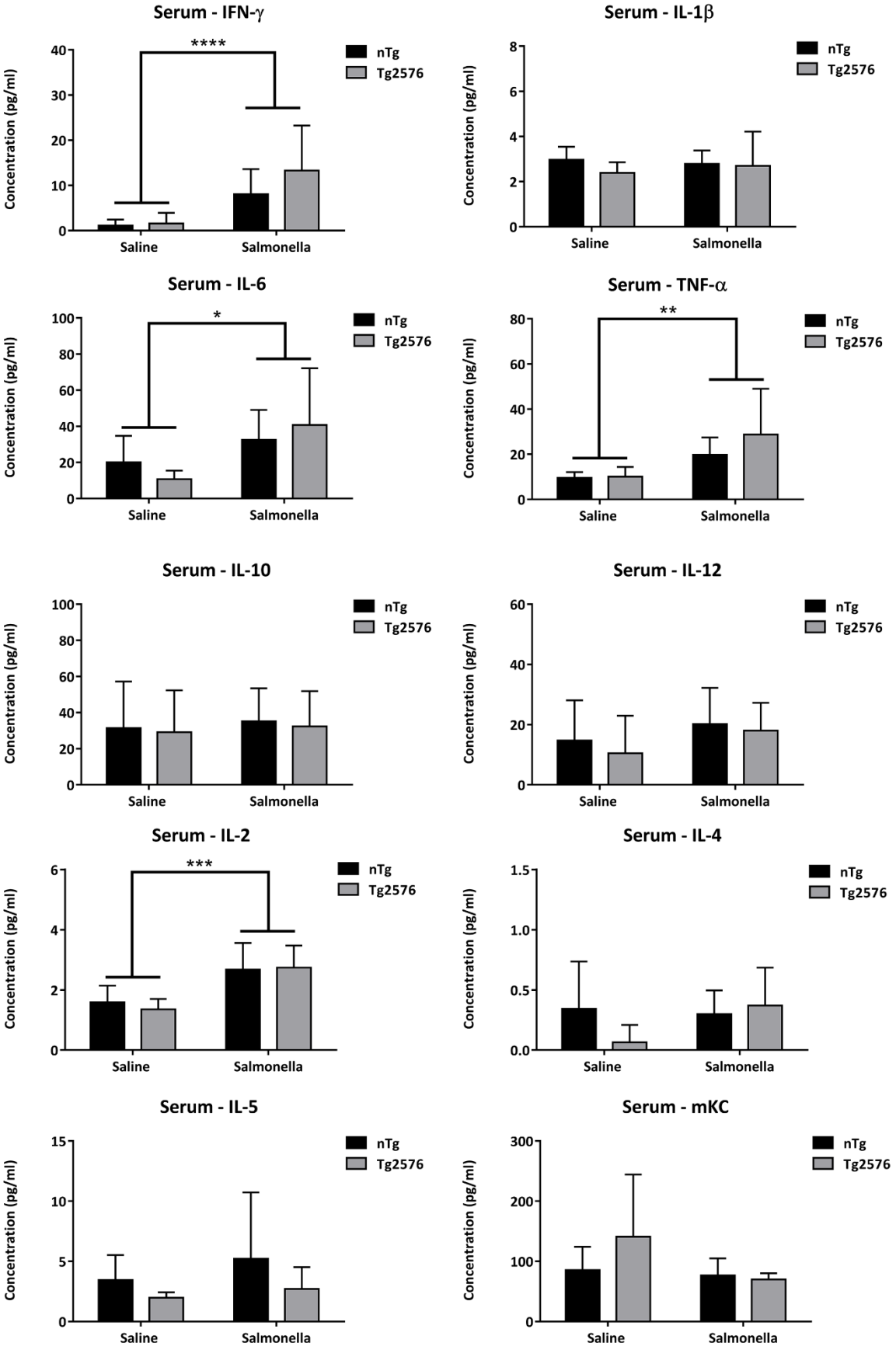
Serum - IFN-γ
Concentration (pg/ml)
****
nTg
Tg2576
Saline
Salmonella
Serum - IL-1β
Concentration (pg/ml)
nTg
Tg2576
Saline
Salmonella
Serum - IL-6
Concentration (pg/ml)
*
nTg
Tg2576
Saline
Salmonella
Serum - TNF-α
Concentration (pg/ml)
**
nTg
Tg2576
Saline
Salmonella
Serum - IL-10
Concentration (pg/ml)
nTg
Tg2576
Saline
Salmonella
Serum - IL-12
Concentration (pg/ml)
nTg
Tg2576
Saline
Salmonella
Serum - IL-2
Concentration (pg/ml)
***
nTg
Tg2576
Saline
Salmonella
Serum - IL-4
Concentration (pg/ml)
nTg
Tg2576
Saline
Salmonella
Serum - IL-5
Concentration (pg/ml)
nTg
Tg2576
Saline
Salmonella
Serum - mKC
Concentration (pg/ml)
nTg
Tg2576
Saline
Salmonella

Fig 6.2:- Cytokine expression levels in serum from Tg2576 transgenic mice and non-transgenic littermates infected with S. Typhimurium. Cytokine levels (pg/ml) in serum from Tg2576 transgenic mice or non-transgenic littermates 4 weeks post infection with S. Typhimurium, or injection with saline. Data was analysed by 2-way ANOVA and Tukey post hoc test (n=4-6), and displayed as mean + SD.

Circulating levels of cytokines were measured in serum samples using a 10-plex immunoassay (Fig 6.2).

Infection with *S*. Typhimurium induced a significant increase in the proinflammatory cytokines IFN-γ (16-fold, $p \leq 0.0001$), IL-6 (5-fold, $p \leq 0.05$) and TNF-α (5-fold, $p \leq 0.01$) and the T-cell growth factor IL-2 (4-fold, $p \leq 0.001$) compared to saline-injected control mice, independent of genotype. This data suggests a prolonged Th1-driven proinflammatory response in the periphery of both Tg2576 and non-transgenic littermates in response to *S*. Typhimurium, 4 weeks post infection.

6.3.2 Neuroinflammatory response in Tg2576 mice and non-transgenic littermates infected with *S.* Typhimurium

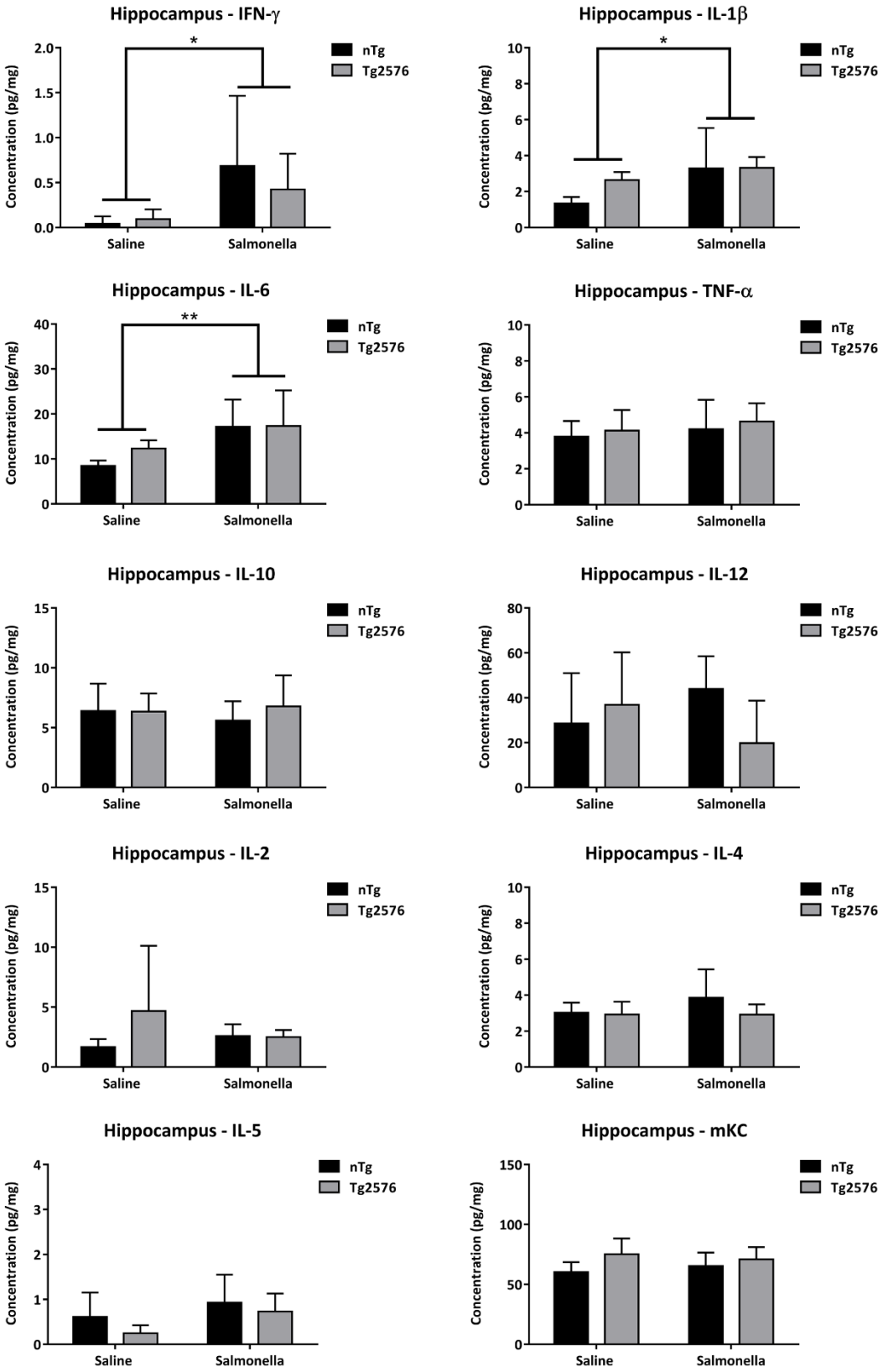

Fig 6.3:- Cytokine expression levels in hippocampal-enriched tissue from Tg2576 transgenic mice and non-transgenic littermates infected with *S*. Typhimurium. Cytokine levels (pg/mg of total protein) in hippocampal-enriched tissue homogenate from Tg2576 transgenic mice or non-transgenic littermates 4 weeks post infection with *S*. Typhimurium, or injection with saline. Data was analysed by 2-way ANOVA and Tukey post hoc test (n=4-6), and displayed as mean + SD.

Levels of brain cytokines were measured in hippocampal-enriched tissue homogenate using a 10-plex immunoassay (Fig 6.3).

Infection with *S*. Typhimurium induced a significant increase in the proinflammatory cytokines IFN-γ (16-fold, $p \leq 0.05$), IL-1β (3-fold, $p \leq 0.05$) and IL-6 (3-fold, $p \leq 0.01$) compared to saline-injected control mice, independent of genotype. This data suggests a prolonged proinflammatory response in the hippocampus of both Tg2576 and non-transgenic littermates in response to *S*. Typhimurium, 4 weeks post infection.

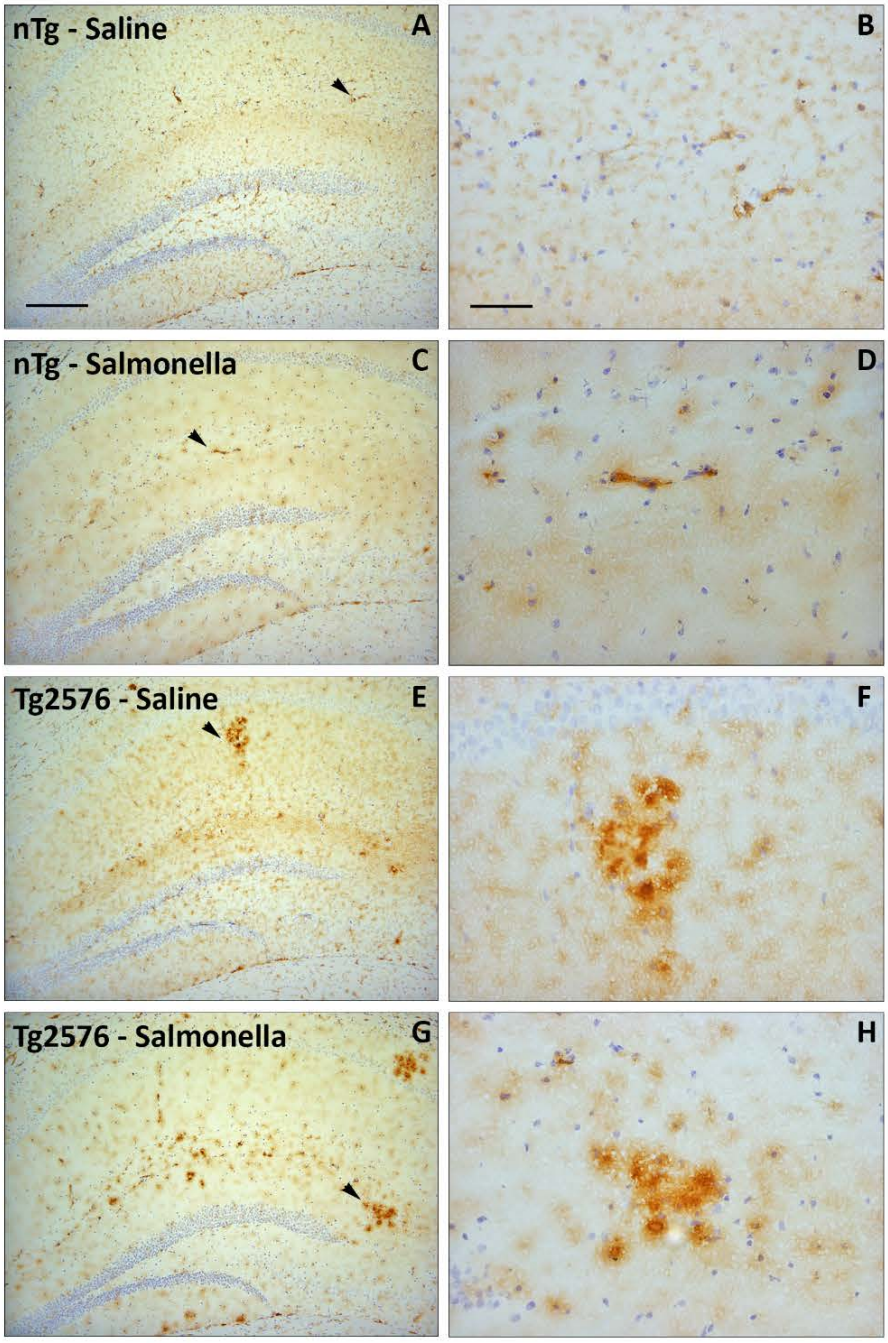
nTg - Saline
A
B
nTg - Salmonella
C
D
Tg2576 - Saline
E
F
Tg2576 - Salmonella
G
H

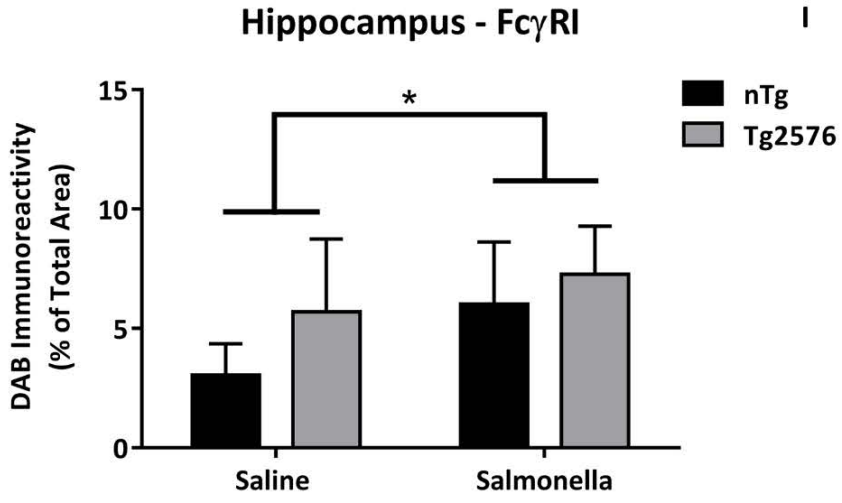
Hippocampus - FcγRI
I
DAB Immunoreactivity (% of Total Area)
15
10
5
0
*
nTg
Tg2576
Saline
Salmonella

Fig 6.4:- FcγRI expression in the hippocampus of Tg2576 transgenic mice and non-transgenic littermates infected with *S*. Typhimurium. Overview of FcγRI expression in Tg2576 transgenic mice (E,G) or non-transgenic littermates (A,C) 4 weeks post infection with *S*. Typhimurium (C,G), or injection with saline (A,E). Scale bar = 200μm. Higher magnification images derived from overview of hippocampus and indicated with black arrows. Scale bar = 50μm. (I) Quantification of FcγRI expression (DAB immunoreactivity (% of total area)) from entirety of hippocampus. Data was analysed by 2-way ANOVA and Tukey post hoc test (n=4-6), and displayed as mean + SD.

To investigate the cellular response to *S*. Typhimurium infection, FcγRI expression on myeloid cells, such as microglia, was assessed by immunohistochemistry (Fig 6.4).

Quantification of FcγRI expression in the hippocampus indicated a significant increase following *S*. Typhimurium infection, in both Tg2576 mice and non-transgenic littermates, compared to saline-injected control mice (1.5-fold, $p \leq 0.05$) (Fig 6.4I). *S*. Typhimurium infection caused a widespread increase in FcγRI expression on microglia, in addition to increases in localised staining, particularly in the hippocampal fissure (Fig 6.4D). In contrast, a greater number of clustered cells expressing FcγRI were observed in Tg2576 mice compared to non-transgenic littermates, with an increased trend in overall FcγRI expression ($p=0.08$).

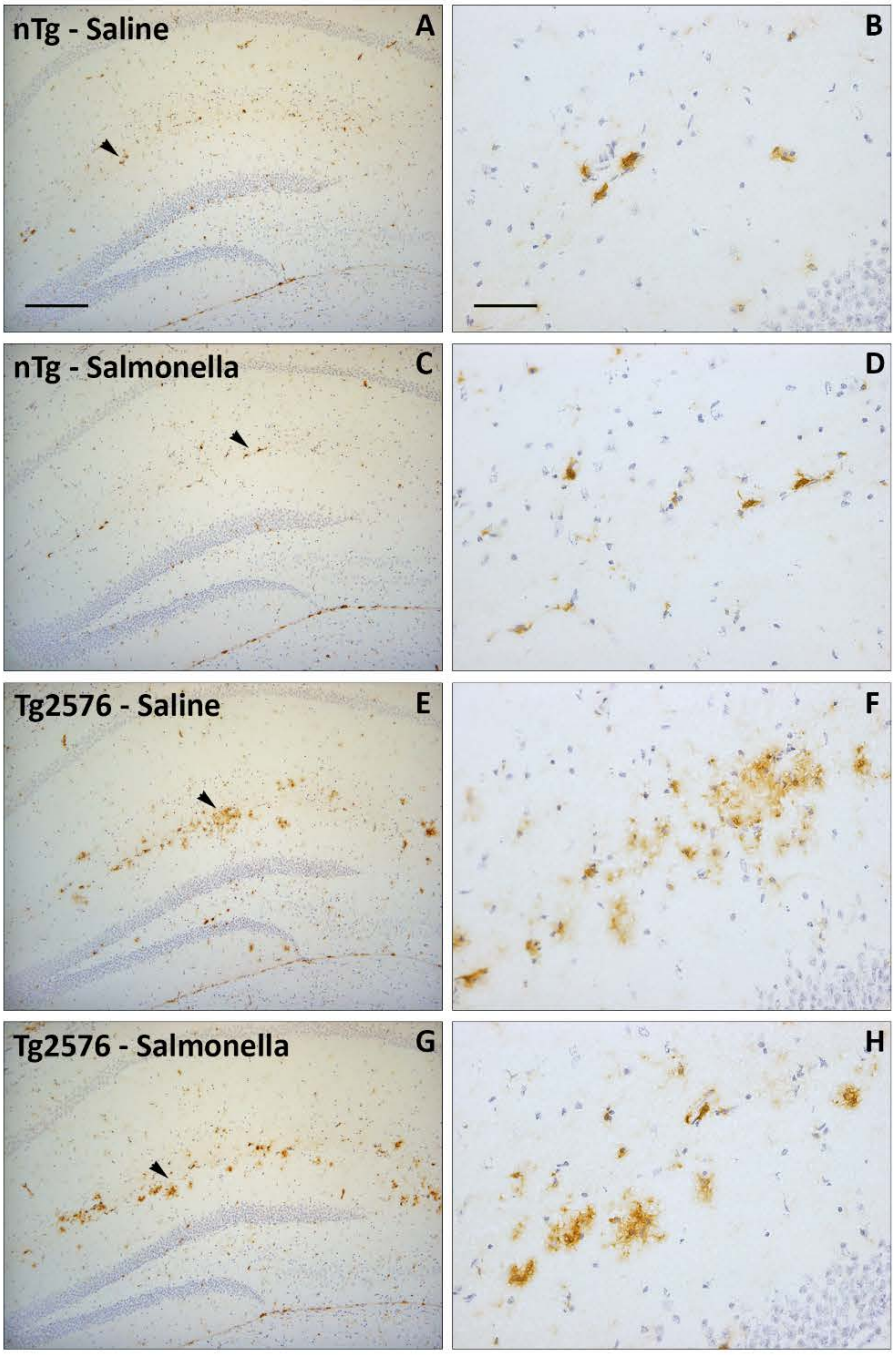
nTg - Saline
A
B
nTg - Salmonella
C
D
Tg2576 - Saline
E
F
Tg2576 - Salmonella
G
H

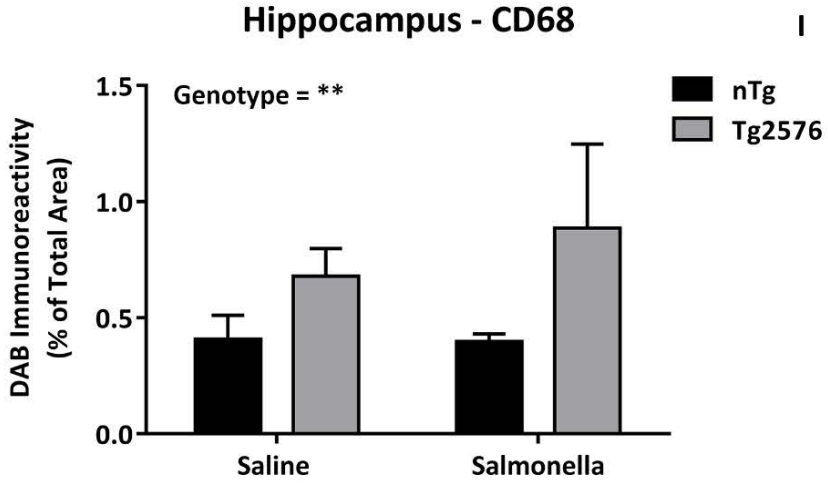
Hippocampus - CD68
I
Genotype = **
nTg
Tg2576
DAB Immunoreactivity
(% of Total Area)
1.5
1.0
0.5
0.0
Saline
Salmonella

Fig 6.5:- CD68 expression in the hippocampus of Tg2576 transgenic mice and non-transgenic littermates infected with *S*. Typhimurium. Overview of CD68 expression in Tg2576 transgenic mice (E,G) or non-transgenic littermates (A,C) 4 weeks post infection with *S*. Typhimurium (C,G), or injection with saline (A,E). Scale bar = 200μm. Higher magnification images derived from overview of hippocampus and indicated with black arrows. Scale bar = 50μm. (I) Quantification of CD68 expression (DAB immunoreactivity (% of total area)) from entirety of hippocampus. Data was analysed by 2-way ANOVA and Tukey post hoc test (n=4-6), and displayed as mean + SD.

To investigate the cellular response to *S*. Typhimurium infection, CD68 expression on myeloid cells, such as microglia, was assessed by immunohistochemistry (Fig 6.5).

Quantification of CD68 in the hippocampus indicated Tg2576 mice had a significantly greater expression (2-fold, $p \leq 0.05$), compared to non-transgenic littermates and independent of infection with *S*. Typhimurium (Fig 6.5I). The pattern of CD68 expression in the hippocampus appeared less widespread, in contrast to FcγRI expression. Localised staining, particularly in the hippocampal fissure was observed to a similar level in non-transgenic mice injected with saline and infected with *S*. Typhimurium (Fig 6.5B,D). Similarly, the greater CD68 expression observed in the Tg2576 mice appeared to be localised along the hippocampal fissure. However, the pattern of CD68 expression is consistent with immunoreactivity described for activated microglia that typically display shorter process length (Fig 6.5F,H). *S*. Typhimurium infection caused no significant change in levels or localisation of CD68 expression, in either Tg2576 mice or non-transgenic littermates.

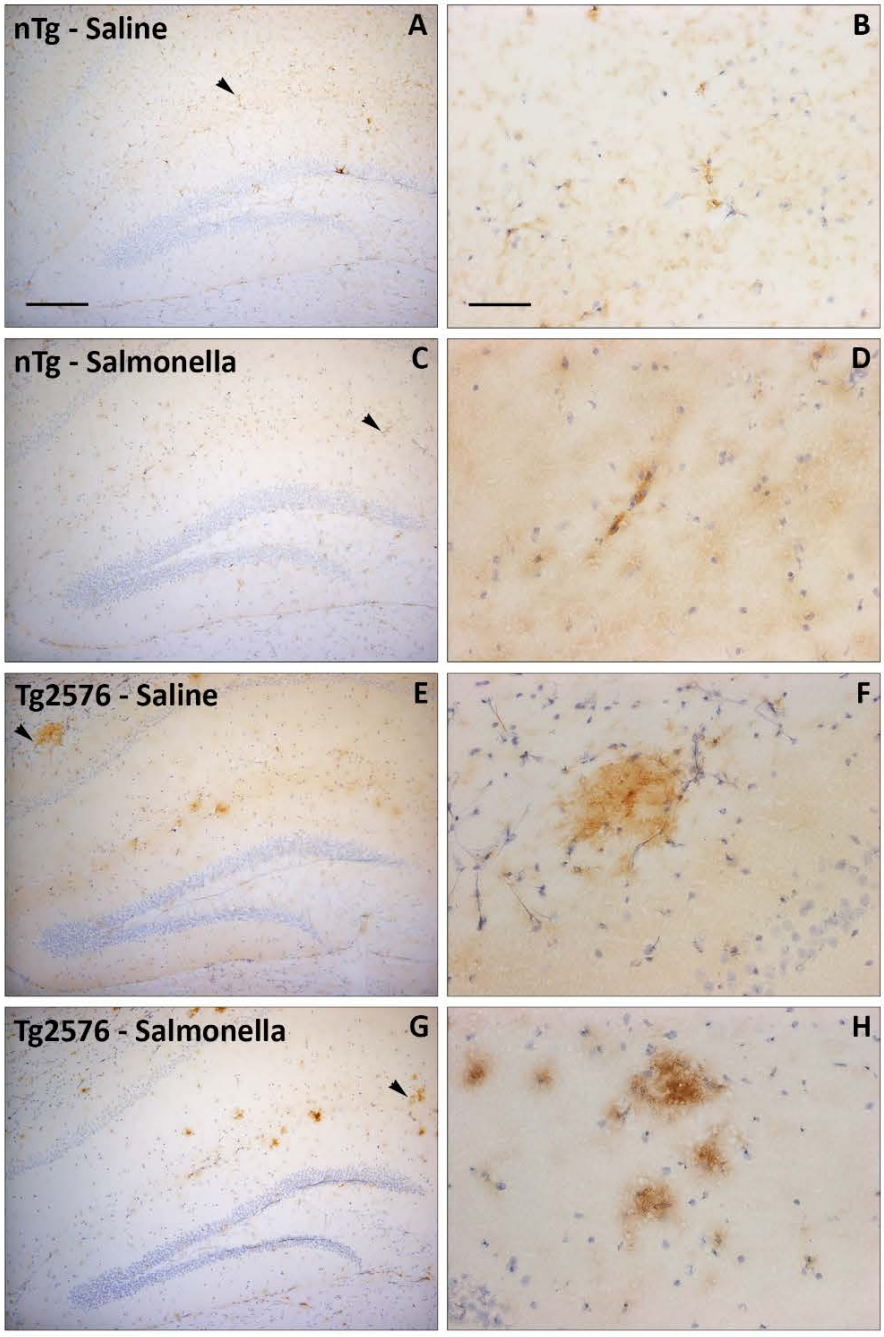
nTg - Saline
A
B
nTg - Salmonella
C
D
Tg2576 - Saline
E
F
Tg2576 - Salmonella
G
H

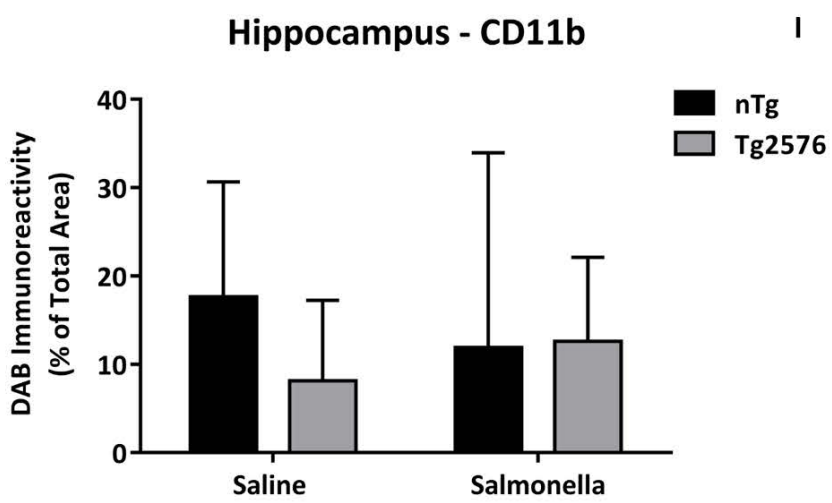
Hippocampus - CD11b
I
nTg
Tg2576
DAB Immunoreactivity
(% of Total Area)
40
30
20
10
0
Saline
Salmonella

Fig 6.6:- CD11b expression in the hippocampus of Tg2576 transgenic mice and non-transgenic littermates infected with *S*. Typhimurium. Overview of CD11b expression in Tg2576 transgenic mice (E,G) or non-transgenic littermates (A,C) 4 weeks post infection with *S*. Typhimurium (C,G), or injection with saline (A,E). Scale bar = 200µm. Higher magnification images derived from overview of hippocampus and indicated with black arrows. Scale bar = 50µm. (I) Quantification of CD11b expression (DAB immunoreactivity (% of total area)) from entirety of hippocampus. Data was analysed by 2-way ANOVA and Tukey post hoc test (n=4-6), and displayed as mean + SD.

To investigate the cellular response to *S*. Typhimurium infection, CD11b expression on myeloid cells, such as microglia, was assessed by immunohistochemistry (Fig 6.6).

Quantification of CD11b expression in the hippocampus was subject to high variability and indicated no significant change following *S*. Typhimurium infection, in both Tg2576 mice and non-transgenic littermates, compared to saline-injected control mice (Fig 6.6I). The pattern of CD11b expression in the hippocampus of non-transgenic mice appeared widespread, with areas of localisation in the hippocampal fissure (Fig 6.6B,D). It was observed that CD11b positive cells clustered throughout the hippocampus (Fig 6.6F,H) in a manner similar to FcγRI. However, the lack of an increased trend when quantified may be due to a lower widespread CD11b expression.

MHCII positive cells were restricted to the choroid plexus and meninges, with moderate increases following infection with *S*. Typhimurium, independent of genotype (Fig 6.7). For this reason, quantification was not performed.

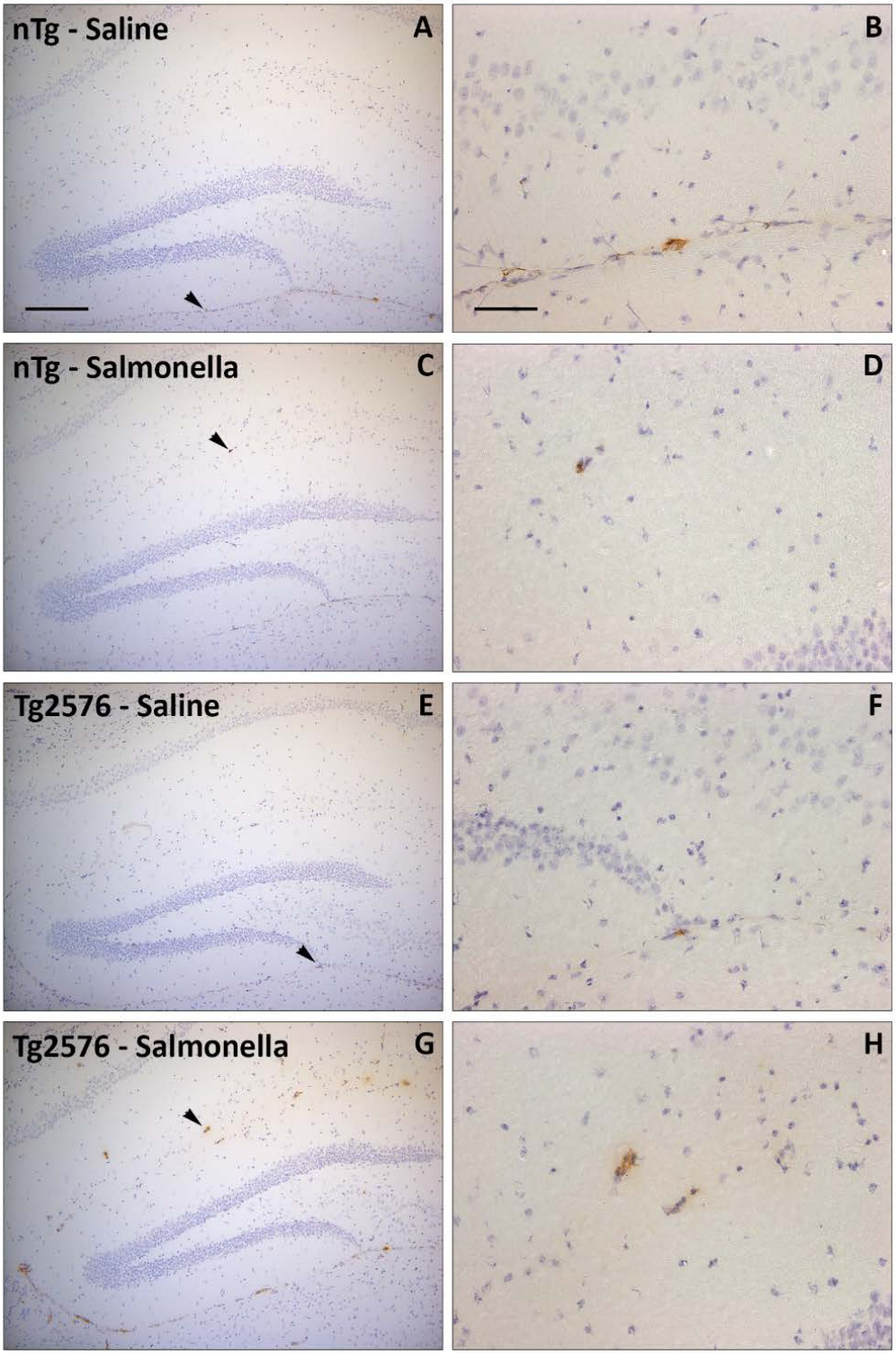

Fig 6.7:- MHCII expression in the hippocampus of Tg2576 transgenic mice and non-transgenic littermates infected with *S*. Typhimurium. Overview of MHCII expression in Tg2576 transgenic mice (E,G) or non-transgenic littermates (A,C) 4 weeks post infection with *S*. Typhimurium (C,G), or injection with saline (A,E). Scale bar = 200µm. (B,D,F,H) Higher magnification images derived from overview of hippocampus and indicated with black arrows. Scale bar = 50µm.

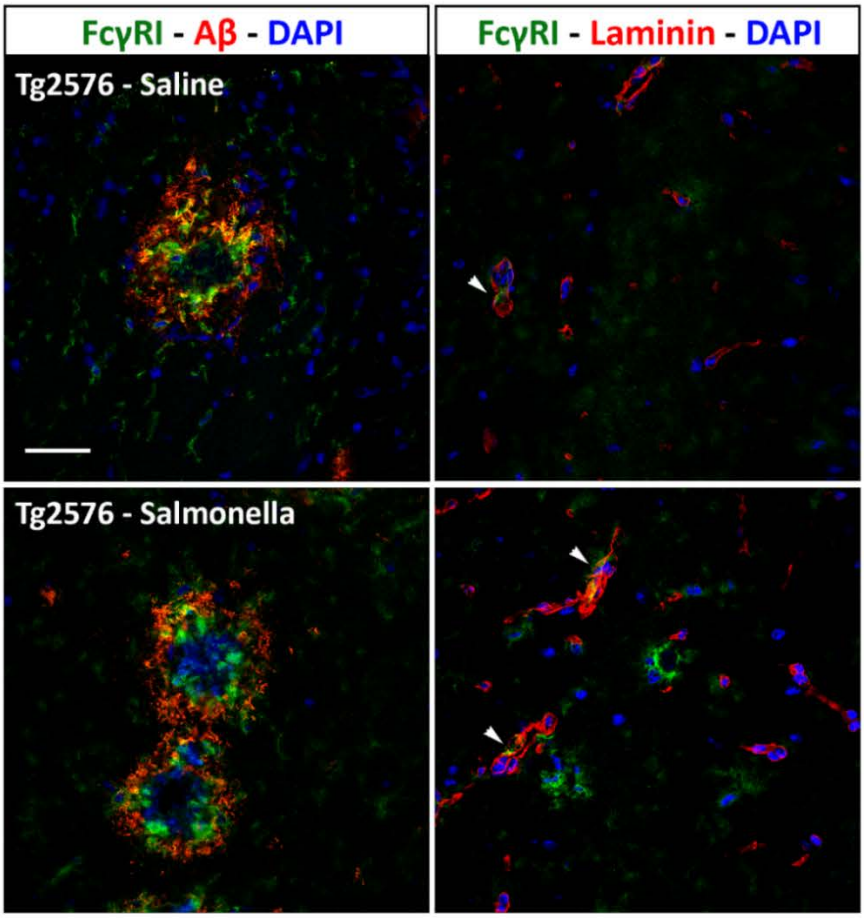
FcγRI - Aβ - DAPI
FcγRI - Laminin - DAPI
Tg2576 - Saline
Tg2576 - Salmonella

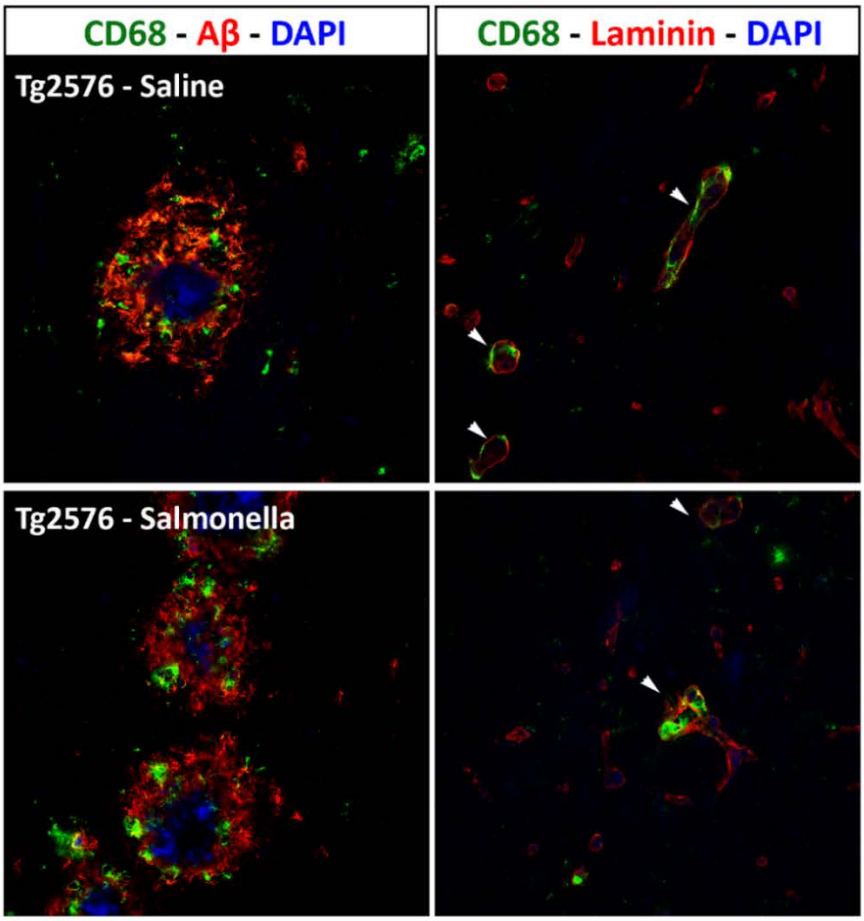
CD68 - Aβ - DAPI
CD68 - Laminin - DAPI
Tg2576 - Saline
Tg2576 - Salmonella

Fig 6.8:- Association of FcγRI/CD68 with Aβ/laminin expression in the hippocampus of Tg2576 transgenic mice infected with *S*. Typhimurium. Representative high magnification confocal images of FcγRI/CD68 positive cells (green) with Aβ/laminin (red) and DAPI (blue), from the hippocampus of Tg2576 transgenic mice 4 weeks post infection with *S*. Typhimurium, or injection with saline. White arrows indicate basement membranes of blood vessels (laminin) associated with FcγRI or CD68 positive cells. Scale bar = 25µm.

To further explore the localisation of FcγRI or CD68 positive cells, co-staining with Aβ or laminin was performed, highlighting amyloid plaque and blood vessel association respectively (Fig 6.8).

Clustering of FcγRI positive cells was observed both in and around many of the Aβ plaques found in the hippocampus of the Tg2576 mice, supporting the increased trend in FcγRI expression observed with DAB staining (Fig 6.4). Co-staining with laminin confirmed the presence of FcγRI positive cells associated with the vasculature as highlighted with white arrows. This latter observation was seen to the same degree in both Tg2576 mice and non-transgenic littermates.

Similarly, CD68 positive cells were observed clustering both in and around many of the Aβ plaques found in the hippocampus of the Tg2576 mice, supporting the significantly higher CD68 expression observed with DAB staining (Fig 6.5). CD68 expression was found associated with laminin (white arrows) in both Tg2576 mice and non-transgenic littermates, in a similar pattern to FcγRI.

6.3.3 Aβ and tau-related pathology in Tg2576 mice and non-transgenic littermates infected with *S.* Typhimurium

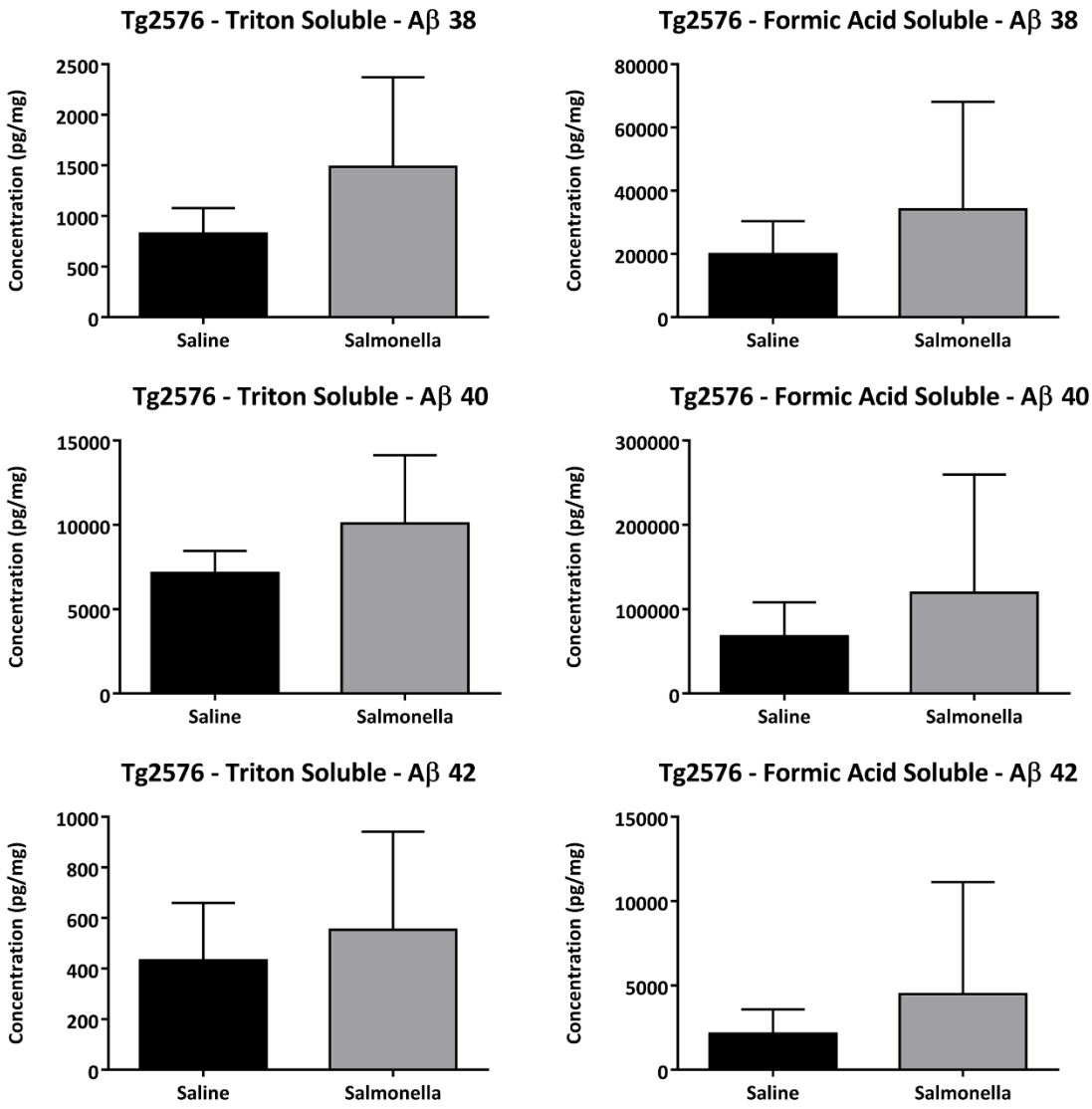

Fig 6.9:- Aβ isoform levels in hippocampal-enriched tissue from Tg2576 transgenic mice infected with *S*. Typhimurium. Human Aβ 38, 40, 42 isoform levels (pg/mg of total protein) in triton-soluble and formic acid-soluble fractions from hippocampal-enriched homogenate. Analysis performed in Tg2576 transgenic mice 4 weeks post infection with *S*. Typhimurium, or injection with saline. Data was analysed by two tailed T-test (n=4-6), and displayed as mean + SD.

To investigate the impact of *S*. Typhimurium infection on Aβ pathology in the brain, human Aβ isoform levels were measured in hippocampal-enriched tissue homogenate from the Tg2576 mice, using a 3-plex immunoassay (Fig 6.9).

There were no significant changes in any of the Aβ isoform levels from the triton soluble or formic acid-soluble fractions assessed. There was a trend for increased Aβ pathology in animals following *S*. Typhimurium infection, with the caveat that there was variability in the data. These data suggest *S*. Typhimurium infection may modify soluble and plaque-associated Aβ levels, however, this is not a consistent effect seen throughout the Tg2576 group.

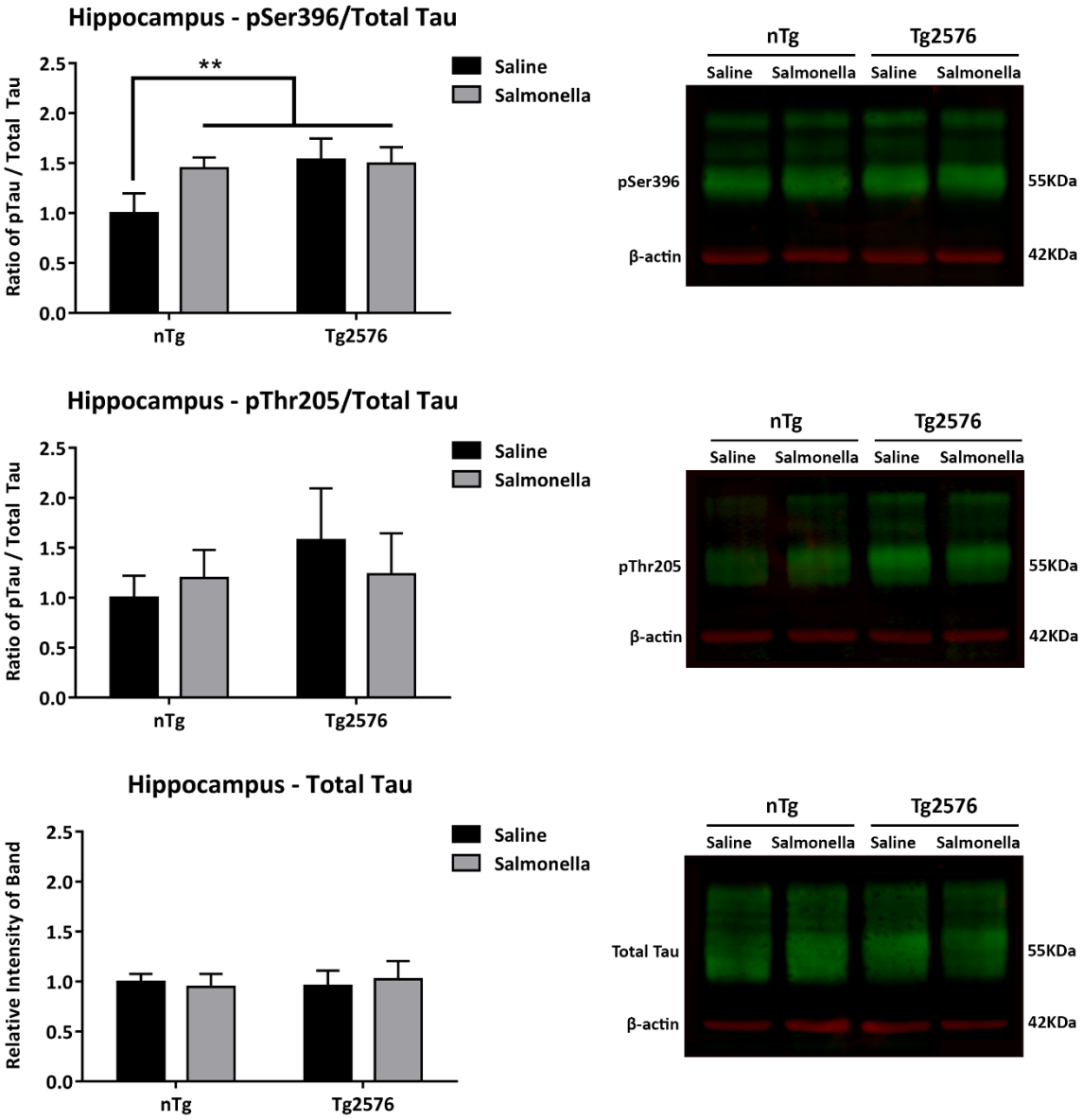

Fig 6.10:- Phosphorylated- and total tau expression levels in hippocampal-enriched tissue from Tg2576 transgenic mice and non-transgenic littermates infected with *S*. Typhimurium.

Expression of pSer396 and pThr205 (ratio of ptau/total tau), and total tau levels (relative intensity) in hippocampal-enriched homogenate from Tg2576 transgenic mice or non-transgenic littermates 4 weeks post infection with *S*. Typhimurium, or injection with saline. Representative western blot membranes demonstrating tau (green) and β-actin (red) immunoreactivity, with the latter used for normalisation of protein loading. Data was analysed by 2-way ANOVA and Tukey post hoc test (n=4-6), and displayed as mean + SD.

To investigate the impact of *S*. Typhimurium infection on tau pathology in the brain, total and phosphorylated-tau levels were measured in hippocampal-enriched tissue homogenate by western blot (Fig 6.10).

Quantification of the bands obtained from western blot demonstrated that saline-injected Tg2576 mice had greater levels of phosphorylation at the Ser396 epitope at baseline, compared to saline-injected non-transgenic mice (1.5-fold, $p \leq 0.01$). Analysis indicated a significant interaction between genotype and *S*. Typhimurium infection for this same epitope ($p \leq 0.01$); post hoc tests showed *S*. Typhimurium infection in non-transgenic mice caused a significant increase in phosphorylation at the Ser396 epitope (1.5-fold, $p \leq 0.01$) compared to the saline-injected counterparts, and in contrast to a lack of change seen in the Tg2576 group. No differences were observed at the phospho-Thr205 epitope or in total tau levels between groups. This data suggests *S*. Typhimurium infection is sufficient to induce selective phosphorylation of tau (pSer396) above basal levels in aged non-transgenic mice, in contrast to Tg2576 mice which have a higher baseline phosphorylation state but do not show further changes in response to the infection.

6.3.4 Phenotypic behaviour in Tg2576 mice and non-transgenic littermates infected with *S*. Typhimurium

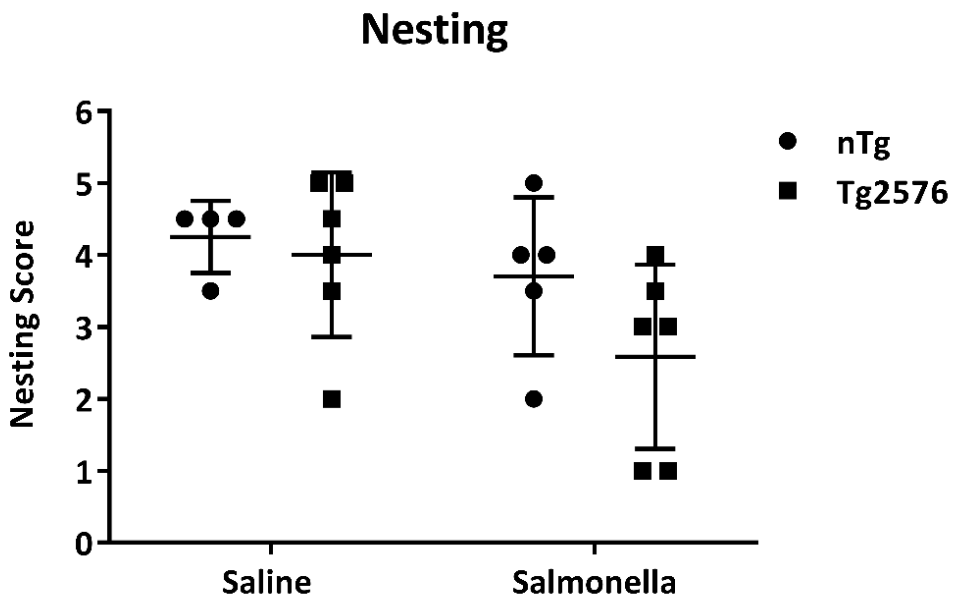

Fig 6.11:- Nesting Behaviour in Tg2576 transgenic mice and non-transgenic littermates infected with S. Typhimurium. Tg2576 transgenic mice or non-transgenic littermates 4 weeks post infection with S. Typhimurium, or injection with saline, were individually isolated the night before day of sacrifice and scored the next day for nesting behaviour. Nesting score of 5 represents complete nest build and 1 represents absent building of nest. Detailed scoring available in chapter methods. Data was analysed by 2-way ANOVA and Tukey post hoc test (n=4-6), and displayed as mean + SD.

Nesting behaviour was performed on the day of sacrifice to determine changes to phenotypic behaviour (Fig 6.11) (Deacon 2012).

Quantification of scores indicated a trend towards decreased nesting behaviour following *S*. Typhimurium infection (p=0.057). This suggests Tg2576 mice do not show overt changes in phenotypic behaviour, but *S*. Typhimurium may cause deficits 4 weeks post infection, independent of genotype status.

6.4 Discussion

There is evidence that systemic inflammation can be detrimental to patients with AD, whereby chronic neuroinflammatory processes already present may be exacerbated by peripheral infections (Barichello et al. 2015; Lim et al. 2015; McManus and Heneka 2017). For example, in patients with AD, those that were reported to experience acute systemic inflammatory events had a higher rate of cognitive decline over a 6 month period, associated with higher serum levels of TNF-α (Holmes et al. 2009). Furthermore, data from animal models has supported these findings with memory deficits and tau phosphorylation shown to be exacerbated in 3xTg mice that received repeated i.p. injections of LPS, over a 6 week period (Sy et al. 2011). However, thus far the majority of studies investigating systemic inflammation in mouse models of AD, have relied heavily on the use of bacterial mimetics, such as LPS. These are administered repeatedly to simulate chronic infection, but as the previous chapters and other groups have shown, the inflammatory profile generated does not accurately model bacterial infection (Püntener et al. 2012). This presents a gap in knowledge of how genuine infections impact the CNS in health and disease. In this chapter, I have looked to address this issue by utilising an attenuated AroA strain of the bacterium *S*. Typhimurium. This was administered to aged Tg2576 mice (16-17 month old), which exhibit amyloid deposition in both the cortex and hippocampus at this time point (Hsiao et al. 1996). Therefore, we examined the influence of a systemic bacterial infection in a model exhibiting advanced age, pre-existing neuroinflammation and amyloid deposition. I hypothesise that these additional risk factors will drive increases in tau phosphorylation, following systemic infection.

Body weight data from this experiment showed a differing trend between the Tg2576 mice and non-transgenic littermates when administered with *S*. Typhimurium. While the non-transgenic mice appeared to lose weight upon infection and maintain this lower bodyweight throughout the 4 weeks, Tg2576 mice recovered quickly from *S*. Typhimurium and gained weight above their previous starting body weight. This discrepancy is additionally seen in starting body weights, with Tg2576 mice exhibiting a significantly lower body weight compared to non-transgenic littermates. These findings suggest a different metabolism state between the two genotypes, in line with a previous

study conducted to investigate preclinical weight loss in AD, utilising the Tg2576 strain (Ishii et al. 2014). It was found that differences in body weight between Tg2576 mice and non-transgenic littermates occurred as early as 3 months of age and this divergence increased with greater age and brain Aβ42 burden.

This weight difference was associated with decreased adiposity and lower plasma leptin levels. Further investigation demonstrated disruption to the hypothalamic arcuate NPY (orexigenic neuropeptide Y) neurons suggesting Aβ accumulation disrupts hypothalamic leptin signalling. Interestingly, this was not associated with food intake but rather an increased energy expenditure as measured by oxygen consumption (Speakman 2013; Ishii et al. 2014). Although these findings support our observations that Tg2576 mice have lower starting body weights, further investigation is required into the greater weight gain seen following infection with *S*. Typhimurium.

One explanation for the differences in weight gain following infection, could lie in the genotypes' immune responses to this challenge. However, both genotypes displayed similar increases in spleen weight and serum cytokine levels following infection with *S*. Typhimurium. Moderate increases in the proinflammatory cytokines IFN-γ, IL-6 and TNF-α together with the T-cell growth factor IL-2, is in accordance with the resolving stages of the *S*. Typhimurium infection. Overall, these results would suggest little difference in peripheral immune response between the genotypes following infection, and therefore it is unlikely to be responsible for the differing weight profiles observed.

Certain conditions have the capacity to prime cells in the brain, resulting in microglial activation and an exaggerated cytokine response following further stimuli such as a systemic challenge with LPS. These prerequisites include ageing (Godbout et al. 2005) and chronic neurodegeneration (Cunningham et al. 2005). Limited research exists for priming in models of amyloid deposition only. Sly et al have previously observed that systemic LPS (25μg/mouse), administered i.v., to 16-month old Tg2576 mice resulted in increased cortical levels of IL-1β mRNA and Aβ42 as early as 2 hours following delivery, compared to non-transgenic littermates (Sly et al. 2001). However, the absence of a saline-injected control group from analysis, leads me to question these findings, as the group had previously shown higher baseline mRNA levels of IL-1β in this model. In the 3xTg model,

Laferla and colleagues showed that multiple i.p LPS challenges (0.5 mg/kg), administered twice weekly, for 6 weeks, to 3xTg mice (4 month old) resulted in elevated levels of IL-1β mRNA, together with increased immunoreactivity of CD45, as an indicator of microglial activation (Kitazawa et al. 2005). Although both these studies indicate increased levels of a proinflammatory cytokine, associated with microglial phenotype changes in the latter article, the lack of required controls in either study does not allow for conclusions to be drawn as to whether an exaggerated immune response, i.e. priming, was observed in these transgenic models.

Using the novel approach of infection with *S*. Typhimurium in the Tg2576 model, increases in central levels of the proinflammatory cytokines IFN-γ, IL-6 and IL-1β have been demonstrated, although baseline levels of these latter two mediators appear to be higher than in the non-transgenic mice. Additionally, *S*. Typhimurium caused a significant upregulation in FcγRI expression, but again baseline expression in Tg2576 mice was higher than controls. No changes in CD68 or CD11b were observed. These results indicate that a moderate proinflammatory response is still apparent 4 weeks post infection, however baseline levels in the Tg2576 appear higher than non-transgenic control mice and no additive effects are observed at this time point and in the brain region selected (hippocampus). Although FcγRI, CD11b and CD68 are found to cluster around the larger plaques found in the hippocampus, only the latter marker is significantly upregulated in the Tg2576 mice, independent of infection. I believe that as the expression of CD68 is less widespread on microglia, its upregulation on activated microglia around plaques in the Tg2576 mice appears quantifiably higher. In contrast, FcγRI and CD11b expression levels do not appear to change, as much of the signal is contributed from microglia that are not associated with plaques. Existing literature supports these findings as activated microglia are found surrounding plaques, both in Tg2576 mice and post-mortem studies from patients with AD (Itagaki et al. 1989; Peress et al. 1993; Frautschy et al. 1998; Kitazawa et al. 2011).

An interesting observation from this study was the lack of MHCII positive staining on the cells associated with the vasculature; a phenomenon seen in both adult and middle-aged C57BL/6 wild-type mice following infection with *S*. Typhimurium. Although this may relate to strain differences, the differential effects of advanced age in the Tg2576 mice and non-

transgenic littermates may be responsible. MHCII expression upon cells of the vasculature such as the endothelium, require stimulation from IFN-γ (Etienne et al. 1999). Cytokine levels from the periphery indicate increases in IFN-γ following infection with *S*. Typhimurium, however, the lack of MHCII expression on the brain endothelium in the Tg2576 mice and non-transgenic littermates would suggest a lack of responsiveness from this cell type with age. MHCII expression on endothelial cells has not previously been investigated with age, however, multiple studies report the upregulation of MHCII on other cells types such as microglia and astrocytes (Lynch 2009). The endothelial cells may have important role in transducing inflammation from the periphery to the brain, and therefore further studies are necessary to understand the impact of endothelial phenotype in healthy ageing and disease.

Manipulation of central and peripheral inflammation in APP transgenic mouse models is a vast field of research, which continues to produce both insight and contradictions as to the relationship between inflammation and Aβ pathology (Birch et al. 2014). For example, in a number of APP models, genetic knock-out for key inflammatory factors such as TNFRI, IL-12 and IFNGR1 has resulted in decreased soluble Aβ levels and plaque load, suggesting proinflammatory processes are detrimental to disease progression (He et al. 2007; Yamamoto et al. 2007; Vom Berg et al. 2012). However, controversy arises when different research models are utilised, as deletion of iNOS has opposing effects on Aβ in the APP/PSI and Tg2576 models (C A Colton et al. 2006; Kummer et al. 2011). One mechanism by which proinflammatory processes may be increasing Aβ, is through increased activity of enzymes that cleave and process APP, such as the β secretase, BACE1. An additional observation from the APP models where proinflammatory processes have been genetically disrupted and Aβ reduced, is the reduction of BACE1 levels (He et al. 2007; Yamamoto et al. 2007). This is supported by reports that i.p LPS injection induces Aβ generation with associated increases in BACE1 activity (Lee et al. 2008). Our results, although not significant, suggest increases in all Aβ isoforms assessed from the triton-soluble fractions of hippocampal homogenate and therefore support the existing literature.

Another consequence of promoting a proinflammatory environment in AD mouse models, is the clearance of Aβ plaque pathology through increased microglial

phagocytosis. The administration of LPS or IL-1β overexpression, in particular, appear to follow this mechanism with a reduction in Aβ plaque levels and upregulation of microglial activation markers (Herber et al. 2007; Shaftel et al. 2007).

The 3D6 antibody was generated recombinantly from the variable domain amino acid sequence of the therapeutic antibody Bapineuzumab (Fuller et al. 2015). Therefore, it recognizes the linear N-terminus of Aβ and binds all forms of Aβ e.g. prefibrillar aggregates and plaques (Moreth et al. 2013). The immunofluorescent staining suggests strong binding of 3D6 to Aβ, however, it is unclear why the core of the plaque remains unstained by the antibody. Staining of the hippocampus from Tg2576 mice shows the emergence of both diffuse and compact plaques by 12 months of age (Sasaki et al. 2002). The examples shown may represent the former and therefore the lack of central staining.

Aβ isoform levels from the formic acid-soluble fractions displayed an increased trend although this was not significant. This would suggest an increase in Aβ associated with plaques, perhaps indicating that an increase in phagocytosis of these structures was not occurring post infection with *S*. Typhimurium. However, increased soluble Aβ levels, as a result of inflammation, may aggregate to increase plaque burden, superseding any increases in phagocytosis that occur. In addition, there is strong evidence that patients with AD have a reduced Aβ efflux at the BBB (Deane et al. 2008). Interestingly, systemic LPS has been shown to mirror this reduction in Aβ efflux with associated downregulation of LRP-1, a transporter found on cells of the brain vasculature (Jaeger et al. 2009). Further investigation into changes at the BBB, with regard to Aβ clearance in our model, would be valuable.

Although fewer studies have been carried out on the effect of systemic inflammation on tau pathology, initial reports suggest a similarly contradictory relationship. For example, overexpression of IL-1β in 3xTg mice results in microglial activation and tau phosphorylation with a contrasting reduction in Aβ pathology (Ghosh et al. 2013). Although APP models, like the Tg2576, do not develop neurofibrillary tangles, they do exhibit increased phosphorylation of the tau protein by 11 months (Otth et al. 2002; Noda-Saita et al. 2004), a feature I aimed to modify by infection with *S*. Typhimurium. The data presented here confirms that Tg2576 mice had increased phosphorylation at the

Ser396 epitope, however, this was not modified by infection with *S*. Typhimurium. Studies using the 3xTg model have shown that administering repeated doses of i.p. LPS results in increased phosphorylation and accumulation of tau in neurons, driven by CDK5 and GSK3β in 4 and 12 month old mice respectively (Kitazawa et al. 2005; Sy et al. 2011). Interestingly, no changes in Aβ levels or plaque pathology were seen, suggesting effects on tau were independent of Aβ and perhaps solely related to the microglial activation observed. The failure to induce further tau phosphorylation in our model may signify that microglia in the 16-month old Tg2576 mice are less responsive to additional immune stimuli provided by systemic inflammation. Alternatively, mutated human tau used in these studies is likely to have a greater propensity for further phosphorylation following a systemic inflammatory challenge. Interestingly, greater phosphorylation of the tau protein was observed in the non-transgenic mice following infection with *S*. Typhimurium. With increased FcγRI expression and proinflammatory cytokine levels additionally observed in these non-transgenic mice following infection, one hypothesis is that ageing has provided a susceptible environment in which these changes have the capacity to drive the phosphorylation of the tau protein. Other markers of ageing such as oxidative stress together with alterations to tau kinase activity, may further elucidate mechanisms involved and help substantiate this claim.

Systemic inflammatory challenges such as LPS or *S*. Typhimurium have been shown to have detrimental effects on behaviours such as burrowing, due to the development of sickness behaviours (Püntener et al. 2012). Additionally, Tg2576 mice show deficits in building nests by 2-3 months, an effect that is exacerbated with age (Wesson and Wilson 2011). When assessing the effect *S*. Typhimurium infection had on nesting behaviour in the Tg2576 mice, a strong trend was seen towards a deficit in mice receiving *S*. Typhimurium, however, the results were subject to large variation within each group. Previously our lab has demonstrated that *S*. Typhimurium causes changes in burrowing at 1 day post infection when serum LPS concentrations are at their highest (Püntener et al. 2012). As this nesting behaviour was performed 4 weeks post infection, it is likely any changes would have already occurred. The addition of behavioural tests at earlier time points may expose changes that are occurring during infection with *S*. Typhimurium.

In summary, this chapter has demonstrated that infection with *S*. Typhimurium elicits both a peripheral and central cytokine response in 16-17 month old mice. The lack of an exaggerated response in Tg2576 mice would suggest Aβ is not a priming influence and/or that infection with *S*. Typhimurium is not an adequate secondary stimulus at the time point assessed, although acute challenges are required to fully analyse this phenomenon. Investigation into microglial phenotype supports previous literature, demonstrating extensive interaction between this cell type and Aβ plaque pathology. The addition of *S*. Typhimurium did not significantly alter this relationship as evidenced by the phenotypic markers utilised, however, moderate change in both soluble and plaque-associated Aβ may suggest more subtle alterations are occurring. The increases in soluble Aβ may be the result of greater Aβ cleavage, through BACE1 activity, or decreased efflux through the brain vasculature. Extensive plaque pathology in the Tg2576 mice would suggest microglia are already struggling to phagocytose Aβ, and therefore increased soluble levels would contribute to the greater plaque-associated Aβ observed. Assessment of plaque size and structure in addition to further investigation of the mechanisms outlined here, would be beneficial in the interpretation of current observations. Furthermore, both processes outlined are likely not mutually exclusive.

The changes seen in non-transgenic littermates, would suggest that systemic inflammation in ageing is sufficient to cause increased phosphorylation of the tau protein. I propose that the higher baseline tau phosphorylation observed in the Tg2576 is a result of microglial activation, in response to the development of Aβ plaque pathology. This activation is mimicked by systemic inflammation in the aged non-transgenic littermates, and therefore a similar increase in tau phosphorylation is observed. There is a suggestion that as Aβ plaques develop and microglia are recruited, these cells become dystrophic from chronic activation and are unable to properly function e.g. phagocytose debris and Aβ (Streit et al. 2014). We may speculate that additional consequences of this include a reduced ability to respond to inflammatory stimuli, such as systemic inflammation, and therefore no further tau phosphorylation is induced.

Chapter 7: General Discussion

With the success of modern medicine and subsequent increase in life expectancy across much of the developed world, new threats have emerged in the form of age-related conditions such as chronic neurodegenerative diseases like AD. Worryingly, over a century after the first descriptions by Alois Alzheimer (Alzheimer 1907), there still remains no disease-modifying treatments available for AD. Therefore, it is critical that the mechanisms and pathways which drive such diseases are identified and therapeutics developed to slow and halt their progression.

One avenue of investigation is in the risk factors that potentiate these disorders, such as systemic inflammation (Barichello et al. 2015; Lim et al. 2015; McManus and Heneka 2017). Epidemiological studies from the 1990s reported that patients taking NSAIDs for arthritis, were at half the risk of developing AD compared to the general population (McGeer et al. 1996). Disappointingly, these positive effects did not translate into clinical trial success (Arvanitakis et al. 2008), highlighting the requirement for earlier intervention and greater exploration into disease mechanism.

The aim of the study presented here was to determine whether the deleterious effects of systemic inflammation, induced by a real life bacterial infection, in the course of neurodegenerative disease, can result in the induction of tau phosphorylation, a hallmark of many of these diseases. Thus far, clinical trials of amyloidocentric therapies have yielded disappointing results with respect to slowing or halting cognitive decline, and a shift in focus to the other two main pathologies in AD, inflammation and tau, is prudent.

Research exploring the relationship between these pathologies has identified a promising pathway which I have chosen to investigate in this set of studies. Peripheral administration of the bacterial mimetic, LPS, has been shown to result in activation of immune cells, such as microglia, in the brain, resulting in elevations of proinflammatory cytokines. In turn, this inflammation propagates to nearby neuronal cells, driving kinase activation and the subsequent phosphorylation of the tau protein (Kitazawa et al. 2005; Bhaskar et al. 2010; Sy et al. 2011; Czapski et al. 2016; Gardner et al. 2016). This pathway

serves as my underlying hypothesis for the events that occur in the CNS following systemic inflammation.

7.1 Multiple LPS v.s. *Salmonella* Typhimurium

In **Chapter 3**, I sought to confirm and expand on the observations in prior published studies that have reported the induction of tau phosphorylation following the systemic administration of LPS (Kitazawa et al. 2005; Roe et al. 2011; Czapski et al. 2016; Gardner et al. 2016). Single or multiple doses of LPS were injected into the peritoneum of young adult (3-4 month old) wild-type C57BL/6 mice, to determine the acute- and long- term effects of systemic LPS-induced inflammation on the brain. Twenty-four hours following a single injection of LPS, a robust inflammatory effect was observed with elevations in both central pro- and anti-inflammatory cytokines e.g. IFN-γ, IL-1β, IL-10. In contrast, multiple injections of LPS showed an attenuated cytokine profile indicative of the development of endotoxin tolerance (ET) or hyporesponsiveness, with only small increases in the levels of IL-1β and mKC still evident.

This observation represents a limitation of the multiple LPS model, when trying to replicate the effects of a common bacterial infection. Following the initial engagement of LPS, the immune response is dampened in order to limit tissue-damaging inflammation from further stimulation (Pardon 2015). However, over the past decade it has emerged the mechanisms that drive ET involve gene reprogramming and immunomodulation rather than a global downregulation of gene expression and function. Indeed, although decreased TLR-4-MyD88 complex formation, impaired IRAK-1 activity and reduced activation of MAPKs and NF-κB is reported, events such as histone acetylation of antimicrobial gene promoters and upregulation of microRNAs suggest complex and multifactorial mechanisms drive ET (for review see (Biswas and Lopez-Collazo 2009)). Furthermore, certain microRNAs such as miR-26a are implicated in the regulation of tau kinases (for review see (Zhao et al. 2017)).

In contrast to central cytokine levels, similar microglial phenotype changes were observed i.e. FcγRI and CD11b, following single and multiple challenges of LPS. This suggests that marker expression is not a reflection of cytokine production and/or affected by ET.

Indeed, it has been shown that FcγRI expression increases in endotoxin tolerant human monocytes (del Fresno et al. 2009). However, there are conflicting reports as to whether cells in the brain become endotoxin tolerant *in vivo* (Püntener et al. 2012; Pardon 2015; Schaafsma et al. 2015; Chu et al. 2016).

Alternatively, one explanation for the differing effects on cytokine levels and microglia phenotype may lie in the source of the former. Cells associated with the brain vasculature such as the endothelia have the capacity to secrete pro- and anti-inflammatory cytokines in response to LPS and cytokine exposure from the circulation (Banks et al. 2015; Varatharaj and Galea 2017). Therefore the attenuation in cytokine levels in the brain may be a result of tolerance in this cell type (Wang et al. 2011; Stark et al. 2016) or decreased stimulation from the reduced levels of circulating cytokines, resulting from peripheral ET. This highlights the possible importance of the BBB, not just in its restriction of pathogens into the brain but also its capacity to propagate inflammation (Bechmann et al. 2007). Determining the source of cytokines through methods such as fluorescent in situ hybridization (FISH) would be useful in deciphering mechanism and targeting therapeutic intervention.

Contrary to previous reports demonstrating the induction of tau phosphorylation following both single and multiple doses of LPS (Kitazawa et al. 2005; Bhaskar et al. 2010; Roe et al. 2011; Czapski et al. 2016; Gardner et al. 2016; Liu et al. 2016), no increases in tau phosphorylation were observed in our studies. I believe this discrepancy arises from both a time- and dose-dependent effect on the induction of tau phosphorylation. For example, Roe and colleagues observed tau phosphorylation with low dose LPS (0.1mg/kg) but only for a maximum for 4 hours post i.p. injection (Roe et al. 2011). Bhaskar et al. demonstrated increases in tau phosphorylation later at 24 hours post infection but only following 10mg/kg, and not a 1mg/kg LPS dose (Bhaskar et al. 2010). With doses above 1mg/kg considered to simulate sepsis (Barron et al. 2016), this again raises the question as to the suitability of LPS in simulating the time course of a real life bacterial infection. Additionally, high doses of LPS may cause disruption to BBB integrity leaving the brain vulnerable to the influx of circulating inflammatory mediators including LPS, and therefore central TLR-4 stimulation in the brain (Varatharaj and Galea 2017) .

To address the limitations of the LPS model, in **Chapter 4**, I took the novel approach of infecting wild-type mice with an attenuated strain of the bacterium S. Typhimurium, in order to determine whether tau phosphorylation was induced by a real life bacterial infection. Our lab had previously shown that *S.* Typhimurium induces a robust inflammatory response in both the periphery and brain for at least 3 weeks post infection (Püntener et al. 2012). Investigating both acute (1 week and 4 week) and long term (8 weeks and 24 week) effects of the infection, the data presented here demonstrates a peripheral elevation of cytokines that peaked at 1 week, was still moderately elevated at 4 weeks and returned to baseline by 8 weeks. These findings are in line with previous studies that report clearance of the bacteria by 40 days (McSorley and Jenkins 2000; Cunningham et al. 2007).

An array of cytokines including IFN-γ, IL-1β, IL-6, TNF-α and mKC were elevated in the brain for at least 4 weeks post infection. This suggests robust and sustained neuroinflammation resulting from the systemic bacterial infection, in contrast to the proposed ET developed in the multiple LPS model. As outlined in the Chapter 1, S. Typhimurium engages numerous pathways including TLR-1,2,4,5,9 and the NLRs, NLRC4 and NLRP3, with the latter family inducing the assembly of the inflammasome (Broz et al. 2012). Furthermore, a range of cell types are involved in the immune response such macrophages, NK cells, neutrophils and dendritic cells. S. Typhimurium results in an intracellular infection and requires an adaptive immune response for elimination including recruitment of both T- and B-cells (Mittrucker and Kaufmann 2000).

However, the inflammation in the brains of mice infected with S. Typhimurium did not appear to induce tau phosphorylation at any of the time points assessed. One explanation for this observation in both models of systemic inflammation, may rely on healthy resolution to the inflammatory challenge. As these experiments were performed in adult wild-type mice, it is likely that mechanisms are in place to successfully resolve inflammation.

The resolution of inflammation is an active process influencing key inflammatory events to promote the return to immune homeostasis (for reviews see (Serhan and Petasis 2011; Sugimoto et al. 2016). Aspects of this process include the counter regulation of cytokines

and chemokines, stimulation of leukocyte apoptosis, clearance of apoptotic cells by macrophages and switching of this cell phenotype from proinflammatory to pro-resolving. Anti-inflammatory effects differ from pro-resolving actions as the former refers to an inhibitory or blocking action while the latter stimulates healing. Examples of specialised pro-resolving mediators (SPMs) include the lipid meditators (LMs) lipoxins, E-series resolvins, D-series resolvins, protectins and maresins (Serhan and Petasis 2011). Importantly for the study of age-related diseases, it has been shown that resolution is delayed in aged (20-month old) mice injected with yeast cell wall particles (zymosan) that initiate acute inflammation (Arnardottir et al. 2014). This effect was associated with reduced levels of SPMs and elevated levels of proinflammatory LMs. Additionally, reduced levels of the SPM lipoxin A4 have been reported in the CSF and hippocampus of AD patients - the former correlating with MMSE cognitive score (Wang et al. 2015). These studies may suggest that in ageing and AD, resolution of inflammation is disrupted and this could be a critical factor in why systemic inflammation has a deleterious impact in neurodegenerative disease.

7.2 Systemic inflammation in middle age

Age is the biggest risk factor for neurodegenerative disease (Niccoli and Partridge 2012), and therefore in **Chapter 5,** the effect of age on tau phosphorylation, following systemic inflammation, was investigated. However, emerging evidence suggests that earlier therapeutic intervention is required to impact chronic neurodegenerative disease, raising the question as to how early the ageing process affects the CNS. Indeed, studies have reported that pathological changes, such as Aβ deposition and glial cell activation, occur decades before symptoms arise in the brains of AD patients (Reiman et al. 2012; Rodriguez-Vieitez et al. 2016). It may follow that the ageing process also adversely impacts the CNS, by 'priming' immune cells, such as the microglia, to react in an exacerbated manner when engaged by a secondary immune stimulus (Godbout et al. 2005). In addition, elevated serum levels of CRP at middle age are associated with an increased risk of dementia (Schmidt et al. 2002; Komulainen et al. 2007), supporting the hypothesis that systemic inflammation may contribute to earlier onset and/or progression of neurodegeneration. Whether systemic inflammation also drives tau

pathology remains to be proven. Therefore, the aim of **Chapter 5** was to determine whether the systemic inflammation resulting from multiple LPS or *S.* Typhimurium infection, had the capacity to induce tau phosphorylation in 12-month old middle-aged mice.

One hypothesis by which this could occur, is through a greater peripheral and central inflammatory response in aged mice. To determine whether this occurs as early as middle age, both serum and brain cytokine levels were assessed in 12-month old wild-type mice following 4 weeks of multiple LPS injections or a single *S.* Typhimurium infection. Although cytokine levels in the hippocampus and serum were not measured 24 hours after a single systemic injection of LPS for comparison, the similar changes in adult and middle-aged mice suggest ET additionally occurs in the latter. Akin to the results from chapter 3, IL-1β and mKC are still elevated in the brain at both ages, with additionally moderate increases in TNF-α, IL-10 and IL-2. Mice infected with *S.* Typhimurium showed elevations in all but one of the serum cytokines, IL-4, with a trend towards a greater increase in middle-aged mice. However, despite causing elevations in a greater range of brain cytokines compared to multiple LPS challenges e.g. IFN-γ and IL-6, *S.* Typhimurium has similar central cytokine effects at both ages. This suggests middle-age may be too early to observe overt changes to the inflammatory response following immune challenge.

In line with cytokine changes, there was increased expression of CD11b and FcγRI on immune cells, such as microglia and perivascular macrophages, following multiple LPS, while infection with *S.* Typhimurium showed increases in FcγRI only. Nevertheless, neither model exhibited significant differences in expression between the adult and middle-aged wild-type mice. Although it was suggested in the previous section that microglia may not be the source of these changes in cytokines and/or marker expression does not represent functional state e.g. cytokine secretion, the data presented here supports cytokine data showing no significant changes to the immune response at middle age.

Multiple LPS challenge and *S.* Typhimurium infection appear to have a different impact on phosphorylation of tau. There was no evidence of changes in tau phosphorylation at either epitope following multiple LPS challenge. On the other hand, an interaction

indicated that, where a decrease in tau phosphorylation at pSer396 and pThr205 was observed following *S.* Typhimurium infection in adult mice, the opposite trend was seen at middle age. Although these effects were modest, as indicated by the non-significant relationship with respective saline-injected control mice, the data presented here may suggest the systemic inflammation resulting from *S.* Typhimurium infection, has the capacity to induce tau phosphorylation at middle age.

An important difference between the two models of systemic inflammation, were changes occurring at cerebral blood vessels. Confocal microscopy revealed the expression of MHCII on cells associated with the vasculature, which presumably could be endothelial in nature, and the infiltration of IgG into the brain parenchyma. A previous study by Sarlus and colleagues utilised intranasal ovalbumin as a chronic model of airway-induced allergy (Sarlus et al. 2012). Investigation in the brains of these C57BL/6 wild-type mice, showed elevations in both parenchymal IgG and IgE levels. Associated with these increases was the phosphorylation of tau at the Ser202/Thr205 (AT8) epitope. Given that parenchymal infiltration of IgG is only a characteristic of the *S.* Typhimurium model in my study, this phenomenon may be critical in the induction of tau phosphorylation observed. However, it is difficult to speculate the signalling pathway involved. Firstly, the data presented here does not show neuronal expression of the IgG receptor, FcγRI, and therefore IgG cannot directly cause tau phosphorylation in this cell type. Secondly, FcγRI engagement on immune cells, such as microglia, is likely to result in elevated cytokine levels. Changes to cytokine levels were similar in both adult and middle-aged mice and therefore cannot account for the different impacts on tau phosphorylation, observed at each age. Future investigations using IgG deficient mice may uncover further mechanistic clues.

The data presented here, implies that at middle age, alternative inflammatory mechanisms and signalling pathways are activated and/or neurons are predisposed to behave differently in response to inflammation. One mediator that may lie between inflammation and tau phosphorylation, is brain-derived neurotrophic factor (BDNF). BDNF has been shown to dephosphorylate tau at Ser202/Thr205 *in vitro*, via activation of PI3-kinase and Akt, with subsequent inhibition of the prominent tau kinase GSK3β (Elliott et al. 2005). BDNF levels are reported to decline in middle-aged rats (Hattiangady et al. 2005) and proinflammatory cytokine exposure, such as IL-1β, reduces BDNF gene

expression (Calabrese et al. 2014). Therefore, the combination of both middle age and inflammation may reduce BDNF to levels that are detrimental to tau phosphorylation. Future studies would benefit from investigation into BDNF levels following systemic inflammation in middle-age.

7.3 Systemic inflammation and Aβ pathology

Although a trend was seen for the induction of tau phosphorylation in middle-aged mice following *S.* Typhimurium, it is possible that additional factors are required to trigger greater and persistent pathological tau phosphorylation. One line of reasoning follows the Amyloid Cascade Hypothesis (ACH) which postulates that the abnormal processing of APP, production of, and subsequent deposition of Aβ plaques are leading events in AD pathogenesis (Hardy and Higgins 1992). Evidence suggests microglia attempt to phagocytose and remove Aβ plaques, but in doing so, release proinflammatory cytokines (Stancu et al. 2014). As cytokines, such as IL-1β, are implicated in driving neuronal kinase activation, this pathway may provide a prominent link between Aβ and tau pathology (Li et al. 2003). Furthermore, the addition of systemic inflammation may further drive the chronic neuroinflammation observed in AD. Indeed, multiple i.p. LPS challenges have been shown to increase tau phosphorylation in transgenic models displaying both amyloid and tau pathology, together with pre-existing neuroinflammation (Kitazawa et al. 2005).

Therefore in **Chapter 6**, I took the novel approach of utilising aged (16-17 month old) APP^{SWE} (Tg2576) transgenic mice, which have extensive amyloid plaque deposition, and administering *S.* Typhimurium to determine the consequences of a common bacterial infection on neuroinflammation and tau phosphorylation. By assessing microglial phenotype and cytokine levels, I aimed to determine whether systemic inflammation did indeed promote the pathway outlined above.

Two different consequences were observed in relation to tau phosphorylation in the Tg2576 mice and non-transgenic littermates, following infection with *S.* Typhimurium. Therefore, I put forward an explanation for each of the genotypes' responses.

Non-transgenic APP^{SWE} mice

In the 16-month old non-transgenic mice, a moderate body weight loss, increase in spleen size and elevations in proinflammatory serum cytokines, including IFN-γ, IL-6 and TNF-α, is observed, indicating that these ageing mice are still responsive to a systemic bacterial infection. Furthermore, increased levels of central cytokines including IFN-γ, IL-1β and IL-6, are seen which may contribute to the increased FcγRI expression on parenchymal cells such as microglia and perivascular macrophages. Similarly to the earlier studies in adult and middle-aged wild-type mice, further investigation is required as to the relative contributions of cytokines from cell types such as microglia and the endothelia. These 16-month old mice display an increase in tau phosphorylation at the Ser396 epitope, following *S.* Typhimurium infection.

This would suggest that advanced age (16-17 month old) predisposes these mice to *S.* Typhimurium-induced tau phosphorylation. While a trend for increased phosphorylation of tau was observed in middle-aged mice in chapter 5, the consequences of ageing are severe enough in these mice to register a significant difference. To my knowledge, this is the first study to show increases in tau phosphorylation following systemic inflammation induced by bacterial infection in aged wild-type animals.

Recently Bodea and colleagues investigated the effects of ageing on tau phosphorylation (Bodea et al. 2017). They found no changes in tau phosphorylation in a transgenic model of accelerated ageing (SAMP8/TaHsd) (Takeda et al. 1981), but when a transgenic mutated human tau model (PR5) (Gotz et al. 2001) was backcrossed onto this strain, increased tau phosphorylation at the Ser202/Thr205 (AT8) epitope was observed. This may suggest that while age alone does not induce tau phosphorylation, an additional factor such as the presence of mutated human tau, which displays progressive tau hyperphosphorylation, or in our case, systemic inflammation, can increase this post-translational modification.

Therefore, it appears the ageing process lowers the threshold for tau phosphorylation to occur. Two possible contributors to this are as follows. Firstly, both mice and humans show signs of BBB breakdown with advancing age (Goodall et al. 2017). Recently, Goodall and colleagues demonstrated a significant decrease in cortical expression of the tight

junction protein ZO-1 at 18, but not 12 months of age, in C57BL/6 wild-type mice. Furthermore, using MRI, it was reported that the human hippocampus displays signs of BBB breakdown with age (Montagne et al. 2015). Interestingly, there was a lack of MHCII positive staining on the cells associated with the vasculature in both genotypes at 16 months of age; a phenomenon previously seen in both the adult and middle-aged C57BL/6 wild-type mice following infection with *S*. Typhimurium. While the 16-month old mice displayed similar increases in proinflammatory cytokines as younger mice, further investigation would be useful in determining what other inflammatory mediators pass into the brain parenchyma when the BBB is compromised with age.

Secondly, changes to cells in the brain, including neurons and microglia, may be increased in advanced age, which lays the foundations for detrimental consequences following further inflammatory stimuli. Numerous alterations occur with ageing including disruption to insulin signalling, DNA modification, impairment of DNA repair, changes in lipid metabolism and increases in oxidative stress (for reviews see (Mattson and Magnus 2006; Wang and Michaelis 2010)). There is evidence that inflammation is linked to the development of insulin resistance, as cytokines such as IL-1β, IL-6 and TNF-α are reported to cause inhibition of neuronal insulin receptor substrate 1 (IRS-1) (Talbot 2014), a critical component of insulin signalling. As insulin inhibits the activation of GSK3β (Cross et al. 1995), a disinhibition of this tau kinase may result in tau phosphorylation. I propose that the combination of ageing and a secondary immune stimulus may lower the threshold for insulin resistance to occur, resulting in GSK3β activation and subsequent tau phosphorylation. As insulin resistance is a characteristic reported in AD patients (Talbot et al. 2012), investigation into this pathway in the *S*. Typhimurium model, may be beneficial in determining the link between systemic inflammation and tau phosphorylation.

Transgenic APP^{SWE} mice

Following *S.* Typhimurium infection in the 16-month old Tg2576 mice, an increase in spleen size and elevations in proinflammatory serum cytokines, including IFN-γ, IL-6 and TNF-α, is observed, indicating that these mice are still responsive to a bacterial infection. However, Tg2576 mice receiving the infection rapidly recovered with regard to bodyweight, and gained weight above both their starting weight and saline-injected

counterparts. As the transgenic mice also had a significantly lower starting bodyweight compared to the non-transgenics, this may indicate an altered metabolism due to hypothalamic dysfunction, a characteristic of patients with mild cognitive impairment (for review see (Ishii and Iadecola 2015)).

In the hippocampus, it was observed that microglia clustered around amyloid plaques with high expression of FcγRI and CD68, as has been reported in other transgenic APP models and AD (Itagaki et al. 1989; Minett et al. 2016). Despite increases in FcγRI expression and the levels of brain IFN-γ, IL-6 and IL-1β following infection with *S.* Typhimurium, these changes appear smaller than those observed in non-transgenic mice.

Investigating pathological changes, there was a trend towards increased levels of both soluble and insoluble Aβ, however, this did not reach statistical significance. It has been shown that i.p. injection of LPS induces Aβ generation through associated increases in the APP secretase BACE1 (Lee et al. 2008), possibly accounting for this increased trend in soluble Aβ. As there is evidence of impaired Aβ clearance and/or microglial phagocytosis in AD models (Krabbe et al. 2013; Wildsmith et al. 2013), these greater soluble levels may aggregate and result in the increased insoluble Aβ observed in this model.

In contrast to the non-transgenic mice, although Tg2576 mice had a significantly higher baseline phosphorylation of tau at the Ser396 epitope, infection with *S*. Typhimurium did not induce any further phosphorylation.

Similarly to ageing, Aβ deposition is thought to evoke an exacerbated response from immune cells when exposed to a secondary immune stimulus i.e. priming (Yin et al. 2017), However, studies assessing this are limited (Sly et al. 2001). Although, priming is commonly assessed with acute stimuli, the data presented here suggests no additional central inflammatory cytokine response following infection with *S.* Typhimurium. On the contrary, the response is relatively limited in comparison to non-transgenic littermates, perhaps suggesting an immunosuppressed environment.

There is strong evidence from the literature that Aβ activates inflammasomes such as NLRP3, resulting in increased production of proinflammatory cytokines such as IL-1β (for review see (White et al. 2017)). It is speculated that because bacteria such as *S.*

Typhimurium and *E*. Coli also present amyloid fibrils on their surface, microglia respond and attempt to clear Aβ in a similar manner to a pathogen. However, with constant endogenous Aβ production in AD, the microglia never succeed in this task and remain in a chronically active and detrimental state (Streit et al. 2014). Eventually, it has been observed this continuous attempt to phagocytose the Aβ leads to a dystrophic or 'burned out' phenotype, as is observed around compact, dense-core plaques (Sheng et al. 1997). It is therefore conceivable that these dystrophic microglia are unable to respond to inflammatory stimulus and therefore, as observed, neuronal tau phosphorylation is not increased.

In summary, chapter 8 supports earlier data suggesting ageing facilitates tau phosphorylation following *S.* Typhimurium infection. We may speculate that ageing predisposes cells in the brain, such as neurons and microglia, and/or induces barrier breakdown allowing a greater influence from systemic inflammation. In contrast, there were limited central immune changes and no increases in tau phosphorylation observed following *S.* Typhimurium infection in the transgenic 16-month old APP^{SWE} mice. As brain immune cells, such as microglia, attempt to clear Aβ, they are chronically activated, eventually resulting in a dystrophic and unresponsive phenotype, unable to respond fully to the *S.* Typhimurium infection. Further investigation into the issues outlined here would be beneficial in fully elucidating disease mechanisms.

7.4 Conclusions

The data presented in this project supports the following conclusions:

1. *S.* Typhimurium provides a model of systemic inflammation that better recapitulates immune activation following a real life bacterial infection, than the multiple LPS protocol which develops ET.
2. There is limited evidence for the induction of tau phosphorylation in healthy adult wild-type mice, possibly due to functional physiological mechanisms that resolve inflammation before aberrant tau pathology can develop and mediate subsequent neuronal demise.

3. Tau phosphorylation increases with age in response to *S.* Typhimurium, suggesting the ageing process lowers the threshold for induction of this post-translational modification.
4. There is an increased basal level of tau phosphorylation in APP^{SWE} transgenic mice and further stimulation by *S.* Typhimurium does not alter this, perhaps due to dystrophic and immunosuppressed microglia.

7.5 The inflammation hypothesis

The inflammation hypothesis of AD, proposed by Dimitrije Krstic and Irene Knuesel, positions chronic inflammation as a leading event in the development of LOAD (Krstic and Knuesel 2012). The hypothesis was formulated, in part, from their own studies which demonstrated that systemic administration of the viral mimic PolyI:C to wild-type mice during late gestation, resulted in neuroinflammation and aggregated Aβ in ageing offspring (Knuesel et al. 2009). Furthermore, a second systemic PolyI:C challenge in 12-month old wild-type offspring, resulted in an exacerbated phenotype with deposition of APP, tau aggregation, microglial activation (CD68) and reactive gliosis (GFAP) (Krstic et al. 2012), supporting the previously outlined 'priming' phenomenon. Unifying results from other studies, a hypothesis was formed whereby, during healthy ageing, misfolded and dysfunctional proteins are efficiently removed from axons in a 'budding' process and these resulting granules are phagocytosed and removed by microglia. However, in the presence of chronic inflammation in the brain, this process is accelerated, tau becomes hyperphosphorylated and microglia switch to a primed phenotype. This results in axonal transport deficits and damage from overactive microglia, increasing metabolic and morphologic stress on the neurons. Paired-helical filaments of tau form and synapses begin to degenerate. The presence of chronic inflammation and axonal transport deficits result in deposition of amyloid plaques, formation of NFTs and neurodegeneration. Crucially, two key characteristics of this model are the causative and early appearance of chronic inflammation and tau hyperphosphorylation respectively.

The data presented in these chapters support the inflammation hypothesis of AD, in that systemic inflammation exacerbates deleterious processes that occur in ageing. For example, in middle-aged wild-type C57BL/6 mice, Knuesel and colleagues reported the

accumulation and aggregation of Reelin-enriched plaques, a neuronal glycoprotein that modulates synaptic function and plasticity, in the hippocampus (Knuesel et al. 2009). Prenatal exposure to PolyI:C increased the number of plaques observed, demonstrating that chronic inflammation had accelerated this ageing characteristic. In chapter 5, middle-aged mice showed a trend toward increased tau phosphorylation following infection with *S.* Typhimurium. This effect was significant in the 16-month old non-transgenic mice. This demonstrates that systemic inflammation accelerates a deleterious process in ageing, in this case tau phosphorylation. Future studies would benefit from investigation into aggregation of Reelin in this model, considering it is common feature of ageing in numerous species including rats and marmoset monkeys (Knuesel et al. 2009), and that dysfunctional Reelin signalling has been reported to result in the increased activity of GSK3β and tau hyperphosphorylation (Ohkubo et al. 2002).

An additional feature of ageing, demonstrated to promote neuroinflammation, is the compromised BBB (Montagne et al. 2015). Accordingly, infection with *S.* Typhimurium resulted in infiltration of IgG into the parenchyma in both adult and middle-aged mice, which is in line with the notion of an impaired BBB. Furthermore, ageing may also facilitate further crosstalk of mediators that promote tau phosphorylation (Sarlus et al. 2012). Therefore, assessing the expression of key structural proteins in the BBB e.g. ZO-1, may help in determining the breakdown in this structure.

A controversial aspect of the inflammation hypothesis, is the role of APP and Aβ. While the misprocessing of APP and aggregation of Aβ are postulated to be leading events in LOAD pathogenesis, the inflammation hypothesis instead claims that APP plays a protective neuronal role and the processing of Aβ is a defence mechanism to neuronal injury (Krstic and Knuesel 2012). Indeed, Reelin associates with APP in the early accumulations observed in ageing (Knuesel et al. 2009). While the inflammation hypothesis applies to sporadic LOAD, the misprocessing of APP is still a central causative factor in familial AD. Therefore, the transgenic Tg2576 mouse model, used in my studies, recapitulates aspects of this form of AD rather than LOAD. The increased tau phosphorylation already present in the Tg2576 mice (Otth et al. 2002; Noda-Saita et al. 2004), may be a result of the Aβ itself and/or activated microglia reacting to the amyloid plaques. The absence of change following *S.* Typhimurium infection may suggest a

dysfunctional immune response characterised by senescent microglia. This would fit with reports of attenuated neuroinflammation in AD patients with increasing age (Hoozemans et al. 2011), and supports the early role of inflammation in the pathogenesis of the disease. Therefore, utilising middle-aged Tg2576 mice may uncover the contribution of systemic inflammation to tau phosphorylation in the early events of AD.

In conclusion, the results presented in these chapters fit with the inflammation hypothesis of AD. It remains to be seen whether all the steps outlined are true to disease pathogenesis, however, I believe that chronic inflammation and tau phosphorylation are early events. There is some evidence to support that additional factors surface during ageing, such as disruption to insulin signalling (Ferreira et al. 2014) and increased oxidative stress (Markesbery 1999), which all contribute to lowering the threshold for pathological tau phosphorylation to occur. I believe systemic inflammation, such as that provided by bacterial infections, drives the outlined deleterious events in early AD pathogenesis. Therefore, therapeutic intervention should target this earlier time window before neurodegeneration has taken place.

7.6 Future directions

In relation to this project, there are numerous aspects that could be explored further. Firstly, the missing component of this hypothesis is the role of the tau kinases. Highly implicated kinases include the tyrosine kinase Fyn and the Serine/Threonine protein kinases GSK3β, CDK5, PKA and the MAP kinases (for review see (Martin et al. 2013)). Investigation of kinases involved suffers a similar issue to cytokines, as it is difficult to identify the location of the kinases using biochemical methods alone. Therefore, to identify the kinases responsible for tau phosphorylation in the neurons, immunochemistry is required. Nevertheless, targeting enhanced activation of kinases, regardless of location, may inhibit the deleterious pathways which ultimately lead to tau phosphorylation. Additionally, although current therapeutics targeting the kinases have issues with specificity (Panza et al. 2016), identification would still provide information on activated pathways.

There is still debate as to whether overall or site-specific phosphorylation is more important in the pathological hyperphosphorylation of tau. I have looked at 2 epitopes implicated in pathology, however, there are 85 residues on which tau can be phosphorylated (Noble et al. 2013). It is possible that while the residues I have chosen are phosphorylated with ageing and systemic inflammation, other epitopes may be important in adulthood or when Aβ pathology is present. Mass spectrometry has recently been utilised to identify post-translational modifications to tau in wild-type and hAPP mice (Morris et al. 2015).

In future this tool may be invaluable in building a complete picture of tau phosphorylation between experimental groups. Furthermore mass spectrometry identifies other post-translational modifications such as acetylation, ubiquitination and methylation, some of which are highly implicated in the development of pathological tau (Martin et al. 2011). I believe that by using an array of methods including mass spectrometry, more targets can be identified for tau-related therapeutics.

In addition to other post-translational modifications on tau, researchers are curious to determine whether slowing the propagation of tau across interconnected brain regions, would be a viable target for therapeutics (Pooler et al. 2015). Asai and colleagues have reported that microglia may be partially responsible, by phagocytosing tau-bearing neurons, and spreading pathological tau species to other regions of the brain via exosome secretion (Asai et al. 2015). Furthermore, depletion of microglia partially inhibits the spread of tau pathology. If microglia and neuroinflammation are important in this pathological spreading process, it would be interesting to determine whether systemic inflammation is an accelerating factor.

As detailed previously, it is difficult to ascertain the source of the elevations in central cytokines observed. Detecting cytokine proteins can be problematic given their transient nature, however, fluorescent in situ hybridization (FISH) could be utilised to detect the source of mRNA transcripts. Deciphering which cell type is responsible for neuroinflammatory changes following systemic inflammation is crucial in tailoring therapeutic intervention. If the contribution from cells associated with the vasculature is significant, treatments may not have to overcome the difficulty of crossing the BBB.

Inhibiting the elevations in peripheral proinflammatory cytokines may be a viable treatment option as has been suggested in early clinical trials (Butchart et al. 2015). However, caution should be taken as it is becoming apparent that mechanisms involved in the resolution of inflammation, require stimulus from mediators in this proinflammatory phase (Serhan and Petasis 2011). Therefore, further investigation into activation of these mechanisms may facilitate novel treatment options.

Emerging evidence suggests greater diversity and fluidity in microglial populations than the M1/M2 phenotype classification dictates (Perry 2016). Using flow cytometry, greater insight into these different populations may be determined and the shift following systemic inflammation. Additionally, transcriptomic studies have begun to reveal the differences between microglial populations in ageing, priming and APP mice (Holtman et al. 2015). The depth of this profiling can help identify different microglial populations and inform on unique markers such as the purinergic receptor P2ry12 (Butovsky et al. 2014). Furthermore, utilising transcriptional single-cell sorting, Keren-Shaul and colleagues have recently identified a disease-specific microglial phenotype (DAM) that is thought to restrict neurodegeneration (Keren-Shaul et al. 2017). Investigating how pathological hallmarks, such as Aβ plaques and NFTs, alter the phenotype of specific microglia, may uncover why broader treatments are not successful, and could be utilised to assess the impact of systemic inflammation.

Despite utilising the *S.* Typhimurium model to engage a diverse spectrum of innate and adaptive immune pathways, this study has focussed on cells from the former for analysis. However, given the decline of the adaptive branch during immunosenescence, it would be beneficial to investigate the changes to T- and B- cells. Recently, Marsh and colleagues generated an immune-deficient AD mouse model that lacked T, B and natural killer cells (Marsh et al. 2016). The microglia in these mice showed increased cytokine production and reduced phagocytic capacity, resulting in a more than 2-fold increase in Aβ pathology. Interestingly, treatment with preimmune IgG enhanced clearance of Aβ. With significant IgG infiltration into the brain parenchyma following *S.* Typhimurium infection, it would be interesting to determine whether greater phagocytosis takes place at this time point or earlier. However, in another study, infiltrating CD4+ T-cells have been shown to produce IFN-γ, activate microglia and increase Aβ plaque burden in an AD model combined with

nasal bortadella pertussis toxin (McManus et al. 2015), demonstrating that further investigation into the role of the adaptive immune system is required.

In this study, I have focussed on the relationship between bacterial infections and tau phosphorylation. However, viral infections such as herpes simplex virus type 1 (HSV-1) and fungal infections such as Candida albicans are also implicated as risk factors for neurodegenerative diseases like AD (for review see (McManus and Heneka 2017)). In addition to relatively acute infections like *S.* Typhimurium, low-grade chronic systemic inflammation is a risk factor for AD. Examples of these conditions include rheumatoid arthritis, obesity, metabolic syndrome, atherosclerosis, and diabetes (for review see (Cunningham and Hennessy 2011)).

With the modest age-dependent increases in tau phosphorylation observed following systemic inflammation, I believe there are crucial stages of life when infections can have deleterious consequences to the brain. As previously outlined, it has been shown that administration of the viral mimic PolyI:C to pregnant wild-type mice, in late gestation, causes the development of AD-like neuropathology during the course of ageing (Krstic et al. 2012). An additional feature was the increased expression of inflammatory cytokines in the foetal brain (Meyer et al. 2006). It may be speculated that this early challenge, during the formation of the BBB, altered the brain immune profile and compromised the offspring when they reached advanced age. Additionally, experimental evidence suggests advanced age and/or ongoing neurodegeneration, when the BBB has been shown to be disrupted, is another vulnerable time for the CNS from acute systemic inflammation (Cunningham et al. 2005; Godbout et al. 2005). Although present for at least 40 days, the *S.* Typhimurium infection utilised in my studies, represents a relatively acute challenge. Therefore, pathological processes such as tau hyperphosphorylation occur when the infection is given in advanced age, as observed, and we may speculate the same occurs if given during foetal development. In contrast, chronic low-grade systemic inflammation throughout life from conditions such as obesity, may be required to alter brain immune profiles, accelerate the process of ageing and bring forward the age of onset for neurodegenerative diseases (Miller and Spencer 2014). Future studies may benefit from investigating models of low-grade chronic inflammation, to determine if this predisposes the brain to pathogenesis in older age.

Neurodegenerative conditions such as AD are multifactorial, and therefore a range of therapeutics are likely to be required. Although results from Aβ-targeted immunotherapy have proved disappointing thus far, I believe a combinational approach with tau-targeted immunotherapy can limit the progression of AD at the earliest stages. With greater understanding of mechanism, I envisage treatments targeting both peripheral and central inflammation playing a key role in this combination therapy. Until that point, prevention of certain inflammatory conditions such as obesity and type-2 diabetes, and the rapid diagnosis and treatment of infection in the elderly would delay the onset and progression of neurodegenerative disease in the general population.

List of References

Abbott, N.J. et al. 2010. Structure and function of the blood–brain barrier. *Neurobiology of Disease* 37(1), pp. 13–25. doi: 10.1016/j.nbd.2009.07.030.

Abramov, A.Y. et al. 2003. Changes in intracellular calcium and glutathione in astrocytes as the primary mechanism of amyloid neurotoxicity. *The Journal of neuroscience : the official journal of the Society for Neuroscience* 23(12), pp. 5088–95.

Ackmann, M. et al. 2000. Nonsaturable binding indicates clustering of tau on the microtubule surface in a paired helical filament-like conformation. *The Journal of biological chemistry* 275(39), pp. 30335–43. doi: 10.1074/jbc.M002590200.

Adams, S.J. et al. 2009. Overexpression of Wild-Type Murine Tau Results in Progressive Tauopathy and Neurodegeneration. *The American Journal of Pathology* 175(4), pp. 1598–1609. doi: 10.2353/ajpath.2009.090462.

Ahmed, T. et al. 2014. Cognition and hippocampal synaptic plasticity in mice with a homozygous tau deletion. *Neurobiology of aging* 35(11), pp. 2474–8. doi: 10.1016/j.neurobiolaging.2014.05.005.

Akira, S. et al. 2006. Pathogen Recognition and Innate Immunity. *Cell* 124(4), pp. 783–801. doi: 10.1016/j.cell.2006.02.015.

Albandar, J.M. and Rams, T.E. 2002. Global epidemiology of periodontal diseases: an overview. *Periodontology 2000* 29, pp. 7–10.

Alberdi, E. et al. 2013. Ca(2+) dependent endoplasmic reticulum stress correlates with astrogliosis in oligomeric amyloid β-treated astrocytes and in a model of Alzheimer's disease. *Aging Cell* 12(2), pp. 292–302. doi: 10.1111/acel.12054.

Alexander, C. and Rietschel, E. 2001. Invited review: Bacterial lipopolysaccharides and innate immunity. *Journal of Endotoxin Research* 7(3), pp. 167–202. doi: 10.1177/09680519010070030101.

Alonso, A. et al. 2001. Hyperphosphorylation induces self-assembly of tau into tangles of paired helical filaments/straight filaments. *Proceedings of the National Academy of Sciences of the United States of America* 98(12), pp. 6923–8. doi: 10.1073/pnas.121119298.

Alonso, A. d. C. et al. 2004. Promotion of Hyperphosphorylation by Frontotemporal Dementia Tau Mutations. *Journal of Biological Chemistry* 279(33), pp. 34873–34881. doi: 10.1074/jbc.M405131200.

Alonso, A.C. et al. 1996. Alzheimer's disease hyperphosphorylated tau sequesters normal tau into tangles of filaments and disassembles microtubules. *Nature medicine* 2(7), pp. 783–7.

Álvarez, G. et al. 2012. Herpes simplex virus type 1 induces nuclear accumulation of hyperphosphorylated tau in neuronal cells. *Journal of Neuroscience Research* 90(5), pp. 1020–1029. doi: 10.1002/jnr.23003.

Alzheimer, A. 1907. Uber eine eigenartige Erkrankung der Hirnrinde. *Allg Zeits Psychiatry Psychisch Y Gerichtlich Med* 64, pp. 146–8. doi: 10.1002/ca.980080612.

Amenta, F. et al. 1998. Astrocyte changes in aging cerebral cortex and hippocampus: A quantitative immunohistochemical study. *Microscopy Research and Technique* 43(1), pp. 29–33. doi: 10.1002/(SICI)1097-0029(19981001)43:1<29::AID-JEMT5>3.0.CO;2-H.

Anderson, C.F. and Mosser, D.M. 2002. A novel phenotype for an activated macrophage: the type 2 activated macrophage. *Journal of leukocyte biology* 72(1), pp. 101–6.

Andorfer, C. et al. 2003. Hyperphosphorylation and aggregation of tau in mice expressing normal human tau isoforms. *Journal of neurochemistry* 86(3), pp. 582–90.

Anforth, H.R. et al. 1998. Biological activity and brain actions of recombinant rat interleukin-1alpha and interleukin-1beta. *European cytokine network* 9(3), pp. 279–88.

Anstey, K.J. et al. 2007. Smoking as a Risk Factor for Dementia and Cognitive Decline: A Meta-Analysis of Prospective Studies. *American Journal of Epidemiology* 166(4), pp. 367–378. doi: 10.1093/aje/kwm116.

Aravalli, R.N. et al. 2007. Toll-like Receptors in Defense and Damage of the Central Nervous System. *Journal of Neuroimmune Pharmacology* 2(4), pp. 297–312. doi: 10.1007/s11481-007-9071-5.

Arnardottir, H.H. et al. 2014. Aging delays resolution of acute inflammation in mice: reprogramming the host response with novel nano-proresolving medicines. *Journal of immunology (Baltimore, Md. : 1950)* 193(8), pp. 4235–44. doi: 10.4049/jimmunol.1401313.

Arvanitakis, Z. et al. 2008. Relation of NSAIDs to incident AD, change in cognitive function, and AD

pathology. *Neurology* 70(23), pp. 2219–25. doi: 10.1212/01.wnl.0000313813.48505.86.

Asai, H. et al. 2015. Depletion of microglia and inhibition of exosome synthesis halt tau propagation. *Nature Neuroscience* 18(11), pp. 1584–1593. doi: 10.1038/nn.4132.

Atwood, C.S. et al. 2003. Amyloid-beta: a chameleon walking in two worlds: a review of the trophic and toxic properties of amyloid-beta. *Brain research. Brain research reviews* 43(1), pp. 1–16.

Babcock, A.A. et al. 2003. Chemokine expression by glial cells directs leukocytes to sites of axonal injury in the CNS. *The Journal of neuroscience : the official journal of the Society for Neuroscience* 23(21), pp. 7922–30.

Bagyinszky, E. et al. 2017. Role of inflammatory molecules in the Alzheimer's disease progression and diagnosis. *Journal of the Neurological Sciences* 376, pp. 242–254. doi: 10.1016/j.jns.2017.03.031.

Balasingam, V. et al. 1994. Reactive astrogliosis in the neonatal mouse brain and its modulation by cytokines. *The Journal of neuroscience : the official journal of the Society for Neuroscience* 14(2), pp. 846–56.

Bamberger, M.E. et al. 2003. A cell surface receptor complex for fibrillar beta-amyloid mediates microglial activation. *The Journal of neuroscience : the official journal of the Society for Neuroscience* 23(7), pp. 2665–74.

Banks, W.A. et al. 1995. Passage of cytokines across the blood-brain barrier. *Neuroimmunomodulation* 2(4), pp. 241–8.

Banks, W.A. et al. 1996. Passage of Cytokines across the Blood-Brain Barrier. *Neuroimmunomodulation* 2(4), pp. 241–248. doi: 10.1159/000097202.

Banks, W.A. et al. 2015. Lipopolysaccharide-induced blood-brain barrier disruption: roles of cyclooxygenase, oxidative stress, neuroinflammation, and elements of the neurovascular unit. *Journal of neuroinflammation* 12, p. 223. doi: 10.1186/s12974-015-0434-1.

Barichello, T. et al. 2015. Does Infection-Induced Immune Activation Contribute to Dementia? *Aging and Disease* 6(5), p. 342. doi: 10.14336/AD.2015.0521.

Barrientos, R.M. et al. 2006. Peripheral infection and aging interact to impair hippocampal memory consolidation. *Neurobiology of Aging* 27(5), pp. 723–732. doi:

10.1016/j.neurobiolaging.2005.03.010.

Barron, M. et al. 2016. A state of delirium: Deciphering the effect of inflammation on tau pathology in Alzheimer's disease. *Experimental Gerontology* . doi: 10.1016/j.exger.2016.12.006.

Bechmann, I. et al. 2007. What is the blood–brain barrier (not)? *Trends in Immunology* 28(1), pp. 5–11. doi: 10.1016/j.it.2006.11.007.

Vom Berg, J. et al. 2012. Inhibition of IL-12/IL-23 signaling reduces Alzheimer's disease-like pathology and cognitive decline. *Nature medicine* 18(12), pp. 1812–9. doi: 10.1038/nm.2965.

von Bernhardi, R. et al. 2015. Microglial cell dysregulation in brain aging and neurodegeneration. *Frontiers in Aging Neuroscience* 7(JUN), p. 124. doi: 10.3389/fnagi.2015.00124.

Bertram, L. et al. 2010. The genetics of alzheimer disease: Back to the future. *Neuron* 68(2), pp. 270–281. doi: 10.1016/j.neuron.2010.10.013.

Bhaskar, K. et al. 2010. Regulation of Tau Pathology by the Microglial Fractalkine Receptor. *Neuron* 68, pp. 19–31. doi: 10.1016/j.neuron.2010.08.023.

Biernat, J. et al. 2002. Protein kinase MARK/PAR-1 is required for neurite outgrowth and establishment of neuronal polarity. *Molecular biology of the cell* 13(11), pp. 4013–28. doi: 10.1091/mbc.02-03-0046.

Biesmans, S. et al. 2013. Systemic immune activation leads to neuroinflammation and sickness behavior in mice. *Mediators of inflammation* 2013, p. 271359. doi: 10.1155/2013/271359.

Biessels, G.J. et al. 2006. Risk of dementia in diabetes mellitus: a systematic review. *The Lancet. Neurology* 5(1), pp. 64–74. doi: 10.1016/S1474-4422(05)70284-2.

Birch, A.M. et al. 2014. Modulation of inflammation in transgenic models of Alzheimer's disease. *Journal of Neuroinflammation* 11(1), p. 25. doi: 10.1186/1742-2094-11-25.

Biswas, S.K. and Lopez-Collazo, E. 2009. Endotoxin tolerance: new mechanisms, molecules and clinical significance. *Trends in Immunology* 30(10), pp. 475–487. doi: 10.1016/j.it.2009.07.009.

Bluthé, R.M., Walter, V., et al. 1994. Lipopolysaccharide induces sickness behaviour in rats by a vagal mediated mechanism. *Comptes rendus de l'Academie des sciences. Serie III, Sciences de la vie* 317(6), pp. 499–503.

Bluthé, R.M., Pawlowski, M., et al. 1994. Synergy between tumor necrosis factor alpha and

interleukin-1 in the induction of sickness behavior in mice. *Psychoneuroendocrinology* 19(2), pp. 197–207.

Bodea, L.-G. et al. 2017. Accelerated aging exacerbates a pre-existing pathology in a tau transgenic mouse model. *Aging Cell* 16(2), pp. 377–386. doi: 10.1111/acel.12565.

Borchelt, D.R. et al. 1997. Accelerated amyloid deposition in the brains of transgenic mice coexpressing mutant presenilin 1 and amyloid precursor proteins. *Neuron* 19(4), pp. 939–45.

Borges, B.C. et al. 2012. Glial cell activity is maintained during prolonged inflammatory challenge in rats. *Brazilian Journal of Medical and Biological Research* 45(8), pp. 784–791. doi: 10.1590/S0100-879X2012007500069.

Bournazos, S. et al. 2016. The Role and Function of Fcγ Receptors on Myeloid Cells. *Microbiology spectrum* 4(6). doi: 10.1128/microbiolspec.MCHD-0045-2016.

Bowman-Rogers, M. 2017. Treating Tau: Finally, Clinical Candidates Are Stepping into the Ring. Available at: http://www.alzforum.org/news/conference-coverage/treating-tau-finally-clinical-candidates-are-stepping-ring.

Braak, E. et al. 1994. A sequence of cytoskeleton changes related to the formation of neurofibrillary tangles and neuropil threads. *Acta neuropathologica* 87(6), pp. 554–67.

Braak, H. et al. 2013. Intraneuronal tau aggregation precedes diffuse plaque deposition, but amyloid-β changes occur before increases of tau in cerebrospinal fluid. *Acta Neuropathologica* 126(5), pp. 631–641. doi: 10.1007/s00401-013-1139-0.

Braak, H. and Braak, E. 1991. Neuropathological stageing of Alzheimer-related changes. *Acta Neuropathologica* 82(4), pp. 239–259. doi: 10.1007/BF00308809.

Breder, C.D. et al. 1994. Regional induction of tumor necrosis factor alpha expression in the mouse brain after systemic lipopolysaccharide administration. *Proceedings of the National Academy of Sciences of the United States of America* 91(24), pp. 11393–7.

Breitner, J.C. et al. 2011. Extended results of the Alzheimer's disease anti-inflammatory prevention trial. *Alzheimer's & Dementia* 7(4), pp. 402–411. doi: 10.1016/j.jalz.2010.12.014.

Bret-Dibat, J.L. et al. 1995. Lipopolysaccharide and interleukin-1 depress food-motivated behavior in mice by a vagal-mediated mechanism. *Brain, behavior, and immunity* 9(3), pp. 242–6.

Brightman, M. 1991. Implication of Astroglia in the Blood-Brain Barrier. *Annals of the New York*

Academy of Sciences 633(1 Glial-Neurona), pp. 343–347. doi: 10.1111/j.1749-6632.1991.tb15625.x.

Brkic, M. et al. 2015. Amyloid Oligomers Disrupt Blood-CSF Barrier Integrity by Activating Matrix Metalloproteinases. *Journal of Neuroscience* 35(37), pp. 12766–12778. doi: 10.1523/JNEUROSCI.0006-15.2015.

Broz, P. et al. 2012. Innate immune response to Salmonella typhimurium, a model enteric pathogen. *Gut microbes* 3(2), pp. 62–70. doi: 10.4161/gmic.19141.

Buée, L. et al. 2000. Tau protein isoforms, phosphorylation and role in neurodegenerative disorders. *Brain Research Reviews* 33(1), pp. 95–130. doi: 10.1016/S0165-0173(00)00019-9.

Bueno, V. et al. 2016. Immune to Brain Communication in Health, Age and Disease: Implications fo Understanding Age-Related Neurodegeneration. In: *The Ageing Immune System and Health*., pp. 125–136.

Butchart, J. et al. 2015. Etanercept in Alzheimer disease: A randomized, placebo-controlled, double-blind, phase 2 trial. *Neurology* 84(21), pp. 2161–2168. doi: 10.1212/WNL.0000000000001617.

Butovsky, O. et al. 2014. Identification of a unique TGF-β-dependent molecular and functional signature in microglia. *Nature neuroscience* 17(1), pp. 131–43. doi: 10.1038/nn.3599.

Caceres, A. and Kosik, K.S. 1990. Inhibition of neurite polarity by tau antisense oligonucleotides in primary cerebellar neurons. *Nature* 343(6257), pp. 461–3. doi: 10.1038/343461a0.

Cai, Z. et al. 2017. Astrocyte and Alzheimer's disease. *Journal of neurology* . doi: 10.1007/s00415-017-8593-x.

Calabrese, F. et al. 2014. Brain-derived neurotrophic factor: a bridge between inflammation and neuroplasticity. *Frontiers in cellular neuroscience* 8, p. 430. doi: 10.3389/fncel.2014.00430.

Calsolaro, V. and Edison, P. 2016. Neuroinflammation in Alzheimer's disease: Current evidence and future directions. *ALZHEIMERS & DEMENTIA* 12(6), pp. 719–732. doi: 10.1016/j.jalz.2016.02.010.

Campuzano, O. et al. 2009. Increased levels of proinflammatory cytokines in the aged rat brain attenuate injury-induced cytokine response after excitotoxic damage. *Journal of Neuroscience Research* 87(11), pp. 2484–2497. doi: 10.1002/jnr.22074.

Carson, M.J. et al. 2006. CNS immune privilege: hiding in plain sight. *Immunological reviews* 213(1), pp. 48–65. doi: 10.1111/j.1600-065X.2006.00441.x.

Carter, S.F. et al. 2012. Evidence for Astrocytosis in Prodromal Alzheimer Disease Provided by 11C-Deuterium-L-Deprenyl: A Multitracer PET Paradigm Combining 11C-Pittsburgh Compound B and 18F-FDG. *Journal of Nuclear Medicine* 53(1), pp. 37–46. doi: 10.2967/jnumed.110.087031.

Catorce, M.N. and Gevorkian, G. 2016. LPS-induced Murine Neuroinflammation Model: Main Features and Suitability for Pre-clinical Assessment of Nutraceuticals. *Current neuropharmacology* 14(2), pp. 155–64. doi: 10.2174/1570159x14666151204122017.

Cazareth, J. et al. 2014. Molecular and cellular neuroinflammatory status of mouse brain after systemic lipopolysaccharide challenge: importance of CCR2/CCL2 signaling. *Journal of Neuroinflammation* 11(1), p. 132. doi: 10.1186/1742-2094-11-132.

Chen, J. et al. 2008. Neuroinflammation and disruption in working memory in aged mice after acute stimulation of the peripheral innate immune system. *Brain, Behavior, and Immunity* 22(3), pp. 301–311. doi: 10.1016/j.bbi.2007.08.014.

Chen, W.-W. et al. 2016. Role of neuroinflammation in neurodegenerative diseases. *MOLECULAR MEDICINE REPORTS* 13(4), pp. 3391–3396. doi: 10.3892/mmr.2016.4948.

Cho, Y.-E. et al. 2017. Neuronal Cell Death and Degeneration through Increased Nitroxidative Stress and Tau Phosphorylation in HIV-1 Transgenic Rats. Eugenin, E. A. ed. *PLOS ONE* 12(1), p. e0169945. doi: 10.1371/journal.pone.0169945.

Chohan, M.O. et al. 2005. Hyperphosphorylation-induced self assembly of murine tau: a comparison with human tau. *Journal of neural transmission (Vienna, Austria : 1996)* 112(8), pp. 1035–47. doi: 10.1007/s00702-004-0241-9.

Chu, C.-H. et al. 2016. Neurons and astroglia govern microglial endotoxin tolerance through macrophage colony-stimulating factor receptor-mediated ERK1/2 signals. *Brain, behavior, and immunity* 55, pp. 260–72. doi: 10.1016/j.bbi.2016.04.015.

Clavaguera, F. et al. 2009. Transmission and spreading of tauopathy in transgenic mouse brain. *Nature cell biology* 11(7), p. 909. doi: 10.1038/ncb1901.

Clavaguera, F. et al. 2015. Invited review: Prion-like transmission and spreading of tau pathology. *Neuropathology and Applied Neurobiology* 41(1), pp. 47–58. doi: 10.1111/nan.12197.

Colton, C.A. et al. 2006. Expression profiles for macrophage alternative activation genes in AD and in mouse models of AD. *Journal of neuroinflammation* 3(1), p. 27. doi: 10.1186/1742-2094-3-27.

Colton, C.A. et al. 2006. NO synthase 2 (NOS2) deletion promotes multiple pathologies in a mouse model of Alzheimer's disease. *Proceedings of the National Academy of Sciences of the United States of America* 103(34), pp. 12867–72. doi: 10.1073/pnas.0601075103.

Cotrina, M.L. and Nedergaard, M. 2002. Astrocytes in the aging brain. *Journal of Neuroscience Research* 67(1), pp. 1–10. doi: 10.1002/jnr.10121.

Coutinho, A.E. and Chapman, K.E. 2011. The anti-inflammatory and immunosuppressive effects of glucocorticoids, recent developments and mechanistic insights. *Molecular and cellular endocrinology* 335(1), pp. 2–13. doi: 10.1016/j.mce.2010.04.005.

Cowan, C.M. and Mudher, A. 2013. Are tau aggregates toxic or protective in tauopathies? *Frontiers in neurology* 4, p. 114. doi: 10.3389/fneur.2013.00114.

Crespo-Biel, N. et al. 2012. Protein tau: prime cause of synaptic and neuronal degeneration in Alzheimer's disease. *International journal of Alzheimer's disease* 2012, p. 251426. doi: 10.1155/2012/251426.

Cross, D.A.E. et al. 1995. Inhibition of glycogen synthase kinase-3 by insulin mediated by protein kinase B. *Nature* 378(6559), pp. 785–789. doi: 10.1038/378785a0.

Crouch, P.J. et al. 2008. Mechanisms of Aβ mediated neurodegeneration in Alzheimer's disease. *Int J Biochem Cell Biol* 40(2), pp. 181–198. doi: S1357-2725(07)00251-8 [pii] 10.1016/j.biocel.2007.07.013 [doi].

Cunningham, A.F. et al. 2007. Salmonella Induces a Switched Antibody Response without Germinal Centers That Impedes the Extracellular Spread of Infection. *The Journal of Immunology* 178(10)

Cunningham, C. et al. 2005. Central and systemic endotoxin challenges exacerbate the local inflammatory response and increase neuronal death during chronic neurodegeneration. *The Journal of neuroscience : the official journal of the Society for Neuroscience* 25(40), pp. 9275–84. doi: 10.1523/JNEUROSCI.2614-05.2005.

Cunningham, C. and Hennessy, E. 2011. Co-morbidity and systemic inflammation as drivers of cognitive decline: new experimental models adopting a broader paradigm in dementia research. *Research & Therapy* 7. doi: 10.1186/s13195-015-0117-2.

Czapski, G.A. et al. 2016. The mechanisms regulating cyclin-dependent kinase 5 in hippocampus during systemic inflammatory response: The effect on inflammatory gene expression. *Neurochemistry International* 93, pp. 103–112. doi: 10.1016/j.neuint.2016.01.005.

Dantzer, R. 2001. Cytokine-Induced Sickness Behavior: Where Do We Stand? *Brain, Behavior, and Immunity* 15(1), pp. 7–24. doi: 10.1006/brbi.2000.0613.

Dantzer, R. 2009. Cytokine, sickness behavior, and depression. *Immunology and allergy clinics of North America* 29(2), pp. 247–64. doi: 10.1016/j.iac.2009.02.002.

Deacon, R. 2012. Assessing Burrowing, Nest Construction, and Hoarding in Mice. *Journal of Visualized Experiments* (59), p. e2607. doi: 10.3791/2607.

Deacon, R.M.J. 2006. Assessing nest building in mice. *Nature protocols* 1(3), pp. 1117–9. doi: 10.1038/nprot.2006.170.

Deane, R. et al. 2008. The role of the cell surface LRP and soluble LRP in blood-brain barrier Abeta clearance in Alzheimer's disease. *Current pharmaceutical design* 14(16), pp. 1601–5.

Deng, X.-H. et al. 2006. Cytokine-induced activation of glial cells in the mouse brain is enhanced at an advanced age. *Neuroscience* 141(2), pp. 645–661. doi: 10.1016/j.neuroscience.2006.04.016.

DeVos, S.L. et al. 2013. Antisense reduction of tau in adult mice protects against seizures. *The Journal of neuroscience : the official journal of the Society for Neuroscience* 33(31), pp. 12887–97. doi: 10.1523/JNEUROSCI.2107-13.2013.

DiCarlo, G. et al. 2001. Intrahippocampal LPS injections reduce Abeta load in APP+PS1 transgenic mice. *Neurobiology of aging* 22(6), pp. 1007–12.

Dickey, C.A. et al. 2007. The high-affinity HSP90-CHIP complex recognizes and selectively degrades phosphorylated tau client proteins. *The Journal of clinical investigation* 117(3), pp. 648–58. doi: 10.1172/JCI29715.

Dixit, R. et al. 2008. Differential regulation of dynein and kinesin motor proteins by tau. *Science (New York, N.Y.)* 319(5866), pp. 1086–9. doi: 10.1126/science.1152993.

Doens, D. et al. 2014. Microglia receptors and their implications in the response to amyloid β for Alzheimer's disease pathogenesis. *Journal of Neuroinflammation* 11(1), p. 48. doi: 10.1186/1742-2094-11-48.

Doody, R.S. et al. 2014. Phase 3 trials of solanezumab for mild-to-moderate Alzheimer's disease.

The New England journal of medicine 370(4), pp. 311–21. doi: 10.1056/NEJMoa1312889.

Dorshkind, K. and Swain, S. 2009. Age-associated declines in immune system development and function: causes, consequences, and reversal. *Current Opinion in Immunology* 21(4), pp. 404–407. doi: 10.1016/j.coi.2009.07.001.

Doty, K.R. et al. 2015. The role of the immune system in neurodegenerative disorders: Adaptive or maladaptive? *BRAIN RESEARCH* 1617(SI), pp. 155–173. doi: 10.1016/j.brainres.2014.09.008.

Dubois, B. et al. 2014. Advancing research diagnostic criteria for Alzheimer's disease: the IWG-2 criteria. *The Lancet. Neurology* 13(6), pp. 614–29. doi: 10.1016/S1474-4422(14)70090-0.

Dunlap, N.E. et al. 1991. A 'safe-site' for Salmonella typhimurium is within splenic cells during the early phase of infection in mice. *Microbial Pathogenesis* 10(4), pp. 297–310. doi: 10.1016/0882-4010(91)90013-Z.

Dunn, N. et al. 2005. Association between dementia and infectious disease: evidence from a case-control study. *Alzheimer disease and associated disorders* 19(2), pp. 91–4.

Dutta, S. and Sengupta, P. 2016. Men and mice: Relating their ages. *Life Sciences* 152, pp. 244–248. doi: 10.1016/j.lfs.2015.10.025.

Duyckaerts, C. et al. 2008. Alzheimer disease models and human neuropathology: similarities and differences. *Acta neuropathologica* 115(1), pp. 5–38. doi: 10.1007/s00401-007-0312-8.

Edison, P. et al. 2008. Microglia, amyloid, and cognition in Alzheimer's disease: An [11C](R)PK11195-PET and [11C]PIB-PET study. *Neurobiology of Disease* 32(3), pp. 412–419. doi: 10.1016/j.nbd.2008.08.001.

Edwards, J.P. et al. 2006. Biochemical and functional characterization of three activated macrophage populations. *Journal of Leukocyte Biology* 80(6), pp. 1298–1307. doi: 10.1189/jlb.0406249.

Elahy, M. et al. 2015. Blood-brain barrier dysfunction developed during normal aging is associated with inflammation and loss of tight junctions but not with leukocyte recruitment. *Immunity & ageing : I & A* 12(1), p. 2. doi: 10.1186/s12979-015-0029-9.

Elliott, E. et al. 2005. Brain-derived neurotrophic factor induces a rapid dephosphorylation of tau protein through a PI-3Kinase signalling mechanism. *European Journal of Neuroscience* 22(5), pp. 1081–1089. doi: 10.1111/j.1460-9568.2005.04290.x.

Erickson, M.A. and Banks, W.A. 2011. Cytokine and chemokine responses in serum and brain after single and repeated injections of lipopolysaccharide: Multiplex quantification with path analysis. *Brain, Behavior, and Immunity* 25(8), pp. 1637–1648. doi: 10.1016/j.bbi.2011.06.006.

Etienne, S. et al. 1999. MHC class II engagement in brain endothelial cells induces protein kinase A-dependent IL-6 secretion and phosphorylation of cAMP response element-binding protein. *Journal of immunology (Baltimore, Md. : 1950)* 163(7), pp. 3636–41.

Fabricius, K. et al. 2013. Effect of age on neocortical brain cells in 90+ year old human females—a cell counting study. *Neurobiology of Aging* 34(1), pp. 91–99. doi: 10.1016/j.neurobiolaging.2012.06.009.

Fahlström, A. et al. 2011. Behavioral changes in aging female C57BL/6 mice. *Neurobiology of Aging* 32(10), pp. 1868–1880. doi: 10.1016/j.neurobiolaging.2009.11.003.

Farhad, S.Z. et al. 2014. The effect of chronic periodontitis on serum levels of tumor necrosis factor-alpha in Alzheimer disease. *Dental research journal* 11(5), pp. 549–52.

Feinstein, S.C. and Wilson, L. 2005. Inability of tau to properly regulate neuronal microtubule dynamics: a loss-of-function mechanism by which tau might mediate neuronal cell death. *Biochimica et Biophysica Acta (BBA) - Molecular Basis of Disease* 1739(2–3), pp. 268–279. doi: 10.1016/j.bbadis.2004.07.002.

Felten, D.L. et al. 1985. Noradrenergic and peptidergic innervation of lymphoid tissue. *Journal of immunology (Baltimore, Md. : 1950)* 135(2 Suppl), p. 755s–765s.

Fenn, A.M. et al. 2012. Lipopolysaccharide-induced interleukin (IL)-4 receptor-α expression and corresponding sensitivity to the M2 promoting effects of IL-4 are impaired in microglia of aged mice. *Brain, behavior, and immunity* 26(5), pp. 766–77. doi: 10.1016/j.bbi.2011.10.003.

Ferreira, S.T. et al. 2014. Inflammation, defective insulin signaling, and neuronal dysfunction in Alzheimer's disease. *Alzheimer's & Dementia* 10(1), pp. S76–S83. doi: 10.1016/j.jalz.2013.12.010.

Floden, A.M. and Combs, C.K. 2011. Microglia demonstrate age-dependent interaction with amyloid-β fibrils. *Journal of Alzheimer's disease : JAD* 25(2), pp. 279–93. doi: 10.3233/JAD-2011-101014.

Franceschi, C. et al. 2000. Inflamm-aging. An evolutionary perspective on immunosenescence. *Annals of the New York Academy of Sciences* 908, pp. 244–54.

Franceschi, C. and Campisi, J. 2014. Chronic Inflammation (Inflammaging) and Its Potential Contribution to Age-Associated Diseases. *The Journals of Gerontology Series A: Biological Sciences and Medical Sciences* 69(Suppl 1), pp. S4–S9. doi: 10.1093/gerona/glu057.

Frandemiche, M.L. et al. 2014. Activity-dependent tau protein translocation to excitatory synapse is disrupted by exposure to amyloid-beta oligomers. *The Journal of neuroscience : the official journal of the Society for Neuroscience* 34(17), pp. 6084–97. doi: 10.1523/JNEUROSCI.4261-13.2014.

Frank-Cannon, T.C. et al. 2008. Parkin Deficiency Increases Vulnerability to Inflammation-Related Nigral Degeneration. *Journal of Neuroscience* 28(43), pp. 10825–10834.

Frank, M.G., Barrientos, R.M., et al. 2006. mRNA up-regulation of MHC II and pivotal pro-inflammatory genes in normal brain aging. *Neurobiology of Aging* 27(5), pp. 717–722. doi: 10.1016/j.neurobiolaging.2005.03.013.

Frank, M.G., Wieseler-Frank, J.L., et al. 2006. Rapid isolation of highly enriched and quiescent microglia from adult rat hippocampus: Immunophenotypic and functional characteristics. *Journal of Neuroscience Methods* 151(2), pp. 121–130. doi: 10.1016/j.jneumeth.2005.06.026.

Frank, S. et al. 2007. Tauopathy models and human neuropathology: similarities and differences. *Acta Neuropathologica* 115(1), pp. 39–53. doi: 10.1007/s00401-007-0291-9.

Frautschy, S.A. et al. 1998. Microglial response to amyloid plaques in APPsw transgenic mice. *The American journal of pathology* 152(1), pp. 307–17.

del Fresno, C. et al. 2009. Potent Phagocytic Activity with Impaired Antigen Presentation Identifying Lipopolysaccharide-Tolerant Human Monocytes: Demonstration in Isolated Monocytes from Cystic Fibrosis Patients. *The Journal of Immunology* 182(10)

Fuller, J.P. et al. 2015. Comparing the efficacy and neuroinflammatory potential of three anti-abeta antibodies. *Acta Neuropathologica* 130(5), pp. 699–711. doi: 10.1007/s00401-015-1484-2.

Fulop, T. et al. 2016. From inflamm-aging to immune-paralysis: a slippery slope during aging for immune-adaptation. *BIOGERONTOLOGY* 17(1), pp. 147–157. doi: 10.1007/s10522-015-9615-7.

Fulop, T. et al. 2016. THE ROLE OF IMMUNOSENESCENCE IN THE DEVELOPMENT OF AGE-RELATED DISEASES. *REVISTA DE INVESTIGACION CLINICA-CLINICAL AND TRANSLATIONAL INVESTIGATION* 68(2, 2), pp. 84–91.

Fuster-Matanzo, A. et al. 2009. Function of tau protein in adult newborn neurons. *FEBS letters* 583(18), pp. 3063–8. doi: 10.1016/j.febslet.2009.08.017.

Galea, I. et al. 2007. What is immune privilege (not)? *Trends in Immunology* 28(1), pp. 12–18. doi: 10.1016/j.it.2006.11.004.

Games, D. et al. 1995. Alzheimer-type neuropathology in transgenic mice overexpressing V717F β-amyloid precursor protein. *Nature* 373(6514), pp. 523–527. doi: 10.1038/373523a0.

Gardner, L.E. et al. 2016. Imatinib methanesulfonate reduces hyperphosphorylation of tau following repeated peripheral exposure to lipopolysaccharide. *Neuroscience* 331, pp. 72–77. doi: 10.1016/j.neuroscience.2016.06.007.

Gasparotto, J. et al. 2015. Increased tau phosphorylation and receptor for advanced glycation endproducts (RAGE) in the brain of mice infected with Leishmania amazonensis. *Brain, Behavior, and Immunity* 43, pp. 37–45. doi: 10.1016/j.bbi.2014.06.204.

Gauthier, S. et al. 2016. Efficacy and safety of tau-aggregation inhibitor therapy in patients with mild or moderate Alzheimer's disease: a randomised, controlled, double-blind, parallel-arm, phase 3 trial. *The Lancet* 388(10062), pp. 2873–2884. doi: 10.1016/S0140-6736(16)31275-2.

Gautier, E.L. et al. 2012. Gene-expression profiles and transcriptional regulatory pathways that underlie the identity and diversity of mouse tissue macrophages. *Nature Immunology* 13(11), pp. 1118–1128. doi: 10.1038/ni.2419.

Ghosh, S. et al. 2013. Sustained Interleukin-1 Overexpression Exacerbates Tau Pathology Despite Reduced Amyloid Burden in an Alzheimer's Mouse Model. *Journal of Neuroscience* 33(11), pp. 5053–5064. doi: 10.1523/JNEUROSCI.4361-12.2013.

Glabe, C.G. 2006. Common mechanisms of amyloid oligomer pathogenesis in degenerative disease. *Neurobiology of Aging* 27(4), pp. 570–575. doi: 10.1016/j.neurobiolaging.2005.04.017.

Glenner, G.G. et al. 1984. The amyloid deposits in Alzheimer's disease: their nature and pathogenesis. *Applied pathology* 2(6), pp. 357–69.

Godbout, J.P. et al. 2005. Exaggerated neuroinflammation and sickness behavior in aged mice following activation of the peripheral innate immune system. *FASEB journal : official publication of the Federation of American Societies for Experimental Biology* 19(10), pp. 1329–31. doi: 10.1096/fj.05-3776fje.

Goedert, M. et al. 1988. Cloning and sequencing of the cDNA encoding a core protein of the paired helical filament of Alzheimer disease: identification as the microtubule-associated protein tau. *Proceedings of the National Academy of Sciences of the United States of America* 85(11), pp. 4051–5.

Goedert, M. and Spillantini, M.G. 2000. Tau mutations in frontotemporal dementia FTDP-17 and their relevance for Alzheimer's disease. *Biochimica et biophysica acta* 1502(1), pp. 110–21.

Goedert, M. and Spillantini, M.G. 2006. A Century of Alzheimer's Disease. *Science* 314(5800), pp. 777–781. doi: 10.1126/science.1132814.

Goedert, M. and Spillantini, M.G. 2011. Pathogenesis of the tauopathies. *Journal of molecular neuroscience : MN* 45(3), pp. 425–31. doi: 10.1007/s12031-011-9593-4.

Goehler, L.E. et al. 1999. Interleukin-1beta in immune cells of the abdominal vagus nerve: a link between the immune and nervous systems? *The Journal of neuroscience : the official journal of the Society for Neuroscience* 19(7), pp. 2799–806.

Goldmann, E. 1913. *Vitalfärbung am Zentralnervensystem. Beitrag zur Physio-Pathologie des Plexus chorioideus und der Hirnhäute.* Berlin: Königl. Akademie der Wissenschaften.

Gómez-Isla, T. et al. 1997. Neuronal loss correlates with but exceeds neurofibrillary tangles in Alzheimer's disease. *Annals of Neurology* 41(1), pp. 17–24. doi: 10.1002/ana.410410106.

González-Marrero, I. et al. 2015. Choroid plexus dysfunction impairs beta-amyloid clearance in a triple transgenic mouse model of Alzheimer's disease. *Frontiers in cellular neuroscience* 9, p. 17. doi: 10.3389/fncel.2015.00017.

Goodall, E.F. et al. 2017. Age-associated changes in the blood-brain barrier: comparative studies in human and mouse. *Neuropathology and Applied Neurobiology* . doi: 10.1111/nan.12408.

Gordon, S. et al. 2014. Macrophage heterogeneity in tissues: phenotypic diversity and functions. *Immunological Reviews* 262(1), pp. 36–55. doi: 10.1111/imr.12223.

Gorlé, N. et al. 2016. The effect of aging on brain barriers and the consequences for Alzheimer's disease development. *Mammalian Genome* 27(7–8), pp. 407–420. doi: 10.1007/s00335-016-9637-8.

Gotz, J. et al. 2001. Tau Filament Formation in Transgenic Mice Expressing P301L Tau. *Journal of Biological Chemistry* 276(1), pp. 529–534. doi: 10.1074/jbc.M006531200.

Grammas, P. and Ovase, R. 2001. Inflammatory factors are elevated in brain microvessels in Alzheimer's disease. *Neurobiology of aging* 22(6), pp. 837–42.

Grundke-Iqbal, I. et al. 1986. Abnormal phosphorylation of the microtubule-associated protein tau (tau) in Alzheimer cytoskeletal pathology. *Proceedings of the National Academy of Sciences of the United States of America* 83(13), pp. 4913–7.

Gruver, A.L. et al. 2007. Immunosenescence of ageing. *The Journal of pathology* 211(2), pp. 144–56. doi: 10.1002/path.2104.

Guest, J. et al. 2014. Changes in Oxidative Damage, Inflammation and [NAD(H)] with Age in Cerebrospinal Fluid. Arendt, T. ed. *PLoS ONE* 9(1), p. e85335. doi: 10.1371/journal.pone.0085335.

Guillot-Sestier, M.-V. et al. 2015. Il10 Deficiency Rebalances Innate Immunity to Mitigate Alzheimer-Like Pathology. *Neuron* 85(3), pp. 534–548. doi: 10.1016/j.neuron.2014.12.068.

Guo, Q. et al. 2012. APP physiological and pathophysiological functions: insights from animal models. *Cell Research* 22(1), pp. 78–89. doi: 10.1038/cr.2011.116.

Hamo, L. et al. 2007. Distinct regulation of MHC molecule expression on astrocytes and microglia during viral encephalomyelitis. *Glia* 55(11), pp. 1169–77. doi: 10.1002/glia.20538.

Hampel, H. et al. 2009. Lithium trial in Alzheimer's disease: a randomized, single-blind, placebo-controlled, multicenter 10-week study. *The Journal of clinical psychiatry* 70(6), pp. 922–31.

Hanger, D.P. et al. 2009. Tau phosphorylation: the therapeutic challenge for neurodegenerative disease. *Trends in Molecular Medicine* 15(3), pp. 112–119. doi: 10.1016/j.molmed.2009.01.003.

Harada, A. et al. 1994. Altered microtubule organization in small-calibre axons of mice lacking tau protein. *Nature* 369(6480), pp. 488–91. doi: 10.1038/369488a0.

Hardy, J. and Higgins, G. 1992. Alzheimer's disease: the amyloid cascade hypothesis. *Science* 256(5054), pp. 184–185.

Hart, A.D. et al. 2012. Age related changes in microglial phenotype vary between CNS regions: Grey versus white matter differences. *Brain, Behavior, and Immunity* 26(5), pp. 754–765. doi: 10.1016/j.bbi.2011.11.006.

Hart, B.L. 1988. Biological basis of the behavior of sick animals. *Neuroscience and biobehavioral reviews* 12(2), pp. 123–37.

Hattiangady, B. et al. 2005. Brain-derived neurotrophic factor, phosphorylated cyclic AMP response element binding protein and neuropeptide Y decline as early as middle age in the dentate gyrus and CA1 and CA3 subfields of the hippocampus. *Experimental Neurology* 195(2), pp. 353–371. doi: 10.1016/j.expneurol.2005.05.014.

He, P. et al. 2007. Deletion of tumor necrosis factor death receptor inhibits amyloid β generation and prevents learning and memory deficits in Alzheimer's mice. *The Journal of Cell Biology* 178(5), pp. 829–841. doi: 10.1083/jcb.200705042.

Hefendehl, J.K. et al. 2014. Homeostatic and injury-induced microglia behavior in the aging brain. *Aging Cell* 13(1), pp. 60–69. doi: 10.1111/acel.12149.

Heneka, M.T. et al. 2005. Focal glial activation coincides with increased BACE1 activation and precedes amyloid plaque deposition in APP[V717I] transgenic mice. *Journal of Neuroinflammation* 2(1), p. 22. doi: 10.1186/1742-2094-2-22.

Heneka, M.T. et al. 2015. Neuroinflammation in Alzheimer's disease. *The Lancet Neurology* 14(4), pp. 388–405. doi: 10.1016/S1474-4422(15)70016-5.

Henry, C.J. et al. 2008. Minocycline attenuates lipopolysaccharide (LPS)-induced neuroinflammation, sickness behavior, and anhedonia. *Journal of Neuroinflammation* 5(1), p. 15. doi: 10.1186/1742-2094-5-15.

Henry, C.J. et al. 2009. Peripheral lipopolysaccharide (LPS) challenge promotes microglial hyperactivity in aged mice that is associated with exaggerated induction of both pro-inflammatory IL-1β and anti-inflammatory IL-10 cytokines. *Brain, Behavior, and Immunity* 23(3), pp. 309–317. doi: 10.1016/j.bbi.2008.09.002.

Herber, D.L. et al. 2007. Microglial Activation is Required for Aβ Clearance After Intracranial Injection of Lipopolysaccharide in APP Transgenic Mice. *Journal of Neuroimmune Pharmacology* 2(2), pp. 222–231. doi: 10.1007/s11481-007-9069-z.

Hickman, S.E. et al. 2013. The microglial sensome revealed by direct RNA sequencing. *Nature neuroscience* 16(12), pp. 1896–905. doi: 10.1038/nn.3554.

Hoiseth, S.K. and Stocker, B.A. 1981. Aromatic-dependent Salmonella typhimurium are non-virulent and effective as live vaccines. *Nature* 291(5812), pp. 238–9.

Holcomb, L. et al. 1998. Accelerated Alzheimer-type phenotype in transgenic mice carrying both mutant amyloid precursor protein and presenilin 1 transgenes. *Nature medicine* 4(1), pp. 97–100.

Holmes, C. et al. 2009. Systemic inflammation and disease progression in Alzheimer disease. *Neurology* 73(10), pp. 768–774. doi: 10.1212/WNL.0b013e3181b6bb95.

Holmes, C. 2013. Review: Systemic inflammation and Alzheimer's disease. *Neuropathology and Applied Neurobiology* 39(1), pp. 51–68. doi: 10.1111/j.1365-2990.2012.01307.x.

Holtman, I.R. et al. 2015. Induction of a common microglia gene expression signature by aging and neurodegenerative conditions: a co-expression meta-analysis. *Acta neuropathologica communications* 3, p. 31. doi: 10.1186/s40478-015-0203-5.

Hong, X.-P. et al. 2010. Essential role of tau phosphorylation in adult hippocampal neurogenesis. *Hippocampus* 20(12), pp. 1339–1349. doi: 10.1002/hipo.20712.

Hoogland, I.C.M. et al. 2015. Systemic inflammation and microglial activation: systematic review of animal experiments. *Journal of neuroinflammation* 12, p. 114. doi: 10.1186/s12974-015-0332-6.

Hoover, B.R. et al. 2010. Tau mislocalization to dendritic spines mediates synaptic dysfunction independently of neurodegeneration. *Neuron* 68(6), pp. 1067–81. doi: 10.1016/j.neuron.2010.11.030.

Hoozemans, J.J. et al. 2011. Neuroinflammation in Alzheimer's disease wanes with age. *Journal of Neuroinflammation* 8(1), p. 171. doi: 10.1186/1742-2094-8-171.

Hsiao, K. et al. 1996. Correlative Memory Deficits, Aβ Elevation, and Amyloid Plaques in Transgenic Mice. *Science* 274(5284)

Ide, M. et al. 2016. Periodontitis and Cognitive Decline in Alzheimer's Disease. *PloS one* 11(3), p. e0151081. doi: 10.1371/journal.pone.0151081.

Imbimbo, B.P. et al. 2011. Therapeutic intervention for Alzheimer's disease with γ-secretase inhibitors: still a viable option? *Expert Opinion on Investigational Drugs* 20(3), pp. 325–341. doi: 10.1517/13543784.2011.550572.

Iqbal, K. et al. 1998. Mechanisms of neurofibrillary degeneration and the formation of neurofibrillary tangles. *Journal of neural transmission. Supplementum* 53, pp. 169–80.

Iqbal, K. et al. 2008. Cytosolic abnormally hyperphosphorylated tau but not paired helical filaments sequester normal MAPs and inhibit microtubule assembly. *Journal of Alzheimer's disease : JAD* 14(4), pp. 365–70.

Ishii, M. et al. 2014. Transgenic mice overexpressing amyloid precursor protein exhibit early metabolic deficits and a pathologically low leptin state associated with hypothalamic dysfunction in arcuate neuropeptide Y neurons. *The Journal of neuroscience : the official journal of the Society for Neuroscience* 34(27), pp. 9096–106. doi: 10.1523/JNEUROSCI.0872-14.2014.

Ishii, M. and Iadecola, C. 2015. Metabolic and Non-Cognitive Manifestations of Alzheimer's Disease: The Hypothalamus as Both Culprit and Target of Pathology. *Cell Metabolism* 22(5), pp. 761–776. doi: 10.1016/j.cmet.2015.08.016.

Itagaki, S. et al. 1989. Relationship of microglia and astrocytes to amyloid deposits of Alzheimer disease. *Journal of neuroimmunology* 24(3), pp. 173–82.

Ittner, L.M. et al. 2009. Phosphorylated Tau Interacts with c-Jun N-terminal Kinase-interacting Protein 1 (JIP1) in Alzheimer Disease. *Journal of Biological Chemistry* 284(31), pp. 20909–20916. doi: 10.1074/jbc.M109.014472.

Ittner, L.M. et al. 2010. Dendritic Function of Tau Mediates Amyloid-β Toxicity in Alzheimer's Disease Mouse Models. *Cell* 142(3), pp. 387–397. doi: 10.1016/j.cell.2010.06.036.

Jackson, A. et al. 2010. Innate immune activation during Salmonella infection initiates extramedullary erythropoiesis and splenomegaly. *Journal of immunology (Baltimore, Md. : 1950)* 185(10), pp. 6198–204. doi: 10.4049/jimmunol.1001198.

Jaeger, L.B. et al. 2009. Lipopolysaccharide alters the blood-brain barrier transport of amyloid beta protein: a mechanism for inflammation in the progression of Alzheimer's disease. *Brain, behavior, and immunity* 23(4), pp. 507–17. doi: 10.1016/j.bbi.2009.01.017.

Jain, N.K. et al. 2002. Modulatory role of cyclooxygenase inhibitors in aging- and scopolamine or lipopolysaccharide-induced cognitive dysfunction in mice. *Behavioural brain research* 133(2), pp. 369–76.

Jho, Y.S. et al. 2010. Monte Carlo Simulations of Tau Proteins: Effect of Phosphorylation. *Biophysical Journal* 99(8), pp. 2387–2397. doi: 10.1016/j.bpj.2010.06.056.

Jin, M. et al. 2011. Soluble amyloid beta-protein dimers isolated from Alzheimer cortex directly induce Tau hyperphosphorylation and neuritic degeneration. *Proceedings of the National Academy of Sciences of the United States of America* 108(14), pp. 5819–24. doi: 10.1073/pnas.1017033108.

Kang, S.-C. et al. 2004. Are the immune responses different in middle-aged and young mice

following bone fracture, tissue trauma and hemorrhage? *Cytokine* 26(5), pp. 223–230. doi: 10.1016/j.cyto.2004.03.005.

Karran, E. and De Strooper, B. 2016. The amyloid cascade hypothesis: are we poised for success or failure? *Journal of Neurochemistry* 139, pp. 237–252. doi: 10.1111/jnc.13632.

Kawarabayashi, T. et al. 2001. Age-dependent changes in brain, CSF, and plasma amyloid (beta) protein in the Tg2576 transgenic mouse model of Alzheimer's disease. *The Journal of neuroscience : the official journal of the Society for Neuroscience* 21(2), pp. 372–81.

Kayed, R. and Lasagna-Reeves, C.A. 2012. Molecular mechanisms of amyloid oligomers toxicity. *Advances in Alzheimer's Disease* 3, pp. 67–78. doi: 10.3233/978-1-61499-154-0-67.

Keren-Shaul, H. et al. 2017. A Unique Microglia Type Associated with Restricting Development of Alzheimer's Disease. *Cell* 169(7), p. 1276–1290.e17. doi: 10.1016/j.cell.2017.05.018.

Khanna, M.R. et al. 2016. Therapeutic strategies for the treatment of tauopathies: Hopes and challenges. *Alzheimer's and Dementia* 12(10), pp. 1051–1065. doi: 10.1016/j.jalz.2016.06.006.

Kimura, T. et al. 2014. Microtubule-associated protein tau is essential for long-term depression in the hippocampus. *Philosophical transactions of the Royal Society of London. Series B, Biological sciences* 369(1633), p. 20130144. doi: 10.1098/rstb.2013.0144.

Kinsey, S.G. et al. 2008. The inflammatory response to social defeat is increased in older mice. *Physiology & behavior* 93(3), pp. 628–36. doi: 10.1016/j.physbeh.2007.11.003.

Kitazawa, M. et al. 2005. Lipopolysaccharide-Induced Inflammation Exacerbates Tau Pathology by a Cyclin-Dependent Kinase 5-Mediated Pathway in a Transgenic Model of Alzheimer's Disease. *Journal of Neuroscience* 25(39), pp. 8843–8853. doi: 10.1523/JNEUROSCI.2868-05.2005.

Kitazawa, M. et al. 2011. Blocking IL-1 signaling rescues cognition, attenuates tau pathology, and restores neuronal β-catenin pathway function in an Alzheimer's disease model. *Journal of immunology (Baltimore, Md. : 1950)* 187(12), pp. 6539–49. doi: 10.4049/jimmunol.1100620.

Kluger, M.J. and Rothenburg, B.A. 1979. Fever and reduced iron: their interaction as a host defense response to bacterial infection. *Science (New York, N.Y.)* 203(4378), pp. 374–6.

Knops, J. et al. 1991. Overexpression of tau in a nonneuronal cell induces long cellular processes. *The Journal of cell biology* 114(4), pp. 725–33.

Knuesel, I. et al. 2009. Age-related accumulation of Reelin in amyloid-like deposits. *Neurobiology*

of Aging 30(5), pp. 697–716. doi: 10.1016/j.neurobiolaging.2007.08.011.

Koike, M.A. et al. 2012. APP knockout mice experience acute mortality as the result of ischemia. Di Giovanni, S. ed. *PloS one* 7(8), p. e42665. doi: 10.1371/journal.pone.0042665.

Komulainen, P. et al. 2007. Serum high sensitivity C-reactive protein and cognitive function in elderly women. *Age and Ageing* 36(4), pp. 443–448. doi: 10.1093/ageing/afm051.

Korzhevskii, D.E. and Kirik, O. V. 2016. Brain Microglia and Microglial Markers. *Neuroscience and Behavioral Physiology* 46(3), pp. 284–290. doi: 10.1007/s11055-016-0231-z.

Kosik, K.S. et al. 1989. Developmentally regulated expression of specific tau sequences. *Neuron* 2(4), pp. 1389–1397. doi: 10.1016/0896-6273(89)90077-9.

Kovacs, G.G. et al. 2013. Neuropathology of the hippocampus in FTLD-Tau with Pick bodies: a study of the BrainNet Europe Consortium. *Neuropathology and Applied Neurobiology* 39(2), pp. 166–178. doi: 10.1111/j.1365-2990.2012.01272.x.

Krabbe, G. et al. 2013. Functional Impairment of Microglia Coincides with Beta-Amyloid Deposition in Mice with Alzheimer-Like Pathology. Priller, J. ed. *PLoS ONE* 8(4), p. e60921. doi: 10.1371/journal.pone.0060921.

Kress, B.T. et al. 2014. Impairment of paravascular clearance pathways in the aging brain. *Annals of Neurology* 76(6), pp. 845–861. doi: 10.1002/ana.24271.

Krstic, D. et al. 2012. Systemic immune challenges trigger and drive Alzheimer-like neuropathology in mice. *Journal of Neuroinflammation* 9

Krstic, D. and Knuesel, I. 2012. Deciphering the mechanism underlying late-onset Alzheimer disease. *Nature Reviews Neurology* 9(1), pp. 25–34. doi: 10.1038/nrneurol.2012.236.

Krstic, D. and Knuesel, I. 2013. The airbag problem-a potential culprit for bench-to-bedside translational efforts: relevance for Alzheimer's disease. *Acta neuropathologica communications* 1(1), p. 62. doi: 10.1186/2051-5960-1-62.

Ksiezak-Reding, H. et al. 1992. Phosphate analysis and dephosphorylation of modified tau associated with paired helical filaments. *Brain research* 597(2), pp. 209–19.

Kuchibhotla, K. V. et al. 2009. Synchronous Hyperactivity and Intercellular Calcium Waves in Astrocytes in Alzheimer Mice. *Science* 323(5918)

Kukull, W.A. et al. 2002. Dementia and Alzheimer disease incidence: a prospective cohort study. *Archives of neurology* 59(11), pp. 1737–46.

Kumar, D.K.V. et al. 2016. Amyloid-β peptide protects against microbial infection in mouse and worm models of Alzheimer's disease. *Science Translational Medicine* 8(340)

Kummer, M.P. et al. 2011. Nitration of tyrosine 10 critically enhances amyloid β aggregation and plaque formation. *Neuron* 71(5), pp. 833–44. doi: 10.1016/j.neuron.2011.07.001.

Kurnellas, M.P. et al. 2013. Amyloid fibrils composed of hexameric peptides attenuate neuroinflammation. *Science translational medicine* 5(179), p. 179ra42. doi: 10.1126/scitranslmed.3005681.

Lalo, U. et al. 2014. Exocytosis of gliotransmitters from cortical astrocytes: implications for synaptic plasticity and aging. *Biochemical Society Transactions* 42(5), pp. 1275–1281. doi: 10.1042/BST20140163.

Lauro, C. et al. 2015. Fractalkine in the nervous system: neuroprotective or neurotoxic molecule? *Annals of the New York Academy of Sciences* 1351(1), pp. 141–148. doi: 10.1111/nyas.12805.

Lawson, L.J. et al. 1992. Turnover of resident microglia in the normal adult mouse brain. *Neuroscience* 48(2), pp. 405–15.

Lee, D.C. et al. 2010. LPS- induced inflammation exacerbates phospho-tau pathology in rTg4510 mice. *Journal of Neuroinflammation* 7(1), p. 56. doi: 10.1186/1742-2094-7-56.

Lee, G. et al. 1998. Tau interacts with src-family non-receptor tyrosine kinases. *Journal of Cell Science* 111(21)

Lee, J. et al. 2008. Neuro-inflammation induced by lipopolysaccharide causes cognitive impairment through enhancement of beta-amyloid generation. *Journal of Neuroinflammation* 5(1), p. 37. doi: 10.1186/1742-2094-5-37.

Lefebvre, T. et al. 2003. Evidence of a balance between phosphorylation and O-GlcNAc glycosylation of Tau proteins—a role in nuclear localization. *Biochimica et Biophysica Acta (BBA) - General Subjects* 1619(2), pp. 167–176. doi: 10.1016/S0304-4165(02)00477-4.

Lei, P. et al. 2012. Tau deficiency induces parkinsonism with dementia by impairing APP-mediated iron export. *Nature medicine* 18(2), pp. 291–5. doi: 10.1038/nm.2613.

Lepekhin, E.A. et al. 2001. Intermediate filaments regulate astrocyte motility. *Journal of*

neurochemistry 79(3), pp. 617–25.

Lesne, S. et al. 2005. NMDA Receptor Activation Inhibits -Secretase and Promotes Neuronal Amyloid- Production. *Journal of Neuroscience* 25(41), pp. 9367–9377. doi: 10.1523/JNEUROSCI.0849-05.2005.

Lewis, J. et al. 2001. Enhanced neurofibrillary degeneration in transgenic mice expressing mutant tau and APP. *Science (New York, N.Y.)* 293(5534), pp. 1487–91. doi: 10.1126/science.1058189.

Li, Y. et al. 2003. Interleukin-1 mediates pathological effects of microglia on tau phosphorylation and on synaptophysin synthesis in cortical neurons through a p38-MAPK pathway. *The Journal of neuroscience : the official journal of the Society for Neuroscience* 23(5), pp. 1605–11. doi: 23/5/1605 [pii].

Lim, S.L. et al. 2015. Infection, systemic inflammation, and Alzheimer's disease. *Microbes and Infection* 17(8), pp. 549–556. doi: 10.1016/j.micinf.2015.04.004.

Lindsay, J. et al. 2002. Risk factors for Alzheimer's disease: a prospective analysis from the Canadian Study of Health and Aging. *American journal of epidemiology* 156(5), pp. 445–53.

Little, C.S. et al. 2004. Chlamydia pneumoniae induces Alzheimer-like amyloid plaques in brains of BALB/c mice. *Neurobiology of Aging* 25(4), pp. 419–429. doi: 10.1016/S0197-4580(03)00127-1.

Liu-Seifert, H. et al. 2015. Delayed-start analysis: Mild Alzheimer's disease patients in solanezumab trials, 3.5 years. *Alzheimer's and Dementia: Translational Research and Clinical Interventions* 1(2), pp. 111–121. doi: 10.1016/j.trci.2015.06.006.

Liu, J. et al. 2016. Suppression of LPS-induced tau hyperphosphorylation by serum amyloid A. *Journal of Neuroinflammation* 13(1), p. 28. doi: 10.1186/s12974-016-0493-y.

Liu, R. et al. 2003. Reversal of age-related learning deficits and brain oxidative stress in mice with superoxide dismutase/catalase mimetics. *Proceedings of the National Academy of Sciences of the United States of America* 100(14), pp. 8526–31. doi: 10.1073/pnas.1332809100.

Llorens-Martin, M. et al. 2012. Tau Isoform with Three Microtubule Binding Domains is a Marker of New Axons Generated from the Subgranular Zone in the Hippocampal Dentate Gyrus: Implications for Alzheimer's Disease. *Journal of Alzheimer's Disease* 29(4), pp. 921–930. doi: 10.3233/JAD-2012-112057.

Lloret, A. et al. 2015. Molecular mechanisms linking amyloid β toxicity and Tau

hyperphosphorylation in Alzheimers disease. *Free Radical Biology and Medicine* 83, pp. 186–191. doi: 10.1016/j.freeradbiomed.2015.02.028.

López-González, I. et al. 2015. Neuroinflammatory Signals in Alzheimer Disease and APP/PS1 Transgenic Mice. *Journal of Neuropathology & Experimental Neurology* 74(4), pp. 319–344. doi: 10.1097/NEN.0000000000000176.

Lopez Gonzalez, I. et al. 2016. Genetic and transcriptomic profiles of inflammation in neurodegenerative diseases: Alzheimer, Parkinson, Creutzfeldt-Jakob and Tauopathies. *International Journal of Molecular Sciences* 17(2), pp. 1–23. doi: 10.3390/ijms17020206.

Lovestone, S. et al. 2015. A phase II trial of tideglusib in Alzheimer's disease. *Journal of Alzheimer's disease : JAD* 45(1), pp. 75–88. doi: 10.3233/JAD-141959.

Lovestone, S. and Reynolds, C.H. 1997. The phosphorylation of tau: a critical stage in neurodevelopment and neurodegenerative processes. *Neuroscience* 78(2), pp. 309–24.

Lu, Y.C. et al. 2008. LPS/TLR4 signal transduction pathway. *Cytokine* 42(2), pp. 145–151. doi: 10.1016/j.cyto.2008.01.006.

Lucas, J.J. et al. 2001. Decreased nuclear beta-catenin, tau hyperphosphorylation and neurodegeneration in GSK-3beta conditional transgenic mice. *The EMBO journal* 20(1–2), pp. 27–39. doi: 10.1093/emboj/20.1.27.

Lue, L.F. et al. 1996. Inflammation, A beta deposition, and neurofibrillary tangle formation as correlates of Alzheimer's disease neurodegeneration. *Journal of neuropathology and experimental neurology* 55(10), pp. 1083–8.

Lull, M.E. and Block, M.L. 2010. Microglial activation and chronic neurodegeneration. *Neurotherapeutics : the journal of the American Society for Experimental NeuroTherapeutics* 7(4), pp. 354–65. doi: 10.1016/j.nurt.2010.05.014.

Lunnon, K. and Mill, J. 2013. Epigenetic studies in Alzheimer's disease: current findings, caveats, and considerations for future studies. *Am J Med Genet B Neuropsychiatr Genet* 162b(8), pp. 789–799. doi: 10.1002/ajmg.b.32201.

Lynch, M.A. 2009. The Multifaceted Profile of Activated Microglia. *Molecular Neurobiology* 40(2), pp. 139–156. doi: 10.1007/s12035-009-8077-9.

Maarouf, C.L. et al. 2011. Alzheimer's disease and non-demented high pathology control

nonagenarians: comparing and contrasting the biochemistry of cognitively successful aging. Mattson, M. P. ed. *PloS one* 6(11), p. e27291. doi: 10.1371/journal.pone.0027291.

Maesako, M. et al. 2012. Environmental enrichment ameliorated high-fat diet-induced Aβ deposition and memory deficit in APP transgenic mice. *Neurobiology of Aging* 33(5), p. 1011.e11-1011.e23. doi: 10.1016/j.neurobiolaging.2011.10.028.

Maher, F.O. et al. 2005. Downregulation of IL-4-induced signalling in hippocampus contributes to deficits in LTP in the aged rat. *Neurobiology of Aging* 26(5), pp. 717–728. doi: 10.1016/j.neurobiolaging.2004.07.002.

Mai, J. et al. 2013. An evolving new paradigm: endothelial cells--conditional innate immune cells. *Journal of hematology & oncology* 6, p. 61. doi: 10.1186/1756-8722-6-61.

Malik, M. et al. 2015. Genetics ignite focus on microglial inflammation in Alzheimer's disease. *Molecular Neurodegeneration* 10(1), p. 52. doi: 10.1186/s13024-015-0048-1.

Maloney, J.A. et al. 2014. Molecular mechanisms of Alzheimer disease protection by the A673T allele of amyloid precursor protein. *Journal of Biological Chemistry* 289(45), pp. 30990–31000. doi: 10.1074/jbc.M114.589069.

Mandelkow, E.-M. et al. 2003. Clogging of axons by tau, inhibition of axonal traffic and starvation of synapses. *Neurobiology of aging* 24(8), pp. 1079–85.

Mantovani, A. et al. 2004. The chemokine system in diverse forms of macrophage activation and polarization. *Trends in immunology* 25(12), pp. 677–86. doi: 10.1016/j.it.2004.09.015.

Maragakis, N.J. and Rothstein, J.D. 2004. Glutamate transporters: animal models to neurologic disease. *Neurobiology of Disease* 15(3), pp. 461–473. doi: 10.1016/j.nbd.2003.12.007.

Marchesi, V.T. 2011. Alzheimer's dementia begins as a disease of small blood vessels, damaged by oxidative-induced inflammation and dysregulated amyloid metabolism: implications for early detection and therapy. *FASEB journal : official publication of the Federation of American Societies for Experimental Biology* 25(1), pp. 5–13. doi: 10.1096/fj.11-0102ufm.

Markesbery, W.R. 1999. The role of oxidative stress in Alzheimer disease. *Archives of neurology* 56(12), pp. 1449–52.

Marsh, S.E. et al. 2016. The adaptive immune system restrains Alzheimer's disease pathogenesis by modulating microglial function. *Proceedings of the National Academy of Sciences of the United*

States of America 113(9), pp. E1316-25. doi: 10.1073/pnas.1525466113.

Martin, L. et al. 2011. Post-translational modifications of tau protein: Implications for Alzheimer's disease. *Neurochemistry International* 58(4), pp. 458–471. doi: 10.1016/j.neuint.2010.12.023.

Martin, L. et al. 2013. Tau protein kinases: Involvement in Alzheimer's disease. *Ageing Research Reviews* 12(1), pp. 289–309. doi: 10.1016/j.arr.2012.06.003.

Masliah, E. et al. 2000. Abnormal Glutamate Transport Function in Mutant Amyloid Precursor Protein Transgenic Mice. *Experimental Neurology* 163(2), pp. 381–387. doi: 10.1006/exnr.2000.7386.

Mattson, M.P. and Magnus, T. 2006. Ageing and neuronal vulnerability. *Nature reviews. Neuroscience* 7(4), pp. 278–94. doi: 10.1038/nrn1886.

McCandless, E.E. et al. 2006. CXCL12 limits inflammation by localizing mononuclear infiltrates to the perivascular space during experimental autoimmune encephalomyelitis. *Journal of immunology (Baltimore, Md. : 1950)* 177(11), pp. 8053–64.

McGeer, P.L. et al. 1996. Arthritis and anti-inflammatory agents as possible protective factors for Alzheimer's disease: a review of 17 epidemiologic studies. *Neurology* 47(2), pp. 425–32.

McManus, R.M. et al. 2015. T Cells—Protective or Pathogenic in Alzheimer's Disease? *Journal of Neuroimmune Pharmacology* 10(4), pp. 547–560. doi: 10.1007/s11481-015-9612-2.

McManus, R.M. and Heneka, M.T. 2017. Role of neuroinflammation in neurodegeneration: new insights. *Alzheimer's Research & Therapy* 9(1), p. 14. doi: 10.1186/s13195-017-0241-2.

McSorley, S.J. and Jenkins, M.K. 2000. Antibody is required for protection against virulent but not attenuated Salmonella enterica serovar typhimurium. *Infection and immunity* 68(6), pp. 3344–8.

Medawar, P.B. 1948. Immunity to homologous grafted skin; the fate of skin homografts transplanted to the brain, to subcutaneous tissue, and to the anterior chamber of the eye. *British journal of experimental pathology* 29(1), pp. 58–69.

Medina, M. and Wandosell, F. 2011. Deconstructing GSK-3: The Fine Regulation of Its Activity. *International journal of Alzheimer's disease* 2011, p. 479249. doi: 10.4061/2011/479249.

Meyer, U. et al. 2006. The Time of Prenatal Immune Challenge Determines the Specificity of Inflammation-Mediated Brain and Behavioral Pathology. *Journal of Neuroscience* 26(18), pp. 4752–4762. doi: 10.1523/JNEUROSCI.0099-06.2006.

Meyer, U. et al. 2008. Relative Prenatal and Postnatal Maternal Contributions to Schizophrenia-Related Neurochemical Dysfunction after In Utero Immune Challenge. *Neuropsychopharmacology* 33(2), pp. 441–456. doi: 10.1038/sj.npp.1301413.

Middeldorp, J. et al. 2016. Preclinical Assessment of Young Blood Plasma for Alzheimer Disease. *JAMA Neurology* 73(11), p. 1325. doi: 10.1001/jamaneurol.2016.3185.

Miller, A.A. and Spencer, S.J. 2014. Obesity and neuroinflammation: A pathway to cognitive impairment. *Brain, Behavior, and Immunity* 42, pp. 10–21. doi: 10.1016/j.bbi.2014.04.001.

Minett, T. et al. 2016. Microglial immunophenotype in dementia with Alzheimer's pathology. *Journal of Neuroinflammation* 13(1), p. 135. doi: 10.1186/s12974-016-0601-z.

Mittelbronn, M. et al. 2001. Local distribution of microglia in the normal adult human central nervous system differs by up to one order of magnitude. *Acta neuropathologica* 101(3), pp. 249–55.

Mittrucker, H.W. and Kaufmann, S.H. 2000. Immune response to infection with Salmonella typhimurium in mice. *J Leukoc Biol* 67(4), pp. 457–463.

Mizuno, Y. et al. 2003. Th1 and Th1-inducing cytokines in Salmonella infection. *Clinical and experimental immunology* 131(1), pp. 111–7. doi: 10.1046/J.1365-2249.2003.02060.X.

Mondragón-Rodríguez, S. et al. 2014. Phosphorylation of tau protein at sites Ser $^{396\text{-}404}$ is one of the earliest events in Alzheimer's disease and Down syndrome. *Neuropathology and Applied Neurobiology* 40(2), pp. 121–135. doi: 10.1111/nan.12084.

Montagne, A. et al. 2015. Blood-Brain Barrier Breakdown in the Aging Human Hippocampus. *Neuron* 85(2), pp. 296–302. doi: 10.1016/j.neuron.2014.12.032.

Montgomery, S.L. et al. 2011. Ablation of TNF-RI/RII expression in Alzheimer's disease mice leads to an unexpected enhancement of pathology: implications for chronic pan-TNF-α suppressive therapeutic strategies in the brain. *The American journal of pathology* 179(4), pp. 2053–70. doi: 10.1016/j.ajpath.2011.07.001.

Moreth, J. et al. 2013. Passive anti-amyloid immunotherapy in Alzheimer's disease: What are the most promising targets? *Immunity and Ageing* 10(1). doi: 10.1186/1742-4933-10-18.

Morris, M. et al. 2011. The Many Faces of Tau. *Neuron* 70(3), pp. 410–426. doi: 10.1016/j.neuron.2011.04.009.

Morris, M. et al. 2015. Tau post-translational modifications in wild-type and human amyloid precursor protein transgenic mice. *Nature Neuroscience* 18(8), pp. 1183–1189. doi: 10.1038/nn.4067.

Mouton, P.R. et al. 2002. Age and gender effects on microglia and astrocyte numbers in brains of mice. *Brain research* 956(1), pp. 30–5.

Mouton, P.R. et al. 2012. The effects of age and lipopolysaccharide (LPS)-mediated peripheral inflammation on numbers of central catecholaminergic neurons. *Neurobiology of aging* 33(2), p. 423.e27-36. doi: 10.1016/j.neurobiolaging.2010.09.025.

Muniz-Junqueira, M.I. et al. 1997. Factors influencing phagocytosis of Salmonella typhimurium by macrophages in murine schistosomiasis. *Revista da Sociedade Brasileira de Medicina Tropical* 30(2), pp. 101–106. doi: 10.1590/S0037-86821997000200003.

Murinello, S. et al. 2014. Fcγ receptor upregulation is associated with immune complex inflammation in the mouse retina and early age-related macular degeneration. *Investigative ophthalmology & visual science* 55(1), pp. 247–58. doi: 10.1167/iovs.13-11821.

Murray, M.E. et al. 2014. Clinicopathologic assessment and imaging of tauopathies in neurodegenerative dementias. *Alzheimer's Research & Therapy* 6(1), p. 1. doi: 10.1186/alzrt231.

Nadeau, S. and Rivest, S. 2000. Role of microglial-derived tumor necrosis factor in mediating CD14 transcription and nuclear factor kappa B activity in the brain during endotoxemia. *The Journal of neuroscience : the official journal of the Society for Neuroscience* 20(9), pp. 3456–68.

Nagele, R.G. et al. 2004. Contribution of glial cells to the development of amyloid plaques in Alzheimer's disease. *Neurobiology of Aging* 25(5), pp. 663–674. doi: 10.1016/j.neurobiolaging.2004.01.007.

Nash, K.R. et al. 2013. Fractalkine overexpression suppresses tau pathology in a mouse model of tauopathy. *Neurobiology of Aging* 34(6), pp. 1540–1548. doi: 10.1016/j.neurobiolaging.2012.12.011.

Nauciel, C. and Espinasse-Maes, F. 1992. Role of gamma interferon and tumor necrosis factor alpha in resistance to Salmonella typhimurium infection. *Infection and immunity* 60(2), pp. 450–4.

Newman, A.B. et al. 2005. Dementia and Alzheimer's Disease Incidence in Relationship to Cardiovascular Disease in the Cardiovascular Health Study Cohort. *Journal of the American Geriatrics Society* 53(7), pp. 1101–1107. doi: 10.1111/j.1532-5415.2005.53360.x.

Niccoli, T. and Partridge, L. 2012. Ageing as a Risk Factor for Disease. *Current Biology* 22(17), pp. R741–R752. doi: 10.1016/j.cub.2012.07.024.

Niederkorn, J.Y. 2006. See no evil, hear no evil, do no evil: the lessons of immune privilege. *Nature immunology* 7(4), pp. 354–9. doi: 10.1038/ni1328.

Nikodemova, M. et al. 2016. Age-dependent differences in microglial responses to systemic inflammation are evident as early as middle age. *Physiological Genomics* (19), p. physiolgenomics.00129.2015. doi: 10.1152/physiolgenomics.00129.2015.

Nimmerjahn, A. et al. 2005. Resting Microglial Cells Are Highly Dynamic Surveillants of Brain Parenchyma in Vivo. *Science* 308(5726)

Nimmerjahn, F. and Ravetch, J. V 2005. Divergent Immunoglobulin G Subclass Activity Through Selective Fc Receptor Binding. *Science* 310(5753), pp. 1510–1512. doi: 10.1126/science.1118948.

Niraula, A. et al. 2016. Microglia Priming with Aging and Stress. *Neuropsychopharmacology* (May), pp. 1–16. doi: 10.1038/npp.2016.185.

Njie, eMalick G. et al. 2012. Ex vivo cultures of microglia from young and aged rodent brain reveal age-related changes in microglial function. *Neurobiology of Aging* 33(1), p. 195.e1-195.e12. doi: 10.1016/j.neurobiolaging.2010.05.008.

Noble, W. et al. 2003. Cdk5 is a key factor in tau aggregation and tangle formation in vivo. *Neuron* 38(4), pp. 555–65.

Noble, W. et al. 2005. Inhibition of glycogen synthase kinase-3 by lithium correlates with reduced tauopathy and degeneration in vivo. *Proceedings of the National Academy of Sciences of the United States of America* 102(19), pp. 6990–5. doi: 10.1073/pnas.0500466102.

Noble, W. et al. 2013. The Importance of Tau Phosphorylation for Neurodegenerative Diseases. *Frontiers in Neurology* 4, p. 83. doi: 10.3389/fneur.2013.00083.

Noda-Saita, K. et al. 2004. Exclusive association and simultaneous appearance of congophilic plaques and AT8-positive dystrophic neurites in Tg2576 mice suggest a mechanism of senile plaque formation and progression of neuritic dystrophy in Alzheimer?s disease. *Acta Neuropathologica* 108(5), pp. 435–442. doi: 10.1007/s00401-004-0907-2.

Nolan, Y. et al. 2005. Role of Interleukin-4 in Regulation of Age-related Inflammatory Changes in the Hippocampus. *Journal of Biological Chemistry* 280(10), pp. 9354–9362. doi:

10.1074/jbc.M412170200.

Oakley, H. et al. 2006. Intraneuronal beta-Amyloid Aggregates, Neurodegeneration, and Neuron Loss in Transgenic Mice with Five Familial Alzheimer's Disease Mutations: Potential Factors in Amyloid Plaque Formation. *Journal of Neuroscience* 26(40), pp. 10129–10140. doi: 10.1523/JNEUROSCI.1202-06.2006.

Oddo, S. et al. 2003. Triple-transgenic model of Alzheimer's disease with plaques and tangles: intracellular Abeta and synaptic dysfunction. *Neuron* 39(3), pp. 409–21.

Office for National Statistics 2015. Population Estimates for UK, England and Wales, Scotland and Northern Ireland, Mid-2014 - ONS. Available at: https://www.ons.gov.uk/peoplepopulationandcommunity/populationandmigration/populationestimates/bulletins/annualmidyearpopulationestimates/2015-06-25 [Accessed: 5 June 2017].

Ogawa, H. et al. 2003. Mechanisms of endotoxin tolerance in human intestinal microvascular endothelial cells. *Journal of immunology (Baltimore, Md. : 1950)* 170(12), pp. 5956–64.

Ohkubo, N. et al. 2002. Apolipoprotein E and Reelin ligands modulate tau phosphorylation through an Apolipoprotein E receptor/diables-1/glycogen synthase kinase-3beta cascade. *The FASEB Journal* 17(2), pp. 295–7. doi: 10.1096/fj.02-0434fje.

Orihuela, R. et al. 2016. Microglial M1/M2 polarization and metabolic states. *British Journal of Pharmacology* 173(4), pp. 649–665. doi: 10.1111/bph.13139.

Otth, C. et al. 2002. AbetaPP induces cdk5-dependent tau hyperphosphorylation in transgenic mice Tg2576. *Journal of Alzheimer's Disease* 4(5), pp. 417–430.

Owen, J.B. et al. 2009. Proteomics-Determined Differences in the Concanavalin-A-Fractionated Proteome of Hippocampus and Inferior Parietal Lobule in Subjects with Alzheimer's Disease and Mild Cognitive Impairment: Implications for Progression of AD. *Journal of Proteome Research* 8(2), pp. 471–482. doi: 10.1021/pr800667a.

Palygin, O. et al. 2010. Ionotropic NMDA and P2X1/5 receptors mediate synaptically induced Ca2+ signalling in cortical astrocytes. *Cell Calcium* 48(4), pp. 225–231. doi: 10.1016/j.ceca.2010.09.004.

Pan, W. et al. 1997. Permeability of the blood-brain and blood-spinal cord barriers to interferons. *Journal of neuroimmunology* 76(1–2), pp. 105–11.

Panza, F. et al. 2016. Tau-Centric Targets and Drugs in Clinical Development for the Treatment of

Alzheimer's Disease. *Biomed Res Int* 2016, p. 3245935. doi: 10.1155/2016/3245935.

Pardon, M.C. 2015. Lipopolysaccharide hyporesponsiveness: Protective or damaging response to the brain? *Romanian Journal of Morphology and Embryology* 56(3), pp. 903–913.

Paresce, D.M. et al. 1996. Microglial cells internalize aggregates of the Alzheimer's disease amyloid beta-protein via a scavenger receptor. *Neuron* 17(3), pp. 553–65.

Pei, J.J. et al. 1998. Accumulation of cyclin-dependent kinase 5 (cdk5) in neurons with early stages of Alzheimer's disease neurofibrillary degeneration. *Brain research* 797(2), pp. 267–77.

Pei, J.J. et al. 1999. Distribution of active glycogen synthase kinase 3beta (GSK-3beta) in brains staged for Alzheimer disease neurofibrillary changes. *Journal of neuropathology and experimental neurology* 58(9), pp. 1010–9.

Pelvig, D.P. et al. 2008. Neocortical glial cell numbers in human brains. *Neurobiology of Aging* 29(11), pp. 1754–1762. doi: 10.1016/j.neurobiolaging.2007.04.013.

Pensalfini, A. et al. 2014. Intracellular amyloid and the neuronal origin of Alzheimer neuritic plaques. *Neurobiology of Disease* 71, pp. 53–61. doi: 10.1016/j.nbd.2014.07.011.

Peppiatt, C.M. et al. 2006. Bidirectional control of CNS capillary diameter by pericytes. *Nature* 443(7112), pp. 700–704. doi: 10.1038/nature05193.

Peress, N.S. et al. 1993. Identification of Fc gamma RI, II and III on normal human brain ramified microglia and on microglia in senile plaques in Alzheimer's disease. *Journal of neuroimmunology* 48(1), pp. 71–9.

Perlmutter, L.S. et al. 1992. MHC class II-positive microglia in human brain: Association with alzheimer lesions. *Journal of Neuroscience Research* 33(4), pp. 549–558. doi: 10.1002/jnr.490330407.

Perry, B. and Wang, Y. 2012. Appetite regulation and weight control: the role of gut hormones. *Nutrition & diabetes* 2(1), p. e26. doi: 10.1038/nutd.2011.21.

Perry, V.H. et al. 1985. Immunohistochemical localization of macrophages and microglia in the adult and developing mouse brain. *Neuroscience* 15(2), pp. 313–326. doi: 10.1016/0306-4522(85)90215-5.

Perry, V.H. et al. 1993. Altered antigen expression of microglia in the aged rodent CNS. *Glia* 7(1), pp. 60–67. doi: 10.1002/glia.440070111.

Perry, V.H. 2014. Microglial priming in neurodegenerative disease. *Nature Rev. Neurol.* 10. doi: 10.1038/nrneurol.2014.38.

Perry, V.H. 2016. Microglia., pp. 1–9. doi: 10.1128/microbiolspec.MCHD-0003-2015.Correspondence.

Perry, V.H. and Teeling, J. 2013. Microglia and macrophages of the central nervous system: The contribution of microglia priming and systemic inflammation to chronic neurodegeneration. *Seminars in Immunopathology* 35(5), pp. 601–612. doi: 10.1007/s00281-013-0382-8.

Pham, O.H. and McSorley, S.J. 2015. Protective host immune responses to Salmonella infection. *Future microbiology* 10(1), pp. 101–10. doi: 10.2217/fmb.14.98.

Philipson, O. et al. 2010. Animal models of amyloid-β-related pathologies in Alzheimer's disease. *FEBS Journal* 277(6), pp. 1389–1409. doi: 10.1111/j.1742-4658.2010.07564.x.

Poltorak, A. et al. 1998. Defective LPS signaling in C3H/HeJ and C57BL/10ScCr mice: mutations in Tlr4 gene. *Science (New York, N.Y.)* 282(5396), pp. 2085–8.

Pooler, A.M. et al. 2012. Dynamic association of tau with neuronal membranes is regulated by phosphorylation. *Neurobiology of Aging* 33(2). doi: 10.1016/j.neurobiolaging.2011.01.005.

Pooler, A.M. et al. 2013. Physiological release of endogenous tau is stimulated by neuronal activity. *EMBO reports* 14(4), pp. 389–394. doi: 10.1038/embor.2013.15.

Pooler, A.M. et al. 2014. A role for tau at the synapse in Alzheimer's disease pathogenesis. *Neuropharmacology* 76, pp. 1–8. doi: 10.1016/j.neuropharm.2013.09.018.

Pooler, A.M. et al. 2015. Amyloid accelerates tau propagation and toxicity in a model of early Alzheimer's disease. *Acta neuropathologica communications* 3, p. 14. doi: 10.1186/s40478-015-0199-x.

Poorkaj, P. et al. 1998. Tau is a candidate gene for chromosome 17 frontotemporal dementia. *Annals of neurology* 43(6), pp. 815–25. doi: 10.1002/ana.410430617.

Prechel, M.M. et al. 1996. Increased interleukin-6 production by cerebral cortical tissue of adult versus young mice. *Mechanisms of ageing and development* 92(2–3), pp. 185–94.

Price, J.L. et al. 2009. Neuropathology of nondemented aging: Presumptive evidence for preclinical Alzheimer disease. *Neurobiology of Aging* 30(7), pp. 1026–1036. doi: 10.1016/j.neurobiolaging.2009.04.002.

Prince, M. et al. 2014. Dementia UK: Update Second edition.

Prince, M. et al. 2015. World Alzheimer Report 2015 The Global Impact of Dementia an analysis of prevalence, incidence, cost and trends.

Püntener, U. et al. 2012. Long-term impact of systemic bacterial infection on the cerebral vasculature and microglia. *Journal of Neuroinflammation* 9(1), p. 668. doi: 10.1186/1742-2094-9-146.

Qiao, X. et al. 2001. Neuroinflammation-induced acceleration of amyloid deposition in the APPV717F transgenic mouse. *The European journal of neuroscience* 14(3), pp. 474–82.

Quan, N. et al. 1998. Time course and localization patterns of interleukin-1beta messenger RNA expression in brain and pituitary after peripheral administration of lipopolysaccharide. *Neuroscience* 83(1), pp. 281–93.

Raetz, C.R.H. and Whitfield, C. 2002. Lipopolysaccharide Endotoxins. *Annual Review of Biochemistry* 71(1), pp. 635–700. doi: 10.1146/annurev.biochem.71.110601.135414.

Ramos-Morales, F. and Francisco 2012. Impact of *Salmonella enterica* Type III Secretion System Effectors on the Eukaryotic Host Cell. *ISRN Cell Biology* 2012, pp. 1–36. doi: 10.5402/2012/787934.

Ransohoff, R.M. and El Khoury, J. 2015. Microglia in Health and Disease. *Cold Spring Harbor perspectives in biology* 8(1), p. a020560. doi: 10.1101/cshperspect.a020560.

Ransohoff, R.M. and Perry, V.H. 2009. Microglial Physiology: Unique Stimuli, Specialized Responses. *Annual Review of Immunology* 27(1), pp. 119–145. doi: 10.1146/annurev.immunol.021908.132528.

Reiman, E.M. et al. 2012. Brain imaging and fluid biomarker analysis in young adults at genetic risk for autosomal dominant Alzheimer's disease in the presenilin 1 E280A kindred: a case-control study. *The Lancet. Neurology* 11(12), pp. 1048–56. doi: 10.1016/S1474-4422(12)70228-4.

del Rey, A. et al. 2009. Re-exposure to endotoxin induces differential cytokine gene expression in the rat hypothalamus and spleen. *Brain, behavior, and immunity* 23(6), pp. 776–83. doi: 10.1016/j.bbi.2009.02.009.

Ridley, A. and Cavanagh, J.B. 1969. The cellular reactions to heterologous, homologous and autologous skin implanted into brain. *The Journal of pathology* 99(3), pp. 193–203. doi:

10.1002/path.1710990303.

Roberson, E.D. et al. 2007. Reducing endogenous tau ameliorates amyloid beta-induced deficits in an Alzheimer's disease mouse model. *Science (New York, N.Y.)* 316(5825), pp. 750–4. doi: 10.1126/science.1141736.

Rochfort, K.D. et al. 2014. Downregulation of blood-brain barrier phenotype by proinflammatory cytokines involves NADPH oxidase-dependent ROS generation: consequences for interendothelial adherens and tight junctions. Koval, M. ed. *PloS one* 9(7), p. e101815. doi: 10.1371/journal.pone.0101815.

Rodriguez-Vieitez, E. et al. 2016. Diverging longitudinal changes in astrocytosis and amyloid PET in autosomal dominant Alzheimer's disease. *Brain* 139(3), pp. 922–936. doi: 10.1093/brain/awv404.

Roe, A.D. et al. 2011. Lipopolysaccharide-induced tau phosphorylation and kinase activity--modulation, but not mediation, by corticotropin-releasing factor receptors. *The European journal of neuroscience* 34(3), pp. 448–56. doi: 10.1111/j.1460-9568.2011.07764.x.

Rosenthal, S.L. and Kamboh, M.I. 2014. Late-Onset Alzheimer's Disease Genes and the Potentially Implicated Pathways. *Current genetic medicine reports* 2(2), pp. 85–101. doi: 10.1007/s40142-014-0034-x.

Rossi, D. 2015. Astrocyte physiopathology: At the crossroads of intercellular networking, inflammation and cell death. *PROGRESS IN NEUROBIOLOGY* 130, pp. 86–120. doi: 10.1016/j.pneurobio.2015.04.003.

Roth, J. and De Souza, G.E. 2001. Fever induction pathways: evidence from responses to systemic or local cytokine formation. *Brazilian journal of medical and biological research = Revista brasileira de pesquisas medicas e biologicas* 34(3), pp. 301–14.

Roubaud-Baudron, C. et al. 2012. Impact of chronic Helicobacter pylori infection on Alzheimer's disease: preliminary results. *Neurobiology of Aging* 33(5), p. 1009.e11-1009.e19. doi: 10.1016/j.neurobiolaging.2011.10.021.

Roubaud-Baudron, C. et al. 2015. An Eighteen-Month Helicobacter Infection Does Not Induce Amyloid Plaques or Neuroinflammation in Brains of Wild Type C57BL/6J Mice. *Journal of Alzheimer's disease : JAD* 45(4), pp. 1045–50. doi: 10.3233/JAD-143129.

Santacruz, K. et al. 2005. Tau Suppression in a Neurodegenerative Mouse Model Improves Memory Function. *Science* 309(5733), pp. 476–481. doi: 10.1126/science.1113694.

Santello, M. et al. 2011. TNFα Controls Glutamatergic Gliotransmission in the Hippocampal Dentate Gyrus. *Neuron* 69(5), pp. 988–1001. doi: 10.1016/j.neuron.2011.02.003.

Santos, R.L. et al. 2001. Animal models of Salmonella infections: enteritis versus typhoid fever. *Microbes and infection* 3(14–15), pp. 1335–44.

Sarlus, H. et al. 2012. Allergy influences the inflammatory status of the brain and enhances tau-phosphorylation. *Journal of Cellular and Molecular Medicine* 16(10), pp. 2401–2412. doi: 10.1111/j.1582-4934.2012.01556.x.

Sasaki, A. et al. 2002. Amyloid cored plaques in Tg2576 transgenic mice are characterized by giant plaques, slightly activated microglia, and the lack of paired helical filament-typed, dystrophic neurites. *Virchows Archiv* 441(4), pp. 358–367. doi: 10.1007/s00428-002-0643-8.

Sastre, M. et al. 2006. Nonsteroidal anti-inflammatory drugs repress β-secretase gene promoter activity by the activation of PPAR. *Proceedings of the National Academy of Sciences* 103(2), pp. 443–448. doi: 10.1073/pnas.0503839103.

Sastre, M. et al. 2008. Interactions between APP secretases and inflammatory mediators. *Journal of neuroinflammation* 5, p. 25. doi: 10.1186/1742-2094-5-25.

Sastre, M. and Gentleman, S.M. 2010. NSAIDs: How they Work and their Prospects as Therapeutics in Alzheimer's Disease. *Frontiers in aging neuroscience* 2, p. 20. doi: 10.3389/fnagi.2010.00020.

Schaafsma, W. et al. 2015. Long-lasting pro-inflammatory suppression of microglia by LPS-preconditioning is mediated by RelB-dependent epigenetic silencing. *Brain, Behavior, and Immunity* 48, pp. 205–221. doi: 10.1016/j.bbi.2015.03.013.

Schmidt, R. et al. 2002. Early inflammation and dementia: A 25-year follow-up of the Honolulu-Asia aging study. *Annals of Neurology* 52(2), pp. 168–174. doi: 10.1002/ana.10265.

Schulz, M. and Engelhardt, B. 2005. The circumventricular organs participate in the immunopathogenesis of experimental autoimmune encephalomyelitis. *Cerebrospinal fluid research* 2(1), p. 8. doi: 10.1186/1743-8454-2-8.

Schwab, C. et al. 2004. Transgenic mice overexpressing amyloid beta protein are an incomplete model of Alzheimer disease. *Experimental neurology* 188(1), pp. 52–64. doi: 10.1016/j.expneurol.2004.03.016.

Selkoe, D.J. and Hardy, J. 2016. The amyloid hypothesis of Alzheimer's disease at 25 years. *EMBO Molecular Medicine* 8(6), pp. 595–608. doi: 10.15252/emmm.201606210.

Serhan, C.N. and Petasis, N.A. 2011. Resolvins and Protectins in Inflammation Resolution. *Chemical Reviews* 111(10), pp. 5922–5943. doi: 10.1021/cr100396c.

Serot, J.-M. et al. 2003. Choroid plexus, aging of the brain, and Alzheimer's disease. *Frontiers in bioscience : a journal and virtual library* 8, pp. s515-21.

Seruga, B. et al. 2008. Cytokines and their relationship to the symptoms and outcome of cancer. *Nature Reviews Cancer* 8(11), pp. 887–899. doi: 10.1038/nrc2507.

Shaftel, S.S. et al. 2007. Sustained hippocampal IL-1β overexpression mediates chronic neuroinflammation and ameliorates Alzheimer plaque pathology. *Journal of Clinical Investigation* 117(6), pp. 1595–1604. doi: 10.1172/JCI31450.

Shaftel, S.S. et al. 2008. The role of interleukin-1 in neuroinflammation and Alzheimer disease: an evolving perspective. *Journal of Neuroinflammation* 5(1), p. 7. doi: 10.1186/1742-2094-5-7.

Shan, Y. et al. 2013. Age-related CD4(+)CD25(+)Foxp3(+) regulatory T-cell responses during Plasmodium berghei ANKA infection in mice susceptible or resistant to cerebral malaria. *The Korean journal of parasitology* 51(3), pp. 289–95. doi: 10.3347/kjp.2013.51.3.289.

Shan, Y. et al. 2016. Aging as a Precipitating Factor in Chronic Restraint Stress-Induced Tau Aggregation Pathology, and the Protective Effects of Rosmarinic Acid. Ying, Z. ed. *Journal of Alzheimer's Disease* 49(3), pp. 829–844. doi: 10.3233/JAD-150486.

Sheffield, L.G. and Berman, N.E. 1998. Microglial expression of MHC class II increases in normal aging of nonhuman primates. *Neurobiology of aging* 19(1), pp. 47–55.

Sheng, J.G. et al. 1996. In vivo and in vitro evidence supporting a role for the inflammatory cytokine interleukin-1 as a driving force in Alzheimer pathogenesis. *Neurobiology of aging* 17(5), pp. 761–6.

Sheng, J.G. et al. 1997. Glial-neuronal interactions in Alzheimer disease: progressive association of IL-1alpha+ microglia and S100beta+ astrocytes with neurofibrillary tangle stages. *Journal of neuropathology and experimental neurology* 56(3), pp. 285–90.

Shi, J.-Q. et al. 2011. Anti-TNF-α reduces amyloid plaques and tau phosphorylation and induces CD11c-positive dendritic-like cell in the APP/PS1 transgenic mouse brains. *Brain Research* 1368,

pp. 239–247. doi: 10.1016/j.brainres.2010.10.053.

Shipton, O.A. et al. 2011. Tau protein is required for amyloid-β induced impairment of hippocampal long-term potentiation. *The Journal of neuroscience : the official journal of the Society for Neuroscience* 31(5), pp. 1688–92. doi: 10.1523/JNEUROSCI.2610-10.2011.

Siemers, E.R. et al. 2016. Phase 3 solanezumab trials: Secondary outcomes in mild Alzheimer's disease patients. *Alzheimer's and Dementia* 12(2), pp. 110–120. doi: 10.1016/j.jalz.2015.06.1893.

Sierra, A. et al. 2007. Microglia derived from aging mice exhibit an altered inflammatory profile. *Glia* 55(4), pp. 412–424. doi: 10.1002/glia.20468.

Silverberg, G.D. et al. 2003. Alzheimer's disease, normal-pressure hydrocephalus, and senescent changes in CSF circulatory physiology: a hypothesis. *The Lancet. Neurology* 2(8), pp. 506–11.

Silverberg, G.D. et al. 2010. Amyloid efflux transporter expression at the blood-brain barrier declines in normal aging. *Journal of neuropathology and experimental neurology* 69(10), pp. 1034–43. doi: 10.1097/NEN.0b013e3181f46e25.

Simón, A.-M. et al. 2009. Overexpression of wild-type human APP in mice causes cognitive deficits and pathological features unrelated to Abeta levels. *Neurobiology of disease* 33(3), pp. 369–78. doi: 10.1016/j.nbd.2008.11.005.

Simpson, J.E. et al. 2010. Astrocyte phenotype in relation to Alzheimer-type pathology in the ageing brain. *Neurobiology of Aging* 31(4), pp. 578–590. doi: 10.1016/j.neurobiolaging.2008.05.015.

Singh-Manoux, A. et al. 2014. Interleukin-6 and C-reactive protein as predictors of cognitive decline in late midlife. *Neurology* 83(6), pp. 486–93. doi: 10.1212/WNL.0000000000000665.

Sly, L.. et al. 2001. Endogenous brain cytokine mRNA and inflammatory responses to lipopolysaccharide are elevated in the Tg2576 transgenic mouse model of Alzheimer's disease. *Brain Research Bulletin* 56(6), pp. 581–588. doi: 10.1016/S0361-9230(01)00730-4.

Smith, L.K. et al. 2015. β2-microglobulin is a systemic pro-aging factor that impairs cognitive function and neurogenesis. *Nature medicine* 21(8), pp. 932–7. doi: 10.1038/nm.3898.

Soni, N. et al. 2014. GLT-1 transporter: An effective pharmacological target for various neurological disorders. *Pharmacology Biochemistry and Behavior* 127, pp. 70–81. doi: 10.1016/j.pbb.2014.10.001.

Sorrells, S.F. and Sapolsky, R.M. 2010. Glucocorticoids can arm macrophages for innate immune battle. *Brain, behavior, and immunity* 24(1), pp. 17–8. doi: 10.1016/j.bbi.2009.10.004.

Soscia, S.J. et al. 2010. The Alzheimer's Disease-Associated Amyloid β-Protein Is an Antimicrobial Peptide. Bush, A. I. ed. *PLoS ONE* 5(3), p. e9505. doi: 10.1371/journal.pone.0009505.

Speakman, J.R. 2013. Measuring energy metabolism in the mouse - theoretical, practical, and analytical considerations. *Frontiers in Physiology* 4 MAR. doi: 10.3389/fphys.2013.00034.

Spillantini, M.G. et al. 1998. Mutation in the tau gene in familial multiple system tauopathy with presenile dementia. *Proceedings of the National Academy of Sciences of the United States of America* 95(13), pp. 7737–41.

Spillantini, M.G. and Goedert, M. 2013. Tau pathology and neurodegeneration. *The Lancet Neurology* 12(6), pp. 609–622. doi: 10.1016/S1474-4422(13)70090-5.

Spittau, B. 2017. Aging Microglia-Phenotypes, Functions and Implications for Age-Related Neurodegenerative Diseases. *Frontiers in aging neuroscience* 9, p. 194. doi: 10.3389/fnagi.2017.00194.

Spooren, A. et al. 2011. Interleukin-6, a mental cytokine. *Brain Research Reviews* 67(1–2), pp. 157–183. doi: 10.1016/j.brainresrev.2011.01.002.

Stancu, I.-C. et al. 2014. Models of β-amyloid induced Tau-pathology: the long and 'folded' road to understand the mechanism. *Molecular neurodegeneration* 9, p. 51. doi: 10.1186/1750-1326-9-51.

Stark, R.J. et al. 2016. Endothelial cell tolerance to lipopolysaccharide challenge is induced by monophosphoryl lipid A. *Clinical science (London, England : 1979)* 130(6), pp. 451–61. doi: 10.1042/CS20150592.

Steinbach, J.P. et al. 1998. Hypersensitivity to seizures in beta-amyloid precursor protein deficient mice. *Cell death and differentiation* 5(10), pp. 858–66. doi: 10.1038/sj.cdd.4400391.

Stewart, C.R. et al. 2010. CD36 ligands promote sterile inflammation through assembly of a Toll-like receptor 4 and 6 heterodimer. *Nature Immunology* 11(2), pp. 155–161. doi: 10.1038/ni.1836.

Strassnig, M. and Ganguli, M. 2005. About a peculiar disease of the cerebral cortex: Alzheimer's original case revisited. *Psychiatry (Edgmont (Pa. : Township))* 2(9), pp. 30–3.

Streit, W.J. et al. 2004. Dystrophic microglia in the aging human brain. *Glia* 45(2), pp. 208–212. doi: 10.1002/glia.10319.

Streit, W.J. et al. 2014. Microglial pathology. *Acta neuropathologica communications* 2, p. 142. doi: 10.1186/s40478-014-0142-6.

Streit, W.J. and Sparks, D.L. 1997. Activation of microglia in the brains of humans with heart disease and hypercholesterolemic rabbits. *Journal of molecular medicine (Berlin, Germany)* 75(2), pp. 130–8.

Sugimoto, M.A. et al. 2016. Resolution of Inflammation: What Controls Its Onset? *Frontiers in immunology* 7, p. 160. doi: 10.3389/fimmu.2016.00160.

Suhara, T. et al. 2002. Abeta42 generation is toxic to endothelial cells and inhibits eNOS function through an Akt/GSK-3beta signaling-dependent mechanism. *Neurobiology of aging* 24(3), pp. 437–51. doi: 10.1016/S0197-4580(02)00135-5.

Sultan, A. et al. 2011. Nuclear Tau, a Key Player in Neuronal DNA Protection. *Journal of Biological Chemistry* 286(6), pp. 4566–4575. doi: 10.1074/jbc.M110.199976.

Sundaram, J.R. et al. 2013. Specific inhibition of p25/Cdk5 activity by the Cdk5 inhibitory peptide reduces neurodegeneration in vivo. *The Journal of neuroscience : the official journal of the Society for Neuroscience* 33(1), pp. 334–43. doi: 10.1523/JNEUROSCI.3593-12.2013.

Swanson, J.A. and Hoppe, A.D. 2004. The coordination of signaling during Fc receptor-mediated phagocytosis. *Journal of leukocyte biology* 76(6), pp. 1093–103. doi: 10.1189/jlb.0804439.

Sy, M. et al. 2011. Inflammation Induced by Infection Potentiates Tau Pathological Features in Transgenic Mice. *The American Journal of Pathology* 178(6), pp. 2811–2822. doi: 10.1016/j.ajpath.2011.02.012.

Takeda, S. et al. 2013. Increased blood–brain barrier vulnerability to systemic inflammation in an Alzheimer disease mouse model. *Neurobiology of Aging* 34(8), pp. 2064–2070. doi: 10.1016/j.neurobiolaging.2013.02.010.

Takeda, T. et al. 1981. A new murine model of accelerated senescence. *Mechanisms of ageing and development* 17(2), pp. 183–94.

Takuma, H. et al. 2003. Isoforms changes of tau protein during development in various species. *Developmental Brain Research* 142(2), pp. 121–127. doi: 10.1016/S0165-3806(03)00056-7.

Talbot, K. et al. 2012. Demonstrated brain insulin resistance in Alzheimer's disease patients is associated with IGF-1 resistance, IRS-1 dysregulation, and cognitive decline. *Journal of Clinical*

Investigation 122(4), pp. 1316–1338. doi: 10.1172/JCI59903.

Talbot, K. 2014. Brain insulin resistance in Alzheimer's disease and its potential treatment with GLP-1 analogs. *Neurodegenerative disease management* 4(1), pp. 31–40. doi: 10.2217/nmt.13.73.

Tariot, P.N. et al. 2011. Chronic Divalproex Sodium to Attenuate Agitation and Clinical Progression of Alzheimer Disease. *Archives of General Psychiatry* 68(8), p. 853. doi: 10.1001/archgenpsychiatry.2011.72.

Teeling, J.L. et al. 2007. Sub-pyrogenic systemic inflammation impacts on brain and behavior, independent of cytokines. *Brain, Behavior, and Immunity* 21(6), pp. 836–850. doi: 10.1016/j.bbi.2007.01.012.

Tegeler, C. et al. 2016. The inflammatory markers CRP, IL-6, and IL-10 are associated with cognitive function—data from the Berlin Aging Study II. *Neurobiology of Aging* 38, pp. 112–117. doi: 10.1016/j.neurobiolaging.2015.10.039.

Tha, K.K. et al. 2000. Changes in expressions of proinflammatory cytokines IL-1beta, TNF-alpha and IL-6 in the brain of senescence accelerated mouse (SAM) P8. *Brain research* 885(1), pp. 25–31.

Trost, A. et al. 2016. Brain and Retinal Pericytes: Origin, Function and Role. *Frontiers in Cellular Neuroscience* 10(February), pp. 1–13. doi: 10.3389/fncel.2016.00020.

UJIIE, M. et al. 2003. Blood-Brain Barrier Permeability Precedes Senile Plaque Formation in an Alzheimer Disease Model. *Microcirculation* 10(6), pp. 463–470. doi: 10.1038/sj.mn.7800212.

VanCott, J.L. et al. 1998. Regulation of host immune responses by modification of Salmonella virulence genes. *Nature Medicine* 4(11), pp. 1247–1252. doi: 10.1038/3227.

VanGuilder, H.D. et al. 2011. Concurrent hippocampal induction of MHC II pathway components and glial activation with advanced aging is not correlated with cognitive impairment. *Journal of neuroinflammation* 8, p. 138. doi: 10.1186/1742-2094-8-138.

Varatharaj, A. and Galea, I. 2017. The blood-brain barrier in systemic inflammation. *Brain, Behavior, and Immunity* 60, pp. 1–12. doi: 10.1016/j.bbi.2016.03.010.

in 't Veld, B.A. et al. 2001. Nonsteroidal Antiinflammatory Drugs and the Risk of Alzheimer's Disease. *New England Journal of Medicine* 345(21), pp. 1515–1521. doi: 10.1056/NEJMoa010178.

Verma, S. et al. 2006. Release of cytokines by brain endothelial cells: A polarized response to

lipopolysaccharide. *Brain, Behavior, and Immunity* 20(5), pp. 449–455. doi: 10.1016/j.bbi.2005.10.005.

Villeda, S.A. et al. 2011. The ageing systemic milieu negatively regulates neurogenesis and cognitive function. *Nature* 477(7362), pp. 90–4. doi: 10.1038/nature10357.

Violet, M. et al. 2014. A major role for Tau in neuronal DNA and RNA protection in vivo under physiological and hyperthermic conditions. *Frontiers in cellular neuroscience* 8, p. 84. doi: 10.3389/fncel.2014.00084.

Walker, D.G. and Lue, L. 2015. Immune phenotypes of microglia in human neurodegenerative disease : challenges to detecting microglial polarization in human brains. *Alzheimer's Research & Therapy* 7, p. 56. doi: 10.1186/s13195-015-0139-9.

Wallin, K. et al. 2012. Midlife rheumatoid arthritis increases the risk of cognitive impairment two decades later: a population-based study. *Journal of Alzheimer's disease : JAD* 31(3), pp. 669–76. doi: 10.3233/JAD-2012-111736.

Wang, H. et al. 2003. Nicotinic acetylcholine receptor α7 subunit is an essential regulator of inflammation. *Nature* 421(6921), pp. 384–388. doi: 10.1038/nature01339.

Wang, W. et al. 2011. TLR4 Activation Induces Nontolerant Inflammatory Response in Endothelial Cells. *Inflammation* 34(6), pp. 509–518. doi: 10.1007/s10753-010-9258-4.

Wang, X. et al. 2015. Resolution of inflammation is altered in Alzheimer's disease. *Alzheimer's & Dementia* 11(1), p. 40–50.e2. doi: 10.1016/j.jalz.2013.12.024.

Wang, X.-L. et al. 2014. Helicobacter pylori filtrate impairs spatial learning and memory in rats and increases β-amyloid by enhancing expression of presenilin-2. *Frontiers in aging neuroscience* 6, p. 66. doi: 10.3389/fnagi.2014.00066.

Wang, X. and Michaelis, E.K. 2010. Selective neuronal vulnerability to oxidative stress in the brain. *Frontiers in Aging Neuroscience* 2, p. 12. doi: 10.3389/fnagi.2010.00012.

Wang, Y. and Mandelkow, E. 2015. Tau in physiology and pathology. *Nature reviews. Neuroscience* 17(1), pp. 22–35. doi: 10.1038/nrn.2015.1.

Wei, L. et al. 2004. Taking glucocorticoids by prescription is associated with subsequent cardiovascular disease. *Annals of internal medicine* 141(10), pp. 764–70.

Weingarten, M.D. et al. 1975. A protein factor essential for microtubule assembly. *Proceedings of*

the National Academy of Sciences of the United States of America 72(5), pp. 1858–62.

Wesson, D.W. and Wilson, D.A. 2011. Age and gene overexpression interact to abolish nesting behavior in Tg2576 amyloid precursor protein (APP) mice. *Behavioural brain research* 216(1), pp. 408–13. doi: 10.1016/j.bbr.2010.08.033.

White, C.S. et al. 2017. Inflammasomes as therapeutic targets for Alzheimer's disease. *Brain Pathology* 27(2), pp. 223–234. doi: 10.1111/bpa.12478.

Whiteman, I.T. et al. 2009. Activated actin-depolymerizing factor/cofilin sequesters phosphorylated microtubule-associated protein during the assembly of alzheimer-like neuritic cytoskeletal striations. *The Journal of neuroscience : the official journal of the Society for Neuroscience* 29(41), pp. 12994–3005. doi: 10.1523/JNEUROSCI.3531-09.2009.

Wildsmith, K.R. et al. 2013. Evidence for impaired amyloid β clearance in Alzheimer's disease. *Alzheimer's research & therapy* 5(4), p. 33. doi: 10.1186/alzrt187.

Williams, D.R. 2006. Tauopathies: classification and clinical update on neurodegenerative diseases associated with microtubule-associated protein tau. *Internal Medicine Journal* 36(10), pp. 652–660. doi: 10.1111/j.1445-5994.2006.01153.x.

Wilson, E.H. et al. 2010. Trafficking of immune cells in the central nervous system. *Journal of Clinical Investigation* 120(5), pp. 1368–1379. doi: 10.1172/JCI41911.

Wischik, C.M. et al. 1996. Selective inhibition of Alzheimer disease-like tau aggregation by phenothiazines. *Proceedings of the National Academy of Sciences of the United States of America* 93(20), pp. 11213–8.

Wynne, A.M. et al. 2010. Protracted downregulation of CX3CR1 on microglia of aged mice after lipopolysaccharide challenge. *Brain, behavior, and immunity* 24(7), pp. 1190–201. doi: 10.1016/j.bbi.2010.05.011.

Xiao, G. and Gan, L.-S. 2013. Receptor-mediated endocytosis and brain delivery of therapeutic biologics. *International journal of cell biology* 2013, p. 703545. doi: 10.1155/2013/703545.

Xie, Z. et al. 2003. Aging and glial responses to lipopolysaccharide in vitro: greater induction of IL-1 and IL-6, but smaller induction of neurotoxicity. *Experimental neurology* 182(1), pp. 135–41.

Yamada, K. et al. 2014. Neuronal activity regulates extracellular tau in vivo. *The Journal of Experimental Medicine* 211(3), pp. 387–393. doi: 10.1084/jem.20131685.

Yamamoto, M. et al. 2007. Interferon-gamma and tumor necrosis factor-alpha regulate amyloid-beta plaque deposition and beta-secretase expression in Swedish mutant APP transgenic mice. *The American journal of pathology* 170(2), pp. 680–92. doi: 10.2353/ajpath.2007.060378.

Yang, Q. et al. 2002. Mortality associated with Down's syndrome in the USA from 1983 to 1997: A population-based study. *Lancet* 359(9311), pp. 1019–1025. doi: 10.1016/S0140-6736(02)08092-3.

Ye, S.M. and Johnson, R.W. 2001a. An age-related decline in interleukin-10 may contribute to the increased expression of interleukin-6 in brain of aged mice. *Neuroimmunomodulation* 9(4), pp. 183–92. doi: 49025.

Ye, S.M. and Johnson, R.W. 2001b. Regulation of interleukin-6 gene expression in brain of aged mice by nuclear factor kappaB. *Journal of neuroimmunology* 117(1–2), pp. 87–96.

Yin, Z. et al. 2017. Immune hyperreactivity of Aβ plaque-associated microglia in Alzheimer's disease. *Neurobiology of Aging* 55, pp. 115–122. doi: 10.1016/j.neurobiolaging.2017.03.021.

Yoshida, M. 2014. Astrocytic inclusions in progressive supranuclear palsy and corticobasal degeneration. *Neuropathology* 34(6), pp. 555–570. doi: 10.1111/neup.12143.

Yoshiyama, Y. et al. 2007. Synapse Loss and Microglial Activation Precede Tangles in a P301S Tauopathy Mouse Model. *Neuron* 53(3), pp. 337–351. doi: 10.1016/j.neuron.2007.01.010.

Yuan, A. et al. 2008. Axonal Transport Rates In Vivo Are Unaffected by Tau Deletion or Overexpression in Mice. *Journal of Neuroscience* 28(7)

Zhang, Y.-H. et al. 2003. Specific roles of cyclooxygenase-1 and cyclooxygenase-2 in lipopolysaccharide-induced fever and Fos expression in rat brain. *The Journal of comparative neurology* 463(1), pp. 3–12. doi: 10.1002/cne.10743.

Zhao, J. et al. 2017. The Role of MicroRNAs in Aβ Deposition and Tau Phosphorylation in Alzheimer's Disease. *Frontiers in neurology* 8, p. 342. doi: 10.3389/fneur.2017.00342.

Zilka, N. et al. 2012. Who fans the flames of Alzheimer's disease brains? Misfolded tau on the crossroad of neurodegenerative and inflammatory pathways. *Journal of neuroinflammation* 9(1), p. 47. doi: 10.1186/1742-2094-9-47.